On the dynamics of a periodically driven spheroid in a variety of fluid flows at low Reynolds numbers

Thesis submitted to the

Indian Institute of Space Science and Technology Thiruvananthapuram

For award of the degree

of

Doctor of Philosophy

by

JOGENDER SINGH

Under the guidance of

Prof. C V Anil Kumar

DEPARTMENT OF MATHEMATICS
INDIAN INSTITUTE OF SPACE SCIENCE AND TECHNOLOGY,
THIRUVANANTHAPURAM-695547, INDIA

December 2022

Department of Mathematics,
Indian Institute of Space Science and Technology, India
An autonomous institute under Department of Space, Govt. of India

Dedicated...

To my family, I couldn't have done this without you.

Thank you for your support...

Department of Mathematics,
Indian Institute of Space Science and Technology, India
An autonomous institute under Department of Space, Govt. of India

Certificate

This is to certify that the thesis entitled **"On the dynamics of a periodically driven spheroid in a variety of fluid flows at low Reynolds numbers"** submitted by **Jogender Singh**, to the Indian Institute of Space Science and Technology Thiruvananthapuram, is a bonafide record of the research work carried out by him under my supervision and I consider it worthy of consideration for the award of the degree of Doctor of Philosophy of the Institute. The contents of this dissertation, in full or in parts, have not been submitted to any other Institute or University for the award of any degree or diploma.

(seal and sign)

Prof. C. V. Anil Kumar
Research Supervisor
Professor, Dept. of Mathematics

(Counter Signature of HoD with seal)

Place: Thiruvananthapuram
December 2022

Department of Mathematics,
Indian Institute of Space Science and Technology, India
An autonomous institute under Department of Space, Govt. of India

Declaration

I hereby certify that

- The work contained in the dissertation entitled "**On the dynamics of a periodically driven spheroid in a variety of fluid flows at low Reynolds numbers**" is original and has been done by myself under the general supervision of **Prof. C V Anil Kumar**.
- This work has not been submitted to any other Institute for any degree or diploma.
- I have followed the guidelines provided by the Institute in writing the dissertation.
- I have confirmed to the norms and guidelines given in the Ethical Code of Conduct of the Institute.
- Whenever I have used materials (text, theoretical analysis and data) from other sources, I have given due credit to them by citing them in the text of the dissertation and giving their details in the references.
- Whenever I have quoted written materials from other sources, I have put its under quotation and given due credit to the source by citing them and giving required details in the references.

Place: Thiruvananthapuram
December 2022

Jogender Singh
Research Scholar
Roll No.: SC16D039

Acknowledgments

The voyage took five years to reach this point to achieve the goal. Several persons have involved in this process and helped me to complete this journey. First and foremost, I owe a lot to my supervisor Prof. C V Anil Kumar, Dept. of Mathematics, IIST, who has given me the opportunity to work under his guidance. I thank him for his stimulating suggestions and encouragement. He has helped me immensely during the research as well as writing of this thesis. I also would like to express my gratitude to Prof. T R Ramamohan (Rtd. Scientist, 4^{th}PI Bangaluru) and thank him for sharing his knowledge and for reviewing my work. Without his guidance and help, this work would not have been possible. I would like to thank Prof. K Satheesh Kumar (Department of Future studies, Kerala University) for his suggestions regarding the numerical simulations. I would like to thank Prof. Raju K George (Department of Mathematics, and Dean R & D IIST) for chairing the DC Sessions.

I also express my gratitude to Dr. Sarvesh Kumar (Associate Professor, Dept. of Mathematics, IIST), Prof N Sabu (Professor, Dept. of Mathematics, IIST), and Prof. A Salih (Professor, Dept. of Aerospace Engineering, IIST) for agreeing to be on my Doctoral Committee. The discussion with Prof. Sarvesh Kumar had increased the quality of the work a lot. Also, I would like to thank Prof. A Salih for accepting be a DC member and teaching me the courses in computational fluid dynamics. Furthermore, I would like to thank Dr. Pradeep Kumar P (Associate Professor, Dept. of Aerospace Engineering, IIST), who taught me a course in

fluid mechanics. It has undoubtedly helped me develop a solid background in my Dissertation.

I am sincerely grateful to all faculty members of the Department of Mathematics, Prof. Subrahamanian Moosath K S, Prof. Deepak T G, Dr. Kaushik Mukherjee, Dr. Natarajan E, Dr. S Sumitra, Dr. Sakthivel K and Dr. Prosenjit Das for their constant support and help. I would like to thank the staff members at Department of Mathematics, especially Mr. Anish J, Mrs. Nisha, Mrs. Pournami, and Mr. Mohd. Kerim A, for being helpful during the period. I express my heartful gratitude to Dr. Tarakanta Nayak, Associate Professor at IIT Bhubaneswar, for teaching me to write a scientific document.

This research would not have been possible without the financial support of the Indian Institute of Space Science and Technology and the Department of Space Science (DoS), Govt. of India, which should be greatly acknowledged. The simulations were performed using the resources provided by the HPC Lab at the Indian Institute of Space Science and Technology, India. I also would like to thank the director of the Institute, for providing facility to complete my research and the thesis.

I also want to thank my colleagues and friends, Manohar, Gyaneshwar, Krishna Tej, Nitesh, Janaki Raman, Narendra, Elangovan, James, and Sweta, who have had an active participation during these years, have helped me, and I have had enriching discussions with them and for making my stay comfortable and for making me feel welcome. I will surely miss our long sessions discussing every other imaginable aspect of physics, education, ethics, politics, and life in general. These discussions increased my confidence as a researcher and probably made me a better person. I want to express my profound gratitude to a very good friend, Sudhanshu, who was busy writing his thesis and helped me on several occasions. I also thank him for encouraging and supporting me.

Finally, the constant loving support from my family has been invaluable to me, and I would like to express my indebted gratitude to my parents and other

family members. My heartfelt gratitude also goes to my brothers, Mr. Raveesh Rajput and Mr. Govind Singh, and sisters, Mrs. Reena Rajput and Mrs. Arati Rajput, for always being with me in difficult times. They support me in taking steps forward; I want to express my gratitude and love to my family and friends in my hometown.

Last but not least, I would like to thank Hostel, Canteen, and medical staff for their services which made me easy to stay in the campus at IIST, despite the worldwide pandemic.

Jogender Singh

IIST Thiruvananthapuram, India

Abstract

The purpose of this thesis is to investigate the orientation dynamics and resonance properties of oscillations of a periodically driven non-spherical micro-spheroid in a set of Newtonian unsteady viscous fluids at low Reynolds numbers. We neglect the particle-particle interactions by assuming a sufficiently diluted suspension. As a first case, we derive and investigate a perturbation solution of motion of the harmonically-forced rectilinear displacement of a weak eccentric spheroid along its axis of symmetry in the presence and absence of memory forces at resonance. The dependence of the body's aspect ratio, free oscillation frequency, and particle–fluid density ratio on the motion solutions is examined and analyzed. A governing equation inclusive of the effect of damping, Basset memory, and second history integral forces at small Reynolds numbers is derived, and then we proceed to obtain an analytical solution of this equation at resonance. Expressions of the conventional Q-curves, amplitude-frequency, and phase-frequency oscillations of the spheroid with the natural frequency are also derived.

Considering the applications of the orientation of particles in three-dimensional systems, we study the dynamics of a rigid particle in a quiescent fluid, uniform flow, and oscillating flow at low Reynolds numbers. We have derived the system of differential equations that describe the motion of an arbitrarily forced spheroid in each flow at a low Reynolds number. These governing equations are non-linear and contain a history term of all the past positions and velocity. Therefore, obtaining their analytical solution is non-trivial, and suitable numerical methods are employed to study the spheroid transport. The novel features of this study

include periodic forces in an arbitrary direction, The hydrodynamic forces arising due to the disturbance of the velocity fluctuations the forces induced due to the non-spherical nature of the rigid body. Next, we consider a periodically forced prolate spheroid suspended in an oscillating Newtonian fluid in the low-Reynolds number limit. We study the characteristics of the solutions of the particle due to the periodic force applied on the spheroid particle and induced hydrodynamic force acting on the particle. We obtain the governing equations of the proposed problem by using an appropriate expression for the hydrodynamic force. We also examine the orientation profile of a rigid body suspension in a time-dependent uniform flow at low Reynolds numbers under the action of an external periodic field.

In summarizing the results and the applications, we see that the problems considered here have significant contributions from fundamental and technological aspects. This proposed work help in understanding the role of aspect ratio, density ratio, and free frequency on the oscillation properties of the particle. The observed phenomena may give new insights into physics, especially regarding the quantum of velocity disturbances due to particle shape. This study can be used to analyze the oscillation variations of particles having arbitrary eccentricity in the presence of history integral terms and/or other external forces like a magnetic force, acoustic radiation force, electric force, etc. Technically, we can use the dependencies of properties on the controllable parameters for devising better particle separation for characterizing suspensions having desired properties. The analytical solutions obtained at resonance might be important in testing software designed for more complicated and realistic systems, hence striking a good balance between complication and tractability. The solutions may have practical applications in experiments involving more complex systems, mainly to understand the effect of acoustic waves on micro-particle transport. The work can be extended further in many directions, especially considering the effect of Brownian motion and particle-particle interactions.

Contents

List of Figures

List of Tables

Notations

$\mathbf{F}^{\mathrm{H}}$	Hydrodynamic Force
$\mathbf{F}^{\mathrm{H}}_{s}$	Stokes or pseudo Hydrodynamic Force
$\mathbf{F}^{\mathrm{H}\parallel}$	Parallel component of the hydrodynamic force
$\mathbf{F}^{\mathrm{H}\perp}$	Perpendicular component of the hydrodynamic force
μ	dynamic viscosity
ν	Kinematic Viscosity
ρ	Density of fluid
ρ_p	Density of particle
k_a	aspect ratio of the spheroid
ϵ	eccentricity of spheroid
V	Volume of the fluid
V_p	Volume of the particle
$\tilde{V}$	Dimensionless Volume of the Particle or displaced fluid amount
ϕ	Volume fraction
Pr	Prandtl number
Re	Reynolds number
Sl	Strouhal number
Pe	Peclet number
$\mathscr{L}$	Laplace Transform
Q_α	Quality factor of the oscillations of the particle corresponding damping force term
Q_β	Quality factor of the oscillations of the particle corresponding Basset memory force term
Q_γ	Quality factor of the oscillations of the particle corresponding new history force term
∇	Differential operator
$\mathbf{\Phi}$	Stokes resistance tensor
$\mathbf{M}$	Transformation tensor defined such that $\boldsymbol{u}_0 = \mathbf{M} \cdot \boldsymbol{u}_s$
$\mathbf{u}_s$	Slip velocity of the particle
$\mathbf{u}_\infty$	Undisturbed fluid velocity

$\mathbf{u}_p$	Velocity of the particle
$\mathbf{y}_s$	Displacement of the particle
U_c	Characteristic velocity of the particle
$\mathbf{u}_0$	Stokes velocity of the particle
F_i	Amplitude of the periodic force associated with i^{th} direction
Re_F	Scaled amplitude of the periodic force
ω	Frequency of the oscillation
a	Semi-major axis of the spheroid, characteristic particle dimension
b	Semi-minor axis of the spheroid
m_p	mass of the particle
m_f	Mass of the fluid displaced by the particle

Chapter 1

Introduction

In the low Reynolds number regime, the dynamics of particles suspended in a viscous Newtonian fluid are fundamentally crucial in characterizing suspensions. There are several studies on the dynamics of spherical and non-spherical bodies for zero Reynolds number. Exploring the dynamics and rheology of non-spherical spheroids, fibers, slender bodies, and other complex geometric particle becomes more complicated than spherical particles, especially in the inclusion of Reynolds numbers. This thesis intends to study the dynamics of the periodically forced spheroids suspended in a viscous Newtonian fluid at the low Reynolds number limit, such as resting flow, oscillating flow, and time-dependent uniform flow.

In this thesis, we derive the governing equations describing the dynamics of spherical and non-spherical particles. Since the differential equations are coupled and nonlinear, finding analytic and /or closed-form solutions may be difficult. Therefore, we have solved them numerically by employing appropriate numerical schemes. In this chapter, we describe the fundamentals and preliminaries of fluid suspensions, expressions required for deriving the respective governing equations, the research work done in the past, and the major objectives of the problem under consideration.

1.1 Objectives

The main objectives of the thesis are as follows:

• To study the resonance response of a slightly eccentric spheroid suspended in a Newtonian fluid in one dimension.

• To analyze the oscillations of the arbitrarily shaped spheroid, which oscillates in the Newtonian fluid with a low Reynolds number in one dimension.

• To study the effect of the resistance of Stokes, Basset force, and new history integral term of force on the oscillations of the particles.

• To study the effects of the drag force, the Basset memory force term, and the new history-integral force term on the spheroid.

• To study the dynamics of a periodically forced prolate spheroid suspended in a quiescent fluid at low Reynolds numbers.

• To examine the effect of parameters such as Reynolds number, the geometry of particles, and the amplitude of the external periodic force influence the dynamics of the prolate spheroid. We also investigate the particle dynamics depending on the shape and size of the particle.

• To analyze the dynamics of a periodically forced prolate spheroid suspended in a time-dependent uniform flow at low Reynolds numbers. We study the effects of parameters such as Reynolds number, aspect ratio, the flow velocity of the fluid, and amplitude of the external periodic force on the dynamics of the prolate spheroid.

• To investigate the dynamics of the spheroid suspended in an oscillating flow field. We investigate how the dynamics respond to Reynolds number, aspect ratio, external force amplitude, and the oscillating fluid field frequency.

1.2 Review of literature

This section reviews investigations of the effects of a periodic force on suspended particles in incompressible Newtonian and non-Newtonian Fluids. In science, engineering, and technology, research on the dynamics of suspension of particles in fluids is significant and plays a vital role in devising new technologies. Particles suspended or scattered in a fluid medium occur in various natural and man-made environments, for example, colloids, slurries, composite materials, proteins, ceramics, polymers, etc. The occurrence of particles will affect the bulk properties of the suspension and, in particular, its rheological parameters, such as effective viscosity. The central theoretical and realistic problem is understanding and predicting the macroscopic balance of these multi-phase materials and the transport properties from their micro-structural mechanism. Micro-structural mechanics involves Brownian, inter-particle, external, and hydrodynamic forces acting or induced on particles and their spatial and temporal distribution. It is commonly called the microstructure of the system. The macroscopic properties may be the rate of sedimentation or aggregation, the self-diffusion coefficient, the thermal conductivity, or the rheology of a suspension of particles. If the distribution of particles were given, in addition to the location and motion of any boundaries and the physical properties of the particles and suspending fluid, one would have to solve (in principle, not necessarily in practice) the well-posed boundary-value problem to determine the behavior of the system. The macroscopic or averaged properties will be determined by averaging this solution over a large volume or many different configurations. The critical steps in this approach are solving the many-body problem, figuring out the micro-structure, and then investigating the macro properties using sample averages. These approaches are daunting but essential in understanding suspension behavior, theoretically.

Understanding the motion of micro bipolar particle inflows at low Reynolds numbers is critical in various practical scenarios. The transport of small bipolar

particles in flows is of great interest because disturbances in velocity fluctuations caused due to the particle suspension may bring the system unstable. As a result, the unsteady hydrodynamic force in these flows must be considered when analyzing particle motion and the bulk properties of the system. It is possible once the hydrodynamic force induced on a suspended body is known as a function of the geometric properties of the body. Many force simplifications depending on the body's geometry are available in the literature. The dynamics of small rigid particle drops and bubbles in a viscous Newtonian fluid at low Reynolds numbers are addressed by Stokes (1851). Basset (1888a;b) has developed the expression for the hydrodynamic force acting on a sphere moving in a quiescent fluid, including the effects of unsteady inertia. Many researchers have studied particle dynamics in linear flows without external force following the work. Some of them are Jeffrey (1922), Bretherton (1962b;a), Leal and Hinch (1971); Leal (1971) and Brenner (1974). Reasonably comprehensive reviews of research published before 1965 are contained in the works by Goldsmith and Mason (1967), Brenner (1966; 1972) and Leal (1979) and Happel and Brenner (2012). Additional topics not mentioned or only briefly mentioned in previous reviews are covered by Cox (1970), Batchelor (1970), Burgers (1995), Acrivos and Lo (1978), Rallison (1978) and, Rallison and Acrivos (1978). Mazur and Bedeaux (1974) have a generalized extension of Faxen's theorem to the non-steady motion of a spherical particle in an incompressible flow. Lawrence and Weinbaum (1986) investigated the axisymmetric motion of a spheroid at low Reynolds numbers. On the other hand, many others, such as Strand and Kim (1992); Ramamohan et al. (1994) have analyzed the dynamics of suspension under the action of an external force.

There is a vast literature on suspended particles in linear flows. Jeffrey (1922) has obtained the dynamics of a rigid isolated ellipsoid revolved in a simple uniform motion at low Reynolds numbers and has confirmed the existence of a closed orbit called Jeffery's orbit. In addition, the use of singularity methods for the Stokes equation to construct solutions for finite single particles has been investigated by

Chwang and Wu (1974) and Chwang (1975). Chwang and Wu (1976) have also studied low Reynolds number flow in general. The main objective was to develop an efficient solution method for bodies of arbitrary shapes. They considered viscous flows generated by the pure rotation of an axisymmetric body having an arbitrary prolate shape, assuming that the inertial forces have a negligible effect on the flow. The resolution method explored in their work has been based on the spatial distribution of singular torsional moments, called rotlets, through which it is possible to represent the rotational motion of a given body. Chwang and Wu (1975) have obtained exact solutions of dynamics of an elongated spheroid in the closed-form using the method of singularities for various quadratic flows of unbounded viscous Newtonian fluid at low Reynolds numbers.

Furthermore, Bretherton (1962a) studied the two-dimensional steady flow of an incompressible viscous fluid around a circular cylinder and described it in terms of asymptotically valid expansions, where the long-range velocity field is a combination of uniform velocity and uniform flow concerning Axes that move with (but do not rotate with) the center of the cylinder. Theoretically, Bretherton (1962b) has therefore investigated that the orbits of a particle of more general shape in a non-uniform shear in the presence of rigid boundaries can be qualitatively similar, where inertial and non-Newtonian effects are entirely neglected. They found that the axis orientation of almost all bodies is a periodic function of time in any unidirectional flow. It is true even if there is a gravitational force on the particle in the direction of the flow lines. Chwang and Wu (1976) analyzed the problem of uniform transverse flow on a spheroid of arbitrary proportions at low Reynolds numbers by the method of coupled asymptotic expansions. The solution depends on two Reynolds numbers, one based on the semi-major axis a, $Re_a = U_c a/\nu$, and the other on the semi-minor axis b, $Re_b = U_c b/\nu$. Here, U_c is the free flow velocity at infinity, perpendicular to the prolate spheroid's major axis, and ν is the kinematic viscosity of the fluid. When Re_a is small, the current resistance formula is reduced to Oberbeck (1876) result for the Stokes curve past a spheroid.

This result, therefore, provides a clear physical picture and explanation of the well-known "Stokes paradox" in viscous flow theory.

Leal (1971) investigated the effect of an external torque on particles suspended in a dilute suspension. They considered the movement of a sphere and arbitrary spheroid subjected to a magnetic field. Also, they numerically evaluated the effective viscosity of the suspension for many cases of the problem. In a later study, Leal and Hinch (1971) investigated the effect of Brownian motion on particle dynamics suspended in a shear flow at zero Reynolds number. Using the findings, they have calculated the specific bulk properties of the suspension. The predicted properties are then compared with the available experimental observation.

Chwang and Wu (1974) have studied the rotation of axisymmetric prolate spheroids at low Reynolds number flow. Lin et al. (1970) investigated inertial effects and suspension rheology of simple shear flow around a sphere, where results were limited to low particle Reynolds numbers (< 1) in the dilute limit. In addition, the motion of a spherical particle in the presence of a fluid-fluid interface has been studied by Lee et al. (1979) and Lee and Leal (1982). First, a solution for a point force close to a planar interface was derived. Then the solution was extended to include the higher-order terms needed to describe the motion of a solid sphere.

MacMillan (1989) analyzed the dynamics of particles in various linear flows and the effect of these particles' orientation on the suspension's properties. Strand (1989) developed a theory for analyzing the dynamics and rheology of non-spherical particles in an external oscillating force field in simple shear flow. The dynamics of suspended particles in linear flows under the action of alternating or rotating external force fields have been considered by some researchers focusing on various practical applications such as magnetostriction of suspensions of ferromagnetic particles (Ignatenko 1984), magneto-fluidization (Buevich et al. 1985), rheological properties of ferromagnetic colloids (Tsebers 1986), and characterization of magnetorheological suspensions (Kashevskii (1986); Cebers (1993a;b)). They con-

sidered external rotational force fields, which can be considered a superposition of two alternating external force fields. Strand and Kim (1992) numerically demonstrated the dynamics and rheology of non-spherical particles in constant external force fields in simple shear flow. Szeri et al. (1992) analyzed the motion of rigid particles in time-dependent flows. The effect of externally induced forces on small particles in homogeneous shear currents has been considered by Brenner (1974). The motion of a force-less spheroidal particle in paraboloid flow has been determined by him, where the spheroid has been shown to rotate around three principal axes with angular velocities governed by Jeffery's orbital equations with the shear rate evaluated at the center of the spheroid.

It is demonstrated that the nonlinear coupling governing equations of the microscopic particles have influenced the macroscopic rheological parameters. The work on periodic forcing on the orientable particles in a simple shear flow has been summarized by Asokan et al. (2005). Patankar and Hu (2002) studied the impact of Reynolds numbers on the rheological properties of a dilute suspension of spherical particles in a Newtonian fluid using Direct Numerical Simulation (DNS). Kulkarni and Morris (2008) has published a work on the role of particle scale inertia of suspensions in a simulated shear flow at finite Reynolds numbers. The rheology of rigid particle suspension has also been investigated by Mueller et al. (2010). Vodop'yanov et al. (2010) have reported the work on the unsteady sedimentation of rigid spherical particles in a viscous fluid. Madhukar et al. (2010) have investigated the particle dynamics and 'normal stress' evaluation of dilute suspensions of periodically forced spheroid in a quiescent fluid in low Reynolds numbers. Ramamohan et al. (2011) have studied the effects of both unsteady and convective inertia on the dynamics and rheology of a dilute suspension of neutrally buoyant sphere under the action of a periodic force in a quiescent fluid at low Reynolds numbers. Ley and Bruus (2016) established a continuum model for numerical investigations of hydrodynamic particle-particle interaction in microfluidic high-concentration suspensions.

Furthermore, we use the formalism of the hydrodynamic force Lovalenti and Brady (1993a), which acts on a particle in the regime of low Reynolds numbers, to obtain the equations of motion of the particle under the influence of an external force and its dynamics under the different test cases. The expression developed by Lovalenti and Brady (1993a) is a good approximation up to $O(Re)$ for spherical particles and $O(ReSl)$ for particles of arbitrary shape, where Re is the number of Reynolds and Sl, is the number of Strouhal. We used the formalism of the hydrodynamic force (Lovalenti and Brady (1993b)) acting on a particle in the low Reynolds number regime to obtain the equations of motion of a particle under the action of an external force and study its dynamics under different test cases. The expression developed by Lovalenti and Brady (1993b) is a good approximation up to $O(Re)$ and $O(ReSl)$ for particles of arbitrary shape, where Re is the Reynolds number and Sl, is the Strouhal number. Once the force acting on a suspension is identified, the governing equations can be written easily using Newton's law of motion. The most important part is deriving a suitable expression for representing the hydrodynamic force acting on a particle as a function of the geometry of the particle. As pointed out earlier, the problem of determining the steady flow over fixed bodies in a slow and uniform flow of viscous incompressible fluid was initially considered by Stokes (1851). He has given a solution by neglecting inertia's effect by taking the zero Reynolds number. Subsequently, Whitehead (1889) has tried to improve this solution by obtaining higher-order approximations of the flow when the Reynolds number is not negligible. He has proposed the usage of a lower order approximation to calculate the inertial terms in the equation of motion, thus developing an iterative procedure. Since the boundary conditions at each iteration step are independent of the Reynolds number, this procedure is equivalent to assuming a flux expansion in powers of the Reynolds number. The hypothesis of a power expansion of the Reynolds number leads to a situation in which it is impossible to satisfy the boundary conditions of the problem in all the terms except the principal. This mathematical phenomenon is called the

"Whitehead paradox." Oseen (1910) resolved the paradox. When a body moves in a viscous Newtonian fluid encountering some resistance, examination of the flow of momentum over a large area surrounding the body shows that the magnitude of the disturbance of the flow becomes zero only in the region of magnitude approximately inverse to the square of the distance to the body. Oseen (1910; 1913) calculated the first correction of the Stokes resistance for small but finite values of the Reynolds number for a sphere. He has realized that the transport properties near the particle are described by Stokes' equations, whereas Oseen's equations are adequate to describe the properties far from the particle. Oseen's equations are:

$$-\boldsymbol{\nabla} p + \mu \nabla^2 \mathbf{u} - \rho \boldsymbol{U} \cdot \boldsymbol{\nabla} \mathbf{u} = 0 \tag{1.1a}$$

$$\boldsymbol{\nabla} \cdot \mathbf{u} = 0 \tag{1.1b}$$

where $\mathbf{u}$ is the velocity vector, p is the pressure, ρ is the fluid density, and μ is the viscosity of the fluid. Oseen constructed a uniformly valid leading-order approximation to the flow field that satisfies (1.1a) and (1.1b) everywhere and obtained the hydrodynamic force, $\mathbf{F}^{\mathrm{H}}_{Os}$ expression due to Oseen as

$$\mathbf{F}^{\mathrm{H}}_{Os} = 6\pi\mu a \boldsymbol{U} \left(1 + \frac{3}{8} Re\right) \tag{1.2}$$

where ρ and μ are density and viscosity of fluid respectively, $Re = a|\boldsymbol{U}|/\nu$ is the Reynolds number, here ν is kinematic viscosity defined as μ/ρ, $\boldsymbol{U}$ is velocity of sphere, and a is radius of the sphere, . Although this result for the force is correct, Oseen has not computed the velocity field accurately to $O(Re)$. Goldstein (1929) has obtained a basic solution using the Oseen technique. Later, Lagerstrom and Cole (1955) solved Oseen's equations to obtain higher-order flow approximations in two and three-dimensional cases. Proudman and Pearson (1957) described

in detail an alternative procedure which involved simultaneous consideration of locally valid (in general) expansions. Lovalenti and Brady (1993b) have summarized the literature before 1993 and also have derived an approximate expression for the hydrodynamic force acting on an arbitrary rigid particle translating with the time-dependent motion in a uniform time-dependent flow field, including the effects of both unsteady and convective inertia at low Reynolds numbers. Vojir and Michaelides (1994) have published a study on the impact of Basset memory term on the dynamics of a solid sphere in a viscous fluid. Lawrence and Weinbaum (1988) have explored the Navier-Stokes equations in linear form to obtain expressions for the force acting on an arbitrary body. They have deduced the results for a slightly eccentric spheroid. They also developed an expression for hydrodynamic force containing the four terms, namely Stokes drag, added mass, Basset force, and a new memory term due to the non-spherical shape of the particle, where the decay of the new memory term is faster than that of Basset force at a long time.

The study of dynamics and rheology of suspension of periodically forced particles in a Newtonian fluid was initiated by Ramamohan and co-workers (Ramamohan et al. (1994)). Their initial work focused on sheared suspension at negligible Reynolds numbers. They have opened up a new class of problems by analyzing the effects of external periodic force fields on the dynamics of micro-scale particles in simple shear flow (Kumar et al. 1995; 1996; Kumar and Ramamohan 1998; Radhakrishnan 1999). They have pioneered the area of chaos in periodically forced suspensions of particles in simple shear flow, and the results are reported in several articles (Ramamohan et al. (1994); Kumar et al. (1996); Radhakrishnan and Ramamohan (2004)). The effect of an external periodic force on the dynamics and rheology of slender rods in a sheared Newtonian fluid has been studied at zero Reynolds number by Kumar and Ramamohan (1995) and Radhakrishnan and Ramamohan (2004). Kumar et al. (1995) have demonstrated the existence of chaos in the dynamics of periodically forced bodies of spheroids moving in a simple

shear flow within the limit of weak Brownian motion. They have reported chaotic dynamics in certain parametric regions with the strong migration dependence of particles on their shape. This strong dependence of spheroid dynamics on the particle aspect ratio is proposed as a potential application for particle separation from fluid suspension, which is essential for the characterization of fluid suspensions used in industries. Kumar and Ramamohan (1997) have also reported a new Class I intermittency near a tangent bifurcation in the dynamics of a periodically forced spheroid suspended in simple shear flow in the limit of weak Brownian motion. A review of the work carried out over a decade on the dynamics and rheology of suspensions of orientable particles in simple shear flow subject to an external periodic force has been published Asokan et al. (2005).

The effect of the eccentricity and the viscosity ratio on the oscillations of solid and gaseous spheroids is investigated byAbbad et al. (2006). The properties of a one-dimensional transport along the major axis of a spheroid suspended in a quiescent fluid under an external periodic force at a very low but non-zero Reynolds number are also reported by Madhukar et al. (2010). They also proposed a technique for separating particles from a fluid based on its dynamic dependence on the shape of the particle. Magnaudet (2011) has derived different versions of the reciprocal theorem presenting the expression of force exerted on an arbitrarily shaped particle translating into an incompressible flow at a given Reynolds number. An analytical investigation of the effects of fluid and particle inertia on the dynamics of axisymmetric spheroids in a simple shear fluid has been reported in the limit of a small Reynolds number and Stokes numbers by Dabade et al. (2016). Recently Marath and Subramanian (2018a) have demonstrated the effect of fluid and particle inertia on the dynamics of spheroid orientation in a planner-linear flow.

From the above research review, we have observed that a lot of research has been done on the suspension of particles in a Newtonian fluid for $Re << 1$, mainly spherical particles. Few researchers have investigated the dynamics of the suspen-

sion of non-spherical particles either in simple shear flow or in a quiescent fluid field. Even then, there are several gaps to investigate the dynamics of suspension of particles in low Reynolds numbers limit. We aim to investigate the dynamics of the spheroid suspended under the action of periodic force in a variety of fluid fields in which we try to characterize the oscillation properties of particles at low Reynolds numbers. The preliminaries and the expression required for deriving the governing equations and for analyzing the numerical solution are explained in the subsequent sessions. The results obtained in the case of the quiescent flow field motivate us to study the suspension behavior in different flows. The derivations, analysis, and results obtained are explained in the subsequent chapters. It is assumed in this analysis that the suspended particles are rigid solids having the geometry of a spheroid in order to avoid complexity. This assumption is rationale in many cases since any body of arbitrary shape can be approximated as a spheroid.

1.3 Governing equations and scaling procedure

In this thesis, we consider a periodically forced spheroid in an infinite body of Newtonian fluid of different velocity profiles and study the effect of an external periodic force acting on the spheroid along the direction of the displacement of the spheroid. Let $\mathbf{F}^{\text{ext}}(t)$ denote the external force acting on the fluid at the time, t, and hence the total force applied on the particle is $\mathbf{F}^{\text{H}}(t) + \mathbf{F}^{\text{ext}}(t)$, where $\mathbf{F}^{\text{H}}(t)$ denotes the effective hydrodynamic force acting on the particle.

In view of Newton's law of motion, the equation of motion for neutrally buoyant particle under the effect of a periodic external force immersed in a Newtonian fluid is given by

$$m_p \frac{d\boldsymbol{u}_p(t)}{dt} = \mathbf{F}^{\text{ext}}(t) + \mathbf{F}^{\text{H}}(t) \tag{1.3}$$

where m_p is the mass of suspended particle of density ρ_p, $\mathbf{F}^{\text{ext}}(t)(= R_F \sin(\omega t))$ is an external periodic force with frequency ω applied on the particle, $\boldsymbol{u}_p(t)$ is the particle velocity, and $\mathbf{F}^{\text{H}}(t)$ is hydrodynamic force induced on the particle. In dimensionless form the above equations reduces to

$$\frac{m_p \dot{\boldsymbol{u}}_p(t)}{\mu a^2 \omega} = \mathbf{F}^{\text{H}}(t) + \mathbf{F}^{\text{ext}}(t), \tag{1.4a}$$

along with

$$\frac{d\mathbf{y}_p(t)}{dt} = \boldsymbol{u}_p(t) \tag{1.4b}$$

where $\mathbf{y}_p(t)$ is the displacement vector of the particle at time, 't'. Particle dynamics can be described by the above equations, once the expression for the hydrodynamics is known. Since it mainly depends on the geometry of the particle, finding the expressions for a body of arbitrary shape is very difficult. But many suspension can be approximated as suspensions of spheroids if aspect ratio having varying from 0 to ∞. Expression for the hydrodynamics as a function of geometry for arbitrary spheroids is available in the literature(Lawrence and Weinbaum 1986; 1988; Abbad et al. 2006).

All terms of forces and pressure terms are non-dimensionalized by $\mu a U_c$ and $\mu U_c/a$, respectively, where a, U_c, and τ are the characteristic particle length, speed, and time. The Reynolds number at the particle scale is (Guazzelli and Morris 2012; Happel and Brenner 2012) which measures inertial effects compared to viscous effects in the Navier-Stokes equation is given by

$$Re = a U_c \rho/\mu \sim \left| \frac{\rho \left(\mathbf{u} \cdot \boldsymbol{\nabla}\right) \mathbf{u}}{\mu \boldsymbol{\nabla}^2 \mathbf{u}} \right|. \tag{1.5}$$

For suspensions, recall that we are usually interested in particles of small length scales, typically between 10^{-2} and $10^2 \mu m$.

The Strouhal number represents the ratio of inertial forces due to the local

acceleration of the flow to the inertial forces due to the convective acceleration. One can define a Strouhal number as(Guazzelli and Morris 2012; Happel and Brenner 2012)

$$Sl = \frac{a}{U_c \tau} \sim \left| \frac{\partial \mathbf{u}/\partial t}{(\mathbf{u} \cdot \boldsymbol{\nabla})\,\mathbf{u}} \right|, \tag{1.6}$$

which is a measure of unsteadiness, corresponding to the convective time a/U_c.

1.4 Particle suspension and Lorentz reciprocal theorem

There is no entirely satisfactory method available to correlate resistance on irregular particles. Settlement behavior has been associated with most of the widely used shape factors. A few simple general results often lead to valuable estimates of arbitrary particle resistance or sedimentation rate for creeping flow. Compared to smooth edges, sharp edges have little effect on drag, while all the most essential features remain unchanged. Also, most particle suspension can be roughly approximated to spheres or spheroids of aspect ratio varying from 0 to ∞. For a slightly deformed sphere, the mean resistance $\bar{c}$ is equal to that of the sphere of the same volume (Happel and Brenner (2012)).

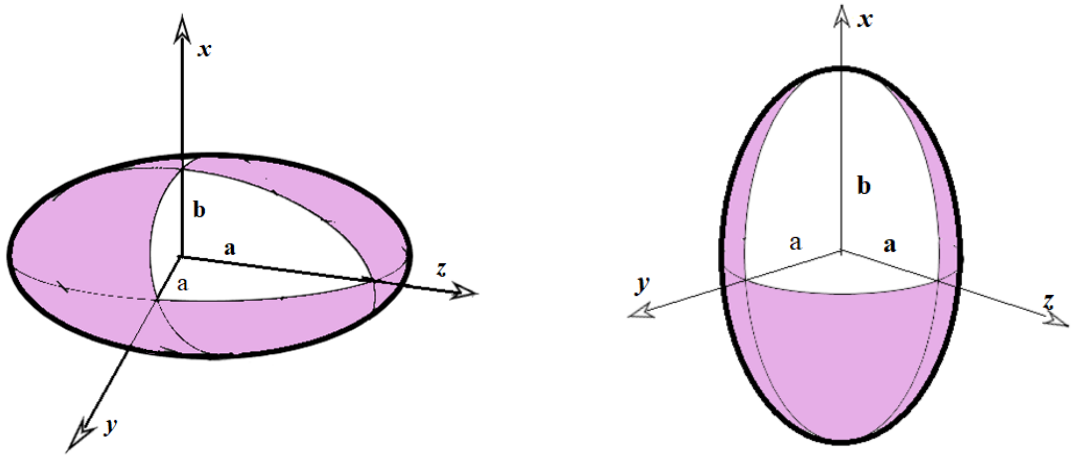

Figure 1.1: The assignment of semi-axes on a spheroid. It is oblate if $b < a$ (left) and prolate if $b > a$ (right). (Schematic)

However, medium resistance is essential and should be used cautiously because even a slight skew in shape will cause a particle to assume a preferred orientation (McNown and Malaika (1950)). Hill and Power (1956) have shown that the Stokes resistance on an arbitrary particle is less than or equal to that of an enclosing body and greater than or equal to that of a body containing it. A judicious choice of circumscribed and inscribed bodies can give strict limits to resistance or settling velocity. Weinberger (1972) showed that the sphere has the highest Stokes resistance settling mean velocity for all bodies of a given volume. Keller et al. (1967) showed that the creeping solutions always underestimate the resistance to *Re* other than zero. Generalization of the results may be possible by considering particles of arbitrary shape. We consider spheroids for the analysis, which are more common than spherical suspensions. The dynamics of spheroidal particles can be analyzed analytically in many cases, and their effect can be studied for shapes ranging from slightly distorted spheres to disks and needles.

Micro-particles and self-propelled particles move and interact in viscous fluid fields. Stokes's flow long-range behavior suggests that hydrodynamic force induced on micro-particle significantly affects particle dynamics and hence affects

rheological parameters. Examples of this are collective dynamics of suspensions, the circular motion of swimmers near boundaries, attraction to surfaces, synchronization of cilia and flagella, interactions, and scattering of pairs of swimmers. The difficulty in determining hydrodynamic force on suspended particles comes because the motion of the particles constitutes boundary conditions. There is an approach to assess the movement of a single particle and hence bypasses the need to calculate the full hydrodynamics. This knowledge has become a standard tool in determining the force.

*The **reciprocal theorem**(Lovalenti and Brady 1993b; Guazzelli and Morris 2012) allows one to determine results for one Stokes flow field based upon the solution of another Stokes flow in the same geometry, i.e., having the same boundaries but for different boundary conditions.* This theorem allows us to approximate the expression for the hydrodynamic force to certain cases in which at least some part of the boundary is a particle surface, allowing us to determine properties of one flow about the body based upon another known solution. Let us consider $(\mathbf{u}, \boldsymbol{\sigma})$ and $(\bar{\boldsymbol{u}}, \bar{\boldsymbol{\sigma}})$ the velocity and stress fields of two Stokes flows which are driven respectively by the external forces $\boldsymbol{f}$ and $\bar{\boldsymbol{f}}$ and by the boundary conditions $\mathbf{u} = \boldsymbol{U}$ and $\bar{\mathbf{u}} = \bar{\boldsymbol{U}}$ on the surface S bounding the fluid volume V . The general form of the theorem is given by

$$\int_V \boldsymbol{f} \cdot \bar{\mathbf{u}} dV + \int_S \bar{\mathbf{u}} \cdot \boldsymbol{\sigma} \cdot \boldsymbol{n} = \int_V \bar{\boldsymbol{f}} \cdot \mathbf{u} dV + \int_S \mathbf{u} \cdot \bar{\boldsymbol{\sigma}} \cdot \boldsymbol{n} \tag{1.7}$$

Lovalenti and Brady (1993b) have used the above reciprocal theorem to compute the hydrodynamic force induced on an arbitrarily shaped particle having arbitrary time-dependent velocity in a time-dependent flowing fluid at low Reynolds numbers, as discussed in the next section.

1.5 Hydrodynamic forces

In 2006, Abbad et al. (2006) have developed an one dimensional expression for the effective hydrodynamic force $\mathrm{F}^{\mathrm{H}}(t)$ due to the perturbed quasi-steady drag force, the added mass force, the Basset memory integral term and the new history force caused by the eccentricity of the spheroid undergoing an arbitrary time dependent motion in the limiting case of low Reynolds number (i.e. $R_e << 1$) in the form,

$$\begin{aligned}\mathrm{F}^{\mathrm{H}}(t) =& 6\pi\mu a\left(1+\frac{4}{5}\epsilon+\frac{2}{175}\epsilon^2\right)U(t)\\ &+\frac{2}{3}\rho\pi a^3\left(1+\frac{16}{5}\epsilon+\frac{604}{175}\epsilon^2\right)\dot{U}(t)\\ &+6\sqrt{\pi}\mu a\left(1+\frac{8}{5}\epsilon+\frac{116}{175}\epsilon^2\right)\int_{-\infty}^{t}\frac{\dot{U}(t)d\tau}{\sqrt{\frac{t-\tau}{\tau_0}}}\\ &+\frac{8}{175}\pi\mu a\epsilon^2\int_{-\infty}^{t}\dot{U}(\tau)G(t-\tau)d\tau+O(\epsilon^3),\end{aligned} \tag{1.8}$$

with

$$\begin{aligned}G(t) =& \Im\left[\sqrt{\frac{w}{3}}\ exp(wt/\tau_0)\ erfc(\sqrt{wt/\tau_0})\right],\\ w =& \frac{3}{2}\left(1+\sqrt{3}\ i\right),\end{aligned} \tag{1.9}$$

and

$$O(\epsilon) << 1.$$

Where $U(t)$ is the velocity of the suspended particle at time t with $U(t) = 0$ for $t \leq 0$ and, μ and ρ are the dynamic viscosity and the density of the ambient fluid respectively. Also, $\dot{U}(t) = \frac{dU}{dt}$ is the particle acceleration, $\tau_0 = a^2/\nu$ is the diffusive time scale and $\nu = \mu/\rho$ is the kinematic viscosity of the fluid, a is characteristic length of the particle, and $\Im$ denotes the imaginary part of considered complex variable. The parameter ϵ denotes the geometrical variation of the particle from a sphere, and the kernel, $G(t)$ is defined as the imaginary part of the corresponding

complex variable.

Lawrence and Weinbaum (1988) have developed a complex formulation for the axisymmetric motion of spheroid to compute the unsteady Stokes field. The expression for the hydrodynamic force, $\mathbf{F}^{\mathrm{H}}(t)$ exerted at time t on an arbitrary particle suspended in a time dependent fluid motion with velocity, $\mathbf{u}_p(t)$ has been derived by Lawrence and Weinbaum (1988) as

$$\begin{aligned}\mathbf{F}^{\mathrm{H}}(t) = &- \mathbf{F}_s \cdot \mathbf{u}_p(t) - \pi^{-1/2}\mathbf{B} \cdot \int_0^t \frac{d\mathbf{u}_p}{d\tau}\,(t-\tau)^{-1/2}\,d\tau - \mathrm{m}_a\frac{d\mathbf{u}_p}{dt} - \\ &e\,(\mathbf{F}_1 - \boldsymbol{B}) \cdot \int_0^t \frac{d\mathbf{u}_p}{d\tau}\,\mathrm{erfc}\left[(t-\tau)^{1/2}\right] d\tau,\end{aligned} \tag{1.10}$$

where m_a is the dimensionless scaled added mass, $\mathbf{F}_s = 6\pi\mu a\boldsymbol{\Phi}$ is the Stokes drag correction factor, μ is the dynamic viscosity of the fluid, $\boldsymbol{\Phi}$ is the frictional resistance tensor of the particle. $\mathbf{F}_1$, defined as $\mathbf{a}\cdot\mathbf{a}$, is tensorial coefficient, and $\mathbf{B}$ is Basset force coefficient. Both $\mathbf{F}_1$ and $\mathbf{B}$ are depends on the shape of the particle and For the perturbed sphere both are identical order up to $O(\epsilon^2)$, where ϵ is sphericity of the deformed sphere.

Later on, Lovalenti and Brady (1993b) obtained the expression for the required hydrodynamic force on an arbitrarily shaped particle in the time-dependent fluid within the long time limit. They have used the reciprocal theorem coupled with Fourier transform in order to drive the following expression for the hydrodynamic force on an arbitrary shaped particle (for more details see Lovalenti and Brady 1993b):

$$\begin{aligned}\mathbf{F}^{\mathrm{H}} =& ReSl\tilde{V}_p\dot{\boldsymbol{u}}_\infty + \mathbf{F}_s^{\mathrm{H}} - ReSl\left\{6\pi\boldsymbol{\Phi}\cdot\boldsymbol{\Phi}\cdot\boldsymbol{\Phi} + \lim_{R\to\infty}\left(\int_{V_f(R)}\mathbf{M}^T\cdot\mathbf{M}\,dV - \frac{9}{2}\boldsymbol{\Phi}\cdot\boldsymbol{\Phi}R\right)\right\}\cdot\dot{\boldsymbol{u}}_s(t) \\ &+\frac{3}{8}\left(\frac{ReSl}{\pi}\right)^{\frac{1}{2}}\left\{\int_{-\infty}^{t}\left[\frac{2}{3}\mathbf{F}_s^{\mathrm{H}\parallel}(t) - \left\{\frac{1}{|\boldsymbol{A}|^2}\left(\frac{\pi^{\frac{1}{2}}}{2|\boldsymbol{A}|}\,\mathrm{erf}(|\boldsymbol{A}|) - \exp(-|\boldsymbol{A}|^2)\right)\right\}\mathbf{F}_s^{\mathrm{H}\parallel}(s)\right.\right. \\ &\left.\left.+\frac{2}{3}\mathbf{F}_t^{\mathrm{H}\perp} - \left\{\exp(-|\boldsymbol{A}|^2) - \frac{1}{2|\boldsymbol{A}|^2}\left(\frac{\pi^{\frac{1}{2}}}{2|\boldsymbol{A}|}\,\mathrm{erf}(|\boldsymbol{A}|) - \exp(-|\boldsymbol{A}|^2)\right)\right\}\mathbf{F}_s^{\mathrm{H}\perp}(s)\right]\frac{2ds}{(t-s)^{\frac{1}{2}}}\right\}\cdot\boldsymbol{\Phi} \\ &- Re\lim_{R\to\infty}\int_{V_f(R)}(\mathbf{u}_0\cdot\boldsymbol{\nabla}\mathbf{u}_0 - \boldsymbol{u}_s(t)\cdot\boldsymbol{\nabla}\mathbf{u}_0)\cdot\mathbf{M}\,dV + o(ReSl) + o(Re)\end{aligned} \tag{1.11}$$

In the above expression (1.11), *Re* represents the Reynolds number indicating the magnitude of the convective inertia related to viscous force, a is the characteristic size of the particle, and *Sl* denotes the Strouhal number, which will be reduced to unity in this dissertation. $\mathbf{M}$ is the second rank tensor, which is a function of the position of the particle and is defined by the condition that $\mathbf{M} \cdot \mathbf{u}_s$ is the Stokes velocity field for the particle translating with velocity $\mathbf{u}_p$ in a stationary fluid. $\mathbf{u}_\infty$ is the velocity of the fluid far from the particle, $\mathbf{\Phi}$ is the Stokes resistance tensor in dimensionless form, $\mathrm{V}_f(R)$ is the volume of fluid surrounding the particle and bounded by a spherical surface of radius R. $\mathbf{u}_s(t) = \mathbf{u}_p(t) - \mathbf{u}_\infty(t)$ is the slip velocity of the particle and $\mathbf{u}_0$ is the velocity induced by the translation of the suspended particle. We also note that the expression is derived from ordering *Re* and *ReSl*. The product *ReSl* measures the relative magnitude of the unsteady inertia of the fluid. The first term of this expression is due to an accelerating reference frame, the second is the pseudo-steady Stokes drag, and the third has been labeled as the acceleration reaction. The fourth term represents the unsteady Oseen correction to the hydrodynamic force. A new history integral replaces the Basset history force at a finite Reynolds number in the long time limit. The last term of this expression can only contribute a force perpendicular to the slip velocity of the particle. To use this expression for a given particle, we only require the steady Stokes drag and the corresponding steady Stokes velocity field created by the translating particle.

Particles subject to Brownian motion tend to adopt random orientations and do not follow the rules. In general, the drag and torque on an arbitrary particle translating and rotating in unbounded fluids are determined by three second-order tensors, which depend on the shape of the body:

(i) A symmetric translation tensor describes the resistance to translational motion.

(ii) A symmetric rotation tensor gives the torques resulting from rotation.

(iii) An asymmetric coupling tensor defines torques resulting from translation and drag forces resulting from rotation.

The use of these resistance tensors has been developed in detail by Happel and Brenner (2012). While enabling the compact formulation of fundamental problems, these tensors have limited application since their components are rarely available, even for simple shapes. Here we discuss specific cases of particle shape without recourse to tensor notation, but some conclusions from the available treatment are of interest. Because the translation tensor is symmetric, it follows that every particle possesses at least three mutually perpendicular axes such that, if the particle is translating without rotation parallel to one of these axes, the total drag force is also parallel to the axis(Happel and Brenner 2012). These axes are usually called principal axes of translation. For an orthotropic particle, the principal axes are normal to the planes of symmetry. For an axisymmetric particle, the axis of symmetry is one of the principal axes. As the name suggests, the Stokes resistance tensor is an opposing force to the particle's motion. The computation of the velocity field for irregular shape is not easy. Lawrence and Weinbaum (1988) have obtained an complex formulation for the axisymmetric motion of a spheroid to compute the unsteady Stokes field. However one can use the concept of the Reciprocal theorem and the idea of a uniformly valid velocity field (see section Lovalenti and Brady (1993b)) to find the unsteady Stokes correction to the pseudo-steady Stokes drag, where $ReSl << 1$. In this dissertation we consider the prolate spheroid as a first example, the polar diameter is greater than the equatorial diameter and the equation describing a prolate spheroid is given by

$$\frac{x^2}{a^2} + \frac{y^2}{b^2} + \frac{z^2}{b^2} = 1 \tag{1.12}$$

where a is the semi-major axis and b is the semi-minor axis and (x, y, z) represent the arbitrary poin on the spheroid. The dimensionless form of Stokes resistance tensor ($\mathbf{\Phi}$) for a prolate spheroid is given by $\mathbf{\Phi} = 8e/3\mathbf{a}$ where e is the eccentricity of the spheroid and $\mathbf{a}$ is a diagonal matrix (Chwang and Wu 1975; Chwang 1975;

Pozrikidis 1992) given by

$$a_{11} = \frac{e^2}{-2e + (1+e^2)\log\left(\frac{1+e}{1-e}\right)}, \quad a_{22} = a_{33} = \frac{-2e^2}{-2e + (1-3e^2)\log\left(\frac{1+e}{1-e}\right)} \tag{1.13}$$

and the 1-axis is aligned with the major axis of the spheroid. As $e \to 0$, $a_{11}, a_{22}, a_{33} \to (3/8)e$, yielding the results for the sphere (Pozrikidis 1992). It will be noted that both the Stokeslets and the potential dipoles in (1.13) are oriented in the direction of translation.

Chwang (1975) showed that the flow produced by the translation of a prolate spheroid may be represented in terms of a distribution of Stokes-lets and potential dipoles over the focal length of the spheroid with constant and parabolic densities respectively. The equations for the fluid velocity field due to the translation of prolate spheroid are given by (Pozrikidis 1992)

$$u_i(\mathbf{x}) = v_k a_{kj} \int_{-c}^{c} \left[G_{ij}(\mathbf{x}, \mathbf{x}_0) - \left(\frac{1-e^2}{2e^2} \right) \left(c^2 - x_0^2 \right) D_{ij}(\mathbf{x}, \mathbf{x}_0) \right] dx_0 \tag{1.14}$$

where e is the eccentricity of the spheroid, defined as $e = c/a$, $0 < e < 1$, where c is the focal length of the spheroid, defined by $c^2 = a^2 - b^2$, and a and b are the major and minor axes of the spheroid, and $\mathbf{x}_0$ is the arbitrary pole (source point) of the spheroid and $\mathbf{x}$ is the observation (field) point. v_k is the velocity of the particle in the k^{th} direction and $\mathbf{a}$ is the diagonal matrix given in (1.13).

The Stokeslet $G_{ij}(\mathbf{x}, \mathbf{x}_0)$ and the potential doublet $D_{ij}(\mathbf{x}, \mathbf{x}_0)$ are given by

$$G_{ij} = \frac{\delta_{ij}}{|\mathbf{X}-\mathbf{X}_0|} + \frac{(\mathbf{X}-\mathbf{X}_0)_i (\mathbf{X}-\mathbf{X}_0)_j}{|\mathbf{X}-\mathbf{X}_0|^3} \tag{1.15}$$

$$D_{ij} = \frac{\delta_{ij}}{|\mathbf{X}-\mathbf{X}_0|^3} - \frac{3(\mathbf{X}-\mathbf{X}_0)_i (\mathbf{X}-\mathbf{X}_0)_j}{|\mathbf{X}-\mathbf{X}_0|^5} \tag{1.16}$$

We obtain singularity representations in forms by expressing the couplet, and the potential dipole in (1.14) and (1.13) in terms of the Green's function are suitable for producing the Faxen relations for the force and torque. We consider

the the force equation (1.11) given by Lovalenti and Brady (1993b) and deduce it to a spheroid undergoing time dependent motion at low Reynolds and Strouhal numbers. In their expression,

$$\mathbf{F}_s^{\mathrm{H}\parallel} = 6\pi \mathbf{u}_s \cdot \mathbf{pp} \qquad \text{and } \mathbf{F}_s^{\mathrm{H}\perp} = 6\pi \mathbf{u}_s \cdot (\boldsymbol{\delta} - \mathbf{pp}) \tag{1.17}$$

where $\boldsymbol{\delta}$ is the idem tensor of order 2 and $\mathbf{p}$ is a unit vector given by

$$\mathbf{p} = \frac{\mathbf{y}_s(t) - \mathbf{y}_s(s)}{|\mathbf{y}_s(t) - \mathbf{y}_s(s)|} \tag{1.18}$$

where $\mathbf{y}_s(t) - \mathbf{y}_s(s)$ is the integrated displacement of the particle relative to the fluid from time s to the current time t and $\mathbf{A}$ is given by the expression,

$$\mathbf{A} = \frac{Re}{2} \left(\frac{t-s}{ReSl}\right)^{\frac{1}{2}} \left(\frac{\mathbf{y}_s(t) - \mathbf{y}_s(s)}{t-s}\right) \tag{1.19}$$

we assume that the velocity of the particle $\mathbf{u}_p = (u_p, v_p, w_p)$ exerted by the fluid on the particle is in the direction of vector $\mathbf{A}$, which itself is parallel to the displacement vector $\mathbf{y}_s(t) - \mathbf{y}_s(s)$ as defined earlier. The Stokes resistance tensor is $6\pi\boldsymbol{\Phi}$ and hence the hydrodynamic force, referred to the pseudo-steady state drag force, acting on the suspended particle translating with slip velocity $\mathbf{u}_s\,(= (u_s, v_s, w_s))$ is given by $\mathbf{F}_s^{\mathrm{H}}(t) = -6\pi\boldsymbol{\Phi} \cdot \mathbf{u}_s(t)$.

The second term $\mathbf{F}_s^{\mathrm{H}}(t)$ in the expression (1.11) can be decomposed into two components parallel $\mathbf{F}_s^{\mathrm{H}\parallel}(t)$ and perpendicular $\mathbf{F}_s^{\mathrm{H}\perp}(t)$ to the vector $\mathbf{A}$.

$$\begin{aligned} \mathbf{F}_s^{\mathrm{H}\parallel}(t) &= -\,6\pi\,(\boldsymbol{\Phi} \cdot \mathbf{u}_s(t)) \\ &= -\,16\pi e\,(e_1 u_s, e_2 v_s, e_2 w_z) \end{aligned} \tag{1.20}$$

and

$$\mathbf{F}_s^{\mathrm{H}\perp} = (0, 0, 0) \tag{1.21}$$

The acceleration reaction term is given by the third term on the right hand side of the hydrodynamic force equation(1.11). Here, we need to investigate the expression given below, which appears in the force equation, over the volume of the fluid surrounding the particle.

$$\int_{V_f(R)} \mathbf{M}^T \cdot \mathbf{M} \tag{1.22}$$

where $\mathbf{M}$ is defined such that $u_i = \mathrm{M}_{ij} v_j$. The above integral diverges as R (the radius of the fluid sphere considered), goes to infinity. However, we find that the following expression converges to a finite value as R tends to infinity.

$$\lim_{R\to\infty} \int_{V_f(R)} \mathbf{M}^T \cdot \mathbf{M} - \frac{9\pi}{2} \mathbf{\Phi} \cdot \mathbf{\Phi}. \tag{1.23}$$

Now from the previous equation (1.14), we can deduce the following

$$\mathbf{M} = (\mathbf{a} \cdot \mathbf{H})^T, \tag{1.24}$$

where,

$$\mathbf{H} = \int_{-c}^{c} \left[G_{ij}(\mathbf{x}, \mathbf{x}_0) - \left(\frac{1 - e^2}{2e^2} \right) \left(c^2 - x_0^2 \right) D_{ij}(\mathbf{x}, \mathbf{x}_0) \right] dx_0. \tag{1.25}$$

Suitable equations were derived for $\mathbf{M}$ and the integral can be performed numerically. The spherical coordinate system can be chosen to perform the integration. The reasons for the above choice are that we would accommodate a more significant number of data points, increasing the accuracy of the integral and easier handling of the integral and making it simpler to understand, and also, the results may make it easy to compare with the radius of the outer boundary. The following formula can be used to evaluate the integral, called the summation approach

of the integration.

$$\int_V f(r,\phi,\theta)r^2\sin(\theta)drd\theta d\phi = \Delta r\Delta\phi\Delta\theta\sum_i\sum_j\sum_k f(r_i,\theta_j,\phi_k)r_i^2\sin(\theta_j). \quad (1.26)$$

The principal components of the 3^{rd} order diagonal matrix representing the acceleration reaction term thus obtain are denoted by $Diag\left(\mathrm{I}_{xx},\mathrm{I}_{yy},\mathrm{I}_{zz}\right)$. Hence the third term of the force(1.11) is given by

$$\begin{aligned}\lim_{R\to\infty}\int_{V_f(R)}\mathbf{M}^T\cdot\mathbf{M}-\frac{9\pi}{2}\mathbf{\Phi}\cdot\mathbf{\Phi} =& ReSlDiag\left(\mathrm{I}_{xx},\mathrm{I}_{yy},\mathrm{I}_{zz}\right)\cdot\dot{\boldsymbol{u}}_s(t)\\ =& ReSlDiag\left(\mathrm{I}_{xx}\dot{u}_s,\mathrm{I}_{yy}\dot{v}_s,\mathrm{I}_{zz}\dot{w}_s\right) \quad (1.27)\end{aligned}$$

The new history integral term in the long time limit at finite Re is the fourth term in the expression of the hydrodynamic force equation (1.11) and given by

$$\begin{aligned}\boldsymbol{T_{nhi}} =& \frac{3}{8}\left(\frac{ReSl}{\pi}\right)^{\frac{1}{2}}\left[\int_{-\infty}^{t}\left\{\frac{2}{3}\mathbf{F}_s^{\mathrm{H}\parallel}(t)-\left[\frac{1}{|\mathbf{A}|^2}\left(\frac{\pi^{\frac{1}{2}}}{2|\mathbf{A}|}\operatorname{erf}(|\mathbf{A}|)-\exp(-|\mathbf{A}|^2)\right)\right]\right.\right.\\ &\left.\mathbf{F}_s^{\mathrm{H}\parallel}(s)+\frac{2}{3}\mathbf{F}_s^{\mathrm{H}\perp}(t)-\left[\exp(-|\mathbf{A}|^2)-\frac{1}{2|\mathbf{A}|^2}\left(\frac{\pi^{\frac{1}{2}}}{2|\mathbf{A}|}\operatorname{erf}(|\mathbf{A}|)-\exp(-|\mathbf{A}|^2)\right)\right]\right.\\ &\left.\left.\mathbf{F}_s^{H\perp}(s)\right\}\frac{2ds}{(t-s)^{\frac{3}{2}}}\right]\cdot\mathbf{\Phi}\\ =&\frac{3}{8}\left(\frac{ReSl}{\pi}\right)^{\frac{1}{2}}\left[\int_{-\infty}^{t}\left\{\frac{2}{3}\times-16\pi e\left(e_1u_s(t),e_2v_s(t),e_2w_s(t)\right)-\right.\right.\\ &\left.\left.B\times-16\pi e\left(e_1u_x(t),e_2u_y(t),e_2u_z(t)\right)\right\}\frac{2ds}{(t-s)^{\frac{3}{2}}}\right]\cdot\mathbf{\Phi}\\ =&\frac{3}{8}\left(\frac{ReSl}{\pi}\right)^{\frac{1}{2}}\left[\int_{0}^{t}\left\{-\frac{32}{3}\times\pi e\times\frac{8e}{3}\left(e_1^2u_s(t),e_2^2v_s(t),e_2^2w_s(t)\right)+\right.\right.\\ &\left.\left.B\times16\pi\frac{8e}{3}e\left(e_1^2u_x(t),e_2^2u_y(t),e_3^2u_z(t)\right)\right\}\frac{2ds}{(t-s)^{\frac{3}{2}}}\right]\\ =&\frac{3}{8}\left(\frac{ReSl}{\pi}\right)^{\frac{1}{2}}\int_{0}^{t}\left\{-\frac{256}{9}\times\pi e^2\times\left(e_1^2u_s(t),e_2^2v_s(t),e_2^2w_s(t)\right)+\right.\end{aligned}$$

$$\frac{128}{3}\pi e^2 B\left(e_1^2 u_x(t), e_2^2 u_y(t), e_3^2 u_z(t)\right)\Big\}\frac{2ds}{(t-s)^{\frac{3}{2}}}, \tag{1.28}$$

where,

$$B = \frac{1}{|\mathbf{A}|^2}\left(\frac{\pi^{\frac{1}{2}}}{2|\mathbf{A}|}\operatorname{erf}(|\mathbf{A}|) - \exp(-|\mathbf{A}|^2)\right)$$

and

$$\mathbf{F}_s^{\mathrm{H}\perp}(s) = \mathbf{0}$$

From the above expression (1.28) of $\boldsymbol{T_{nhi}}$, we can see that there is a singularity at $s = t$. In order to avoid the singularity at $s = t$, we split the history integral term into two over the intervals $[0, t-\epsilon]$ and $[t-\epsilon, t]$, where ϵ is arbitrary. Introducing this, we obtained the integral over $[0, t-\epsilon]$ as,

$$\begin{aligned}\boldsymbol{T'_{nhi}} =& \frac{3}{8}\left(\frac{ReSl}{\pi}\right)^{\frac{1}{2}}\Big\{\frac{-512}{9}\pi e^2\left(e_1^2 u_s(t), e_2^2 v_s(t), e_2^2 w_s(t)\right)\left(t^{-\frac{1}{2}} - \epsilon^{-\frac{1}{2}}\right)\\ &+\frac{256}{3}\pi e^2 B\int_0^{t-\epsilon}\left(e_1^2 u_s(s), e_2^2 v_s(s), e_2^2 w_s(s)\right)\frac{ds}{(t-s)^{\frac{3}{2}}}\Big\}\\ =& \frac{3}{8}\left(\frac{ReSl}{\pi}\right)^{\frac{1}{2}}\Big\{\frac{1024}{9}\pi e^2\left(e_1^2 u_s(t), e_2^2 v_s(t), e_2^2 w_s(t)\right)\left(t^{-\frac{1}{2}} - \epsilon^{-\frac{1}{2}}\right)\\ &+\frac{256}{3}\pi e^2 B\int_0^{t-\epsilon}\left(e_1^2 u_s(s), e_2^2 v_s(s), e_2^2 w_s(s)\right)\frac{ds}{(t-s)^{\frac{3}{2}}}\Big\}\end{aligned} \tag{1.29}$$

Similarly, the integral over $[t-\epsilon, t]$ is given by

$$\begin{aligned}\boldsymbol{T''_{nhi}} =& \frac{3}{8}\left(\frac{ReSl}{\pi}\right)^{\frac{1}{2}}\Big\{\frac{1024}{9}\pi e^2\left(e_1^2 u_s(t), e_2^2 v_s(t), e_2^2 w_s(t)\right)\frac{1}{\epsilon^{-\frac{1}{2}}}\\ &+\frac{256}{3}\pi e^2 B\int_{t-\epsilon}^{t}\left(e_1^2 u_s(s), e_2^2 v_s(s), e_2^2 w_s(s)\right)\frac{ds}{(t-s)^{\frac{3}{2}}}\Big\}\end{aligned} \tag{1.30}$$

Note that the integral converges to a finite value in the limiting case of $s \to t$ and

hence the value of the integral in the range $[t-\epsilon, t]$ can be neglected by choosing ϵ very small. Hence new history integral term $\boldsymbol{T_{nhi}}$ is equal to $\boldsymbol{T'_{nhi}}$.

1.6 Computation of lift force term

The next task is the evaluation of the lift force, which is given the last term in the force expression. We need to integrate the following expression for getting the lift force term.

$$\lim_{R\to\infty} \int_{V_f(R)} (\mathbf{u}_0 \cdot \boldsymbol{\nabla}\mathbf{u}_0 - \mathbf{u}_s(t) \cdot \boldsymbol{\nabla}\mathbf{u}_0) \cdot \mathbf{M}. \tag{1.31}$$

In the above expression we the the expression for $\mathbf{M}$ given in equation (1.24). We have to find the expression for the $\mathbf{u}_0$ and $\mathbf{u}_s(t)$, $\mathbf{u}_s(t)$ is the slip velocity given by the expression,

$$\mathbf{u}_s(t) = \mathbf{u}_p(t) - \mathbf{u}_\infty(t).$$

By the definition of Stokes velocity, $\mathbf{u}_0 = \mathbf{M} \cdot \mathbf{u}_s(t)$. We note that the particle velocity is a function of time alone. Thus, there required expression for the lift force, say, the vector $\boldsymbol{L} = (L_1, L_2, L_3)$ can be evaluated as an integral. It can be found separately as a function of aspect ratio.

As shown in the expression for the hydrodynamic force, we derived expressions for and solved two integral terms, i.e. the acceleration reaction term and the lift force. We also described the derivations and the implementation of the strategy for solving the integral terms in the hydrodynamic force(1.11). Using these simplifications, we obtain the expression for the hydrodynamic force exerted by the

fluid on the spheroid as

$$\begin{aligned}\mathbf{F}^{\mathrm{H}}(t) =& ReSl\mathrm{V}_p\dot{\mathbf{u}}_\infty - 16\pi e\left(e_1, e_2, e_3\right)\cdot\mathbf{u}_s(t) - ReSl\left(I_{xx}, I_{yy}, I_{zz}\right)\cdot\dot{\mathbf{u}}_s(t) + \\ & \frac{3}{8}\left(\frac{ReSl}{\pi}\right)^{\frac{1}{2}}\left\{\frac{1024}{9}\pi e^2\left(e_1^2, e_2^2, e_3^2\right)\cdot\mathbf{u}_s(t)\left(t^{-\frac{1}{2}} - \epsilon^{-\frac{1}{2}}\right)\right. \\ & \left. + \frac{256}{3}\pi e^2\int_0^{t-\epsilon} B\left(e_1^2, e_2^2, e_3^2\right)\cdot\mathbf{u}_s(s)\frac{2ds}{(t-s)^{\frac{3}{2}}}\right\} - Re\left(L_1, L_2, L_3\right)\end{aligned} \tag{1.32}$$

1.7 Organization of the thesis

The organization of this dissertation is as follows. The fundamental concepts and preliminary results are explained in Chapter 1. Chapter 2 introduces the equations governing the dynamics of a periodically driven micro spheroid in an unsteady viscous fluid with low Reynolds numbers. Its oscillation properties in the presence/absence of memory forces are reported. The central part of the derivation is a perturbation analysis of the motion of a sphere. The calculated solutions correspond to those available in the literature in the limiting case of a sphere. The dependence of the solutions on the shape (k_a), the free oscillation frequency (ω_0), and the density ratio of the particulate fluid (κ) are calculated. The maximum amplitude of the oscillations of an oblate spheroid is greater than that of a prolate spheroid, demonstrating that the velocity disturbance for an oblate spheroid is greater in the presence/absence of memory strength. The increase in k_a leads to the increase (reduction) of the amplitude peaks in the case of the flattened spheroid (prolate) in the presence and more dominant in the absence of the force. There is also a reduction in the amplitude of many multiple spheroid oscillations due to memory force. Stronger oscillation variations are observed with the variation of ω_0 or κ compared to k_a. The variations of the phase value are similar for the two spheroids, like the variation of ω_0 and d_r. In contrast, they are inverted on the variable α. The linear scaling of the amplitude on α observed for spheroids can give an idea of physics, particularly regarding the quantum of

the velocity disturbances due to the size of the particles. The slopes are high in the absence and force, confirming that the presence of force strongly increases the resistance of the spheroid motion. The dependencies of the oscillations on the parameters can be used to separate the particles better or characterize the suspension. The novel ideas use in the problem and deriving analytical solutions help in developing software that tests for more complex and realistic systems and strike a good balance between complication and traceability.

Chapter 3 highlights the equation governing the dynamics of a solid micro spheroid periodically forced of moderate aspect ratio in a viscous fluid oscillating along with one of its damping actions; Basset's memory and the history-integral forces of the second stage are derivatives of a small Reynolds number. Determine the amplitude and phase of oscillations by focusing on when resonance occurs at the natural frequency of the particles. The amplitude becomes larger but does not deviate due to the quasi-steady Stokes friction. The effect of the aspect of ratio (k_a) of the particles, the density ratio of the particulate fluid (κ), and the natural frequency (ω_0) in the modification of conventional Q-curves are studied for prolate spheroids. Unlike other cases, the change in the Q-curves, especially the curve corresponding to the second force in history, is significantly more significant. We demonstrate qualitative changes in oscillations due to the impact of hydrodynamic forces. The effect of the additional history integral term on the translational characteristics of the forced spheroid of moderate aspect ratio was noted. Changes in amplitude are confirmed in the presence of other forces, whereas only the presence of Basset memory causes a phase shift of the oscillations, and the phase shift decreases as any parameter increases. The qualitative change observed in motion and Q-curves clarifies the role of memory forces concerning the amplitude and phase relationships of oscillations. Either way, the strength of the Basset memory reduces the resonance curves. The solutions are analytical to be helpful as experiments for more complex systems. Observations can be of practical importance when acoustic waves affect micro-particle transport.

Chapter 4 seeks a set of ordinary differential equations governing the migration of an arbitrarily forced spheroid in a low Reynolds number quiescent flow formulated and discussed, assuming a suspension sufficient diluted to neglect particle-particle interactions. The equations are nonlinear and contain a historical term of all past position and velocity and, therefore, impossible to solve symbolically. Spheroid transport is studied numerically by varying Reynolds numbers, particle aspect ratio, and external forces. Interestingly, the size of the attractor increases with increasing aspect ratio and/or force, whereas it decreases with increasing Reynolds number. This decrease is due to the increase in the inertia of the particles. There is a delay with the velocity at the maximum position, as shown by the respective time series. The delay could be that in the absence of inertia, when the velocity reaches its maximum, the position is at its minimum, and when the particle undergoes the maximum deviation, the velocity is at its minimum. Since the change in position is almost sinusoidal, the velocity will also be sinusoidal with a phase shift of almost $\pi/2$. The net migration of the particle is negligible and is expected to increase as the number increases. The inertia should significantly change this at values higher than the Reynolds number. The dependence of position and velocity on the parameters can be a potential application in particle separation.

Chapter 5 attempted to determine the dynamics of a prolate spheroid forcing periodically in a Newtonian fluid flow with a uniform time-dependent velocity at low Reynolds numbers. Inertial effects have been included to study the behavior more realistically. The numerical values of the acceleration reaction term for different aspect ratios have been presented. It is observed that these values decrease with an increase in the aspect ratio. The spheroid is seen to oscillate under periodic forcing. A preferred direction of movement is observed, and the spheroid shows a net displacement along that direction over time. The effect of the system variables is studied in detail, and we see that the increase in Re limits the particle's movement and, therefore, the attractor's size. By increasing the

amplitude of the periodic force, we see that the size of the attractor increases. The effect of the shape of the particles is studied by varying the aspect ratio. The size of the attractor increases with increasing aspect ratio due to weaker inertial effects. Detailed physical arguments supplemented the results, and, where possible, various tests were conducted to substantiate the results. The ultimate goal is rheology, which can be further achieved using the results of this article as this will determine the stress and strain behavior and determine the processing parameters for these suspensions. It is hoped that this work will stimulate further research in this area. Future work could address the non-uniform aspects of this movement. It would also be interesting to study the effects of rotation-translation coupling.

Then in Chapter 6, In this work, we consider the motion of a periodically forced prolate spheroid suspension in an oscillating Newtonian fluid within the limit of low-Reynolds number. The characteristics of the particle dynamics due to an external periodic force have been studied. The governing equations in the form of a system of integro-differential equations (IDEs) are derived using the expression developed by Lovalenti and Brady (1993b) for the hydrodynamics force.

We also compute the dynamics of a particle and analyze it in detail. The investigation is continued by varying the system parameters such as particle aspect ratio, Reynolds number, amplitude, and frequency of the external force. We observed that the spheroid's amplitude of velocity and displacement increases as frequency, aspect ratio, or/and force increases.

Then in chapter 7, we summarize the dissertation and include some applications and novelty of the research. Moreover, we explain some future aspects of the research. This dissertation extends the ideas and the corresponding methodology to Newtonian fluid suspensions at low Reynolds numbers in various fluid flow fields, like quiescent fluid, oscillating, time-dependent uniformly fluid flow fields. We derive the governing equations under the action of an arbitrary external periodic force on the dynamics of an arbitrarily shaped particle for different flow fields. The study of dynamics of a rigid particle in a fluid at low Reynolds numbers with

inertia emanates an additional term in the governing equation representing a fading memory for the entire history of the motion. The memory term becomes nonlinear with the introduction of convective inertia. The equations are numerically solved for some parameters, and the results are discussed in detail. The effect of periodic force applies to a spheroidal particle in an arbitrary direction, the hydrodynamic forces arise due to the disturbance of the velocity fluctuations, and the forces induced due to the non-spherical nature of the rigid body likely result in some novel features, which may be utilized for the development of new technologies.

Chapter 2

Oscillations of a periodically forced slightly eccentric spheroid in an unsteady viscous flow at low Reynolds number

2.1 Introduction

There is significant research on the transport of micro sized particles in a variety of flows, where a substantial portion of the unsteadiness appears due to the disturbance of fluctuations of velocity components. The presence of micro particles with different shapes and sizes might result in novel features, which could be tapped for developing new technologies. The oscillation of suspended particles at low Reynolds number has attracted the attention of many researchers in suspension rheometry and colloidal suspension because of its use in many industries like food, petroleum, printing, pharmaceutical etc. Madhukar et al. (2010); Lawrence and Weinbaum (1988). The effects of the unsteady hydrodynamics force on a suspended particle is very important in developing smart fluids and the source

of the unsteadiness is a consequence of the disturbance of velocity fluctuations Ouellette (2004). In most practical situations, the suspended particles are non-spherical in geometry and irregular in size. There is a relative velocity between the viscous fluid and the rigid body moving in the fluid at low Reynolds number. The dynamics and resonance properties of oscillations of such micro-bodies are very sensitive to its geometry and size. In this article, we discuss the resonance properties of oscillations of a slightly eccentric spheroid under the influence of an external periodic force, where the suspension is sufficiently diluted so that interactions between particle and particle can be neglected. There is a vast literature in the area of motion and rheology of suspended particles and its technological importance. The nonlinear behavior of a periodically forced spheroid under negligible Brownian motion has been discussed in detail by Kumar et al. (1995) and Kumar and Ramamohan (1998). Ramamohan et al. (2011) have simplified the hydrodynamic force expression for a spherical particle suspended in a quiescent Newtonian-fluid and studied the particle dynamics under the action of a periodic force at small Reynolds numbers.

In 2010, Madhukar et al. (2010) have reported a study of the particle dynamics and the normal-stress for a dilute suspension of spheroids in a quiescent fluid at small values of Reynolds numbers under the action of a periodic force. The effects of an external periodic force on the dynamics of slender rods and spheroids have been investigated by many other researchers Asokan et al. (2005); Kumar et al. (1995); Kumar and Ramamohan (1997; 1998); Ramamohan et al. (2011). A review of the research work carried out over a period of 10 years on the motion of orient particles in simple shear flow under the action of a periodic force has been reported Asokan et al. (2005). Candelier et al. (2005) have demonstrated the Boussinesq-Basset force effect on the radial migration of Stokes particle in a vortex. Stepanyants and Yeoh (2009) have also investigated the dynamics of particles and bubbles in creeping flow and the dynamics of nano-particles in a viscous fluid at low Reynolds numbers. The tiny oscillations of spherical particles under the

influence of a periodic force have been studied by Hassan et al. (2017). They have reported that the memory integral representing the drag force [cf. Eqs.(2.5) and (2.6)] influences the characteristics of the oscillations at low Reynolds numbers. The present study also substantiates their observations. The resonance widening and peak reduction observed in the analysis are significant in micro and nano-suspensions as reported earlier Stepanyants and Yeoh (2010). The drift in the orientation of prolate and oblate spheroid arising due to weak inertial term was analytically studied in the limiting case of small Stokes and Reynolds numbers Dabade et al. (2016). The orientation due to weak inertial drift of certain spheroid particles was analytically investigated by Marath and Subramanian (2018b). A set of non-linear ordinary differential equations governing the transport of an arbitrary forced spheroid in a quiescent flow at low Reynolds number with the inclusion of past position and velocity is analyzed by Singh and Kumar (2019).

Practically in many suspensions, the suspended particles will be non-spherical with different size and shape. Hence it generates interests to study the transport behavior of such particles. Recently, Stepanyants and his group have investigated the dynamics of suspended particles as well as of bubbles in a viscous fluid under the influence of an acoustic radiation force Hassan et al. (2017); Ostrovsky and Stepanyants (2018). Hassan and Stepanyants (2017) have also studied the properties of resonance of oscillations of forced particles and gaseous bubbles of spherical shape at low Reynolds number, where the external force is sinusoidal in nature. As reported by Hassan and Stepanyants (2017), the oscillation characteristics of the motion of an arbitrary oscillator in the presence of Basset memory force have not been addressed to the best of our knowledge. They observed the possibility of characterizing the resonance properties of the oscillations by amplitude and phase. They have studied the influence of the drag force on the oscillations of a spherical drop of a solid particle and a gaseous bubble.

The results of the variant of this problem might be of important particularly in the context of acoustic streaming. In this work, we analyze the forced oscilla-

tions of a near-sphere under the action of an external oscillatory force and study the dependence of oscillation properties on the geometry and shape of the non-spherical particles. As a first case, we consider oscillations of slightly eccentric spheroids in an unsteady viscous fluid at small Reynolds number under the action of a periodic force. Following the approach of Lawrence and Weinbaum (1986), we obtain the governing equation of motion of oscillation of suspended particles in non-dimensional form moving in a single direction. This study proposes the perturbation solution of the solid sphere under the action of a periodic force in low Reynolds number limit and hence the core part of the derivation is a perturbation analysis of motion of a sphere. Also, we studied the well-known Q-curve for the particle under an imposed oscillatory force. This incremental work demonstrates the role of small eccentricity in modifying the known Q-curve for a sphere, where the change in the Q-curve is notable. So the present work is one of the possible extensions of the work done by Hassan and Stepanyants (2017) say, the dynamics of arbitrary shaped particles in a viscous fluid at very small Reynolds numbers.

We demonstrate the result of dynamics of a solid slightly eccentric spheroid constrained to one-dimensional oscillations, and solves the one dimensional equation of motion for the particle where the motion is caused by a periodic external force. We provide solutions to the particle dynamics equations, using fluid mechanic solutions available in the literature. The sensitive dependencies on particle shape of amplitude and phase-frequency of oscillations of a slightly eccentric spheroid is numerically investigated and reported in this article. This analysis is of some utility in terms of clarifying the role of the memory force particularly with regard to the phase relationship of the forced oscillations. It proposes a potential application to separate particles of certain shapes from a suspension of particles with similar size and different shapes. Another possible situation to which the solutions of the problem might be applicable would be damped small amplitude oscillations of a periodically forced pendulum. The results obtained may have scientific and technological impact and may open up new methodologies for char-

acterization of fluid suspensions.

In short, we study the properties of oscillations of slightly eccentric oblate and prolate spheroids in an unsteady viscous fluid driven by a periodic force at small Reynolds number in the presence and absence of the memory drag force. The governing equation of oscillations are derived accordingly, where the eccentricity parameter (ϵ), frequency of free oscillation (ω_0) and density ratio (κ) of the particle found in the equation influence the oscillation properties. In the limiting case, $\epsilon \to 0$, the results match with the results of Hassan and Stepanyants (2017) and thus verify the formulation of the problem and validate the results presented in this work. We demonstrate that the oscillation properties depend on the geometry and shape of suspended particle. What follows is the formulation of the problem proposed.

2.2 The problem

The equation of a spheroid is given by

$$\frac{x^2}{a^2} + \frac{y^2}{b^2} + \frac{z^2}{b^2} = 1$$

where, $2a$ and $2b$ are respectively the major and minor axes and the triplet (x, y, z) represents an arbitrary point on the spheroid. Since it is of interest to study the oscillation properties of a slightly eccentric spheroid, we assume that $b = a(1+\epsilon)$ for an oblate spheroid and $b = a(1-\epsilon)$ for a prolate spheroid, where a is considered to be the characteristic length of the spheroid and $\epsilon << 1$. The solution to the problem considered in this analysis involves the expression for the hydrodynamic force in the limit of low Reynolds number representing the magnitude of the convective inertia related to viscous force.

It is trivial that the eccentricity of the spheroid, $\sqrt{2\epsilon - \epsilon^2}$ reduces approximately to $\sqrt{2\epsilon}$ for small ϵ. In this analysis, we take $\epsilon << 1$. Also, assume that

a near-sphere i.e. a spheroid of small eccentricity, moves from rest with a time dependent velocity $U(t)$ parallel to its axis of symmetry. As given by Abbad et al. (2006), the effective hydrodynamic force due to the perturbed quasi-steady drag force, the added mass force, the Basset memory integral term and the new history force caused by the eccentricity of the spheroid undergoing an arbitrary time dependent motion in the limiting case of low Reynolds number (i.e. $Re << 1$) is in the form,

$$\begin{aligned}
\mathrm{F^H} =& 6\pi\mu a\left(1+\frac{4}{5}\epsilon+\frac{2}{175}\epsilon^2\right)U(t)\\
&+\frac{2}{3}\rho\pi a^3\left(1+\frac{16}{5}\epsilon+\frac{604}{175}\epsilon^2\right)\dot{U}(t)\\
&+6\sqrt{\pi}\mu a\left(1+\frac{8}{5}\epsilon+\frac{116}{175}\epsilon^2\right)\int_{-\infty}^{t}\frac{\dot{U}(t)d\tau}{\sqrt{\frac{t-\tau}{\tau_0}}}\\
&+\frac{8}{175}\pi\mu a\epsilon^2\int_{-\infty}^{t}\dot{U}(\tau)G(t-\tau)d\tau+O(\epsilon^3),
\end{aligned}\tag{2.1}$$

with

$$\begin{aligned}
G(t) =& \Im\left[\sqrt{\frac{w}{3}}\ exp(wt/\tau_0)\ erfc(\sqrt{wt/\tau_0})\right]\\
\text{and } w =& \frac{3}{2}\left(1+\sqrt{3}\ i\right),
\end{aligned}\tag{2.2}$$

where, $U(t)$ is the velocity of the suspended particle at time t with $U(t)=0$ for $t\leq 0$ and, μ and ρ are the dynamic viscosity and the density of the ambient fluid respectively. Also, $\dot{U}(t)=\frac{dU}{dt}$ is the particle acceleration, $\tau_0=a^2/\nu$ is the diffusive time scale and $\nu=\mu/\rho$ is the kinematic viscosity of the fluid. The parameter ϵ denotes the geometrical variation of the particle from a sphere and the kernel, $G(t)$ is defined as the imaginary part of the corresponding complex variable. The one-dimensional transport of a suspended particle under the hydrodynamic force

F^{H} and an external force $\mathrm{F}^{\mathrm{ext}}$ at small Reynolds number can be expressed as

$$\frac{d^2y}{dt^2} + \bar{\omega_0}^2 y + \frac{\mathrm{F}^{\mathrm{H}}}{m_p} = \frac{\mathrm{F}^{\mathrm{ext}}}{m_p}, \tag{2.3}$$

where y is the displacement of the particle from equilibrium position in one-direction, m_p denotes the mass of the particle and $\tilde{\omega_0}$ symbolizes the natural oscillation frequency of the particle in the absence of dissipation. The ${\omega_0}^2 y$ appears as an additional external force, like spring force, that restores the particles position to the origin. Assume that the dynamics is under the action of an external periodic force given by $\mathrm{F}^{\mathrm{ext}} = A_0 \sin(\tilde{\omega}\ t)$ having amplitude A_0 and frequency $\tilde{\omega}$. On simplification, by incorporating the above assumptions, we obtain the governing equation of oscillations of a spheroid as

$$\begin{aligned}&\left(\kappa + \frac{1}{2}k_2\right)\frac{d^2y}{dt^2} + \frac{9\mu}{2a^2\rho}k_1\frac{dy}{dt} + \frac{9}{2a}k_3\sqrt{\frac{\mu}{\pi\rho}}\int_{-\infty}^{t}\frac{d^2y}{d\tau^2}\frac{d\tau}{\sqrt{t-\tau}}\\ &+ \frac{3\mu}{4\rho a^2}k_4\int_{-\infty}^{t}\frac{d^2y}{d\tau^2}G(t-\tau)d\tau + \frac{\tilde{\omega}_0^2}{(1+\epsilon)^2}y - \frac{\tilde{A}}{(1+\epsilon)^2}\sin(\tilde{\omega}t) = 0,\end{aligned} \tag{2.4}$$

where

$$k_1 = \frac{\left(1 + \frac{4}{5}\epsilon + \frac{2}{175}\epsilon^2\right)}{(1+\epsilon)^2},\ k_2 = \frac{\left(1 + \frac{16}{5}\epsilon + \frac{604}{175}\epsilon^2\right)}{(1+\epsilon)^2}$$

$$k_3 = \frac{\left(1 + \frac{8}{5}\epsilon + \frac{116}{175}\epsilon^2\right)}{(1+\epsilon)^2},\ k_4 = \frac{\frac{8}{175}\epsilon^2}{(1+\epsilon)^2},\ \text{and}\ \tilde{A} = \frac{A_0}{(4/3)\pi a^3\rho}$$

$\kappa \equiv \rho_p/\rho$ is the density ratio of the particle to the fluid. It is evident from above that k_1, k_2, k_3 and k_4 are functions of eccentricity parameter ϵ of the spheroid. The presence of k_2 in the first term indicates the consideration of added mass forces and k_4 represents the presence of additional history force due to the suspension of eccentric spheroid particle. The first term in Eq.(2.4) represents the effective force on the particle due to inertia and added mass effect. The second term of the equation describes the Stokes drag force. The third and forth integral terms describe the two history memory forces namely the Boussinesq-Basset drag

force Basset (1888a) known as *Basset memory force* and the new memory integral term Lawrence and Weinbaum (1986) called *additional history force* respectively. The last term indicates presence of external force. Assume that the particle starts moving with velocity $U(t)$ along its axis of symmetry and having an initial velocity $U(0) = U_0$. These considerations can be incorporated by expressing the velocity component, $\frac{dy}{dt}$ by $H(t) : \left(\frac{dy}{dt}\right)^* = H(t)(\frac{dy}{dt})_+,\ -\infty < t < \infty$, where $(dy/dt)^*$ is the instantaneous effective velocity of moving spheroid at any time t and $(dy/dt)_+$ is the velocity when $t > 0$ Hassan and Stepanyants (2017). Trivially, the acceleration is given as

$$\left(\frac{d^2y}{dt^2}\right)^* = \delta(t)\left(\frac{dy}{dt}\right)_+ + H(t)\left(\frac{d^2y}{dt^2}\right)_+,$$

where $H(t)$ represents the unit Heaviside step function and its derivative $\delta(t) \equiv dH(t)/dt$ denotes the Dirac delta function defined on $(-\infty, \infty)$. The governing equation Eq.(2.4) of motion in one-dimension for positive time can be expressed as

$$\left(\kappa + \frac{1}{2}k_2\right)\frac{d^2y}{dt^2} + \frac{9\mu}{2a^2\rho}\left[k_1\frac{dy}{dt} + \frac{aU_0}{\sqrt{\pi\nu\ t}}k_3 + a\ k_3\sqrt{\frac{\rho}{\pi\mu}}\int_{0+}^{t}\frac{d^2y}{d\tau^2}\frac{d\tau}{\sqrt{t-\tau}}\right] +$$
$$\frac{3\mu U_0}{4\rho\, a^2}G(t)k_4 + \frac{3\mu}{4\rho a^2}k_4\int_{0+}^{t}\frac{d^2y}{d\tau^2}G(t-\tau)d\tau + \frac{\tilde{\omega}_0^2}{(1+\epsilon)^2}y - \frac{\tilde{A}}{(1+\epsilon)^2}\sin(\tilde{\omega}t) = 0, \qquad (2.5)$$

using the result $\int_{-c}^{c} f(t)\delta(t) = f(0)$, where the symbols, $\left(\frac{dy}{dt}\right)_+$ and $\left(\frac{d^2y}{dt^2}\right)_+$ are replaced by $\left(\frac{dy}{dt}\right)$ and $\left(\frac{d^2y}{dt^2}\right)$ respectively for convenience. The non-dimensionalized form of expression given in Eq.(2.5) can be again manipulated on scaling length by a, time by $a^2\rho/9\mu$ and velocity by $9\mu/a\rho$ On substitution using

$$Z = y/a\ , \theta = \frac{9\mu t}{a^2\rho},\ \upsilon_0 = \frac{U_0 a\ \rho}{9\mu},$$

the reduced equation in non-dimensional form is obtained as

$$\frac{d^2Z}{d\theta^2} + \frac{k_1}{2\kappa + k_2}\frac{dZ}{d\theta} + \frac{3k_3}{(2\kappa + k_2)\sqrt{\pi}}\left(\frac{\upsilon_0}{\sqrt{\theta}} + \int_0^{\theta}\frac{d^2Z}{d\vartheta^2}\frac{d\vartheta}{\sqrt{\theta - \vartheta}}\right) + \frac{k_4}{6(2\kappa + k_2)}\times$$

$$\left\{ \upsilon_0 G\left(\frac{\rho a^2}{\sqrt{9\mu}}\theta\right) + \int_0^\theta \frac{d^2Z}{d\vartheta^2} G\left(\frac{a^2\rho}{9\mu}\theta - \vartheta\right) d\vartheta \right\} + \frac{2\tilde{\omega}_0^2 a^4 \rho^2}{81(1+\epsilon)^2(2\kappa+k_2)\mu^2} Z - \frac{2\tilde{A}}{(1+\epsilon)^2(2\kappa+k_2)} \frac{a^3\rho^2}{81\mu^2} \sin(\frac{\tilde{\omega}\rho a^2}{9\mu}\theta) = 0. \tag{2.6}$$

Equivalently,

$$\frac{d^2Z}{d\theta^2} + \alpha\frac{dZ}{d\theta} + \frac{\beta}{\sqrt{\pi}}\left(\frac{\upsilon_0}{\sqrt{\theta}} + \int_0^\theta \frac{d^2Z}{d\vartheta^2}\frac{d\vartheta}{\sqrt{\theta-\vartheta}}\right) + \gamma\left\{\upsilon_0 G\left(\frac{a^2\rho}{9\mu}\theta\right) + \int_0^\theta \frac{d^2Z}{d\vartheta^2} G\left(\frac{a^2\rho}{9\mu}(\theta-\vartheta)\right) d\vartheta\right\} + \omega_0^2 Z - A\sin(\omega\theta) = 0, \tag{2.7}$$

where

$$\alpha = \frac{k_1}{2\kappa+k_2},\ \beta = \frac{3k_3}{(2\kappa+k_2)},\ \gamma = \frac{k_4}{6(2\kappa+k_2)}$$

$$\omega_0 = \tilde{\omega}_0\sqrt{\frac{2a^4\rho^2}{81(1+\epsilon)^2(2\kappa+k_2)\mu^2}}\ ,\quad \omega = \frac{\tilde{\omega}\rho a^2}{9\mu}$$

$$A = \frac{2\tilde{A}}{(1+\epsilon)^2(2\kappa+k_2)}\frac{a^3\rho^2}{81\mu^2}\ .$$

Equivalently, the non-autonomous integro-differential equation, Eq.(2.7) can be expressed as a nonlinear autonomous integro-differential equation and can be solved numerically. It is verified that the equation, Eq.(2.7) reduces to the equation derived by Hassan and Stepanyants (2017) who has studied the dynamics of spherical particles.

The following analysis is conceptually important for an arbitrary body whose shape is significantly different from sphere. Similar to the Basset force, the term involving γ is also a memory integral force induced due to the history acceleration of the body, where the kernel function $G(t)$ is given by Eqs.(2.2), which decays exponentially faster than the kernel due to Basset history force. In most cases, the contribution from $G(t)$ is negligibly small and is applicable only for small values of ϵ. However, the new additional history force term due to non-sphericity of particle is numerically evaluated and found that it is negligibly small compared

to the contribution of the term containing β and other terms as reported earlier Lawrence and Weinbaum (1986), on restricting $\epsilon << 1$. Otherwise also, the part of force containing γ (or k_4) due to the additional history vanishes when $\epsilon \to 0$ as evident from the expressions for γ and k_4. The additional history term due to the eccentricity of the particle vanishes as ϵ tends to 0, and the contribution of the other history force proportional to β does not vanish in the limit of $\epsilon \to 0$ as can be seen from the present analysis and the demonstration of Abbad et al. (2006). At the same time, they have demonstrated that the Basset memory force prevails over the other forces like added-mass and Stokes force, when the pulsation is up to 60% of the total drag force. Naturally, the effect of additional history term on the hydrodynamics force can be ignored as $\epsilon \to 0$ and hence the term is ignored in the present analysis. This study is of interest, since an arbitrary particle can be approximated as a spheroid in many cases. For the present analysis we assume that the hydrodynamics force induced due to the influence of additional history force is negligibly small and hence the motion is free from the influence of additional history force (i.e. $\gamma = 0$). Further, we assume that the fluid viscosity is relatively small in such a way that the free oscillations ω_0 are much greater than the parameters α and β, where the Reynolds number is small ($<< 1$). Similar assumptions are made by Hassan and Stepanyants (2017). Thus the transport of the particle is reduced to a second order linear non-autonomous integro-differential equation as

$$\frac{d^2Z}{d\theta^2} + \alpha\frac{dZ}{d\theta} + \beta\frac{1}{\sqrt{\pi}}\left(\frac{\upsilon_0}{\sqrt{\theta}} + \int_0^\theta \frac{d^2Z}{d\vartheta^2}\frac{d\vartheta}{\sqrt{\theta-\vartheta}}\right) + \frac{\gamma}{4\sqrt{3}}\left(\frac{1}{4\sqrt{3}}\frac{\upsilon_0}{(\theta-\vartheta)\sqrt{\theta-\vartheta}}\right.$$
$$\left. + \int_0^\theta \frac{d^2Z}{d\vartheta^2}\frac{d\vartheta}{(\theta-\vartheta)\sqrt{\theta-\vartheta}}\right) + \omega_0^2 Z - A\sin(\omega\theta) = 0, \tag{2.8}$$

2.3 Results and discussion

Following Hassan and Stepanyants (2017), we find out the simplest possible solution, to equation (2.8) in the form of

$$Z(\theta) = R_1 \cos(\omega\theta) + R_2 \sin(\omega\theta) = R(\omega, \omega_0) \cos(\omega\theta - \phi),$$

with initial values $Z(0) = Z_0 = 0 = v_0 = \dot{Z}(0)$. On simplification, we have the expressions:

$$R_1 = - \frac{-A\left(\omega\alpha + \frac{\beta\omega^{3/2}}{2\sqrt{2}} - \gamma\sqrt{\frac{\pi}{3}}\frac{\omega^{3/2}}{4\sqrt{3}}\right)}{\left(\omega_0^2 - \omega^2 - \frac{\beta\omega^{3/2}}{2\sqrt{2}} - \gamma\sqrt{\frac{\pi}{3}}\frac{\omega^{3/2}}{4\sqrt{3}}\right)^2 + \left(\alpha\omega + \frac{\beta\omega^{3/2}}{2\sqrt{2}} - \gamma\sqrt{\frac{\pi}{3}}\frac{\omega^{3/2}}{4\sqrt{3}}\right)^2} \tag{2.9}$$

$$R_2 = - \frac{A\left(\omega_0^2 - \omega^2 - \frac{\beta\omega^{3/2}}{2\sqrt{2}} - \gamma\sqrt{\frac{\pi}{3}}\frac{\omega^{3/2}}{4\sqrt{3}}\right)}{\left(\omega_0^2 - \omega^2 - \frac{\beta\omega^{3/2}}{2\sqrt{2}} - \gamma\sqrt{\frac{\pi}{3}}\frac{\omega^{3/2}}{4\sqrt{3}}\right)^2 + \left(\alpha\omega + \frac{\beta\omega^{3/2}}{2\sqrt{2}} - \gamma\sqrt{\frac{\pi}{3}}\frac{\omega^{3/2}}{4\sqrt{3}}\right)^2} \ . \tag{2.10}$$

The amplitude $R(\omega, \omega_0)$ and the fundamental phase $\phi(\omega, \omega_0)$ are found to be

$$R(\omega, \omega_0) = \sqrt{R_1^2 + R_2^2} \qquad \text{and} \qquad \phi(\omega, \omega_0) = tan^{-1}\left(R_2/R_1\right)$$

$$\text{i.e. } R(\omega, \omega_0) = \frac{-A}{\sqrt{\left(\omega_0^2 - \omega^2 - \frac{\beta\omega^{3/2}}{2\sqrt{2}} - \gamma\sqrt{\frac{\pi}{3}}\frac{\omega^{3/2}}{4\sqrt{3}}\right)^2 + \left(\alpha + \frac{\beta\omega^{3/2}}{2\sqrt{2}} - \gamma\sqrt{\frac{\pi}{3}}\frac{\omega^{3/2}}{4\sqrt{3}}\right)^2}} \tag{2.11}$$

and

$$\phi = \ \tan^{-1}\left(-\frac{\omega\alpha + \frac{\beta\omega^{3/2}}{2\sqrt{2}} - \gamma\sqrt{\frac{\pi}{3}}\frac{\omega^{3/2}}{4\sqrt{3}}}{\omega_0^2 - \omega^2 - \frac{\beta\omega^{3/2}}{2\sqrt{2}} - \gamma\sqrt{\frac{\pi}{3}}\frac{\omega^{3/2}}{4\sqrt{3}}}\right). \tag{2.12}$$

The equations Eq.(2.11) and Eq.(2.12) can be reformulated by normalizing ω by $\omega = n\omega_0$ and introducing the two quality ratios Q_α and Q_β Hassan and Stepanyants (2017); Klepper and Kolenkow (2014) defined by $Q_\alpha = \omega_0/\alpha$, $Q_\beta = 8\omega_0/\beta^2$ and $Q_\gamma = 96/\pi\omega_0\gamma^2$ for the conventional characterization of oscillations. The amplitude of the particle oscillation is also normalized by choosing $A_n = \omega_0^2 R/A$. The expressions for amplitude and phase of oscillations of particles as a functions

of Q_α and Q_β for a given n are exactly same as the expressions given by Hassan and Stepanyants (2017) and are

$$A_n(Q_\alpha, Q_\beta) = \frac{1}{\sqrt{\left(1-n^2-n\sqrt{\frac{n}{Q_\beta}}-n^2\sqrt{\frac{n}{Q_\gamma}}\right)^2+\left(\frac{n}{Q_\alpha}+n\sqrt{\frac{n}{Q_\beta}}-n^2\sqrt{\frac{n}{Q_\gamma}}\right)^2}}. \tag{2.13}$$

$$\phi_n(Q_\alpha, Q_\beta) = \tan^{-1}\left(-\frac{\frac{n}{Q_\alpha}+n\sqrt{\frac{n}{Q_\beta}}-n^2\sqrt{\frac{n}{Q_\gamma}}}{1-n^2-n\sqrt{\frac{n}{Q_\beta}}-n^2\sqrt{\frac{n}{Q_\gamma}}}\right). \tag{2.14}$$

Although, similar expressions for A_n and ϕ_n as given in Eq.(2.13) and Eq.(2.14) are obtained, the quality ratios Q_α and Q_β differ in forms which will be reduced to the corresponding expressions obtained by them on making $\epsilon = 0$. This validates the expressions given in Eq.(2.13) to Eq.(2.14). Also, the amplitude (resonance) and phase frequency dependencies in the limiting case of Basset memory term, $Q_\beta, Q_\gamma \to \infty$ (i.e. $\beta, \gamma \to 0$) are reduced to

$$A_n(Q_\alpha, Q_\beta)|_{\beta=0} = \frac{1}{\sqrt{(1-n^2)^2+\frac{n^2}{Q_\alpha^2}}} \tag{2.15}$$

$$\phi_n(Q_\alpha, Q_\beta)|_{\beta=0} = \tan^{-1}\left(-\frac{\frac{n}{Q_\alpha}}{1-n^2}\right) \tag{2.16}$$

The amplitude curve given in Eq.(2.15) attains its maximum at $n_m = \sqrt{1+\frac{1}{4Q_\alpha^2}}$ and equals to $(A_n)_{max} = \frac{1}{\sqrt{\frac{5}{16Q_\alpha^4}+\frac{1}{Q_\alpha^2}}}$.

As evident from Eq.(2.13) to Eq.(2.16), the amplitude and phase frequencies depend on the parameters ϵ, κ and ω_0. Since ϵ characterizes the shape of the suspended non-spherical particles (for spheres, $\epsilon = 0$), the parameter plays a significant role on its oscillation properties. For numerically analyzing the effect of eccentricity on the dynamics of the particle, ϵ is assumed to be +ve for oblate spheroids and is replaced by $-\epsilon$ for prolate spheroids in all the expressions detailed above. For a comprehensive analysis on the oscillation properties of the spheroid

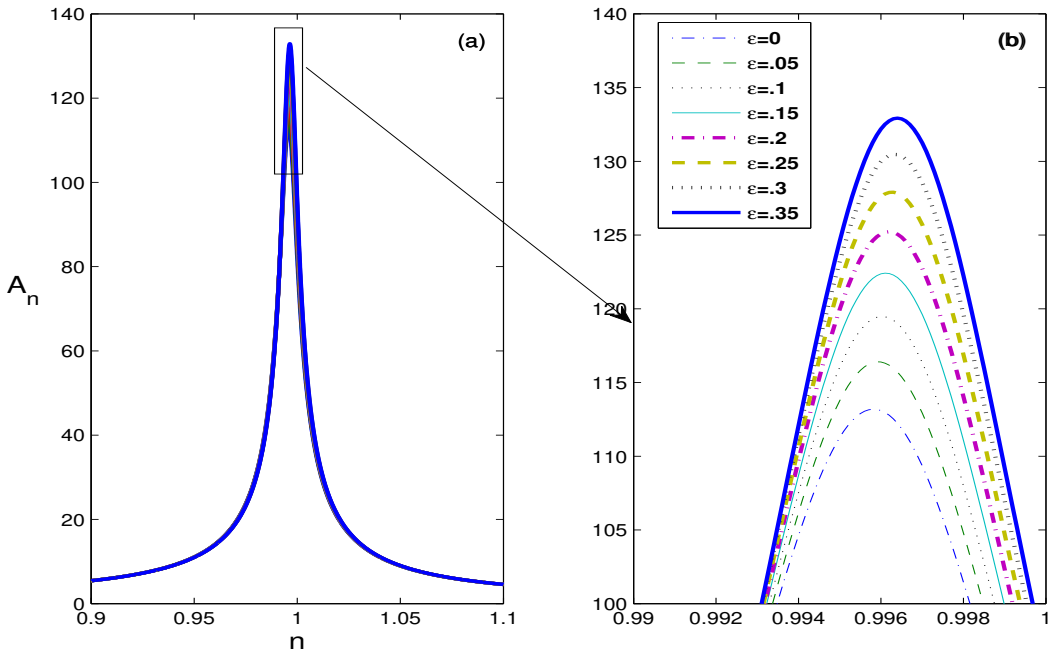

Figure 2.1: (a) The amplitude dependency of the oscillating oblate spheroids as a function of n in the presence of Basset memory force for $\kappa = 4$, $\omega_0 = 200$, $\epsilon = 0.0, 0.05 \ldots 0.35$. (b) A magnified portion of the graph given in (a).

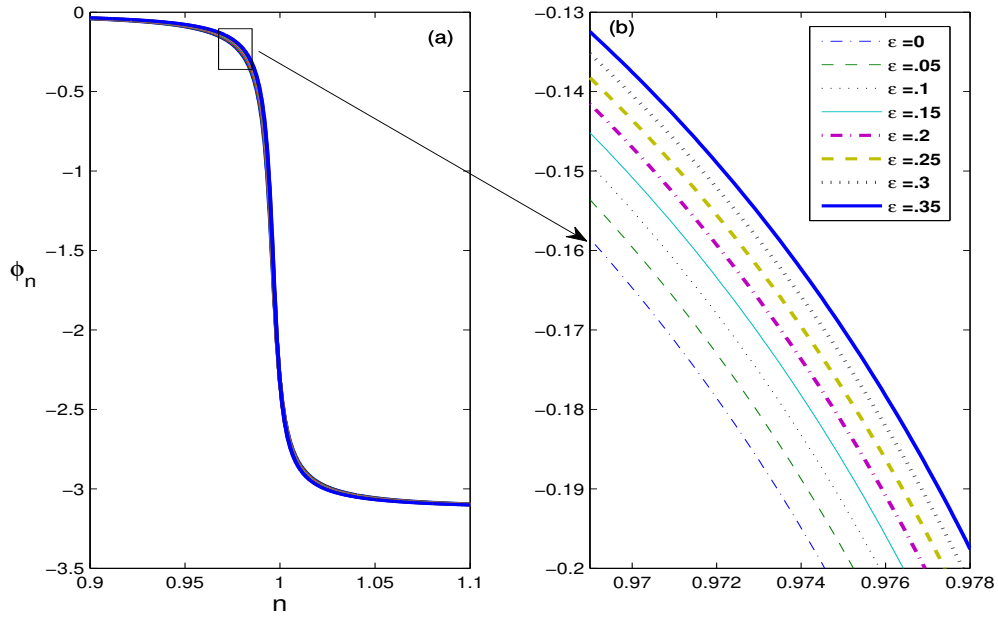

Figure 2.2: (a) The phase-frequency dependency of the oscillating oblate spheroids as a function of n in the presence of Basset memory integral for $\kappa = 4$, $\omega_0 = 200$ and $\epsilon = 0.0$, $0.05 \ldots 0.35$. (b) The magnified plot of the selected portion given in (a).

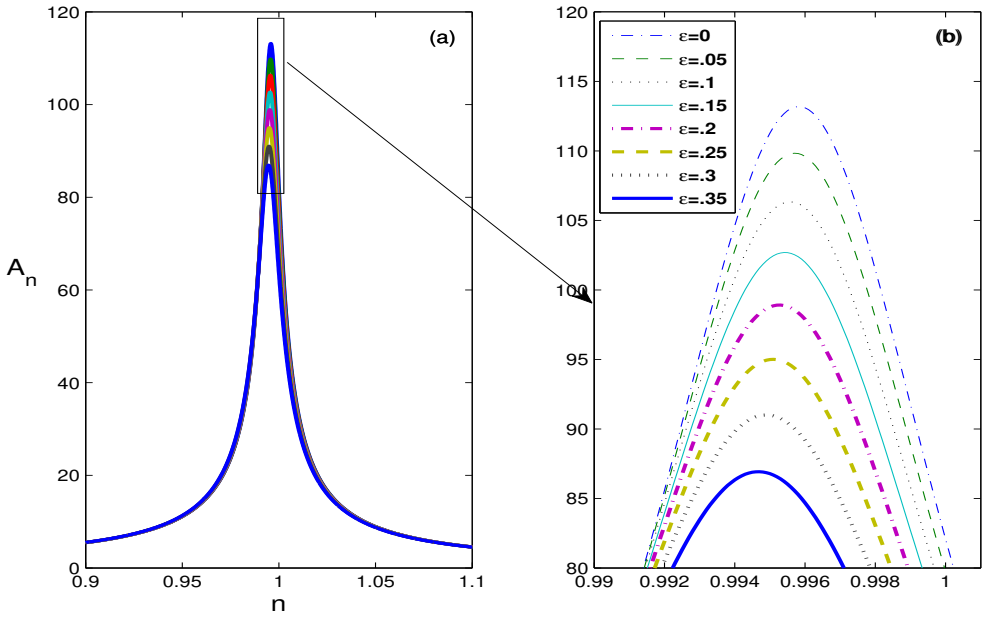

Figure 2.3: (a) The amplitude dependency of the oscillating prolate spheroids as a function of n in the presence of the Basset memory integral for $\kappa = 4$, $\omega_0 = 200$, $\epsilon = 0.0, 0.05 \ldots 0.35$. (b) A magnified plot of the selected portion given in (a).

dynamics the change in particle geometry (ϵ), amplitude of free oscillations (ω_0) and the density ratio (κ) are varied systematically for both the oblate and prolate spheroids in the presence as well as in the absence of Basset memory integral term expecting a variety of results having scientific interest. As a first case, we keep $\omega_0 = 200$, $\kappa = 4$ and vary ϵ from 0 to 0.35 in step of 0.05. The numerical results thus obtained are analyzed in detail. It is observed from Figs.2.1 and 2.2 that the amplitude dependence increases for an oblate spheroid for all n, whereas the phase frequency value increases (decreases) when $n < 1 (n > 1)$ as the non-sphericity measure, ϵ of the particle increases. This dependence on ϵ is very significant, since the hydrodynamic force exerted on the particle differs as ϵ increases. Figs.2.3 and 2.4 depict that the oscillation properties observed for oblate spheroid are reversed on replacing the suspended body by a prolate spheroid, i.e. the amplitude dependency decreases as ϵ increases for any n and the phase frequency value decreases when $n < 1$ and it increases when $n > 1$, in

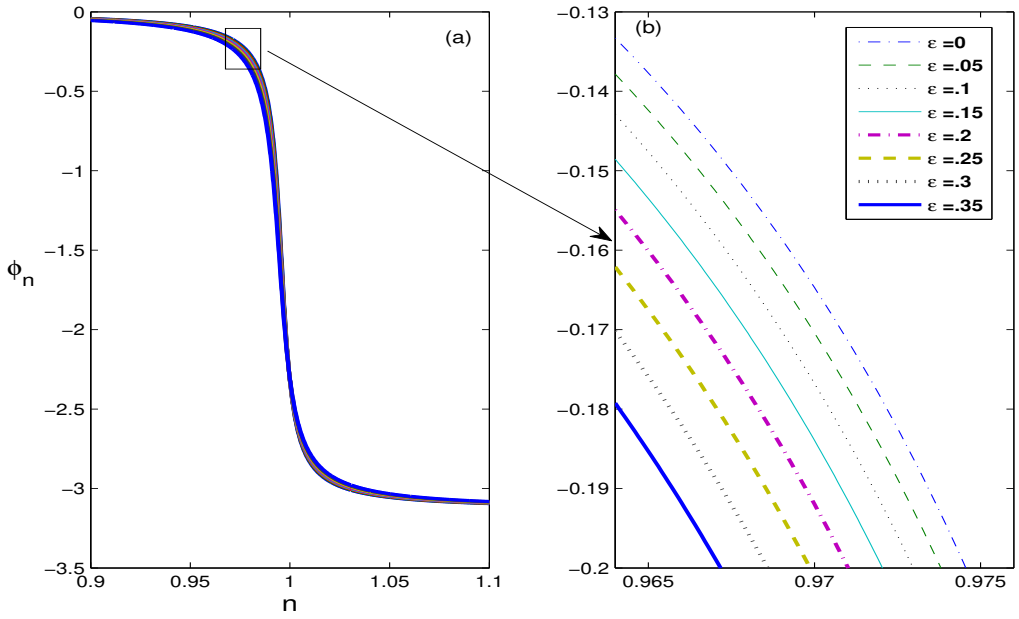

Figure 2.4: (a) The phase-frequency variation of the oscillating prolate spheroids as a function of n in the presence of Basset memory integral for $\kappa = 4$, $\omega_0 = 200$ and $\epsilon = 0.0$, $0.05 \ldots$ 0.35. (b) A magnified plot of the selected portion given in (a).

the case of a prolate spheroid, indicating its influence on the force exerted.

This argument is substantiated by the Fig.2.5 showing maximum amplitude and phase frequency variations for both oblate and prolate spheroids for a given set of values of the parameters, ϵ, ω_o and κ. It is of interest to observe that the maximum amplitude values are higher for an oblate spheroid than a prolate spheroid for a given ϵ as evident from Fig.2.5(a). This analysis shows that the disturbance in velocity due to the presence of particle increases (decreases) as the eccentricity of the spheroid increases in the case of an oblate (prolate) spheroid. For the typical plot shown in Fig.2.5(a), the maximum amplitude, $(A_n)_{max}$, of an oblate spheroid is about 1.5 times larger than that of that of a prolate spheroid, whereas the phase frequency of oscillations of an oblate spheroid is less (greater than) that of a prolate spheroid when $n > 1$ ($n < 1$) as evident from Fig.2.5(b). We summaries the argument as revealed from Figs.2.1 to 2.5 that the oscillation attains its maximum amplitude at a point left to $n = 1$ for any spheroid and the

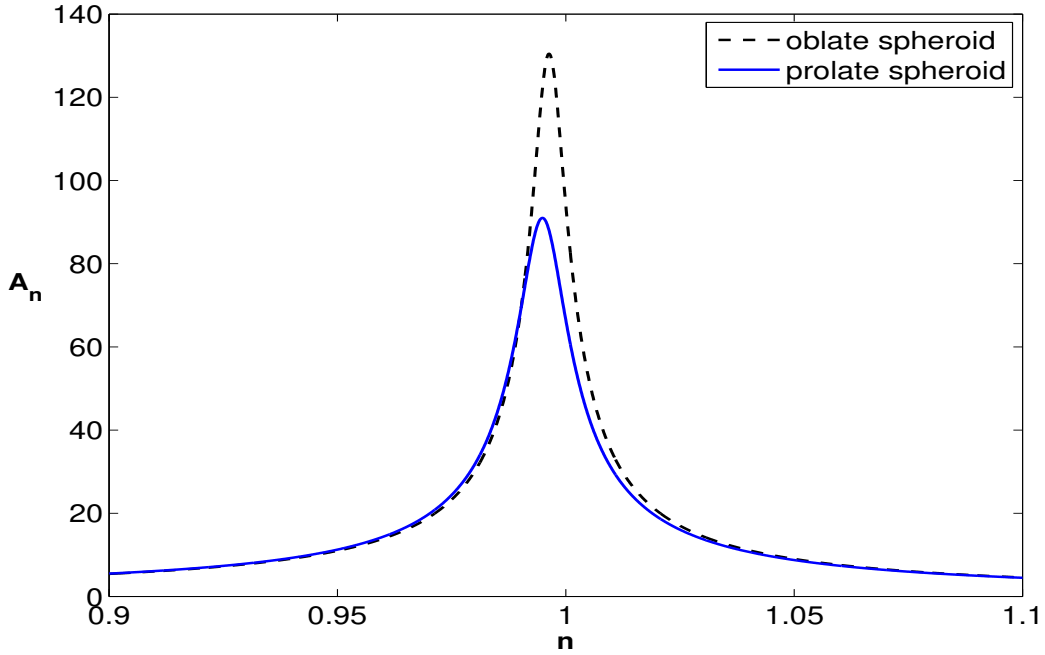

(a)

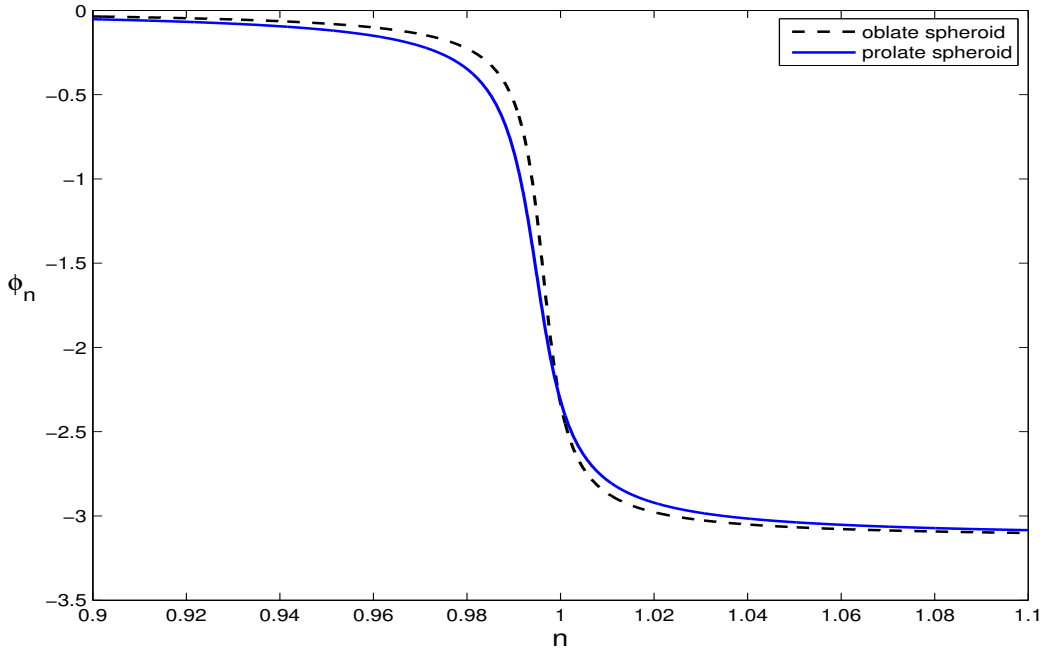

(b)

Figure 2.5: The plot of (a) amplitudes and (b) phase-frequencies of a prolate and oblate spheroids as function of n for $\epsilon = 0.3$, $\omega_0 = 200$ and $\kappa = 4$, showing the difference of oscillation properties of the particles in the presence of Basset memory force.

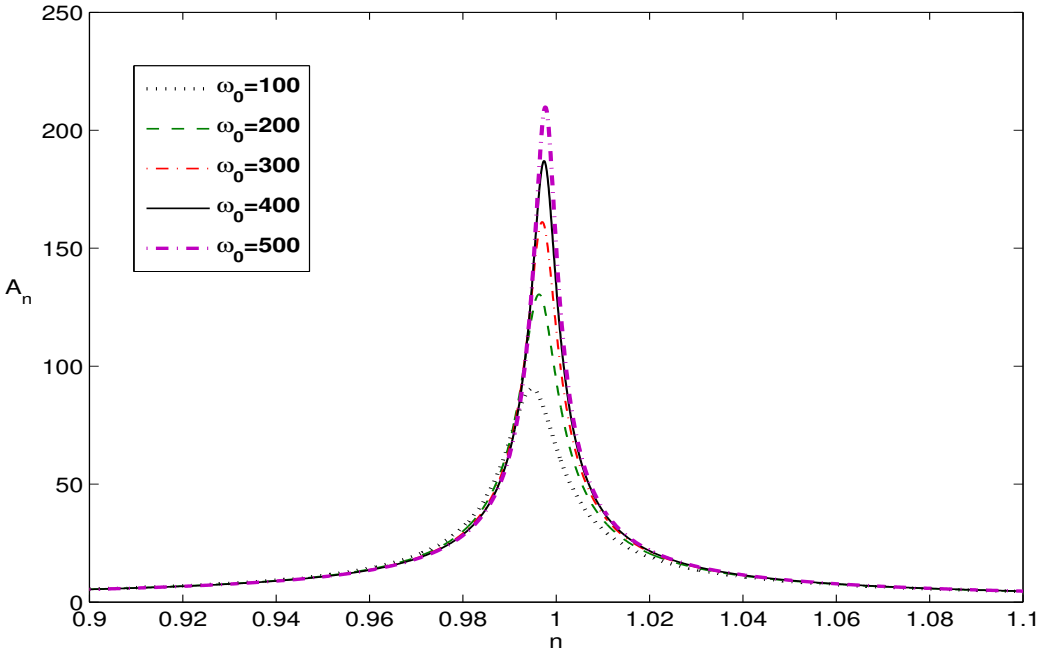

(a)

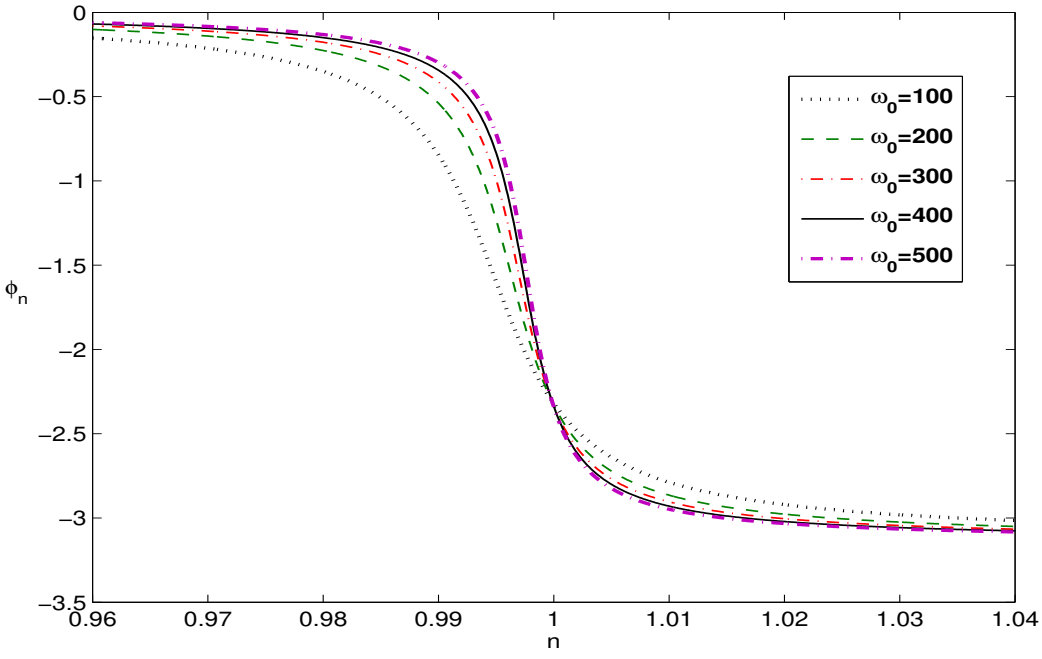

(b)

Figure 2.6: The plot of (a) amplitudes (b) phase frequencies of oscillations of oblate spheroids in the presence of Basset history force for $\kappa = 4$, $\epsilon = 0.3$ and oscillating with different free frequencies, $\omega_0 = 100, 200, ..., 500$.

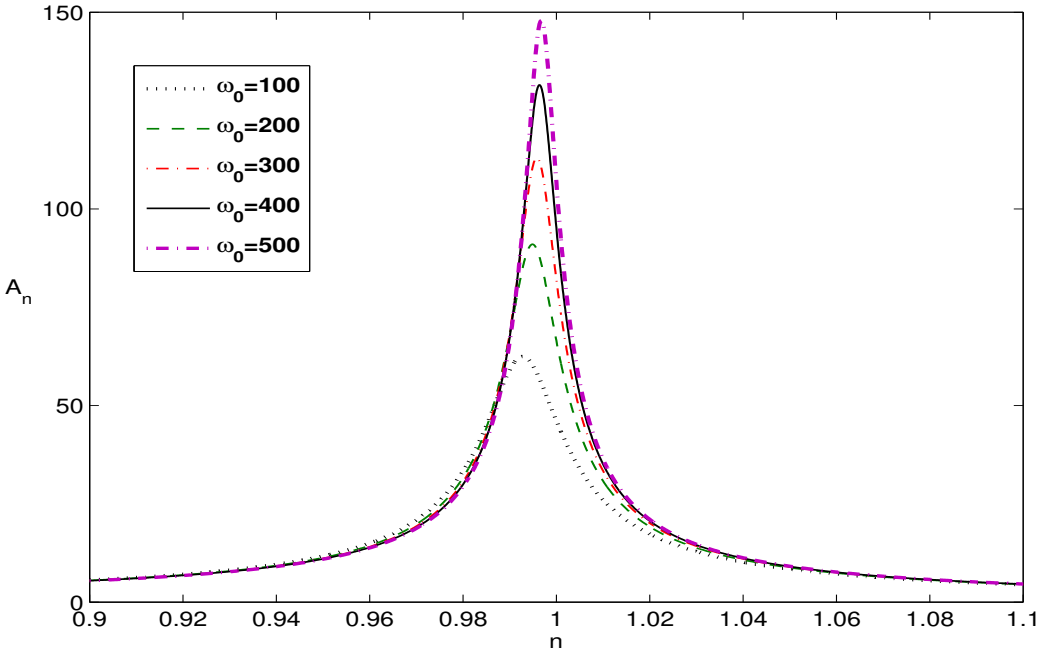

(a)

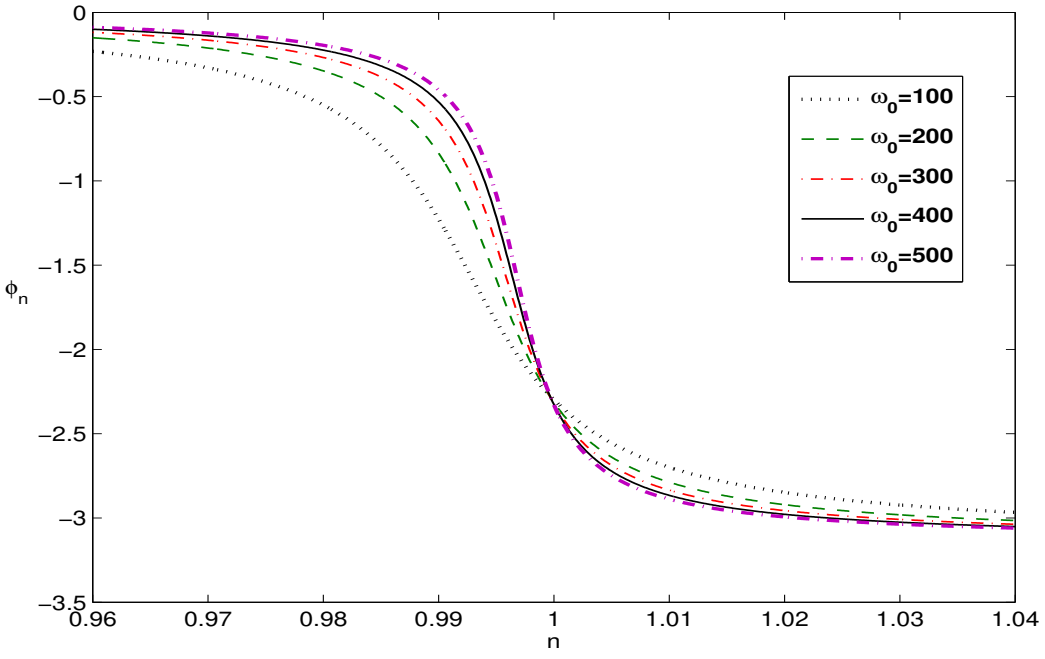

(b)

Figure 2.7: The plot of (a) amplitudes (b) phase frequencies of oscillations of prolate spheroids in the presence of Basset history force for $\kappa = 4$, $\epsilon = 0.3$ and oscillating with different free frequencies, $\omega_0 = 100, 200, ..., 500$.

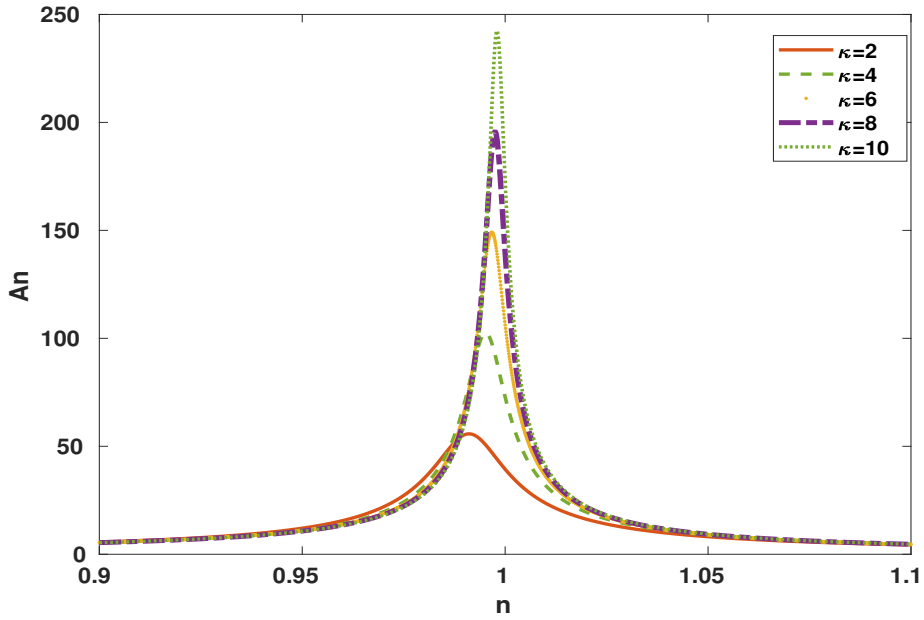

(a)

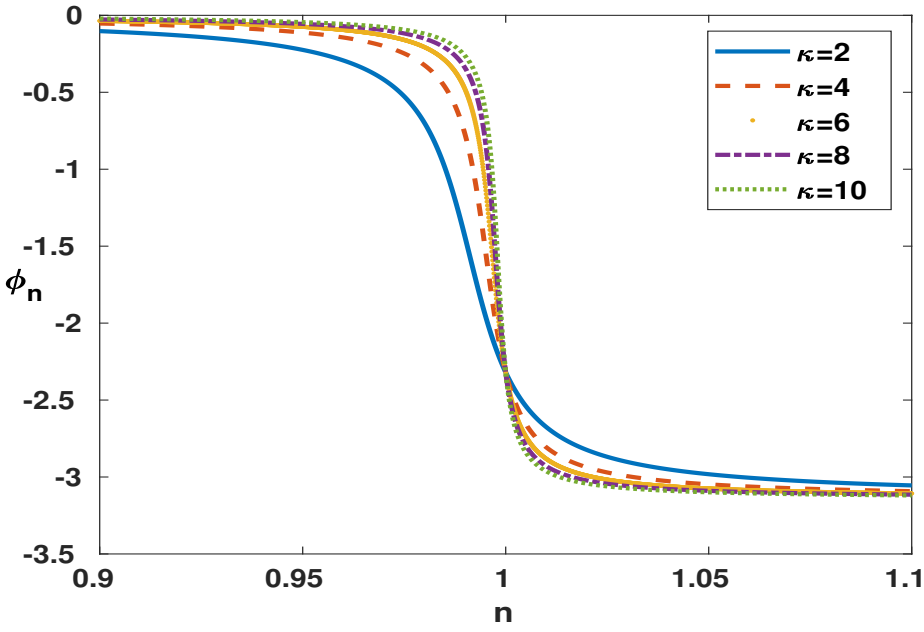

(b)

Figure 2.8: The plot of (a) amplitudes (b) phase frequencies of oscillations of prolate spheroids in the presence of Basset history force for $\epsilon = 0.3, \omega_0 = 200$ and for different density ratios, $\kappa = 2, 4, ..., 10$.

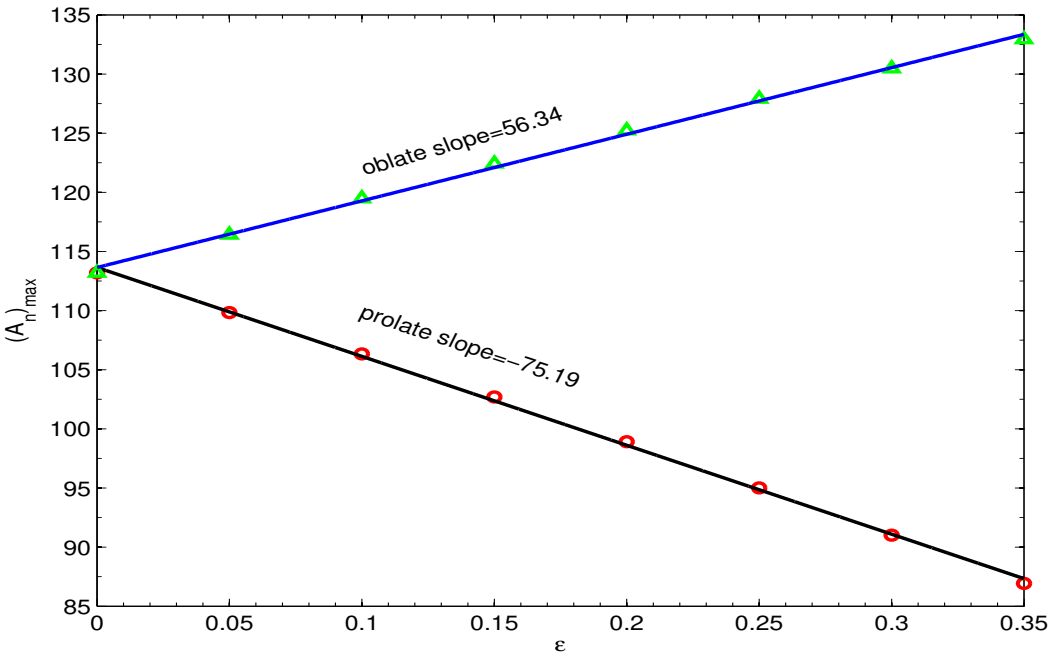

Figure 2.9: The plot showing the variation of numerically computed maximum amplitudes for both the spheroids as a function of ϵ in the presence of Basset memory integral term, showing a linear scaling on eccentricity for $\omega_0 = 200$ and $\kappa = 4$.

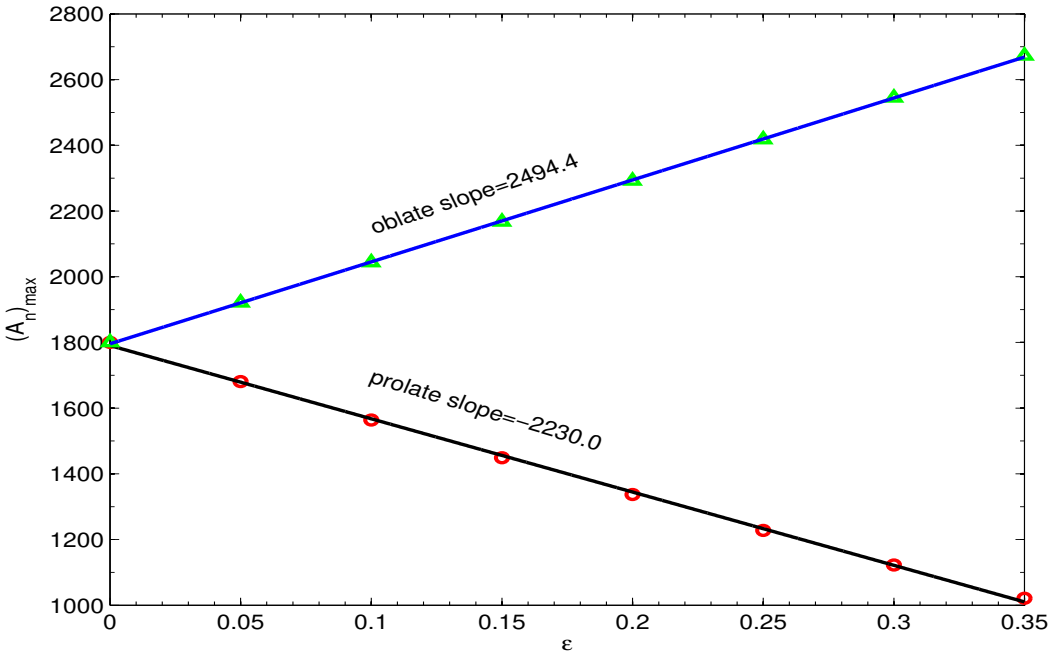

Figure 2.10: The plot showing the variation of numerically computed maximum amplitudes for both the spheroids as a function of ϵ in the absence of Basset memory integral term, showing a linear scaling on eccentricity with higher slopes for $\omega_0 = 200$ and $\kappa = 4$.

phase frequency increases when $n < 1$ and decreases when $n > 1$ for an oblate spheroid as ϵ increases. At the same time the behavior is opposite to this for a prolate spheroid with a higher speed of variation as evident from the figures. The other parameters κ and ω_0 are also varied to study their influence on the oscillation properties of the suspended spheroids. Interestingly, the amplitude of the oscillations increases for all n and the phase value also increases to the left of $n = 1$ and decreases to the right of $n = 1$, surprisingly for both the oblate and prolate spheroids, on increasing the frequency ω_0 of free oscillations in steps of 100. The variation on amplitude and phase values of oscillations of the spheroids on changing the frequency of the free oscillations are dominantly seen from the figures and the variations are greater than that obtained on varying ϵ, as can be seen from the Fig.2.6 and Fig.2.7. Figs. 2.5, 2.6(a) and 2.7(a) also demonstrate that the amplitude of oscillations for an oblates spheroid is more than that of a prolate one for a given eccentricity.

A similar rather stronger variation of properties of oscillations is observed on varying the density ratio of the particle (κ) instead of changing the frequency of free oscillations (ω_0). A pair of typical plots substantiating this argument is shown in Fig.2.8 which resembles the variation shown in Fig.2.7. In short, the phase variations on the change of ω_0 and κ are similar for both the spheroids, whereas it is opposite for oblate and prolate spheroids on changing ϵ.

It is significant to compare the influences of Stokes drag force on the oscillation characteristics of spheroids in the presence as well as in the absence of Basset memory integral force for different values of ϵ. The numerically computed maximum amplitude of oscillations of both the types of oblate and prolate spheroids in the presence and absence of Basset memory integral term for a set values of ϵ is depicted in Figs.2.9 and 2.10. As can be noticed from these figures and Fig.2.5, the oscillation curves of an oblate spheroid are taller than that of a prolate spheroid for a given eccentricity.

It is of interest to record that the maximum value of amplitude increases

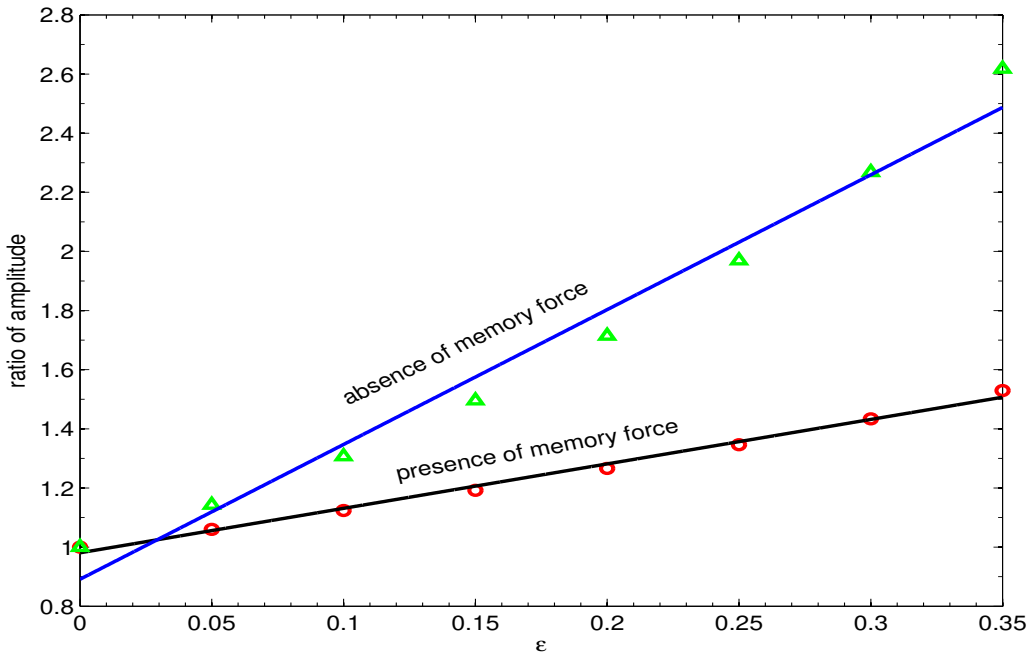

Figure 2.11: A plot of ratios of maximum amplitude of oscillations of an oblate spheroid to that of a prolate spheroid in the presence as well as in the absence of Basset memory integral term for different values of ϵ, $\omega_0 = 200$ and $\kappa = 4$.

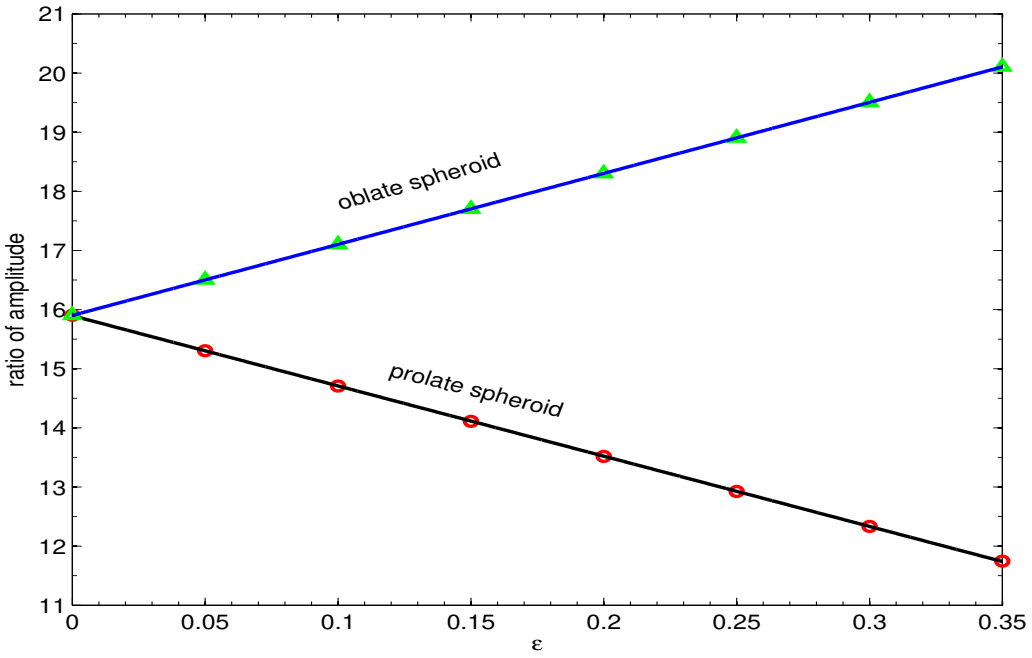

Figure 2.12: A plot of ratios of maximum amplitude of oscillations of a spheroid in the absence of the history integral to that in the presence of the integral, showing the magnitude of reduction of oscillations due to the memory term for different values of ϵ, $\omega_0 = 200$ and $\kappa = 4$.

linearly with slope nearly 56 for oblate spheroids and that decreases linearly with slope nearly -75 for prolate spheroids in the presence of Basset memory integral term as the eccentricity increases as evident from the linear fit shown in Fig.2.9. Fig.2.10 shows that the maximum amplitude varies linearly with slope 2494 and -2230 for oblate and prolate spheroids respectively as ϵ varies in the absence of the Basset memory force. The values of the slopes confirm that the variation of properties of oscillation is high and positive for oblate spheroids, whereas it is high and negative for prolate spheroids in the absence of the memory force. It is also evident from the slopes that the added influence of Basset memory integral force weakens many times the characteristic properties of the oscillations of both oblate and prolate spheroids as can observed from the comparatively small values of the slopes computed.

The ratios of the maximum amplitude of an oblate spheroid to that of a prolate spheroid for a given ϵ in the absence as well as in the presence of the Basset memory force are plotted in the Fig. 2.11. In both situations oscillations of oblate spheroids are larger than that of the prolate spheroids. There is nearly 1 to $2\frac{1}{2}$ times reduction of maximum amplitude on replacing an oblate spheroid by a prolate spheroid in the absence of the memory force, whereas the reduction is only 1 to $1\frac{1}{2}$ times on replacing the particle in the presence of memory force. Another comparison of maximum amplitude of oscillations in absence of the memory integral to that of oscillations in the presence of the term is displayed in the Fig.2.12 for both oblate and prolate spheroids. In this, the maximum amplitude reduction of the oscillations under the influence of the memory force is 16 to 20 times for the case of motion of an oblate spheroid. At the same time, the reduction of maximum amplitude for a prolate spheroid under the effect of the memory integral has come down to 12-16. However, the analysis demonstrates that the presence of memory force increases the resistance to the motion of a spheroid, as expected.

2.4 Conclusion

The results of the work can be summarized as follows. The influence of the memory force on the oscillation properties of rigid particles of different shapes in a viscous flow subjected to an external periodic is significant. The shape, free oscillation frequencies and the density ratio of the particle to suspended fluid have significant impact on the migration properties of a suspended particle. The change in shape leads to the enhancement (reduction) of amplitude peaks in the case of oblate (prolate) spheroid in presence and absence of memory force as the eccentricity increases. It is important to note the amplitude of fluctuations becomes smaller and smaller in the case of prolate spheroids, whereas it becomes larger and larger in the case of oblate spheroid as the eccentricity of the spheroid increases. This means that increase in ϵ suppresses (enhances) the oscillations of particles for prolate (oblate) spheroids. The influence of the other two parameters, density ratio (κ) and frequency of the oscillations (ω_0) is also studied and analyzed in detail. A stronger variation of oscillations on changing these two parameters is observed in comparison with the variations observed due to change in eccentricity. The strong dependence of oscillations on the free oscillation frequency and density ratio of particles is also interesting, whereas the variations of phase values are similar for both the oblate and prolate spheroid on varying ω_0 and κ, but the variations are reversed on replacing oblate spheroids by the prolate spheroids as the eccentricity parameter, ϵ varies.

A linear scaling of maximum amplitude on the eccentricity of both the spheroid in the presence as well as in the absence of Basset memory integral force is observed. Note that the influence of eccentricity on the oscillation properties is linear and high for both oblate and prolate spheroids in the absence of the Basset memory force and hence the presence of the force increases the resistance of the motion of the particle. This linearity may give new insight into the physics of the problem, especially regarding the quantum of velocity disturbances due to the

size of the particle. There is a maximum amplitude reduction of the oscillations under the influence of the memory force and the reduction is many times the amplitude of the oscillation observed in the absence of the force. The amplitude and phase dependence of oscillations on shape of the particle can be utilized for better separation of particles from the suspension to characterize the fluid suspension.

The solutions obtained for the system under consideration are analytical and hence they might have value as tests for more complicated systems. Hence, the problem under consideration in this paper has novelty and strikes a good balance between complication and tractability. The fact that analytical solutions are obtained makes the work valuable for testing software developed for more realistic situations. The study can be extended to analyze the oscillation variation of particles having arbitrary eccentricity in the presence of history integral term (γ) and/or other external forces like magnetic force, acoustic radiation force, electric force etc. Here we have investigated the oscillatory motion of a slightly eccentric spheroid oscillating in a viscous Newtonian fluid at low Reynolds numbers. We have demonstrated the effects of the shape and size of the particle on the oscillations of motion. Also, we have analyzed the effects of the force terms such as damping, Basset memory force, and new history force, individually on the particle's oscillations of motion. we have considered the dynamics o near sphere in this analysis and the properties investigated motivate to extend the study to the dynamics of arbitrary shaped particle. In next chapter we shall investigate the characteristics of oscillations of motion of arbitrary spheroid suspended in viscous Newtonian fluid in low Reynolds numbers limit.

Chapter 3

Periodically driven spheroid in a viscous fluid at low Reynolds numbers

3.1 Introduction

The hydrodynamic forces acting on a body undergoing time-dependent motion, the oscillation properties of particles in a Stokes flow at low Reynolds numbers and the qualitative experiments to validate the predicted quantitative mathematical results developed interest among the researchers working in the area of micro-particle transport and related topics. The authors, Basset (1888b;a); Buchanan (1890); Jeffrey (1922); Taylor (1923); Bretherton (1962b); Williams (1966); Riley (1967); Looker and Carnie (2004); Vasil'ev and Chashechkin (2009) have proposed models and analysed them for the characterization of the transport phenomena. Lawrence and Weinbaum (1988) obtained a general general tensor expression for the functional form of the hydrodynamic force exerted on an arbitrary spheroid of moderate aspect ratio within the range 0.1 to 10 suspended in an unsteady flow field at low Reynolds numbers. Also, the expression for the hydrodynamic forces

such as Stokes drag force, frictional tensor, Basset coefficient and the second history integral force induced on an arbitrary shaped rigid particle undergoing time-dependent fluid motion at low Reynolds number has been introduced in terms of the geometry of the body by Lovalenti and Brady (1993b). The effect of the history force on an oscillating rigid sphere and that of the memory force on slightly eccentric spheroid at low Reynolds number have been analyzed in detail (Abbad and Souhar 2004; Abbad et al. 2006). Resonance properties of motion of sphere and a comparison of motion of rigid spherical particles and gaseous bubbles suspended in a viscous fluid under the influence of an external sinusoidal force in the limit of low Reynolds number has been studied by Stepanyants and Yeoh (2009); Hassan et al. (2017); Hassan and Stepanyants (2017); Ostrovsky and Stepanyants (2018), where the buoyancy force, Stokes drag force, and memory-integral drag force are taken into account. The oscillation properties of solid particles of different shapes in a viscous flow under the action of an external periodic force are significantly important since the dependencies of motion on the system parameters can be utilized for better separation of particles from the fluid or for characterizing the suspension (Kumar et al. (1995); Hassan et al. (2017); Singh and Kumar (2019), and the references therein).

In a recent paper, Singh and Kumar (2021) have investigated motion of the harmonically-forced rectilinear displacement of a weak eccentric spheroid along its axis of symmetry. They have done an incremental advance on the work of Hassan et al. (2017) and also discarded the new memory term, in view of $O(e^2)$, that exists for a non-spherical particle. Their rationale for doing so is that for a near-sphere this new term decays much faster than the Basset term and thus should not affect the particle dynamics too much. While the additional memory term is small for a slightly eccentric spheroid as demonstrated by Singh and Kumar (2021), it is important to note an approximate formula proposed by Lawrence and Weinbaum (1988) for the hydrodynamic force on a spheroid of moderate aspect ratio, for which the effect of the additional memory term on the translation of suspended

particle is not small. These observations motivate the study of the motion of spheroid particles of different shapes in the limit of low Reynolds numbers.

In this study, we derive the transport equation of a spheroid using the expression of the hydrodynamics force developed by Lawrence and Weinbaum (1988) and examine the oscillation properties of dynamics of a spheroid particle in an unsteady viscous flow in the limit of low Reynolds numbers. We find expressions of the conventional Q-curves, amplitude-frequency and phase-frequency of the oscillations of the spheroid at resonance with the natural frequency. We also discuss and compare the effect of damping force, Basset memory force, and the second history integral term on the amplitude and phase oscillations of a spheroid. This study can be utilized to analyze the oscillation variations of particles having arbitrary eccentricity in the presence of history integral term and/or other external forces like a magnetic force, acoustic radiation force, electric force, etc. and to understand how the oscillation properties depend to the change of aspect ratio, density ratio, and free frequency.

3.2 The problem formulation

The displacement, $\boldsymbol{y}$ at time t of a particle of mass, m_p suspended in a fluid at a small Reynolds number, Re is given by the fundamental expression, $m_p \frac{d^2\boldsymbol{y}}{dt^2} = \Sigma\mathbf{F}$; where, $\Sigma\mathbf{F}$ represents the sum of the forces exerted on the particle. In this work, we consider the motion of a periodically forced spheroid subjected to forces due to the natural frequency, ω_0; the hydrodynamic forces, $\mathbf{F}^{\mathrm{H}}(t)$ due to the disturbance in fluid in the vicinity of particle; and an external force, $\mathbf{F}^{\mathrm{ext}}(t)$. What follows is the derivation of the dynamics of a suspended rigid spheroid with equatorial radius, b and polar radius, a of the spheroid. A spheroid particle can be classified as prolate if $k_a > 1$, spherical if $k_a = 1$ and oblate if $k_a < 1$ where the ratio, $k_a = a/b$ is called the aspect ratio of the particle.

The expression for the hydrodynamic force, $\mathbf{F}^{\mathrm{H}}(t)$ exerted at time t on an

arbitrary particle suspended in a time dependent fluid motion with velocity, $\boldsymbol{U}(t)$ has been derived by Lawrence and Weinbaum (1988) as

$$\begin{aligned}\mathbf{F}^{\mathrm{H}}(t) = &- \mathbf{F}_s^{\mathrm{H}}(t)\cdot\boldsymbol{U}(t) - \pi^{-1/2}\boldsymbol{B}\cdot\int_0^t \frac{d\boldsymbol{U}}{d\tau}\,(t-\tau)^{-1/2}\,d\tau - \boldsymbol{m_a}\cdot\frac{d\boldsymbol{U}}{dt} - \\ &e\,(\mathbf{F}_1 - \boldsymbol{B})\cdot\int_0^t \frac{d\boldsymbol{U}}{d\tau}\,\mathrm{erfc}\left[(t-\tau)^{1/2}\right]d\tau,\end{aligned} \tag{3.1}$$

where $\mathbf{F}_s^{\mathrm{H}} = 6\pi\mu a\boldsymbol{\Phi}$ is the Stokes drag correction factor, μ is the dynamic viscosity of the fluid, $\boldsymbol{\Phi}$ is the frictional resistance tensor of the spheroid and is given by $\boldsymbol{\Phi} = \frac{8}{3}e\mathbf{a}$ (Lovalenti and Brady 1993a;b), where e is eccentricity of the spheroid. The tensor, $\mathbf{a} = a_{ij}, \quad i,j = 1,2,3$ is a diagonal matrix and is given by Singh and Kumar (2019) as

$$\begin{aligned}\mathrm{a}_{11} &= \frac{e^2}{-2e + (1+e^2)\log(\frac{1+e}{1-e})},\\ \mathrm{a}_{22} &= \frac{-2e^2}{-2e + (1-3e^2)\log(\frac{1+e}{1-e})},\\ \mathrm{a}_{33} &= \mathrm{a}_{22},\\ \text{and} \qquad \mathrm{a}_{ij} &= 0 \qquad for \qquad i \neq j.\end{aligned} \tag{3.2}$$

For convenience, we prefer the notations $\mathrm{a}_{11} = e_1$; $\mathrm{a}_{22} = \mathrm{a}_{33} = e_2$. The symbols, $\mathbf{F}_1$ and $\boldsymbol{B}$ denote the coefficients of the first-order corrections at low and high frequency in tensor form. Note that $\boldsymbol{B}$ is identified as the Basset coefficient for the spheroid (Lawrence and Weinbaum 1988) and $\mathbf{F}_1 = \mathbf{a}\cdot\mathbf{a}$. The other symbols, $\boldsymbol{m}_a$ and $erfc(t)$ denote the scaled added mass and the standard error function respectively. The Eq.(3.1) represents a more general approximation of the hydrodynamic force for a spheroid of aspect ratio within the range $0.1 < k_a < 10$, with reasonable accuracy.

As explained above, the equation governing the motion of a rigid particle suspended in a fluid subjected to the hydrodynamics force, $\mathbf{F}^{\mathrm{H}}$; force due to natural

frequency, $\tilde{\omega}_0^2 \boldsymbol{y}$; and an external force, $\mathbf{F}^{\text{ext}}(t)$ is given by

$$m_p \frac{d^2 \boldsymbol{y}(t)}{dt^2} + \tilde{\omega}_0^2 \boldsymbol{y}(t) = \mathbf{F}^{\text{ext}}(t) + \mathbf{F}^{\text{H}}(t), \tag{3.3}$$

where $\boldsymbol{y}(t)$ is the displacement of the particle from equilibrium position, m_p is the mass of particle and $\tilde{\omega}_0$ is the Brunt-Vaisala (or buoyancy) natural frequency of oscillations of particle in the absence of dissipation. Inserting Eq.(3.1) in Eq. (3.3), we obtain the following equation of motion in 1-dimensional form.

$$\begin{aligned} \frac{d^2 y(t)}{dt^2} + \tilde{\omega}_0^2 y(t) = & \frac{1}{m_p} \left\{ -\mathrm{F}_s U(t) - \pi^{-\frac{1}{2}} B \int_0^t \frac{dU}{d\tau} (t-\tau)^{-\frac{1}{2}} \, d\tau - m_a \frac{dU}{dt} \right. \\ & \left. - e\,(\mathrm{F}_1 - B) \int_0^t \frac{dU}{d\tau} \operatorname{erfc}\left[(t-\tau)^{\frac{1}{2}}\right] d\tau \right\} + \frac{\mathrm{F}^{\text{ext}}(t)}{m_p}. \end{aligned} \tag{3.4}$$

Making the changes,

$$y(t) = y,$$

$$U(t) = \frac{dy(t)}{dt} = \frac{dy}{dt},$$

and

$$\frac{dU(t)}{dt} = \frac{d^2 y}{dt^2}.$$

and taking $\mathrm{F}^{ext} = A_0 \sin(\tilde{\omega}\, t)$ as the external periodic force having amplitude A_0 and frequency $\tilde{\omega}$, the Eq.(3.4) modifies to

$$\begin{aligned} & \frac{d^2 y}{dt^2} + \tilde{\omega}_0^2 y + \frac{\mathrm{F}_s}{m_p} \frac{dy}{dt} + \frac{\pi^{-\frac{1}{2}} B}{m_p} . \int_0^t \frac{d^2 y}{d\tau^2} (t-\tau)^{-\frac{1}{2}} \, d\tau + \frac{m_a}{m_p} \frac{d^2 y}{dt^2} \\ & + \frac{e\,(\mathrm{F}_1 - B)}{m_p} \int_0^t \frac{d^2 y}{d\tau^2} \operatorname{erfc}\left[(t-\tau)^{\frac{1}{2}}\right] d\tau = \frac{A_0 \sin(\tilde{\omega}\, t)}{m_p}. \end{aligned} \tag{3.5}$$

For the spheroid, it is found that

$$\mathrm{F}_1 = \frac{6\pi\mu a}{(\pi\nu)^{1/2}},$$

$$\mathrm{a}_{11}^2 = \frac{6\pi\mu a}{(\pi\nu)^{1/2}} e_1^2$$

and

$$B = \frac{4\pi\mu a\,(1+e^2)}{(\pi\nu)^{1/2}} \left[\frac{e}{(1+e^2)^{\frac{1}{2}}} - \frac{9}{2} m_a\right]^2 \left[\frac{(2+e^2)}{(1+e^2)^{\frac{1}{2}}} \sinh^{-1}\left(\frac{1}{e}\right) - 1\right],$$

where ν is the kinematic viscosity of the fluid. Assuming ρ_p and ρ as the densities of the solid spheroid and the fluid respectively, the mass of the spheroid, m_p is $\frac{4}{3}\pi a^2 b \rho_p$ and the equivalent mass of the fluid displaced by the spheroid, m_a is $\frac{4}{3}\pi a^2 b\rho$ By taking, $\kappa = \frac{\rho_p}{\rho}$, we have

$$\begin{aligned}(\kappa+1)\frac{d^2y}{dt^2} + \frac{3}{4}\frac{F_s}{\pi a^2 b\rho}\frac{dy}{dt} + \frac{3}{4}\frac{\pi^{-1/2}B}{\pi a^2 b\rho}\int_0^t \frac{d^2y}{d\tau^2}\frac{d\tau}{(t-\tau)^{1/2}} \\ + \frac{3}{4}\frac{e\,(F_1 - B)}{\pi a^2 b\rho}\int_0^t \frac{d^2y}{d\tau^2}\,\mathrm{erfc}\left[(t-\tau)^{\frac{1}{2}}\right] d\tau + \kappa\tilde{\omega}_0^2 y = \frac{A_0\sin(\tilde{\omega}t)}{\frac{4}{3}\pi a^2 b\rho}.\end{aligned} \tag{3.6}$$

By taking,

$$\alpha = \frac{12 e e_1}{(1+\kappa)\,k_a}$$

$$\beta = \frac{9B_1}{2\,(1+\kappa)\,k_a}$$

$$\gamma = \frac{9e}{2\,(1+\kappa)\,k_a}\left(e_1^2 - B_1\right)$$

$$A = \frac{3A_0 a\rho}{4\,(1+\kappa)\,\pi\mu^2},$$

$$\omega_0^2 = \kappa\frac{\tilde{\omega}_0^2 a^3\rho^2}{(1+\kappa)\,\mu^2},$$

and

$$\omega = \frac{a^2}{\nu}\tilde{\omega},$$

and non-dimensionalizing t by a^2/ν and all lengths by a, the governing equation

Eq.(3.6) reduces to

$$\begin{aligned}&\frac{d^2y}{dt^2}+\alpha\frac{dy}{dt}+\beta\int_0^t\frac{d^2y}{d\tau^2}\frac{d\tau}{(t-\tau)^{1/2}}+\gamma\int_0^t\frac{d^2y}{d\tau^2}\,\mathrm{erfc}\left[(t-\tau)^{\frac{1}{2}}\right]d\tau\\&+\omega_0^2y-A\sin(\omega t)=0.\end{aligned}\tag{3.7}$$

The above integro-differential equation represents the motion of a periodically driven spheroid in a viscous fluid at low Reynolds number, where α represents the effect of the damping force, the integral containing β corresponds to the Basset memory force and the second integral containing γ is the history force due to the memory of the previous acceleration of the particle having kernels like $t^{-1/2}$ and an error function of $t^{1/2}$.

3.3 Solutions and discussions

We attempt a trial solution to Eq.(3.7), similar to the classical one outlined by Hassan et al. (2017). A simplest possible trial solution to the Eq.(3.7) can be obtained in the form of

$$\begin{aligned}y(t)=&R_1\cos(\omega t)+R_2\sin(\omega t)\\=&R(\omega,\omega_0)\cos(\omega t-\phi),\end{aligned}$$

with initial values $y_0=y(0)=0$ and $v_0=\dot{y}(0)=0$. Applying Laplace transformation techniques (for calculation of integrals terms in the governing equation see A.2), the amplitude, $R(\omega,\omega_0)$ and the fundamental phase, $\phi(\omega,\omega_0)$ of the trial solution are found using the identities $R(\omega,\omega_0)=\sqrt{R_1^2+R_2^2}$ and $\phi(\omega,\omega_0)=tan^{-1}\left(R_2/R_1\right)$, as

$$R(\omega,\omega_0)=\frac{A}{\sqrt{\left(\alpha\omega+\gamma\omega+\beta\frac{\omega^{\frac{3}{2}}}{2}\sqrt{\frac{\pi}{2}}\right)^2+\left(\omega_0^2-\omega^2-\beta\frac{\omega^{\frac{3}{2}}}{2}\sqrt{\frac{\pi}{2}}\right)^2}},\tag{3.8a}$$

$$\phi(\omega,\omega_0)=\tan^{-1}\left(-\frac{\omega_0^2-\omega^2-\beta\frac{\omega^{\frac{3}{2}}}{2}\sqrt{\frac{\pi}{2}}}{\alpha\omega+\gamma\omega+\beta\frac{\omega^{\frac{3}{2}}}{2}\sqrt{\frac{\pi}{2}}}\right). \tag{3.8b}$$

Clearly, $R(\omega,\omega_0)$ and $\phi(\omega,\omega_0)$ depend on the parameters, κ, k_a and ω_0. We characterize oscillation properties of the spheroid by analysing the solutions at resonance. To have solutions at resonance, amplitude and phase expressions given in Eq.(3.8a) and Eq.(3.8b) are normalized using $\omega = n\omega_0$(i.e. at resonance). For the conventional characterization, two quality factors, Q_α, Q_β (Hassan et al. 2017; Klepper and Kolenkow 2014) corresponding to the effect of damping force and Basset memory term respectively are introduced by choosing $Q_\alpha = \frac{\omega_0}{\alpha}$, $Q_\beta = \frac{8\omega_0}{\pi\beta^2}$ to proceed further. A third quality factor, Q_γ representing the effect of second history integral is newly proposed by taking $Q_\gamma = \frac{\omega_0}{\gamma}$. All the Q-actors are functions of κ, k_a, and ω_0. The amplitude of the particle oscillation is also normalized by choosing $A_n = \omega_0^2\frac{R}{A(\omega,\omega_0)}$. Hence, the expressions Eqs.(3.8a) and (3.8b) reduce to the following for a given n.

$$A_n\left(Q_\alpha,Q_\beta,Q_\gamma\right)=\frac{1}{\sqrt{\left(\frac{n}{Q_\alpha}+\frac{n}{Q_\gamma}+n\sqrt{\frac{n}{Q_\beta}}\right)^2+\left(1-n^2-n\sqrt{\frac{n}{Q_\beta}}\right)^2}}, \tag{3.9a}$$

$$\phi\left(Q_\alpha,Q_\beta,Q_\gamma\right)=\tan^{-1}\left(-\frac{1-n^2-n\sqrt{\frac{n}{Q_\beta}}}{\frac{n}{Q_\alpha}+\frac{n}{Q_\gamma}+n\sqrt{\frac{n}{Q_\beta}}}\right), \tag{3.9b}$$

To understand the dependencies of damping force, Basset memory term, and second history integral on κ, k_a, and ω_0; all the Q-factors are graphed as a function of the parameters. The graphs show that all the factors depend on the parameters κ, k_a, and ω_0, and in particular the dependency is more on k_a than κ, and ω_0. The typical plots of the Q-factors given in Fig.3.1(a-c) reveals that each factor increases as the aspect ratio or/and density ratio or/and natural frequency increases. Interestingly, Q_β values increases more rapidly than Q_α and Q_γ values, whereas the Q_γ increments are less compared to the values of Q_α as the parameter

values increase. In other words, the impact of Q_β, that is the influence of Basset memory force on particle dynamics is high compared to the other two hydrodynamic forces as the parameters varies as can be seen from Fig.3.1(d). The change in Q-curves shows that all the hydrodynamic forces influence the dynamics of a solid particle suspended in a viscous fluid. Most importantly, the role of the new integral force in the transport of suspensions is not negligible at least in the case of dynamics of particles of arbitrary shapes. We use trial solutions at resonance for a detailed study of the transport phenomena

The resonance and phase curves representing the trial solutions are studied by varying the parameters in the presence or/and absence of damping, Basset memory, and second history forces to characterize its effect on oscillations. The sample plot, Fig.3.2 showing the amplitude and phase variations reveals that the new history force plays a significant role in particle dynamics in comparison with the Basset memory force. It is also evident that the impact of damping on particle dynamics is higher than the effect of the other two forces, whereas the quality factor, Q_α indicating damping force is less than the factor, Q_β representing Basset memory force. In short, we find that all the three forces influence the magnitude of the motion: the amplitude increases with the force of damping as well as the second historical integral force, while the presence of Basset memory decreases it. Notably, Basset force causes a phase-shift in oscillations, while the other two forces have no effect on the phase. What follows is a detailed analysis to substantiate these observations. The changes in amplitude and phase of the oscillations of a prolate spheroid at the normalized frequency near 1 are plotted in Fig.3.3 fot $\kappa = 4$, $\omega_0 = 500$, and $k_a = 2, 3, ..., 10$. As the aspect ratio increases, the amplitude increases from 75 to 400 units as can be seen from Fig.3.3a. At the same time, the respective phases moves above for the value of $n \leq 1$ and below for the value of $n \geq 1$ as shown in Fig. 3.3b. Similar amplitude variations and phase-frequency shifts of different scales are observed as the free frequencies and density ratios vary as evident from the Figs.3.4 and 3.5. One can notice from

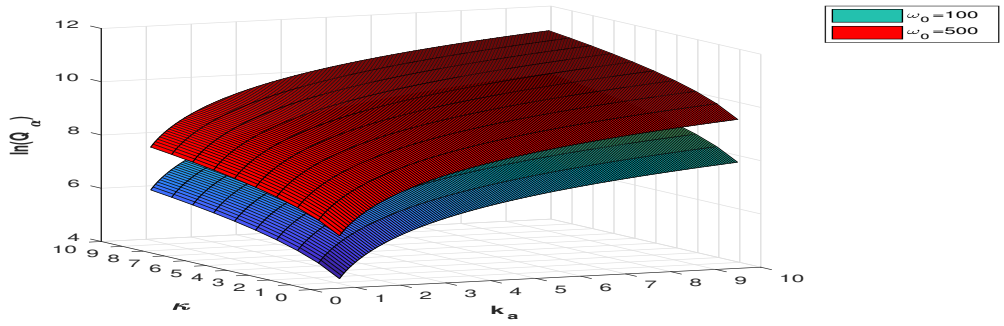

(a)

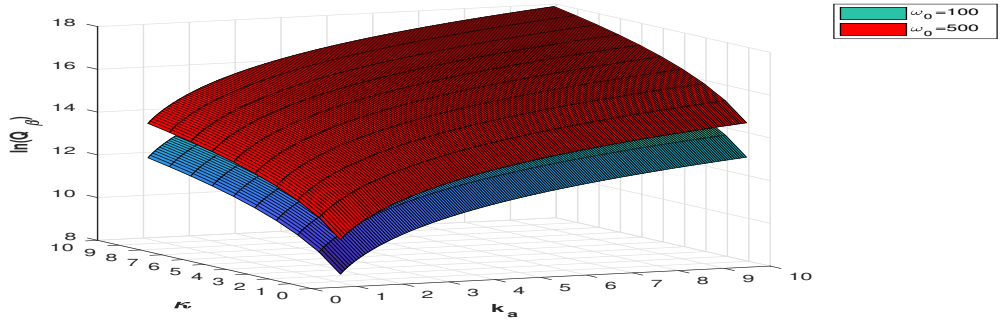

(b)

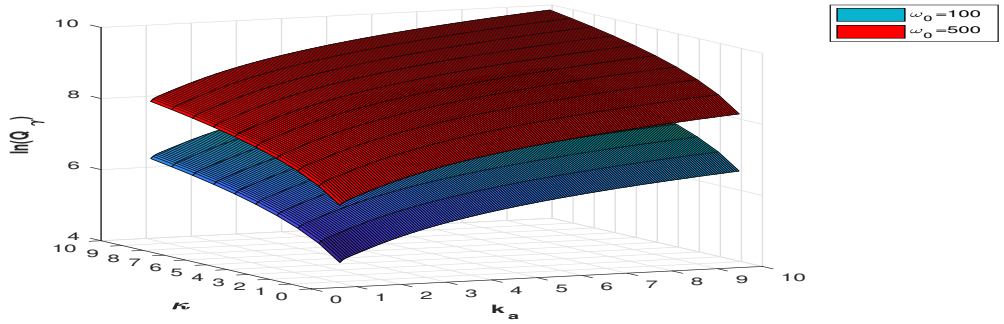

(c)

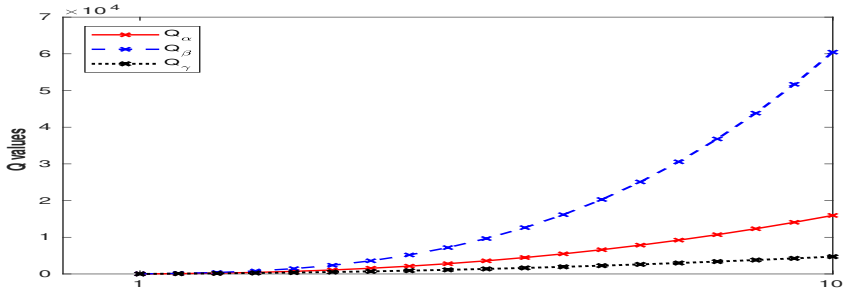

(d)

Figure 3.1: The surface plot of values of (a) Q_α corresponds to damping force, (b) Q_β corresponds to Basset memory integral, (c) Q_γ corresponds to history integral force for κ, k_a, =1,2,3 ... 10, and ω_0 =100, 500. Also, the line plot of values of (d) Q_α, Q_β, and Q_γ for κ, k_a varies from 1 to 10 in steps of 0.5.

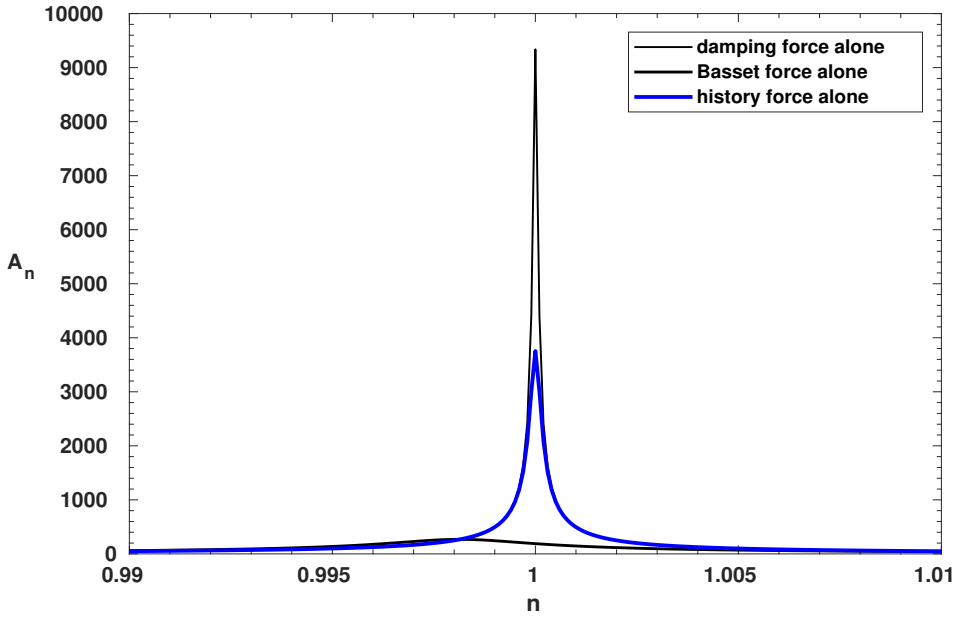

(a)

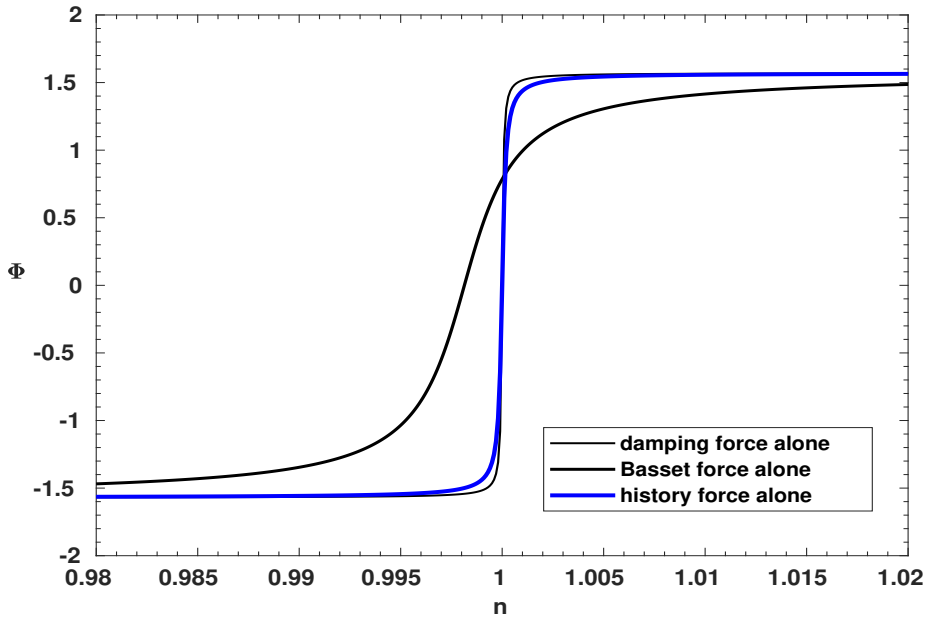

(b)

Figure 3.2: The plot of (a) amplitudes (b) phase oscillations of the trial solutions of a spheroid motion for density ratio $\kappa = 5$, free frequency $\omega_0 = 500$ and aspect ratio $k_a = 5$ showing the effect of the damping force, the Basset memory force and the new history integral force on particle motion

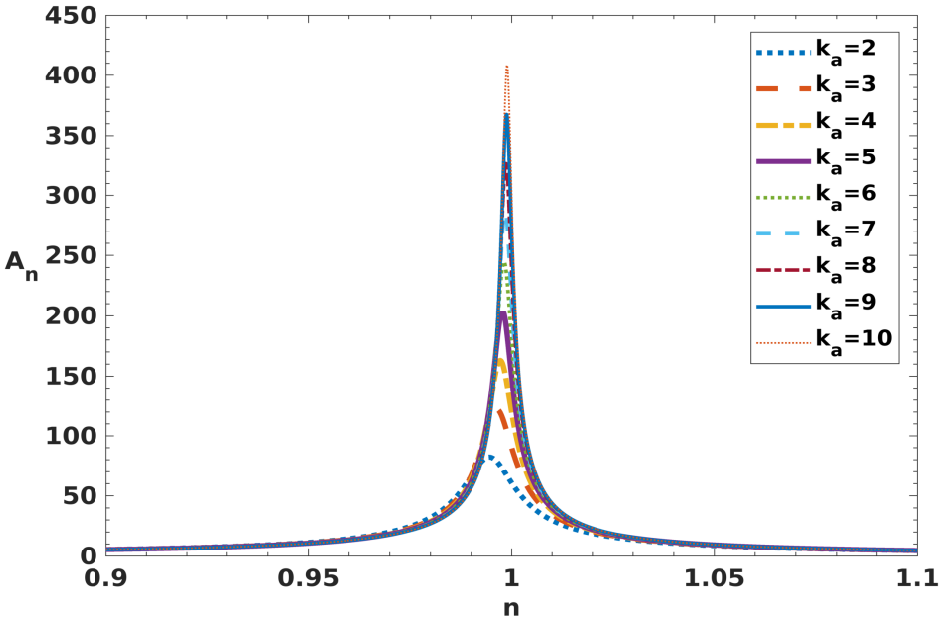

(a)

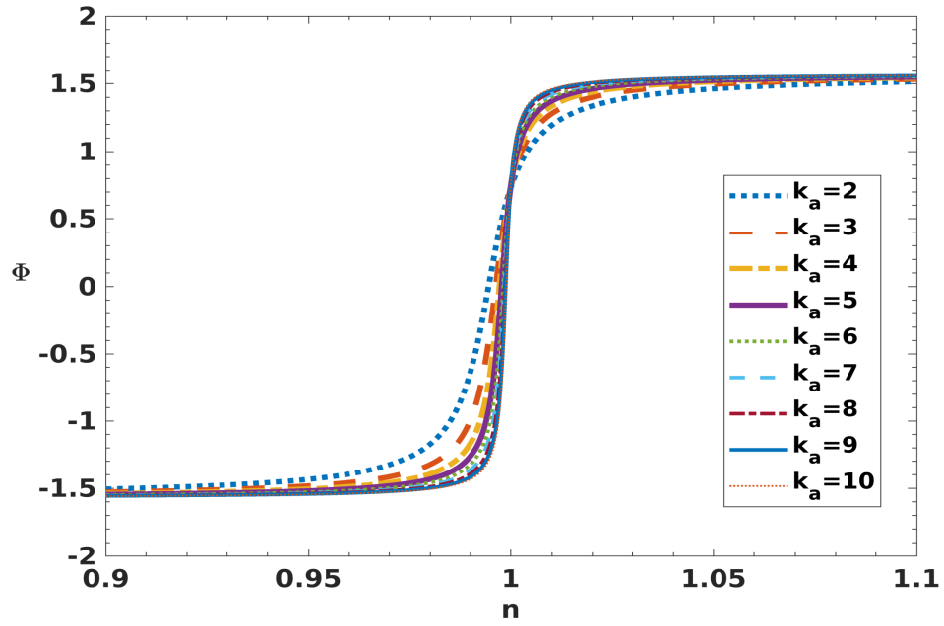

(b)

Figure 3.3: The plot of (a) amplitudes (b) phase oscillations of a prolate spheroid for density ratio $\kappa = 4$, free frequency $\omega_0 = 500$ and different aspect ratios $k_a = 2, 3, ..., 10$

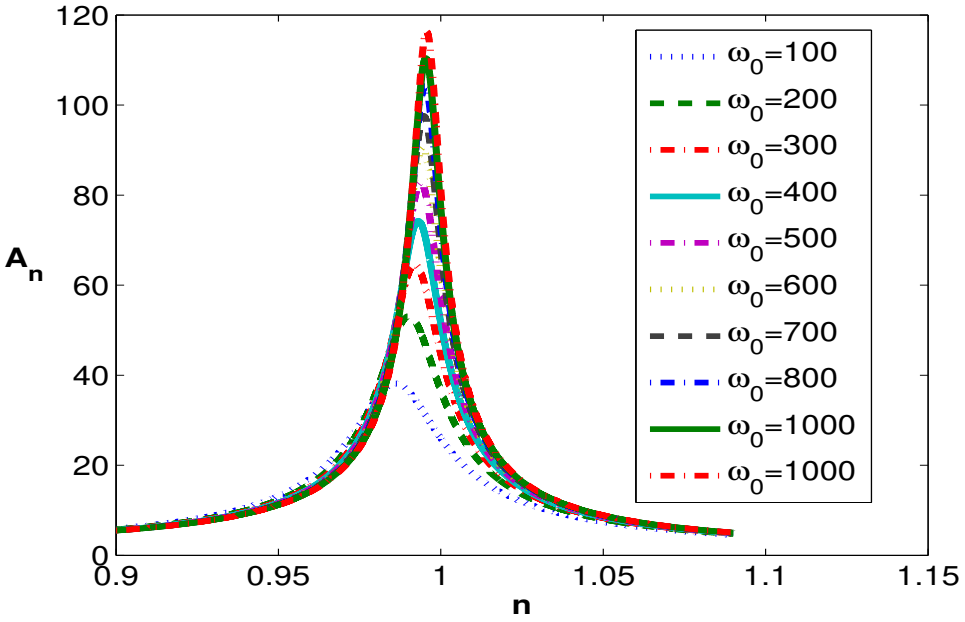

(a)

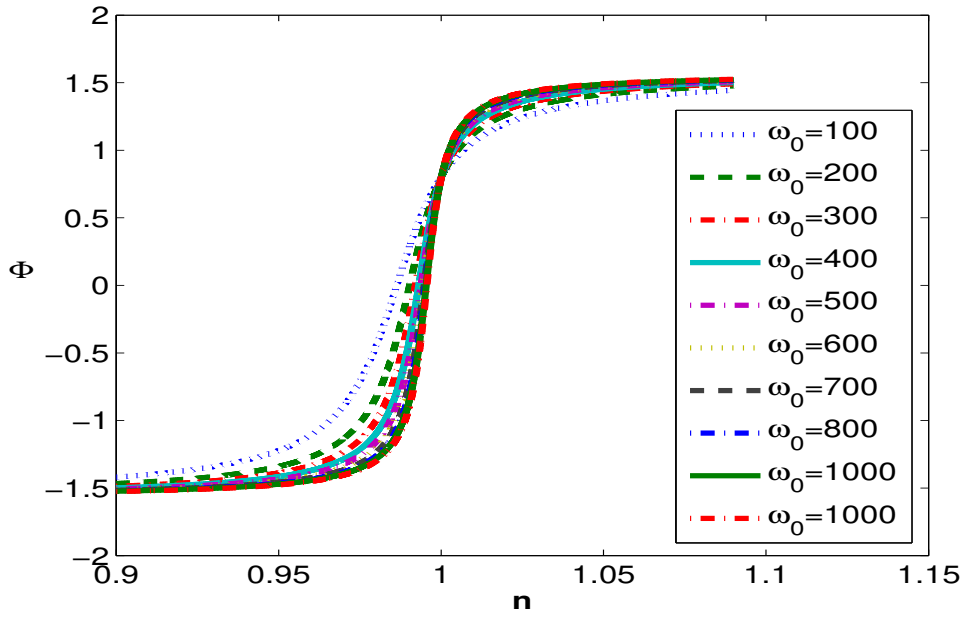

(b)

Figure 3.4: The plot of (a) amplitudes (b) phase oscillations of a prolate spheroid for density ratio $\kappa = 4$, aspect ratio $k_a = 2$ and free frequencies $\omega_0 = 100, 200, ..., 1000$.

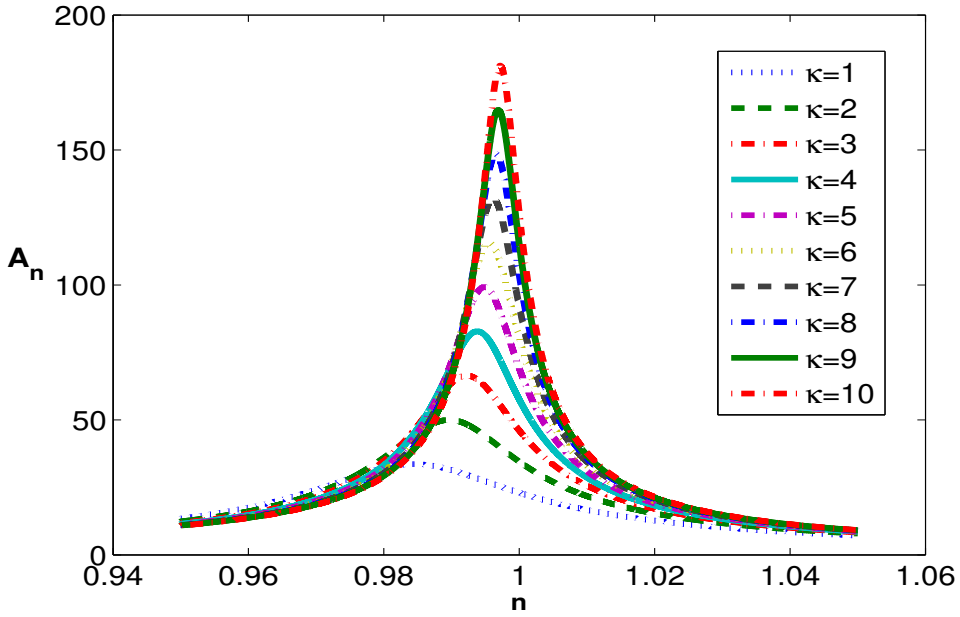

(a)

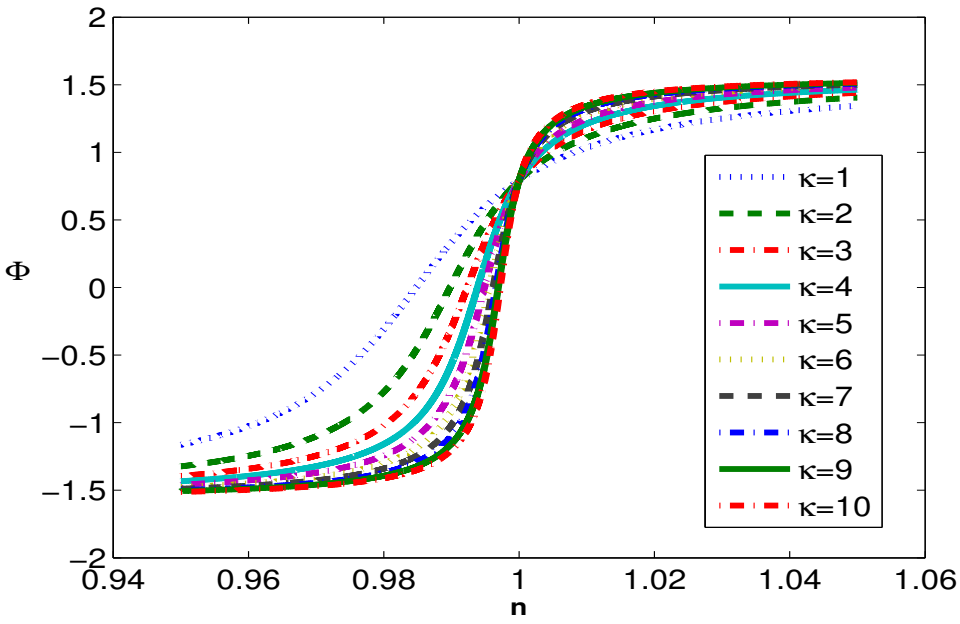

(b)

Figure 3.5: The plot of (a) amplitudes (b) phase oscillations of a prolate spheroid for free frequency $\omega_0 = 500$, aspect ratio $k_a = 2$ and density ratios, $\kappa = 1, 2, ..., 10$.

the Figs. 3.3, 3.4 and 3.5 that the amplitudes get multiplied many times in the presence of the forces as the system parameter increases, whereas the resonant curves change from $n = 1$ to the left of it for all values of the parameters. At the same time, this shifting moves close to $n = 1$ and synchronizes with it for larger values of the parameters. Interestingly, the upward phase-frequency shifting due to the density-ratio variation is higher than that due to the change in aspect ratio and free frequency values as can be seen from the Figs.3.3(b), 3.4(b) and 3.5(b). The shifting due to the Basset memory force prevails even in the presence of damping and second history integral term force as can be seen from the Figs.3.3, 3.4 and 3.5. By and large, these variations in phase shift are comparatively higher for $n \leq 1$ than that for $n \geq 1$ as evident from Fig.3.5b. These findings propose the possibility of reduction/enhancement and phase shifting of the resonance curves by controlling the system parameters.

The above analysis pertains to the cases when all the three forces are accommodated for the study apart from the external periodic force. So, a comparison of oscillations in the presence or/and absence of these forces is worth and may lead to a wide range of phenomenal changes. The spheroid motion due to the effect of the hydrodynamics forces are given in Figs.3.6 and 3.7 for some parameter values. The Figs.3.6(a) and 3.7(a) depict that the amplitude curves of the oscillations coincide each other and hence, the motion is not sensitive to aspect ratio as well as to density ratio in the absence of the hydrodynamic forces. It is clear from the Figs.3.6(b) and 3.7(b), that the amplitude variations due to the damping depend on the aspect ratio and density ratio, whereas no change in phase values is observed for the change in the parameters. There is a reduction in amplitude and a shift in phase to the left side of $n = 1$, once Basset memory is introduced along with the effect of the damping force as can be seen from the figures Figs.3.6(c) and 3.7(c).

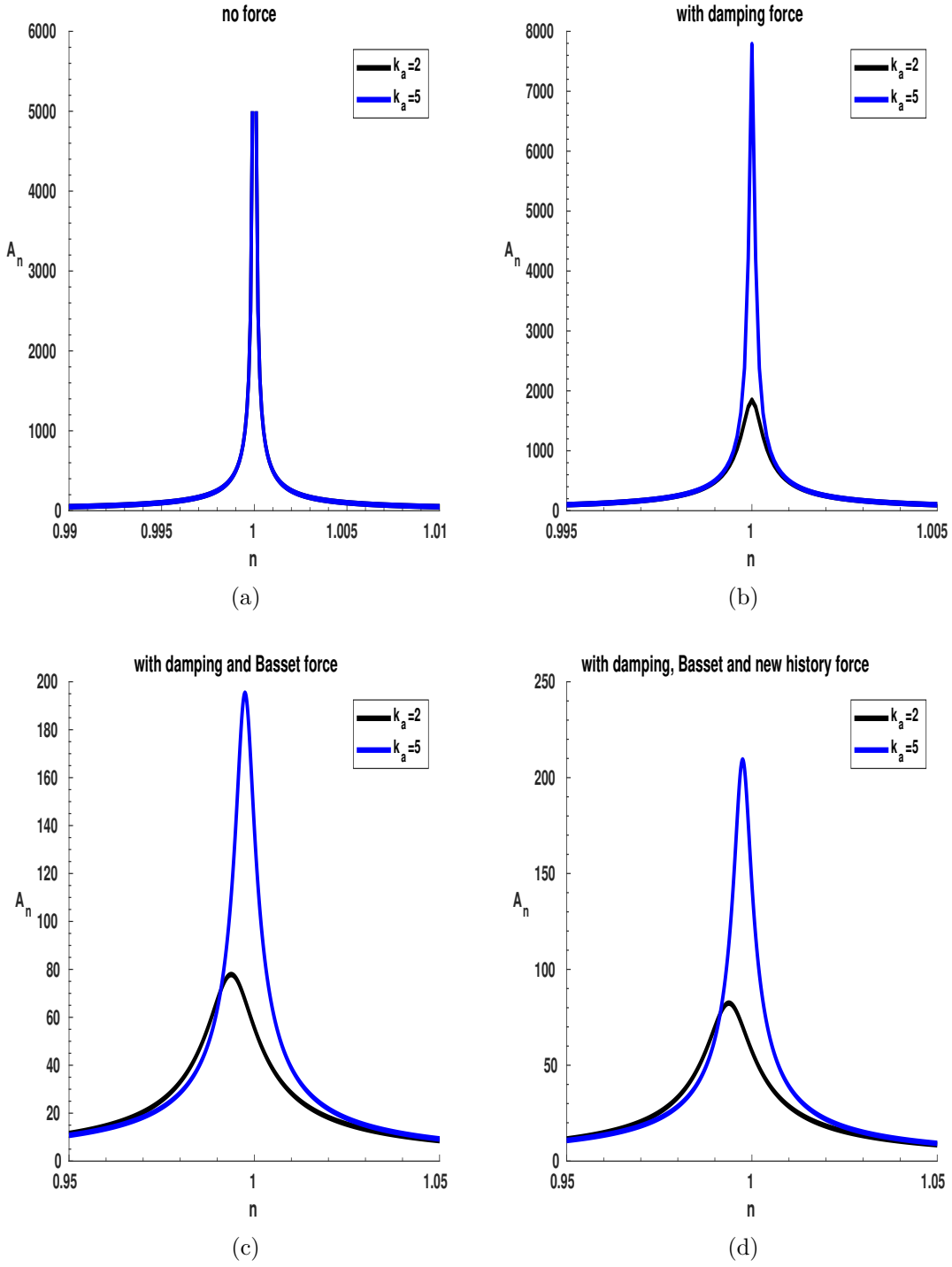

Figure 3.6: The plot of amplitude oscillations of the dynamics in the presence of (a) no hydrodynamic force (b) damping force alone (c) damping force and Basset memory force, and (d) damping force, Basset memory force, and the new history integral term together for $\omega_0 = 500$, $\kappa = 4$, and $k_a = 2, 5$.

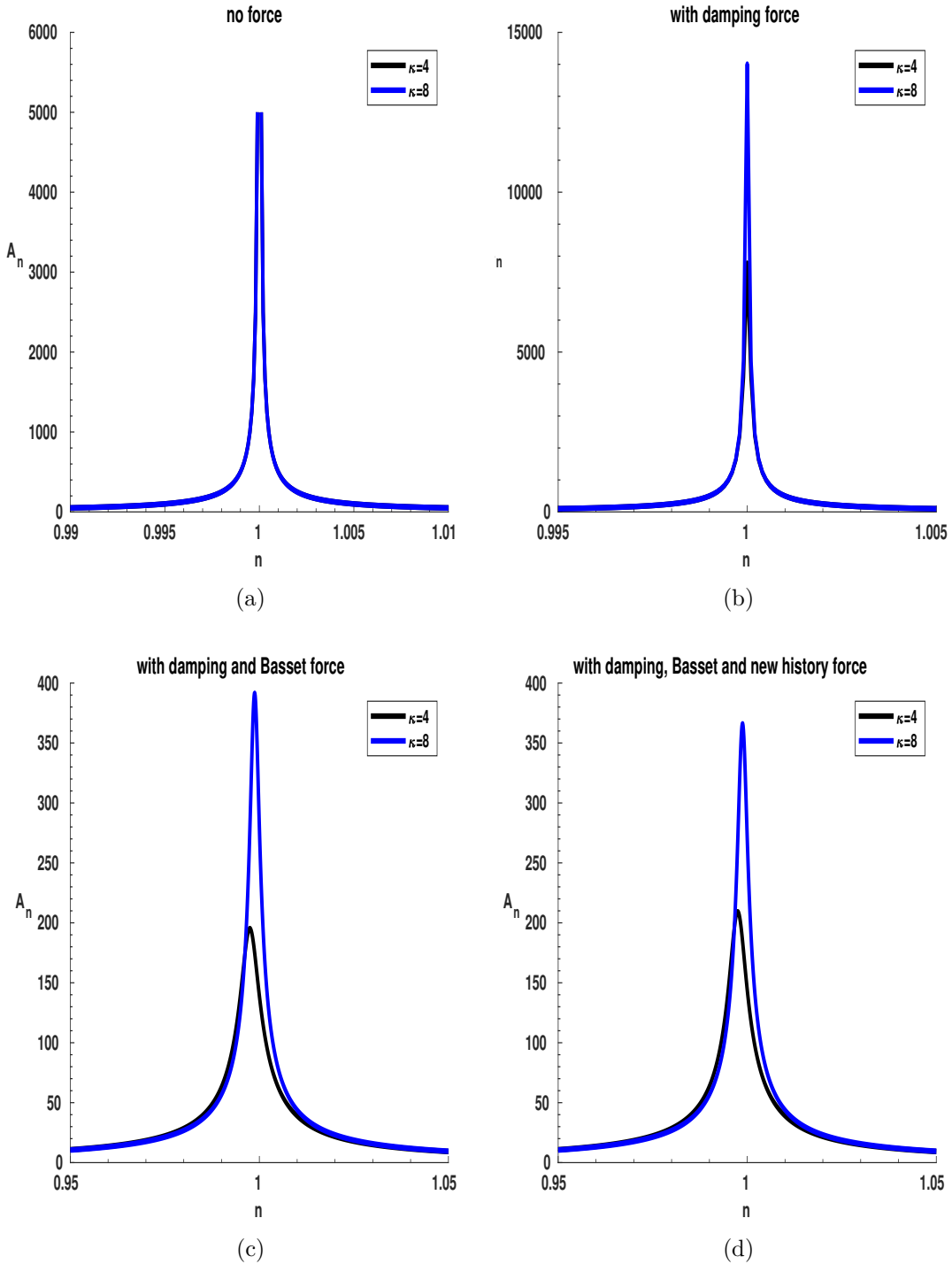

Figure 3.7: The plot of amplitude oscillations of the dynamics in the presence of (a) no hydrodynamic force (b) damping force (c) damping force and Basset memory force, and (d) damping force, Basset memory force, and the new history integral term for $\omega_0 = 500$, $k_a = 5$, and $\kappa = 4, 8$.

This means that change in shape suppresses the oscillations of non-spherical particles due to Basset force. Interestingly, the introduction of the history integral makes a further reduction in amplitude, but maintains the phase shift as evident from the Figs.3.6(d) and 3.7(d). So, the influence of the newly identified history force term on the amplitude of oscillations of spheroids cannot be ignored, unlike spheres and slightly eccentric spheroids as reported earlier Hassan et al. (2017); Singh and Kumar (2021).

3.4 Conclusion

Lawrence and Weinbaum (1986) have provided a general expression of the hydrodynamic force for an unsteady stokes flow of an axisymmetric body in arbitrary motion; then Abbad et al. (2006) have narrowed the derivation to the specific case of a slightly eccentric spheroid. Hassan et al. (2017) have solved a differential equation governing the dynamics of periodically forced bubbles/solid particles of spherical shape; Singh and Kumar (2021) have derived the equation of motion giving a perturbed solution of sphere constrained to one-dimensional oscillations and solved the equation, where the motion is caused by a periodic external force in the limiting case of a small Reynolds number. In this work, we derive an equation of dynamics of periodically forced micro solid spheroids of moderate aspect ratio in a viscous fluid at low Reynolds number under the action of damping, Basset memory, and new history forces. This work provides exact solutions to the dynamics of a spheroid of moderate aspect ratio, using fluid mechanic solutions. The trial solutions of the integrodifferential equation containing the classical Q-factors are investigated at resonance. The results are validated by comparing them with those derived by Hassan et al. (2017); Singh and Kumar (2021) for the limiting case of spherical and near-spherical particles. We also study the well-known Q-curves for a particle under an imposed oscillatory force, which has some utility in terms of clarifying the role of the memory forces particularly

about the phase relationship of the forced oscillations. Unlike the other works, where a drift due to zero or very small eccentricity of spheroid causing no change or negligible change in properties over time is noticed, the change in the Q-curves observed in this problem of spheroid having moderate shape is significantly large as can be seen from the figures. We observe that Q_β varies more rapidly than the other two Q-values in response to the parameter changes. The newly introduced factor, Q_γ corresponding to the new history force depends on the particle aspect ratio (k_a), particle-fluid density ratio (κ) and the natural frequency (ω_0) and also plays a significant role in spheroid dynamics.

The qualitative changes in amplitude and phase shift due to the impact of the damping force, the Basset memory force, and the new history integral are investigated, characterized and compared. Amplitude changes are observed in the presence of all the forces, whereas the shift changes are observed only due to the Basset memory force. This study confirms the significance of second history integral in particle transport as can be seen from the amplitude changes, especially when the particle is geometrically different from a sphere. We demonstrate the role of the parameters k_a, κ, and ω_0 in modifying the Q-curves for a prolate spheroid. The fact that analytic solutions are obtained for a physically realizable system makes the work important for testing software developed for more realistic situations. This study may give insight into the motion of particles under the action of an oscillatory force field due to an acoustic standing wave and hence may be of interest in the context of acoustic streaming. The novelty of the problem strikes a reasonably good balance between complication and tractability. This analysis is of some utility in terms of clarifying the role of the memory force particularly about the phase relationship of the forced oscillations. In This chapter, we have studied the dynamics of an arbitrary spheroidal particle oscillating in a viscous Newtonian fluid at low Reynolds numbers. In this chapter and previous chapter we have analysed dynamics of particles in one dimensional system. The rotational dynamics of particles in 3-dimensional system is also important. Since

it play a major role in describing the rheological parameters of the fluid suspension. The Orientation dynamics of spheroids in quiescent flow will be presented in the next chapter.

Chapter 4

Dynamics of a periodically forced spheroid in a quiescent fluid in the limit of low Reynolds numbers

4.1 Introduction

The study of the motion of micro dipolar particles in flows at low Reynolds numbers is important in a variety of practical situations. There is a considerable interest in the transport of small particles in flows, since a large part of the unsteadiness arises from the disturbance of velocity fluctuations. Hence the unsteady hydrodynamic force in these flows must be considered for analyzing particle motion. The literature is vast in this area starting with the work of Basset (1888b) who developed the expression for the hydrodynamic force acting on a sphere moving in a quiescent fluid including the effects of unsteady inertia. Many researchers have been studied the particle dynamics in linear flows in the absence of external force Jeffrey (1922); Bretherton (1962b); Leal (1971); Brenner (1974)

whereas many others Strand and Kim (1992); Ramamohan et al. (1994) have been analysed the dynamics of suspension under the action of an external force. Mazur and Bedeaux (1974) have generalized the Faxen's theorem to non-steady motion of a spherical particle in an arbitrary incompressible flow. Lawrence and Weinbaum (1986) have studied the axisymmetric motion of a spheroid at low Reynolds numbers. An analysis of axisymmetric flow surrounding a spheroid particle to the the action of the force depending on the aspect ratio is pertinent in the history of fluid analysis Lawrence and Weinbaum (1988). Lovalenti and Brady (1993b) have summarized the literature prior to 1993 and also have derived an approximate expression for the hydrodynamic force acting on an arbitrary rigid particle translating with the time dependent motion in a uniform time dependent flow field including the effects of both unsteady and convective inertia at low Reynolds numbers. Vojir and Michaelides (1994) have published a study on the effect of Basset memory term on the motion of rigid sphere in a viscous fluid. Lawrence and Weinbaum (1988) have explored the Navier-Stokes equations in linear form to obtain expressions for the force acting on an arbitrary body. They deduced the results for a slightly eccentric spheroid and obtained the force expression containing the four terms, namely Stokes drag, added mass, Basset force and a new memory term due to the non-spherical shape of the particle, where the decay of the new memory term is faster than that of Basset force at long time. Kumar et al. (1995) have demonstrated the existence of chaos in the dynamics of periodically forced bodies of spheroids moving in a simple shear flow in the limit of weak Brownian motion. They have seen the existence of chaotic dynamics in certain parametric regions with the strong migration dependence of particles on its shape. This strong dependence of spheroid dynamics on the particle aspect ratio is proposed as a potential application for particle separation from fluid suspension, which is very essential for the characterization of fluid suspensions used in industries. Kumar and Ramamohan (1997) reported a new Class I intermittency near a tangent bifurcation in the dynamics of a periodically forced spheroid suspended in simple

shear flow in the limit of weak Brownian motion.

The group headed by Ramamohan pioneered the area of chaos in periodically forced suspensions of particles in simple shear flow and the results are reported in a number of articles (Ramamohan et al. (1994); Kumar et al. (1996); Radhakrishnan and Ramamohan (2004)). The effect of an external periodic force on the dynamics and rheology of slender rods in a sheared Newtonian fluid has been studied at zero Reynolds number by Kumar and Ramamohan (1995) and, Radhakrishnan and Ramamohan (2004). A review of the work carried out for over a decade, on the dynamics and rheology of suspensions of orientable particles in simple shear flow subject to an external periodic force has been published Asokan et al. (2005). The effect of the eccentricity and the viscosity ratio on the oscillations of solid and gaseous spheroids is investigated by Abbad et al. (2006). The properties of an one dimensional transport along the major axis of a spheroid suspended in a quiescent fluid under an external periodic force at very low Reynolds number are also reported by Madhukar et al. (2010). They also proposed a technique for separating particles from a fluid based on its dynamic dependence on the shape of the particle. Magnaudet (2011) has derived different versions of the reciprocal theorem presenting expression of force exerted on an arbitrary shaped particle translating in an incompressible flow at a given Reynolds number. An analytical investigation of effects of fluid and particle inertia on the dynamics of axisymmetric spheroids in a simple shear fluid has been reported in the limit of a very small Reynolds number and Stokes numbers by Dabade et al. (2016). Recently Marath and Subramanian (2018a) have demonstrated the effect of fluid and particle inertia on the dynamics of spheroid orientation in a planner-linear flow.

In the present work, we extend the results given in Asokan et al. (2005) to the regime of low Reynolds numbers including the effects of both fluid and particle inertia. We derive the governing equations to study the effect of an arbitrary external periodic force on the dynamics of an arbitrary shaped particle, following

the formalism given by Lovalenti and Brady (1993b). This study of dynamics of a rigid particle in a quiescent fluid at low Reynolds numbers with the inclusion of inertia emanate an additional term in the governing equation that represents a fading memory for the entire history of the motion. The memory term becomes nonlinear on the introduction of convective inertia. The equations are numerically solved for some parameters and the results are discussed in detail. The effect of periodic force applies on a spheroidal particle in an arbitrary direction, the hydrodynamic forces arise due to the disturbance of the velocity fluctuations and the forces induce due to the non-spherical nature of the rigid body likely result in a number of novel features, which may be utilized for the development of new technologies.

4.2 Problem statement

The equation of a prolate spheroid in an arbitrary point $\boldsymbol{x} = (x, y, z)$ on it is given by

$$\frac{x^2}{a^2} + \frac{y^2 + z^2}{b^2} = 1, \qquad a > b$$

where a and b are polar and equatorial radii of spheroid respectively. The eccentricity is defined as

$$e = \frac{\sqrt{a^2 - b^2}}{a}$$

and the aspect ratio k_a is defined as a/b. Lovalenti and Brady (1993b) have derived the expression for the required hydrodynamic force on an arbitrary shaped particle, in the long time limit using Fourier transform and reciprocal theorem. As developed by them, the expression for the force on a spheroid undergoing an arbitrary time dependent motion at low Reynolds and Strouhal numbers is obtained as a function of time, $'t'$ in the form,

$$\mathbf{F}^{\mathrm{H}}(t) = ReSl\tilde{V}_p\dot{\mathbf{u}}^{\infty}(t) + \mathbf{F}_s^{\mathrm{H}}(t) - ReSl\left[6\pi\boldsymbol{\Phi}\cdot\boldsymbol{\Phi}\cdot\boldsymbol{\Phi} + \lim_{R\to\infty}\left(\int_{V_f(R)}\mathbf{M}^T\cdot\mathbf{M}dV - \frac{9\pi}{2}\boldsymbol{\Phi}\cdot\boldsymbol{\Phi}R\right)\right]$$

$$\cdot\,\dot{\mathbf{u}}_s(t) + \frac{3}{8}\left(\frac{ReSl}{\pi}\right)^{\frac{1}{2}}\left[\int_{-\infty}^{t}\left\{\frac{2}{3}\mathbf{F}_s^{\mathrm{H}\parallel}(t) - \left[\frac{1}{|\mathbf{A}|^2}\left(\frac{\pi^{\frac{1}{2}}}{2|\mathbf{A}|}erf(|\mathbf{A}|) - exp(-|\mathbf{A}|^2)\right)\right]\mathbf{F}_s^{\mathrm{H}\parallel}(s)\right.\right.$$
$$\left.\left. + \frac{2}{3}\mathbf{F}_s^{\mathrm{H}\perp}(t) - \left[\exp(-|\mathbf{A}|^2) - \frac{1}{2|\mathbf{A}|^2}\left(\frac{\pi^{\frac{1}{2}}}{2|\mathbf{A}|}erf(|\mathbf{A}|) - exp(-|\mathbf{A}|^2)\right)\right]\mathbf{F}_s^{\mathrm{H}\perp}(s)\right\}\frac{2ds}{(t-s)^{\frac{3}{2}}}\right]\cdot\mathbf{\Phi}$$
$$- Re\lim_{R\to\infty}\int_{V_f(R)}(\mathbf{u_0}\cdot\nabla\mathbf{u_0} - \mathbf{u_s(t)}\cdot\nabla\mathbf{u_0})\cdot\mathbf{M}dV + o(ReSl) + o(Re), \tag{4.1}$$

where the first term of the equation is due to the accelerating reference frame, the second term $\mathbf{F}_s^{\mathrm{H}}(t)$ is due to the pseudo-steady state Stokes drag force exerted on the particle, the third is called the acceleration reaction term similar to the added mass and the fourth term represents the unsteady Oseen correction which replaces the Basset memory integral in the long time limit at a finite Reynolds number. The last integral induces a force, normal to the direction of motion of the particle called Lift force. In the above expression, Re represents the Reynolds number indicating the magnitude of the convective inertia related to viscous force, Sl denotes the Strouhal number which will be reduces to 1 in this analysis, $\mathbf{M}$ is the second order tensor depending on the geometry of the particle and is defined such that the vector $\mathbf{M}\cdot\mathbf{u}_p$ is the Stokes velocity field with respect to the particle traveling with velocity $\mathbf{u}_p$ and $\mathbf{M^T}$ is the transpose of $\mathbf{M}$. $\mathbf{u}_0$ is the steady Stokes velocity field in a stationary fluid induced by the movement of the particle, $\mathbf{u}^\infty$ is the velocity of the undisturbed flow with slip velocity $\mathbf{u_s}(t) = \mathbf{u}_p(t) - \mathbf{u}^\infty(t)$ which tend to zero as it is away from particle. $V_f(R)$ is the fluid volume bounded by a spherical surface of radius R surrounding the suspended body and V_p is the particle volume. Note that the expression given in Eq.(4.1) is derived in $o(Re)$ and $o(ReSl)$, where the product $ReSl$ measures the relative magnitude of the unsteady inertia of the fluid. The Stokes resistance tensor $\mathbf{\Phi}$ as the name suggests is an opposing force to the motion of the particle. The dimensionless form of Stoke's resistance tensor for a prolate spheroid is given by $\mathbf{\Phi} = \frac{8}{3}e\mathbf{a}$, where e is the

eccentricity of the spheroid and **a** is the diagonal matrix stated by

$$\begin{aligned} a_{11} &= \frac{e^2}{-2e + (1+e^2)\log(\frac{1+e}{1-e})}, \\ a_{22} &= \frac{-2e^2}{-2e + (1-3e^2)\log(\frac{1+e}{1-e})}, \\ a_{33} &= a_{22}, \\ \text{and} \qquad a_{ij} &= 0 \qquad for \qquad i \neq j. \end{aligned} \tag{4.2}$$

For convenience, we prefer the notations $a_{11} = e_1$; $a_{22} = a_{33} = e_2$. Lawrence and Weinbaum (1988) have given a complex formulation for the axisymmetric motion of a spheroid to compute unsteady Stoke's field, but have failed to find solution for regular perturbation. One can use the concept of Reciprocal theorem and the idea of uniformly valid velocity field to find the unsteady Stoke's correction to pseudo-steady Stoke's drag in the limiting case $ReSl << 1$. We investigate the complex dynamics of a prolate spheroid suspended in a quiescent fluid under the action of a periodic force applies to the body in an arbitrary direction. As a first case, we discuss the dynamics of a prolate spheroid in the fluid at rest and hence assume that $\mathbf{u}^{\infty}(t) = 0$, which leads to $\dot{\mathbf{u}}^{\infty}(t) = 0$. Therefore the first term of Eq.(4.1) becomes

$$\begin{aligned} T_1 =& ReSl\tilde{V}_p \dot{u}^{\infty}(t) \\ =& 0. \end{aligned}$$

As given by Lovalenti and Brady (1993b), the second term $T_2 = \mathbf{F}_s^{\mathrm{H}}(t)$ can be decomposed into two parts namely, $\mathbf{F}_s^{\mathrm{H}\parallel}(s)$ and $\mathbf{F}_s^{\mathrm{H}\perp}(s)$ parallel and perpendicular vectors to the vector **A**. In their expressions,

$$\mathbf{F}_s^{\mathrm{H}\parallel} = 6\pi \mathbf{u}_s \cdot \mathbf{pp} \qquad \text{and} \qquad \mathbf{F}^{\mathrm{H}\perp} = 6\pi \mathbf{u}_s \cdot (\delta - \mathbf{pp}),$$

where δ is the idem tensor of order 2, $\mathbf{p}$ is the unit vector along $\mathbf{y}_s(t) - \mathbf{y}_s(s)$ which is the integrated displacement of the particle relative to fluid from the past time s to the current time t and $\mathbf{A}$ is given by the expression,

$$\mathbf{A} = \frac{Re}{2}\left(\frac{t-s}{ReSl}\right)^{\frac{1}{2}}\left(\frac{\mathbf{y}_s(t)-\mathbf{y}_s(s)}{t-s}\right), \tag{4.3}$$

which itself is parallel to the displacement vector $\mathbf{y}_s(t)-\mathbf{y}_s(s)$. The pseudo-steady state drag force acting on the suspended particle translating with slip velocity $\mathbf{u}_s(t)$ can be written as

$$\mathbf{F}_s^{\mathrm{H}}(t) = -6\pi\mathbf{\Phi}\cdot\mathbf{u}_s(t),$$

where $6\pi\mathbf{\Phi}$ is the Stokes resistance tensor. Hence we have,

$$\begin{aligned}\mathbf{F}_s^{H(t)\parallel}(s) =& 6\pi\left(\mathbf{\Phi}\cdot\mathbf{u}_s(s)\right)\\ =& 6\pi\left(\mathbf{\Phi}\cdot\mathbf{u}_p(s)\right).\end{aligned} \quad \text{and} \quad \mathbf{F}_s^{H\perp}(s) = (0,0,0) \tag{4.4}$$

Representing the velocity, $\mathbf{u}_p$ of the particle exerted by the fluid as $\mathbf{u_p} = (u_x, u_y, u_z)$, we have,

$$T_2 = -16\pi e\left(e_1 u_x(s), e_2 u_y(s), e_2 u_z(s)\right).$$

The acceleration reaction term is given by the third term, T_3 on the right hand side of Eq.(4.1). The equation for the velocity field of the fluid due to the translation of a prolate spheroid is given by Pozrikidis (1992). Chwang (1975) have shown that the velocity field induced by the translation of a prolate spheroid can be written in terms of Stokes-lets, G_{ij} and potential dipoles, D_{ij} which are distributed over the focal length of the spheroid with constant and parabolic densities as given below:

$$v_i(\mathbf{x}) = u_k a_{kj}\int_{-c}^{c}\left[G_{ij}(\mathbf{x},\mathbf{x_0}) - \left(\frac{1-e^2}{2e^2}\right)\left(c^2 - x_0^2\right)D_{ij}(\mathbf{x},\mathbf{x_0})\right]dx_0 \tag{4.5}$$

Here, u_k is the velocity of the particle in the k^{th} direction and $\mathbf{a}$ is the diagonal matrix given above. The Stokeslets, G_{ij} and the potential doublet, D_{ij} are respectively given by

$$G_{ij}(\mathbf{x}, \mathbf{x_0}) = \frac{\delta_{ij}}{|\mathbf{x} - \mathbf{x_0}|} + \frac{(\mathbf{x} - \mathbf{x_0})_i (\mathbf{x} - \mathbf{x_0})_j}{|\mathbf{x} - \mathbf{x_0}|^3} \tag{4.6a}$$

$$D_{ij}(\mathbf{x}, \mathbf{x_0}) = \frac{\delta_{ij}}{|\mathbf{x} - \mathbf{x_0}|^3} - \frac{3(\mathbf{x} - \mathbf{x_0})_i (\mathbf{x} - \mathbf{x_0})_j}{|\mathbf{x} - \mathbf{x_0}|^5} \tag{4.6b}$$

where, $c^2 = a^2 - b^2$, $e = c/a$, $0 < e < 1$, a is the major axis, b is the minor axis, $\mathbf{x_0}$ is the arbitrary pole of the spheroid and $\mathbf{x}$ is the observation point. Now we need to evaluate the integral expression

$$\int_{V_f(R)} \mathbf{M}^T \cdot \mathbf{M} \, dV \tag{4.7}$$

over the volume of the fluid surrounding the particle, where $\mathbf{M}$ is the tensor defined by $v_i = \mathrm{M}_{ij} u_j$. The above integral diverges as the radius of the fluid sphere R, goes to infinity. However we found that the term

$$\int_{V_f(R)} \mathbf{M}^T \cdot \mathbf{M} \, dV - \frac{9\pi}{2} \mathbf{\Phi} \cdot \mathbf{\Phi} R \tag{4.8}$$

converges to a finite value as R approaches infinity. Now, from Eqs.(4.5) and (4.6), we can deduce the following:

$$\mathbf{M} = (\mathbf{a} \cdot \mathbf{H})^T \tag{4.9}$$

where

$$\mathbf{H} = \int_{-c}^{c} \left[G_{ij}(\mathbf{x}, \mathbf{x_0}) - \left(\frac{1 - e^2}{2e^2} \right) (c^2 - x_0^2) D_{ij}(\mathbf{x}, \mathbf{x_0}) \right] dx_0 \tag{4.10}$$

The integral given in Eq.(4.10) can be computed numerically using the expression derived for $\mathbf{M}$. The reason for the above choice is that we could accommodate a larger number of data points, increasing the accuracy of the integral. Incorporating all these, the third term of the force reduces to

$$\begin{aligned}\mathbf{T_3} =& ReSlDiag(I_{xx}, I_{yy}, I_{zz}) \cdot \dot{\mathbf{u}}_\mathbf{s} \\ =& ReSl\left[I_{xx}\dot{u}_x(t), I_{yy}\dot{u}_y(t), I_{zz}\dot{u}_z(t)\right],\end{aligned} \tag{4.11}$$

where the 3^{rd} order diagonal matrix representing the expression within the square brackets in the acceleration reaction term given in Eq.(4.11) is denoted by

$$Diag(I_{xx}, I_{yy}, I_{zz}) \tag{4.12}$$

The new history integral in the long time limit at finite Re is the forth term in the force expression and is given by

$$\begin{aligned}T_4 =& \frac{3}{8}\left(\frac{ReSl}{\pi}\right)^{\frac{1}{2}}\left[\int_{-\infty}^{t}\left\{\frac{2}{3}\mathbf{F}_s^{H\parallel}(t) - \left[\frac{1}{|\mathbf{A}|^2}\left(\frac{\pi^{\frac{1}{2}}}{2|\mathbf{A}|}erf(|\mathbf{A}|) - \exp(-|\mathbf{A}|^2)\right)\right]\mathbf{F}_s^{H\parallel}(s) + \frac{2}{3}\mathbf{F}_s^{H\perp}(t)\right.\right. \\ & \left.\left. - \left[\exp(-|\mathbf{A}|^2) - \frac{1}{2|\mathbf{A}|^2}\left(\frac{\pi^{\frac{1}{2}}}{2|\mathbf{A}|}erf(|\mathbf{A}|) - \exp(-|\mathbf{A}|^2)\right)\right]\mathbf{F}_s^{H\perp}(s)\right\}\frac{2ds}{(t-s)^{\frac{3}{2}}}\right]\cdot\mathbf{\Phi} \\ =& \frac{3}{8}\left(\frac{ReSl}{\pi}\right)^{\frac{1}{2}}\left[\int_0^t\left\{\frac{2}{3}\times -16\pi e\left(e_1u_x(t), e_2u_y(t), e_2u_z(t)\right) - \right.\right. \\ & \left.\left. B\times(-16)\pi e\left(e_1u_x(s), e_2u_y(s), e_2u_z(s)\right)\right\}\frac{2ds}{(t-s)^{\frac{3}{2}}}\right]\cdot\mathbf{\Phi} \\ =& \frac{3}{8}\left(\frac{ReSl}{\pi}\right)^{\frac{1}{2}}\int_0^t\left\{-\frac{256}{9}\pi e^2\left(e_1^2u_x(t), e_2^2u_y(t), e_2^2u_z(t)\right) + \right. \\ & \left.\frac{128}{3}\pi e^2B\left(e_1^2u_x(s), e_2^2u_y(s), e_2^2u_z(s)\right)\right\}\frac{2ds}{(t-s)^{\frac{3}{2}}},\end{aligned} \tag{4.13}$$

where

$$B = \frac{1}{|\mathbf{A}|^2}\left(\frac{\pi^{\frac{1}{2}}}{2|\mathbf{A}|}erf(|\mathbf{A}|) - \exp(-|\mathbf{A}|^2)\right) \qquad \text{and} \qquad \mathbf{F}_s^{H\perp}(s) = \mathbf{0}. \tag{4.14}$$

As can be seen from the term T_4, there is a singularity at $s = t$. In order to avoid the singularity, we split the history integral into two integrals over the non-overlapping intervals $[0, t-\epsilon]$ and $(t-\epsilon, t]$, where ϵ is arbitrary. The integrals are denoted by T_4' and T_4'' respectively. Hence, we have

$$\begin{aligned} T_4' =& \frac{3}{8}\left(\frac{ReSl}{\pi}\right)^{\frac{1}{2}}\left\{\frac{-512}{9}\pi e^2\left(e_1^2u_x(t), e_2^2u_y(t), e_2^2u_z(t)\right) \times (-2)\left(t^{-\frac{1}{2}} - \epsilon^{-\frac{1}{2}}\right)\right. \\ &\left. + \frac{256}{3}\pi e^2 \int_0^{t-\epsilon} B\left(e_1^2u_x(s), e_2^2u_y(s), e_2^2u_z(s)\right)\frac{ds}{(t-s)^{\frac{3}{2}}}\right\} \\ =& \frac{3}{8}\left(\frac{ReSl}{\pi}\right)^{\frac{1}{2}}\left\{\frac{1024}{9}\pi e^2\left(e_1^2u_x(t), e_2^2u_y(t), e_2^2u_z(t)\right)\left(t^{-\frac{1}{2}} - \epsilon^{-\frac{1}{2}}\right)\right. \\ &\left. + \frac{256}{3}\pi e^2 \int_0^{t-\epsilon} B\left(e_1^2u_x(s), e_2^2u_y(s), e_2^2u_z(s)\right)\frac{ds}{(t-s)^{\frac{3}{2}}}\right\}. \end{aligned} \tag{4.15}$$

We observe that the numerical integral converges to a finite value in the limiting case of $s \to t$ and hence the value of integral in the range $(t-\epsilon, t]$ can be neglected by choosing ϵ very small. Numerical computation of the second integral also shows that $T_4'' \to 0$ as $\epsilon \to 0$. Hence $T_4 = T_4'$. The next task is the evaluation of the lift force given by the $5th$ term of the force equation. We need to integrate the following expression T_5, for computing the lift force.

$$T_5 = \lim_{R\to\infty} \int_{V_f(R)} (\mathbf{u_0} \cdot \mathbf{\Delta u_0} - \mathbf{u_s(t)} \cdot \mathbf{\Delta u_0})\mathbf{M}\, dV. \tag{4.16}$$

where the expressions for $\mathbf{M}$, $\mathbf{u_s}$ are given earlier. The initial velocity, $\mathbf{u_0}$ of the fluid is to be found out. Since the flow under consideration is a quiescent fluid medium, we have $u^\infty(t) = (0, 0, 0)$ and thus, $u_s(t) = u_p(t)$. Also by definition,

$u_0 = \mathbf{M} \cdot \mathbf{u}_s(t)$. Thus, the required expression for the lift force, say, the vector $\mathbf{L} = (L_1, L_2, L_3)$ can be evaluated separately.

Introducing all these simplifications, the expression given in Eq.(4.1) for the hydrodynamic force deduces to,

$$\begin{aligned} F^H(t) = &- 16\pi e \left(e_1 u_x(t), e_2 u_y(t), e_2 u_z(t)\right) - ReSl \left(I_{xx}\dot{u}_x(t), I_{yy}\dot{u}_y(t), I_{zz}\dot{u}_z(t)\right) + \\ &\frac{3}{8}\left(\frac{ReSl}{\pi}\right)^{\frac{1}{2}} \left\{ \frac{1024}{9}\pi e^2 \left(e_1^2 u_x(t), e_2^2 u_y(t), e_2^2 u_z(t)\right) \left(t^{-\frac{1}{2}} - \epsilon^{-\frac{1}{2}}\right) \right. \\ &\left. + \frac{256}{3}\pi e^2 \int_0^{t-\epsilon} B\left(e_1^2 u_x(s), e_2^2 u_y(s), e_2^2 u_z(s)\right) \frac{ds}{(t-s)^{\frac{3}{2}}} \right\} - Re \left(L_1, L_2, L_3\right). \end{aligned} \tag{4.17}$$

The Eq.(4.17) represents the hydrodynamic force induced on a neutrally buoyant spheroid in an infinite body of quiescent fluid. In addition to the hydrodynamic force given in Eq.(4.17), we assume that there is an external periodic force denoted by $\mathbf{F}^{ext}$ acting on the spheroid. Following the Newton's law of motion, the equation of motion for neutrally buoyant particle immersed in a Newtonian fluid under the effect of the external periodic force in dimensionless form is given by

$$\frac{m_p \dot{\mathbf{u}}_p(t)}{\mu a^2 \omega} = \mathbf{F}^{\mathrm{H}}(t) + \mathbf{F}^{ext}(t) \tag{4.18}$$

and the displacement of the particle $\mathbf{y}_p(t) = (y_x(t), y_y(t), y_z(t))$ can be evaluated from

$$\frac{d\mathbf{y}_p(t)}{dt} = \mathbf{u}_p(t),$$

where $\mathbf{u}_p(t) = (u_x(t), u_y(t), u_z(t))$. Taking, $\mathbf{F}^{ext} = (F_1, F_2, F_3)\sin(t)$, (4.18) can be written as

$$\frac{du_x(t)}{dt} = \frac{1}{C_1 Re}\left[F_1 \sin(t) - 16\pi e e_1 u_x(t) - \frac{3}{8}\left(\frac{ReSl}{\pi}\right)^{\frac{1}{2}} (P_1 + Q_1) - ReL_1\right] \tag{4.19a}$$

$$\frac{du_y(t)}{dt} = \frac{1}{C_2 Re}\left[F_2\sin(t) - 16\pi e e_2 u_y(t) - \frac{3}{8}\left(\frac{ReSl}{\pi}\right)^{\frac{1}{2}}(P_2+Q_2) - ReL_2\right] \quad (4.19b)$$

$$\frac{du_z(t)}{dt} = \frac{1}{C_3 Re}\left[F_3\sin(t) - 16\pi e e_2 u_z(t) - \frac{3}{8}\left(\frac{ReSl}{\pi}\right)^{\frac{1}{2}}(P_3+Q_3) - ReL_3\right] \quad (4.19c)$$

$$\frac{dy_x(t)}{dt} = u_x(t), \qquad \frac{dy_y(t)}{dt} = u_y(t), \qquad \frac{dy_z(t)}{dt} = u_z(t). \quad (4.20)$$

where

$$C_1 = \frac{4\pi}{3}\left(\frac{b}{a}\right)^2 + SlI_{xx} \qquad C_2 = \frac{4\pi}{3}\left(\frac{b}{a}\right)^2 + SlI_{yy} \qquad C_3 = \frac{4\pi}{3}\left(\frac{b}{a}\right)^2 + SlI_{zz}$$

$$P_1 = \frac{256\pi e^2}{3}\int_0^{t-\epsilon} Be_1^2 u_x(s)\,(t-s)^{-\frac{3}{2}}\,ds \qquad P_2 = \frac{256\pi e^2}{3}\int_0^{t-\epsilon} Be_2^2 u_y(s)\,(t-s)^{-\frac{3}{2}}\,ds$$

$$P_3 = \frac{256\pi e^2}{3}\int_0^{t-\epsilon} Be_2^2 u_z(s)\,(t-s)^{-\frac{3}{2}}\,ds \qquad Q_1 = \frac{1024}{9}\pi e^2 e_1^2 u_x(t)\left(t^{-1/2} - \epsilon^{-1/2}\right)$$

$$Q_2 = \frac{1024}{9}\pi e^2 e_2^2 u_y(t)\left(t^{-1/2} - \epsilon^{-1/2}\right) \qquad Q_3 = \frac{1024}{9}\pi e^2 e_2^2 u_z(t)\left(t^{-1/2} - \epsilon^{-1/2}\right).$$

and the time t has been scaled with respect to the frequency of the external periodic force.

The validity of the Eqs.(4.19) and (4.20) governing the dynamics of a spheroid is verified in two ways. The effect of both convective and unsteady inertia on the dynamics of a dilute suspension of periodically forced neutrally buoyant spherical particles in a quiescent Newtonian fluid at low Reynolds numbers has been studied by Ramamohan et al. (2011), where they have considered external force along the direction of the x-axis. Since the external force has been applied along the direction of transport of the sphere, the lift force on it has been vanished. It is verified that the Eqs.(4.19) and (4.20) analytically deduces to the equations given by them on choosing $k_a = 1$ which corresponds to a sphere, and $\mathbf{L} = \mathbf{0}$ which

means no lift force experiences. Secondly it is demonstrated that the Eqs.(4.19) and (4.20) reduces to the equations derived by Madhukar et al. (2010) who have demonstrated the dynamics of a spheroid in a quiescent fluid at low Reynolds number on restricting the external force along the x component alone. In both cases, the numerical computation of lift force shows that it is negligibly small for a movement of a sphere and spheroid under the action of a force along x direction. It is numerically verified that the results obtained in the our analysis is in good agreement with the work of Madhukar et al. (2010).

4.3 Results and discussion

After obtaining all the necessary expressions and values for different aspect ratios, we proceed to solve the more general set of ODEs given in Eqs.(4.19) and (4.20) for different sets of parameters. We should note the following facts about the differential equation. It is evident from the equations that the system of differential equations is nonlinear and contains a history term of all the past values of the position, $\mathbf{y_p}(t)$ and the corresponding velocity, $\mathbf{u_p}(t)$ and hence impossible to solve symbolically. As an alternative, it has to be simulated numerically for further analysis. A spherical coordinate system is suggested for evaluating the integral numerically. A set of codes in MATLAB is written to compute the expressions involved in the equations and to solve the final set of differential equations. As a first case, we consider forces $F = F_1 = F_2 = F_3$ and the numerical computation of the lift force shows that its effect on the transport of particles is in the order of $o(10^{-10})$ and hence ignored for the present analysis. The position, $\mathbf{y_p}(t)$ and velocity, $\mathbf{u_p}(t)$ are computed from the ODE's as a function of time. To understand the long time behavior of the system, we plot the position and velocity trajectories after removing the transient dynamics, where all trajectories are computed assuming the initial position of the spheroid as $\mathbf{y_p} = (0, 0, 0)$. For a preliminary analysis, plots are generated from the simulation for different sets of

parameters k_a, R_e and F. The aspect ratio k_a is varied over the range $1 \leq k_a \leq 10$ in steps of 1, where as the external force F and the Reynolds number Re are varied over the ranges $0 \leq F \leq 4.0$ and $0 \leq Re \leq 0.5$ in steps 0.5 and 0.05 respectively. A set of typical plots showing the oscillations of x-component of attractors of position and the corresponding velocity of migration of the spheroid, unveiling the variation on amplitude, and phase shift as a function of k_a, F and Re are shown in Figs.4.1-4.3 respectively. The dependence of position and velocity of migration of spheroids on particle size is evident from the Fig.4.1. The particles are settled in different positions for a given time with different velocities for different aspect ratios, as can be seen from the Fig.4.1. The position and velocity oscillate with almost equal wave length for different aspect ratios, whereas the amplitude of the oscillations changes as the aspect ratio changes. Interestingly, the maximum amplitude of both the oscillations increases as the particle size increases as evident from Figs 4.1 and 4.5(a). Similar variations are observed in the oscillation of position and velocity on varying the external force, keeping the other two parameters k_a and Re same, as can be seen from the Figs.4.2 and 4.5(b). It is evident from Figs.4.1 and 4.2 that the size of the attractor of position and velocity of spheroid dynamics increases in the long run on increasing the particle aspect ratio or/and external force. This variation of oscillations observed on the aspect ratio or/and external force demonstrates a strong dependence of solution on external force and aspect ratio. As the amplitude of the periodic force increases, the particle also oscillates with greater amplitude, covering greater surface area in the attractor plot as revealed from the Fig.4.2. On the other hand, it is observed that the size of the attractor of position and velocity shrinks as the Reynolds number increases as can be seen from the typical plot, Fig.4.3 showing the variation of attractor size for different R_e values. As the parameter Re, increases the position and velocity waves oscillate with the almost same period, whereas the amplitude of both waves slowly decreases as observed from Figs.4.3 and 4.5(c). This shows how the inertia slows down the migration of a spheroid particle having the same size under

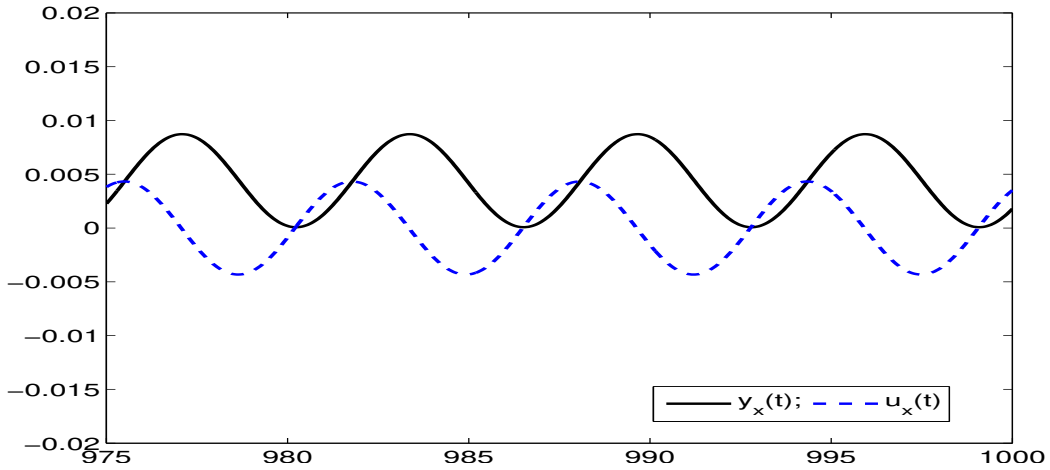

(a) $k_a = 2$

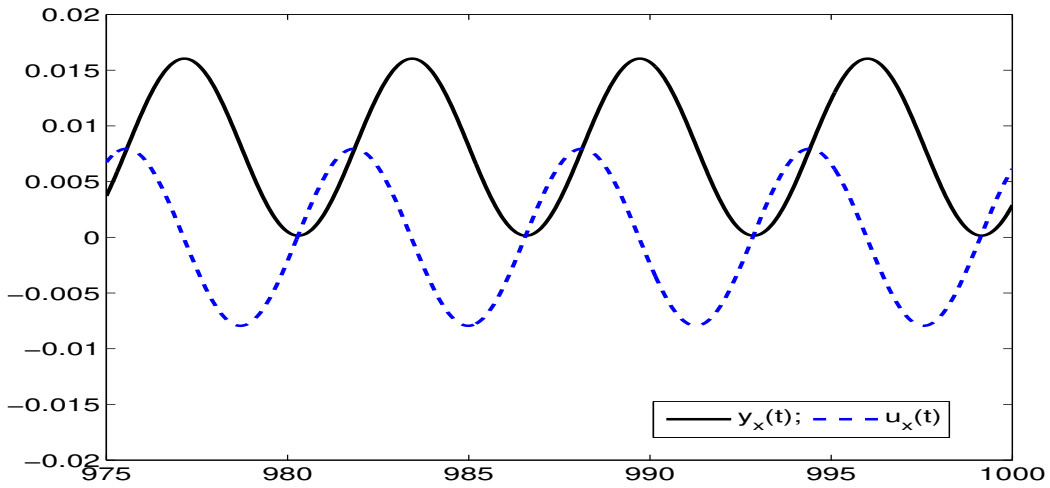

(b) $k_a = 6$

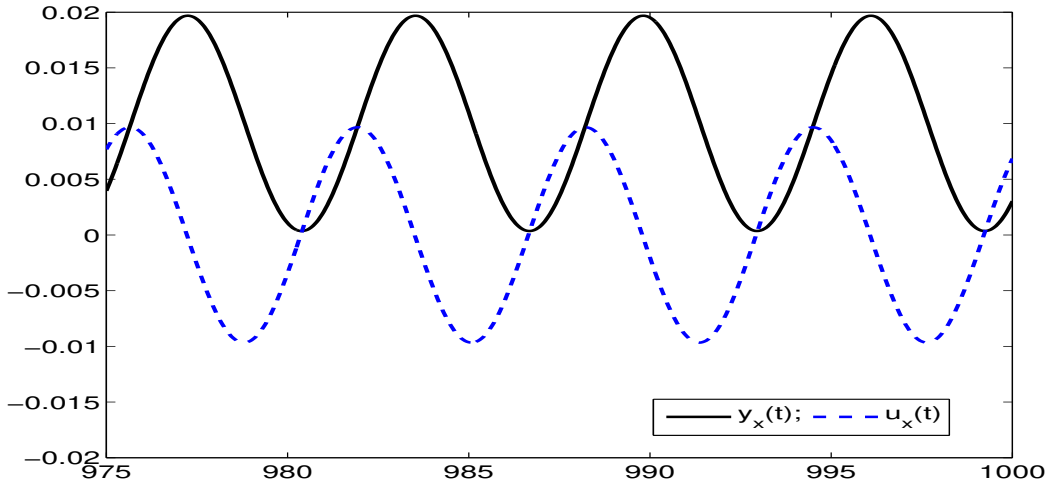

(c) $k_a = 10$

Figure 4.1: The time series plots of x-component of position and velocity showing amplitude, phase changes and characteristic frequency for $Re = 0.05$, $F = 0.05$ and different values of k_a.

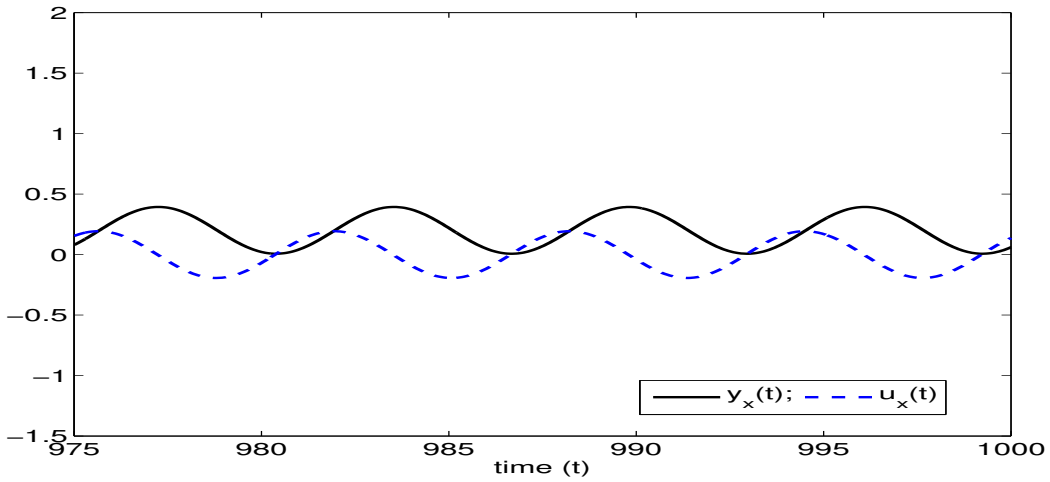

(a) $F = 1.0$.

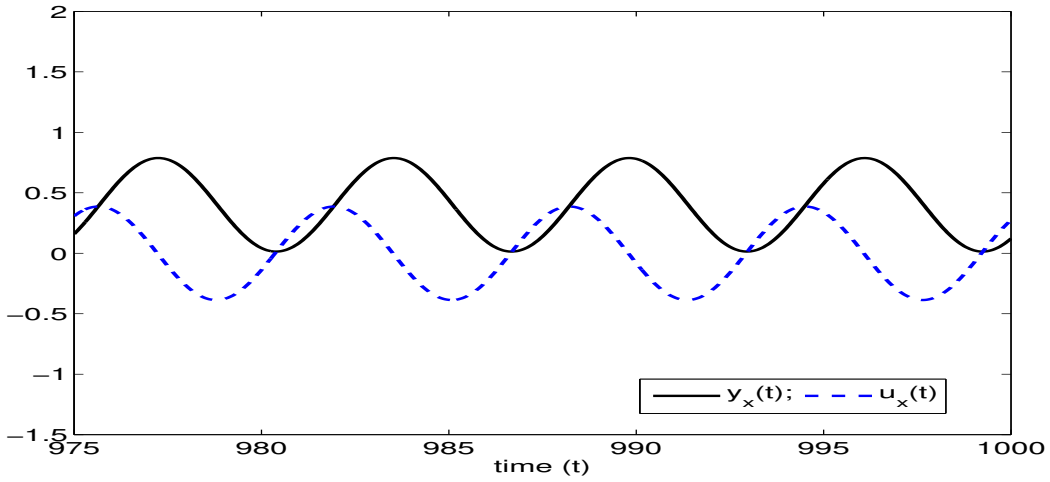

(b) $F = 2.0$.

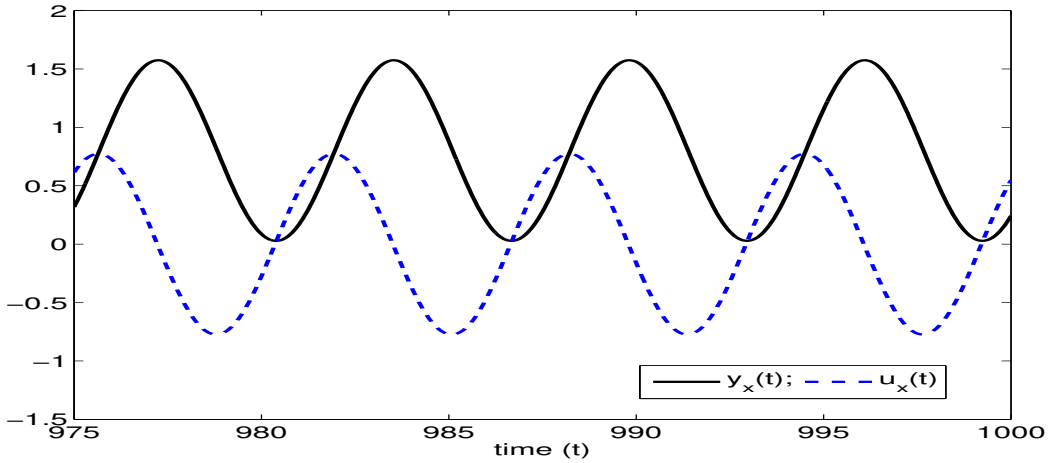

(c) $F = 4.0$.

Figure 4.2: The time series plots of x-component of position and velocity showing amplitude, phase changes and characteristic frequency for $Re = 0.05$, $k_a = 10$ and different values of F.

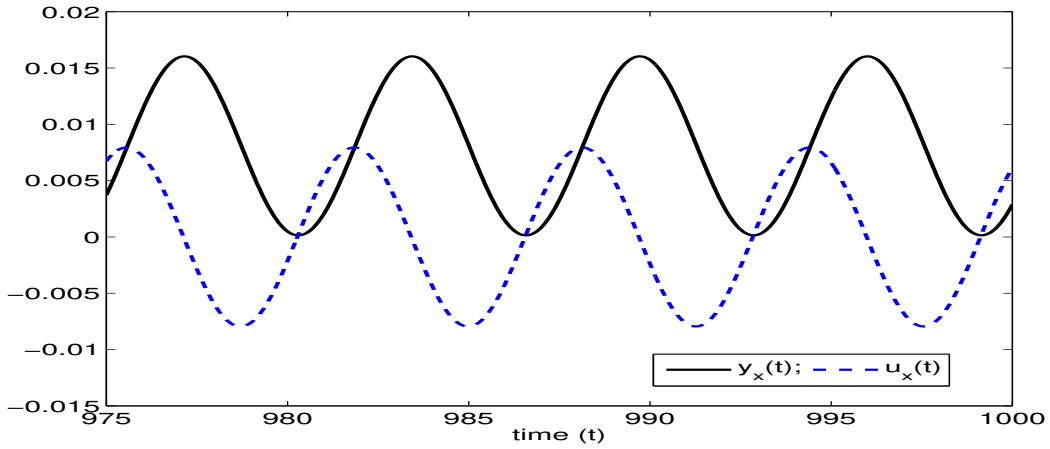

(a) $Re = 0.05$.

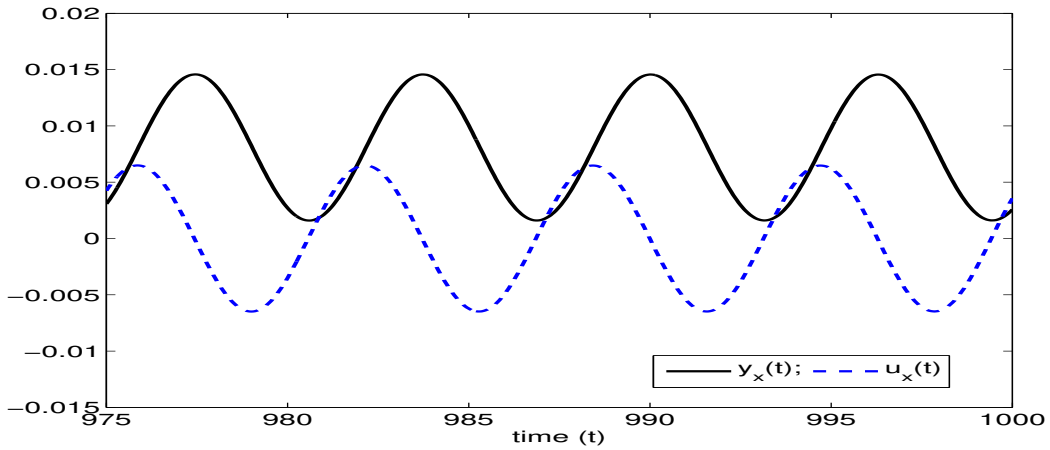

(b) $Re = 0.25$.

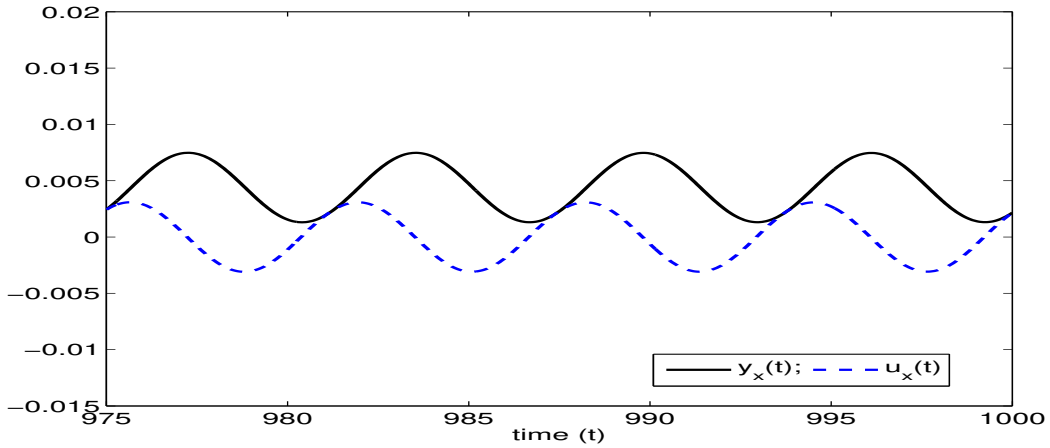

(c) $Re = 0.45$.

Figure 4.3: The time series plots of x-component of position and velocity showing amplitude, phase changes and characteristic frequency for $F = 0.05, k_a = 6$ and different values of Re.

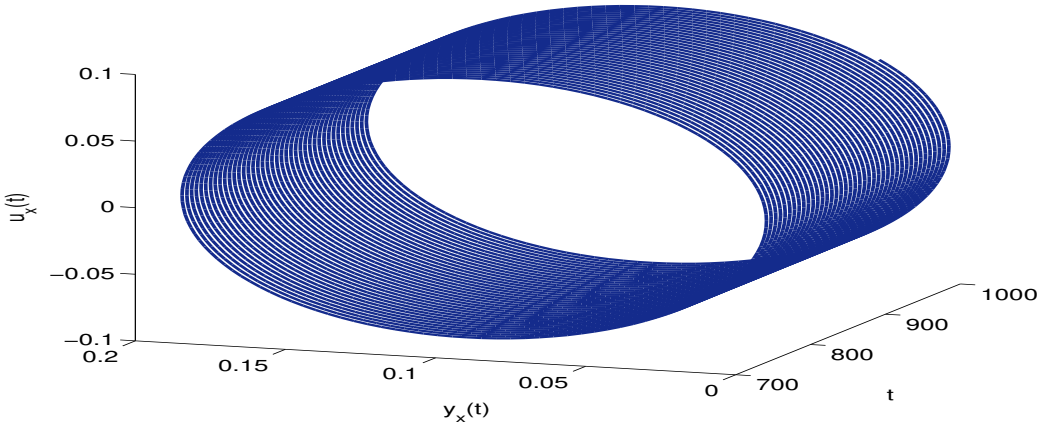

(a) $Re = 0.05$.

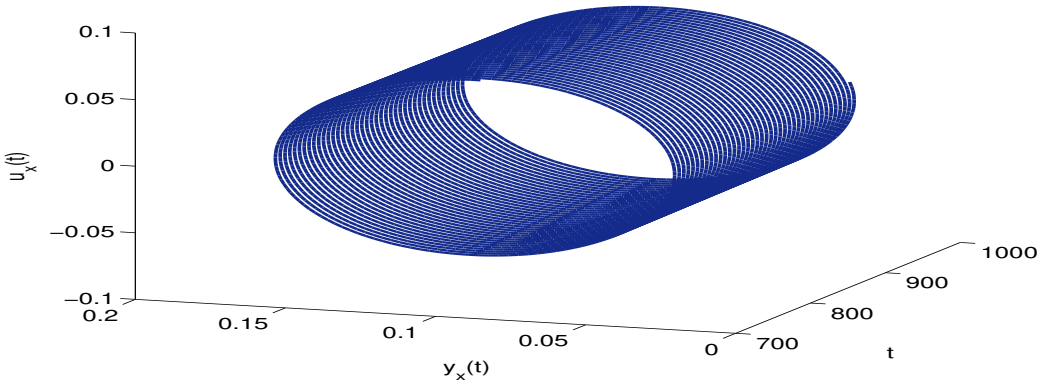

(b) $Re = 0.25$.

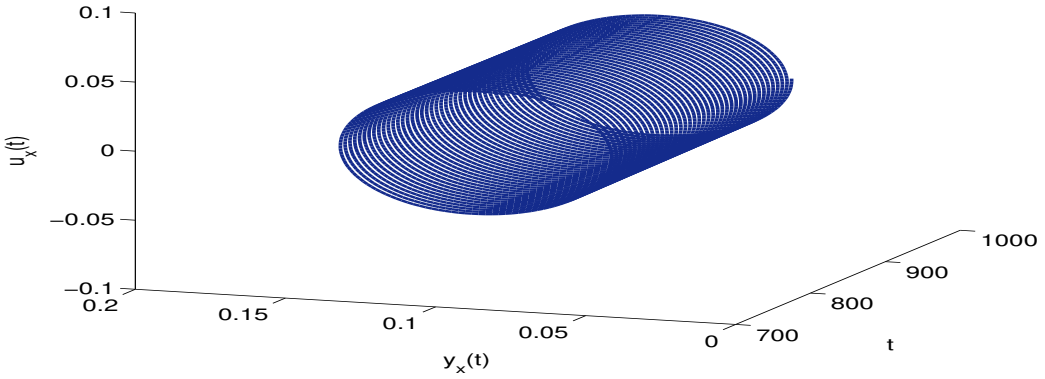

(c) $Re = 0.45$.

Figure 4.4: The phase space plot of position, velocity and time plotted for the evolution of the dynamics for $F = 0.5$, $k_a = 10$ and different values of Reynolds number.

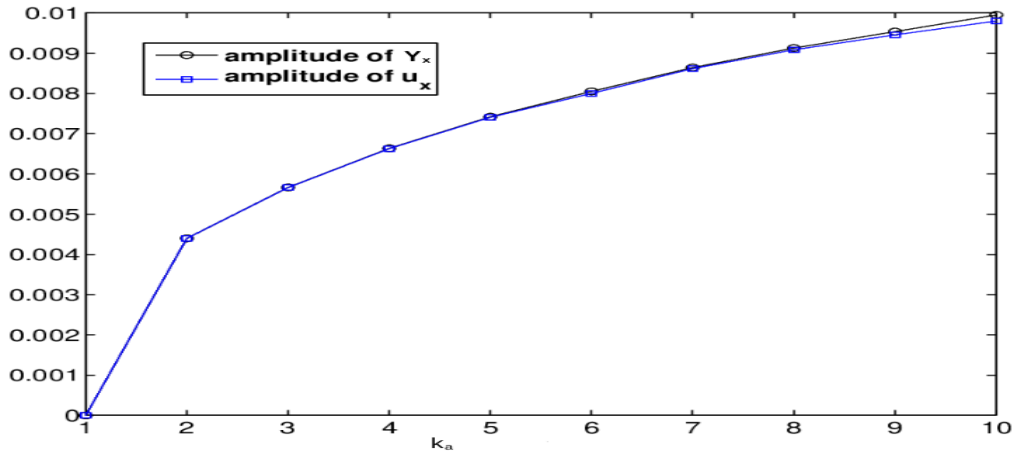

(a) $Re = 0.05$ and $F = 0.05$.

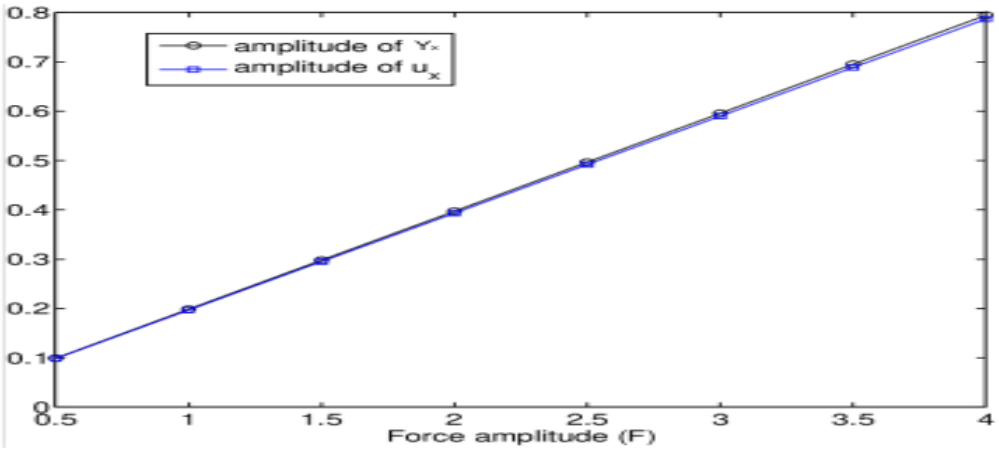

(b) $Re = 0.05$ and $k_a = 10$.

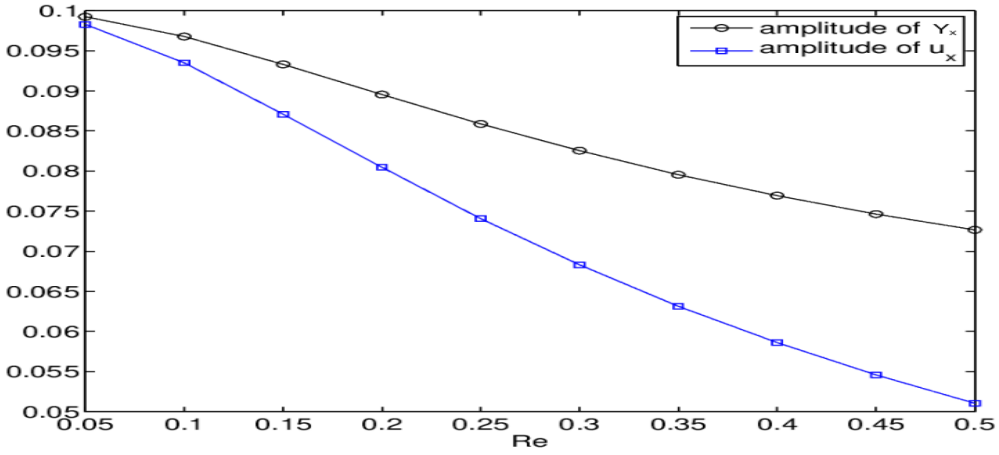

(c) $k_a = 10$ and $F = 0.5$.

Figure 4.5: The plot of maximum amplitude of position and velocity as a function of (a) k_a, (b)force amplitude F, and (c) Reynolds numbers,Re.

the action of the same external force amplitude. As Re increases, the resistance to change in motion increases and as a result the attractor size diminishes. This decrement in size of the oscillations is happened due to the influence of increase of inertia, where the Reynolds number stands for a measure of particle inertia. The observation can be again confirmed from the phase space plot of x components of position and velocity given in Fig.4.4 as a function of time for different values of R_e. The decrement of area of reach of the phase space plot on increment of Re is dominantly seen in Fig.4.4. The change in attractor size also demonstrates the strong dependence of dynamics on R_e.

As explained above, the movement of particle decreases as the inertia increases, whereas the movement can be accelerated by increasing the external force or/and particle size. Fig.4.5 (a) and (b) depict that the maximum amplitude of position and velocity increases non-linearly as the aspect ratio increases, whereas it increases linearly as the external force increases. Also, note that the maximum amplitude of position and velocity coincides for every choice of aspect ratio or external force as can be seen in Fig.4.5(a) and (b). The nonlinear change observed in Fig.4.5(a), shows that the migration of non-spherical particles is more complex than spherical particles. This manifests that the geometrical deviations of suspended particle from its spherical shape accelerate the complexity of the particle dynamics. If there is a proportional increase in amplitude with the external force then it is still a linear phenomenon as can be observed from the Fig.4.5(b). Also, the maximum amplitude of both position and velocity vary non linearly as the Reynolds numbers vary and the numbers representing resistance bring additional complexity in the dynamics as evident from Fig. 4.5(c). If, however, the change in amplitude is not proportional to increase in Re, that will be a nonlinear effect which can be attributed to nonlinear inertial terms. If the mean position of the variation in position is not zero that deviation from zero can be attributed to inertia, since in Stokes flow, the mean position of the oscillation will be zero. The deviation of the mean position from zero should be in the direction of the first

motion of the particle, namely, dependent on the sign of the external force. This is so since the direction of the first motion will be determined by the sign, which is already demonstrated by Madhukar et al. (2010). Interestingly, the inertia brings down the velocity oscillations compare to the position oscillations as can be summarized from Fig.4.5(c). The particle exhibits larger particle oscillations as the external force/ aspect ratio increases and smaller oscillations as the Reynolds number increases, as evident from Figs.4.1-4.4 and also from Fig.4.5.

In short, significant differences in the behavior of the particle migration can be found from the Figs.4.1-4.4. Since the dynamics is very sensitive to shape of the particle, inertia and the external force, particle separation of different shapes of similar spheroids is possible. From the Fig.4.1-4.3 a shifting of the velocity series compared to its position series is observed for the choice of any set of the controlling parameters. The external field causes migration of particles due to internal velocity is high, which resulted in a delay of movement of particles. We believe that the shift is due to the fact that in the absence of inertia, the time at which the velocity reaches its maximum, the position is at its minimum and when the particle experiences its maximum deviation the velocity is at its minimum. The variation of position is almost sinusoidal in nature and hence if we assume that the position variation is sinusoidal the velocity which is its derivative with respect to time will also be sinusoidal with a phase shift of $\pi/2$. The shift of nearly $\pi/2$ in the velocity variation with respect to the position variation is clearly evident from the plots given in Figs.4.1 to 4.3. Inertia should change this to a larger extent at higher values of Reynolds numbers. The net migration at zero Reynolds number will be negligible and should increase with the increase in the number. Also, if we replace the external force with negative of it, the direction of the net migration is also reverse. Hence, the dynamics of the particles of different shapes at low Reynods number are numerically demonstrated. The change in k_a and R_e brings nonlinear changes, whereas and the change in amplitude of external force brings linear changes in the maximum amplitude of oscillations of the particles in its

position and velocity as observed in Fig.4.5.

4.4 Conclusion

The dynamics dependencies of particles on the parameters are evident in this analysis, which can be used for separating particles of different shape with similar sizes. This chapter has analysed the numerical simulations of the dynamics of rigid spheroid suspensions in quiescent Newtonian fluid as a function of aspect ratio, external force amplitude, and Reynolds number. In this work, we have observed some fundamentally important properties of suspensions in a fluid at rest. We extend this work to an oscillating flow field as explained in the next chapter.

Chapter 5

Dynamics of forced particles in an oscillating flow at low Reynolds numbers

5.1 Introduction

The dynamics of suspended particles is significant in many industries such as oil recovery and refinery, printing and paper-making, pharmaceuticals, food processing and so on. The study of suspension rheology leads to insights that may lead to better control of fluid stress deformation behaviour and may lead to appropriate changes in processing technologies. In most situations, the dynamics of the particles are very sensitive to the orientation distribution of the suspended particles due to the irregular and non-spherical shape of the particles. The motion of non-spherical particles in a shear flow at vanishingly small Reynolds numbers has been studied theoretically for a long time and is summarized by Singh and Kumar (2021). It has been known, since the work of (Jeffrey 1922) at zero Reynolds numbers that in the absence of inertia, an axisymmetric particle in a simple shear flow rotates periodically in one of an infinite single-parameter family of closed 'Jeffery'

orbits. In the absence of hydrodynamic interactions, Brownian motion, etc., the particular orbit followed by the particle depends on the initial conditions, rendering the inertia-less limit indeterminate. Later it is substantiated by Bretherton (1962b). Nilsen and Andersson (2013) have investigated the chaotic behaviour of particle dynamics of a spheroid with strong inertia for the large Stokes numbers. They have observed that the chaos has occurred only for Stokes's number larger than certain critical number. Li and Sarkar (2005) have done a numerical simulation of dynamics of a drop in an oscillating extensional flow at finite Reynolds numbers. They have studied the effect of inertia on rheology of dropes and periodic forcing at low, but finite inertia. In this work we have study the dynamics in an oscillating flow, in the presence of inertial terms.

5.2 Formulation and methodology

The general expression of hydrodynamic force on a rigid particle suspended in a time-dependent Newtonian fluid developed by Lovalenti and Brady (1993b) is given as (See Eq.(1.11) in chapter1)

$$
\begin{aligned}
\mathbf{F}^{\mathrm{H}}(t) =& ReSl\tilde{V}_p\dot{\mathbf{u}}_\infty(t) + \mathbf{F}_s^{\mathrm{H}}(t) - \\
& ReSl\left[6\pi\mathbf{\Phi}\cdot\mathbf{\Phi}\cdot\mathbf{\Phi} + \lim_{R\to\infty}\left(\int_{V_f(R)}\mathbf{M}^T\cdot\mathbf{M}dV - \frac{9\pi}{2}\mathbf{\Phi}\cdot\mathbf{\Phi}R\right)\right]\cdot\dot{\mathbf{u}}_s(t) + \\
& \frac{3}{8}\left(\frac{ReSl}{\pi}\right)^{\frac{1}{2}}\left[\int_{-\infty}^{t}\left\{\frac{2}{3}\mathbf{F}_s^{\mathrm{H}\parallel}(t) - \left[\frac{1}{|\mathbf{A}|^2}\left(\frac{\pi^{\frac{1}{2}}}{2|\mathbf{A}|}erf(|\mathbf{A}|) - exp(-|\mathbf{A}|^2)\right)\right]\mathbf{F}_s^{\mathrm{H}\parallel}(s)\right.\right. \\
& \left. + \frac{2}{3}\mathbf{F}_s^{\mathrm{H}\perp}(t) - \left[\exp(-|\mathbf{A}|^2) - \frac{1}{2|\mathbf{A}|^2}\left(\frac{\pi^{\frac{1}{2}}}{2|\mathbf{A}|}erf(|\mathbf{A}|) - exp(-|\mathbf{A}|^2)\right)\right]\right. \\
& \left.\left. \mathbf{F}_s^{\mathrm{H}\perp}(s)\right\}\frac{2ds}{(t-s)^{\frac{3}{2}}}\right]\cdot\mathbf{\Phi} \\
& - Re\lim_{R\to\infty}\int_{V_f(R)}(\mathbf{u_0}\cdot\boldsymbol{\nabla}\mathbf{u_0} - \mathbf{u}_s(\boldsymbol{t})\cdot\boldsymbol{\nabla}\mathbf{u_0})\cdot\mathbf{M}dV + o(ReSl) + o(Re)
\end{aligned}
\tag{5.1}
$$

We assume that fluid flow far from the particle ($\mathbf{u}_\infty$ (t)) with unsteady uniform velocity field is $\mathbf{u}_\infty(t) = (u_\infty(t), v_\infty(t), w_\infty(t))$. Also, we assume that the velocity of the particle $\mathbf{u}_p(t) = (u_p(t), v_p(t), w_p(t))$ exerted by the fluid on the particle is in the direction of the vector $\mathbf{A}$, which itself is parallel to the displacement vector $\mathbf{y}_s(t) - \mathbf{y}_s(s)$ as given earlier. Therefore, the slip velocity of the fluid is given by $\mathbf{u}_s(t) = \mathbf{u}_p(t) - \mathbf{u}_\infty(t)$. All velocities $\mathbf{u}_s(t), \mathbf{u}_p(t)$ and $\mathbf{u}_\infty(t)$ are non-dimensionalized by the characteristic velocity U_c and the acceleration (i.e., by U_c/τ_c), and all length dimensions non-dimensionalized by a. Here, a and U_c are the characteristic particle dimension and the slip velocity of particle and hence the characteristic timescale is defined as $\tau_c = a/U_c$. The Stokes resistance tensor associated with the particle is $6\pi\mathbf{\Phi}$ and hence the pseudo-steady state drag force, acting on the suspended particle translating with slip velocity $\mathbf{u}_s$ is given by, $\mathbf{F}_s^{\mathrm{H}}(t)(t) = -6\pi\mathbf{\Phi}\cdot\mathbf{u}_s(t)$. The second order tensor $\mathbf{\Phi} = \frac{8e}{3}\mathbf{a}$, where e is the eccentricity of prolate spheroid and $\mathbf{a}$ is a diagonal matrix defined by

$$\mathrm{a}_{11} = \frac{e^2}{-2e + (1+e^2)\log(\frac{1+e}{1-e})} \tag{5.2a}$$

$$\mathrm{a}_{22} = \frac{-2e^2}{-2e + (1-3e^2)\log(\frac{1+e}{1-e})} \tag{5.2b}$$

$$\mathrm{a}_{33} = \mathrm{a}_{22}, \tag{5.2c}$$

$$\text{and} \qquad \mathrm{a}_{ij} = 0 \qquad \text{for} \qquad i \neq j. \tag{5.2d}$$

The first term on the right side of the Eq. (5.1) is due to an accelerating frame of reference translating with the particle, and the second term is the pseudo-steady Stokes drag (Stokes's force). The third one is the unsteady Oseen correction to the hydrodynamic force. It is a history integral that replaces the Basset memory term, and the fourth term is an acceleration reaction term. The last integral

term is the contribution of a force orthogonal to the direction of particle velocity, called 'lift force'. In their expression, the pseudo-Stokes force $\mathbf{F}_s^{\mathrm{H}}$ can be split into parallel and perpendicular components to the displacement vector. The parallel and perpendicular components of pseudo-Stokes force can be given respectively by

$$\mathbf{F}_s^{\mathrm{H}\parallel}(t) = 6\pi \mathbf{u}_s \cdot \mathbf{pp},$$

and

$$\mathbf{F}_s^{\mathrm{H}\perp}(t) = 6\pi \mathbf{u}_s \cdot (\delta - \mathbf{pp}).$$

Where δ is the idem tensor of order 2 and $\boldsymbol{p}$ is the unit vector given by

$$\mathbf{p} = \frac{\mathbf{y}_s(t) - \mathbf{y}_s(s)}{|\mathbf{y}_s(t) - \mathbf{y}_s(s)|} \tag{5.3}$$

where $\mathbf{y}_s(t) - \mathbf{y}_s(s)$ is the integrated displacement of the particle relative to fluid from time s to the current time t and $\mathbf{A}$ has been defined as

$$\mathbf{A} = \frac{Re}{2}\left(\frac{t-s}{ReSl}\right)^{\frac{1}{2}}\left(\frac{\mathbf{y}_s(t) - \mathbf{y}_s(s)}{t-s}\right) \tag{5.4}$$

We consider the motion of a spheroid moving along the major (polar radius) axis of the body suspended in an oscillating flow. An arbitrary point, (x, y, z) on the surface of the spheroid having major axis, $2a$ and minor (equatorial radius) axis, $2b$ satisfies the expression,

$$\frac{x^2}{a^2} + \frac{y^2 + z^2}{b^2} = 1. \tag{5.5}$$

There are three cases, say $a < b$ for an oblate spheroid; and $a > b$ for a prolate spheroid; and $a = b$ for a sphere, where $k_a = b/a$ is the aspect ratio of the particle. In this analysis, we consider the motion of a prolate spheroid (i.e., $k_a < 1$ whose eccentricity is

$$e = \sqrt{\frac{a^2 - b^2}{a^2}}.$$

The dominant hydrodynamic forces induced on a spheroid suspended in a fluid are (a) a downward force due to gravity, (b) an upward buoyant force, and (c) the hydrodynamic force $\mathbf{F}^{\mathrm{H}}$ due to the disturbance of the fluid flow in the vicinity of the particle and (d) the applied external force $\mathbf{F}^{\mathrm{ext}}$. Using these the respective governing equation can be deriveed as done in chapter 4.

5.2.1 Governing equations for the problem

From the expression given for the hydrodynamic force, we solve the two integral terms, i.e. the acceleration term and the lift force. Incorporating all these simplifications, we get the expression for the hydrodynamic force exerted by the fluid on the particle as

$$\begin{aligned}
\mathbf{F}^{\mathrm{H}}(t) =& ReSl\left(\tilde{V}_p\dot{\mathbf{u}}_\infty + (I_{xx}, I_{yy}, I_{zz})\cdot\dot{\mathbf{u}}_\infty\right) \\
&- 16\pi e\left(e_1u_s(t), e_2v_s(s), e_3w_s(t)\right) \\
&- ReSl\left(I_{xx}\dot{u}_p(t), I_{yy}\dot{v}_p(t), I_{zz}\dot{w}_p(t)\right) + \frac{3}{8}\left(\frac{ReSl}{\pi}\right)^{\frac{1}{2}} \\
&\left\{\frac{1024}{9}\pi e^2\left(e_1^2u_s(t), e_2^2v_s(t), e_3^2w_s(t)\right)\left(t^{-\frac{1}{2}} - \epsilon^{-\frac{1}{2}}\right)\right. \\
&\left.+\frac{256}{3}\pi e^2\int_0^{t-\epsilon} B\left(e_1^2u_s(s), e_2^2v_s(s), e_3^2w_s(s)\right)\frac{2ds}{(t-s)^{\frac{3}{2}}}\right\} \\
&- Re\left(L_1, L_2, L_3\right)
\end{aligned} \tag{5.6}$$

where L_1, L_2, L_3 are the components of the lift force

$$\lim_{R\to\infty}\int_{v_f}\left(\mathbf{u}_0\cdot\boldsymbol{\Delta}\mathbf{u}_0 - \mathbf{u}_s(t)\cdot\boldsymbol{\Delta}\mathbf{u}_0\right)\cdot\mathbf{M}dV \tag{5.7}$$

From the numerical simulations, we note that the lift force contributes a force only in the perpendicular direction. We found and numerically verified that it is very small and amounts to $O(10^{-8})$, in this case. The expression for $\mathbf{M}$ is known

in the literature, whereas we need to find out expression for $\mathbf{u}_0$ and $\mathbf{u}_s(t)$. $\mathbf{u}_s(t)$ is the slip velocity and is given by $\mathbf{u}_s(t) = \mathbf{u}_p(t) - \mathbf{u}_\infty(t)$. The expression for B is given as

$$B = \frac{1}{|\mathbf{A}|^2}\left(\frac{\pi^{\frac{1}{2}}}{2|\mathbf{A}|}erf(|\mathbf{A}|) - \exp(-|\mathbf{A}|^2)\right). \tag{5.8}$$

It is assumed that the external periodic force $\mathbf{F}^{\text{ext}} = (F_1\sin(t), F_2\sin(t), F_3\sin(t))$ is dimensionless, where time has been scaled with $\tau_c(= a/U_c)$. The characteristic velocity U_c is assumed to be $a\omega_1$, where ω_1 is the frequency of the external periodic force. We use expression (5.6) for $\mathbf{F}^{\text{H}}$ to obtain the governing equations of the motion of a prolate spheroid in the fluid, starting with zero velocity at $t = 0$. Let $\mathbf{u}_s = (u_p, v_p, 0) - (u_\infty\sin(\omega t), v_\infty\sin(\omega t), 0)$ and is scaled by $U_c = a\omega_1$, the size of particle and frequency of external force ω_1. The $\boldsymbol{y}_p(t)(= (x, y, z))$ denotes the displacement vector and $\mathbf{u}_p(t)$ is the velocity vector of the particle.

Let $\mathbf{F}^{\text{ext}}$ denote the external force acting on the particle, and hence the effective force is $\mathbf{F}^{\text{H}}(t)+\mathbf{F}^{\text{ext}}(t)$. The governing equations of motion for a suspended prolate spheroid in an oscillating Newtonian fluid under the effect of a periodic external force are formulated as,

$$m_p\dot{\mathbf{u}}_p = \mathbf{F}^{\text{H}}(t) + \mathbf{F}^{\text{ext}}(t). \tag{5.9}$$

In dimensionless form the above equations reduced to

$$\frac{m_p\dot{\mathbf{u}}_p}{\mu a^2/U_c} = \mathbf{F}^{\text{H}}(t) + \mathbf{F}^{\text{ext}}(t). \tag{5.10}$$

The above expression are substituted in Eq.(5.10) and are simplified. The set of IDEs modeled for $\mathbf{u}_p(t)$ along with

$$\frac{d\mathbf{y}_p(t)}{dt} = \mathbf{u}_p$$

are

$$\frac{du_p(t)}{dt} = \frac{1}{C_1 Re}\left[F_1 \sin(t) + ReSl\left(\frac{4}{3}\pi\alpha^2 + I_{xx}\right) u_\infty \omega \cos(\omega t) \right. \\ \left. -16\pi e e_1 u_s(t) - \frac{3}{8}(P_1 + Q_1) - ReL_1\right] \tag{5.11a}$$

$$\frac{dx(t)}{dt} = u_p(t) \tag{5.11b}$$

$$\frac{dv_p(t)}{dt} = \frac{1}{C_1 Re}\left[F_1 \sin(t) + ReSl\left(\frac{4}{3}\pi\alpha^2 + I_{yy}\right) v_\infty \omega \cos(\omega t) \right. \\ \left. -16\pi e e_2 v_s(t) - \frac{3}{8}(P_2 + Q_2) - ReL_2\right] \tag{5.11c}$$

$$\frac{dy(t)}{dt} = v_p(t) \tag{5.11d}$$

$$\frac{dw_p(t)}{dt} = \frac{1}{C_1 Re}\left[F_1 \sin(t) + ReSl\left(\frac{4}{3}\pi\alpha^2 + I_{zz}\right) w_\infty \omega \cos(\omega t) \right. \\ \left. -16\pi e e_2 w_s(t) - \frac{3}{8}(P_3 + Q_3) - ReL_3\right] \tag{5.11e}$$

$$\frac{dz(t)}{dt} = w_p(t), \tag{5.11f}$$

where,

$$C_1 = \frac{4\pi}{3}\left(\frac{b}{a}\right)^2 + SlI_{xx},$$
$$C_2 = \frac{4\pi}{3}\left(\frac{b}{a}\right)^2 + SlI_{yy},$$
$$C_3 = \frac{4\pi}{3}\left(\frac{b}{a}\right)^2 + SlI_{zz},$$

$$P_1 = \frac{256\pi e^2}{3}\int_0^{t-\epsilon} Be_1^2 u_s(s)\,(t-s)^{-\frac{3}{2}}\,ds,$$

$$P_2 = \frac{256\pi e^2}{3} \int_0^{t-\epsilon} B e_2^2 v_s(s) \, (t-s)^{-\frac{3}{2}} \, ds,$$

$$P_3 = \frac{256\pi e^2}{3} \int_0^{t-\epsilon} B e_2^2 w_s(s) \, (t-s)^{-\frac{3}{2}} \, ds,$$

$$Q_1 = \frac{1024}{9} \pi e^2 e_1^2 u_s(t) \left(t^{-1/2} - \epsilon^{-1/2} \right),$$

$$Q_2 = \frac{1024}{9} \pi e^2 e_2^2 v_s y(t) \left(t^{-1/2} - \epsilon^{-1/2} \right),$$

$$Q_3 = \frac{1024}{9} \pi e^2 e_2^2 w_s(t) \left(t^{-1/2} - \epsilon^{-1/2} \right).$$

The lift force is numerically computed using the expression in Eq.(5.7). The acceleration reaction term (I_{xx}, I_{yy}, I_{zz}) is computed using the expression given by Pozrikidis (1992); Chwang (1975). After calculating all necessary expressions and values for different parameters, we solve the more general set of the equation given above. We solve the equations using a finite difference method. These results are validated by perturbation analysis as explained in next section 5.3.

5.3 Numerical simulation of the dynamics

The integro-differential equations are solved numerically using one step finite-difference routine. In order to accommodate the nonlinear integral term, the trapezoidal product rule was implemented. We select the value of ϵ as 1×10^{-4}. The set of 20000 data points with the time step $\delta t = 0.0001$ in both the characteristic position and velocity is generated using a MATLAB code. Further decrease in time step and increase in resolution did not yield any significant changes in the results and hence we use these values for all computations.

The perturbed solutions are used to validate the study investigated in this

paper. The perturbed solutions are found by the Taylor series expansions for nonlinear integral terms obtained in the governing equations. We use the Reynolds number Re as the perturbation parameter. Note that the hydrodynamic force expression for an arbitrarily shaped particle given by Lovalenti and Brady (1993b) is valid up to $O(Re)$. The numerical solutions are compared with the perturbed solution of the system of equations (5.11) along with (5.12). The perturbed solutions of the equations (5.11) are given (for more details see Nayfeh (1981)) by

$$\begin{aligned} x(t) =& \frac{-F_1}{256\pi^2 e^2 e_1^2 + {C_1}^2 Re^2}\left[16\pi e\ e_1 \cos(t) + C_1 Re\left(\sin(t) + \frac{C_1 Re}{16\pi e\ e_1}\exp\left(\frac{-16\pi e\ e_1}{C_1 Re}t\right)\right)\right] \\ &+ \frac{F_1}{16\pi e\ e_1} + \frac{16\pi e\ e_1 u_\infty}{256\pi^2 e^2 e_1^2 + \omega^2 {C_1}^2 Re^2}\left[\frac{-16\pi e\ e_1}{\omega}\cos(\omega t) + \omega\left(2\pi ReSl - C_1 Re\right)\right. \\ &\left.\left(\frac{\sin(\omega t)}{\omega} + \frac{ReC_1}{16\pi e\ e_1}\exp\left(\frac{-16\pi e\ e_1}{ReC_1}t\right)\right)\right] + \frac{u_\infty \omega Re^2 {C_1}^2 Sl\cos(\omega t)}{256\pi^2 e^2 e_1^2 + \omega^2 {C_1}^2 Re^2} + \frac{u_\infty}{\omega} \end{aligned} \tag{5.13a}$$

$$\begin{aligned} y(t) =& \frac{-F_2}{256\pi^2 e^2 {e_2}^2 + {C_2}^2 Re^2}\left[16\pi e\ e_2 \cos(t) + C_2 Re\left(\sin(t) + \frac{C_2 Re}{16\pi e\ e_2}\exp\left(\frac{-16\pi e\ e_2}{C_2 Re}t\right)\right)\right] \\ &+ \frac{F_2}{16\pi e\ e_2} + \frac{16\pi e\ e_2 v_\infty}{256\pi^2 e^2 {e_2}^2 + \omega^2 {C_2}^2 Re^2}\left[\frac{-16\pi e\ e_2}{\omega}\cos(\omega t) + \omega\left(2\pi ReSl - C_2 Re\right)\right. \\ &\left.\left(\frac{\sin(\omega t)}{\omega}\frac{ReC_2}{16\pi e\ e_2}\exp\left(\frac{-16\pi e\ e_2}{ReC_2}t\right)\right)\right] + \frac{v_\infty \omega Re^2 {C_2}^2 Sl\cos(\omega t)}{256\pi^2 e^2 {e_2}^2 + \omega^2 {C_2}^2 Re^2} + \frac{v_\infty}{\omega} \end{aligned} \tag{5.13b}$$

$$\begin{aligned} z(t) =& \frac{-F_3}{256\pi^2 e^2 {e_2}^2 + {C_3}^2 Re^2}\left[16\pi e\ e_2 \cos(t) + C_3 Re\left(\sin(t) + \frac{C_3 Re}{16\pi e\ e_2}\exp\left(\frac{-16\pi e\ e_2}{C_3 Re}t\right)\right)\right] \\ &+ \frac{F_3}{16\pi e\ e_2} + \frac{16\pi e\ e_2 w_\infty}{256\pi^2 e^2 {e_2}^2 + \omega^2 {C_3}^2 Re^2}\left[\frac{-16\pi e\ e_2}{\omega}\cos(\omega t) + \omega\left(2\pi ReSl - C_3 Re\right)\right. \\ &\left.\left(\frac{\sin(\omega t)}{\omega} + \frac{ReC_3}{16\pi e\ e_2}\exp\left(\frac{-16\pi e\ e_2}{ReC_3}t\right)\right)\right] + \frac{w_\infty \omega Re^2 {C_3}^2 Sl\cos(\omega t)}{256\pi^2 e^2 {e_2}^2 + \omega^2 {C_3}^2 Re^2} + \frac{w_\infty}{\omega} \end{aligned} \tag{5.13c}$$

$$u_p(t) = \frac{F_1}{256\pi^2 e^2 e_1^2 + {C_1}^2 Re^2}\left[16\pi e e_1 \sin(t) + C_1 Re\left(\exp\left(\frac{-16\pi e e_1}{C_1 Re}t\right) - \cos(t)\right)\right] + \frac{16\pi e e_1 u_\infty}{256\pi^2 e^2 e_1^2 + \omega^2 {C_1}^2 Re^2}\left[16\pi e\ e_1 \sin(\omega t) + \omega\left(2\pi ReSl - C_1 Re\right)\left(\cos(\omega t) - \exp\left(\frac{-16\pi e\ e_1}{C_1 Re}t\right)\right)\right] + \frac{\omega^2 Re^2 Sl {C_1}^2 \sin(\omega t) u_\infty}{256\pi^2 e^2 e_1^2 + \omega^2 {C_1}^2 Re^2} \tag{5.14a}$$

$$v_p(t) = \frac{F_2}{256\pi^2 e^2 e_2^2 + {C_2}^2 Re^2}\left[16\pi e e_2 \sin(t) + C_2 Re\left(\exp\left(\frac{-16\pi e e_2}{C_2 Re}t\right) - \cos(t)\right)\right] + \frac{16\pi e e_2 v_\infty}{256\pi^2 e^2 {e_2}^2 + \omega^2 {C_2}^2 Re^2}\left[16\pi e\ e_2 \sin(\omega t) + \omega\left(2\pi ReSl - C_2 Re\right)\left(\cos(\omega t) - \exp\left(\frac{-16\pi e\ e_2}{C_2 Re}t\right)\right)\right] + \frac{\omega^2 Re^2 Sl {C_2}^2 \sin(\omega t) v_\infty}{256\pi^2 e^2 e_2^2 + \omega^2 {C_2}^2 Re^2} \tag{5.14b}$$

$$w_p(t) = \frac{F_3}{256\pi^2 e^2 e_2^2 + {C_3}^2 Re^2}\left[16\pi e e_2 \sin(t) + C_3 Re\left(\exp\left(\frac{-16\pi e e_2}{C_3 Re}t\right) - \cos(t)\right)\right] + \frac{16\pi e e_2 w_\infty}{256\pi^2 e^2 {e_2}^2 + \omega^2 {C_3}^2 Re^2}\left[16\pi e\ e_2 \sin(\omega t) + \omega\left(2\pi ReSl - C_3 Re\right)\left(\cos(\omega t) - \exp\left(\frac{-16\pi e\ e_2}{C_3 Re}t\right)\right)\right] + \frac{\omega^2 Re^2 Sl {C_3}^2 \sin(\omega t) w_\infty}{256\pi^2 e^2 e_2^2 + \omega^2 {C_3}^2 Re^2}. \tag{5.14c}$$

5.4 Results and discussion

The time series variations in positions and velocity are plotted in the figures 5.1 and 5.2 for the aspect ratios 2,4,6,8,10, $R_F = 0.5$ and Re=0.1 and $\omega = .2$. These graphs reveal that there are significant increases in the amplitude of position, whereas only very small increments in the amplitude of velocity are noticed. This shows the response of the motion to the change in aspect ratio k_a. Also, the phase variations of oscillations are given in figure 5.3a (a) for the aspect ratios 2,4,6,8, (b) for the Reynolds numbers 0.02, 0.04, 0.06, 0.08, where $R_F = 0.5$ and $Re = 0.1$ and $\omega = 0.2$. This graph shows the variations in phase with respect to the change in aspect ratio of the spheroid and the Reynolds number is significant.

The variations of the amplitudes of position and velocity are investigated for

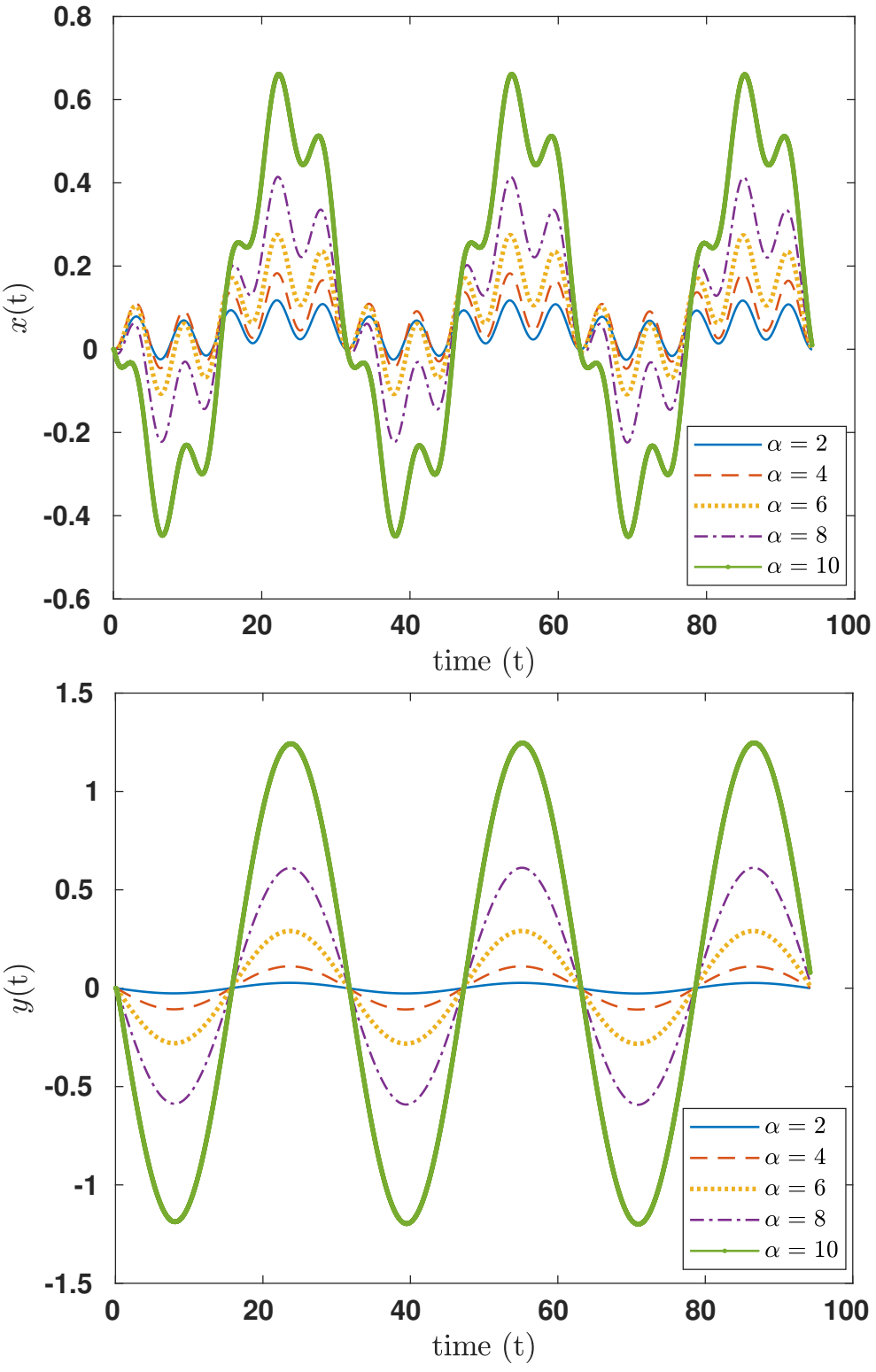

Figure 5.1: The plots showing the variation of x- and y-components of position time series with respect to aspect ratio k_a for $Re = 0.1$, $R_F = 0.5$ and $\omega = 0.2$.

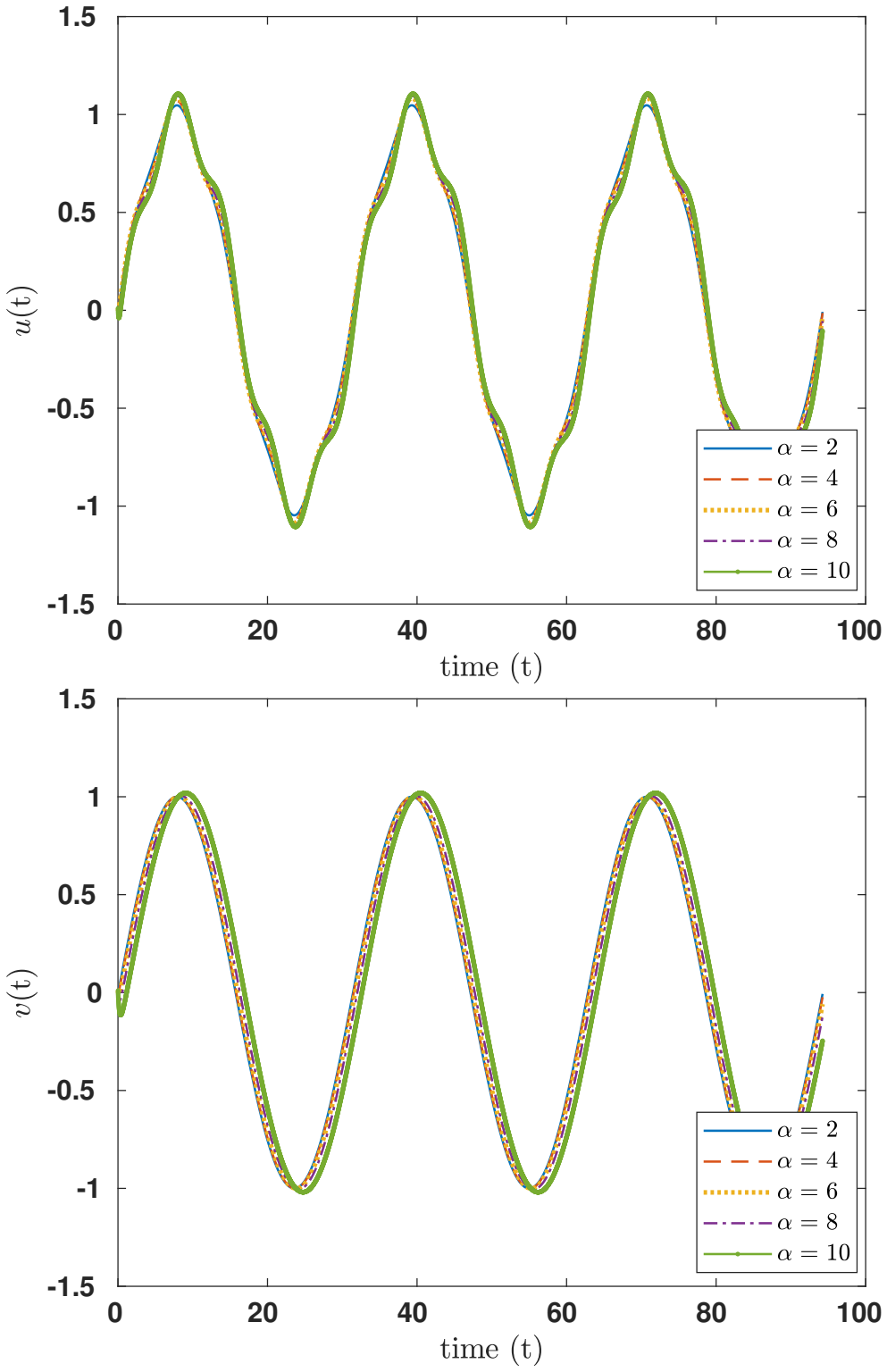

Figure 5.2: Plots showing the variation of x- and y-components of velocity time series with respect to aspect ratio k_a for $Re = 0.1$, $R_F = 0.5$ and $\omega = 0.2$.

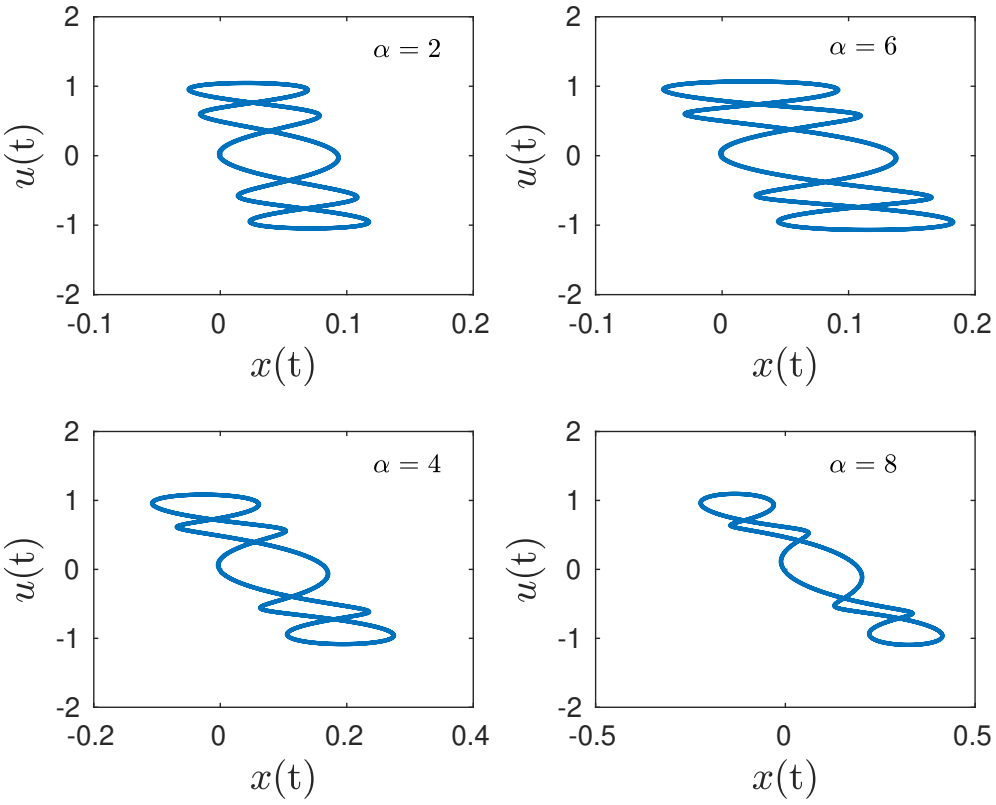

(a)

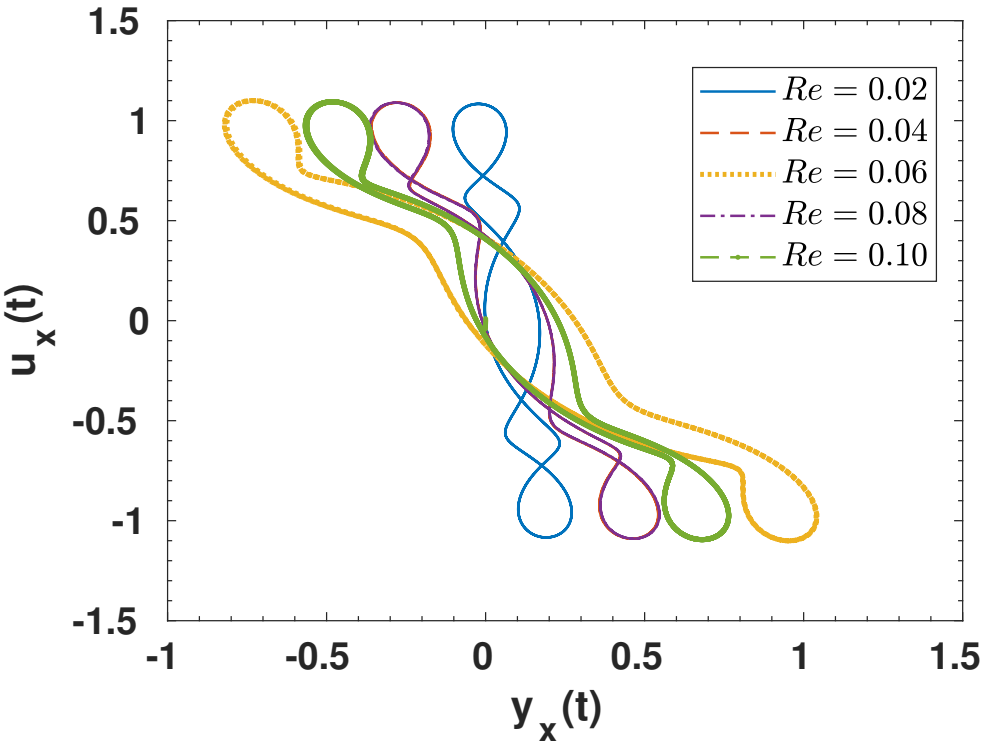

(b)

Figure 5.3: The phase plots drawn for $R_F = 0.5$, $\omega = 0.2$, (a) $Re = 0.1$, and $k_a = 2, 4, 6,$ and 8, (b) $k_a = 6$, and $Re = 0.02, 0.04, 0.06,$ and 0.08.

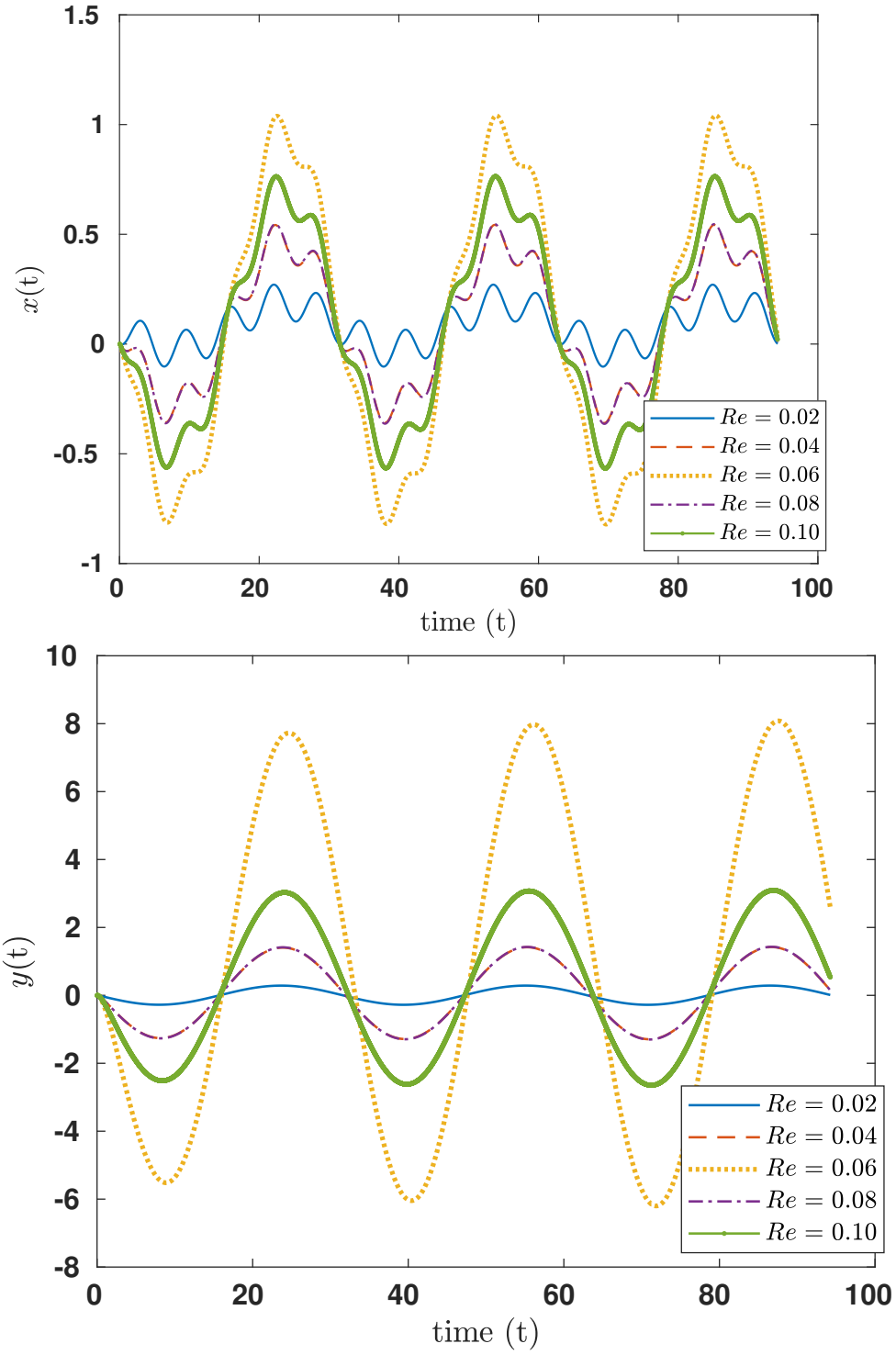

Figure 5.4: The plots showing the variation of x- and y-components of position time series for different values of Re, where $k_a = 6$, $R_F = 0.5$ and $\omega = 0.2$.

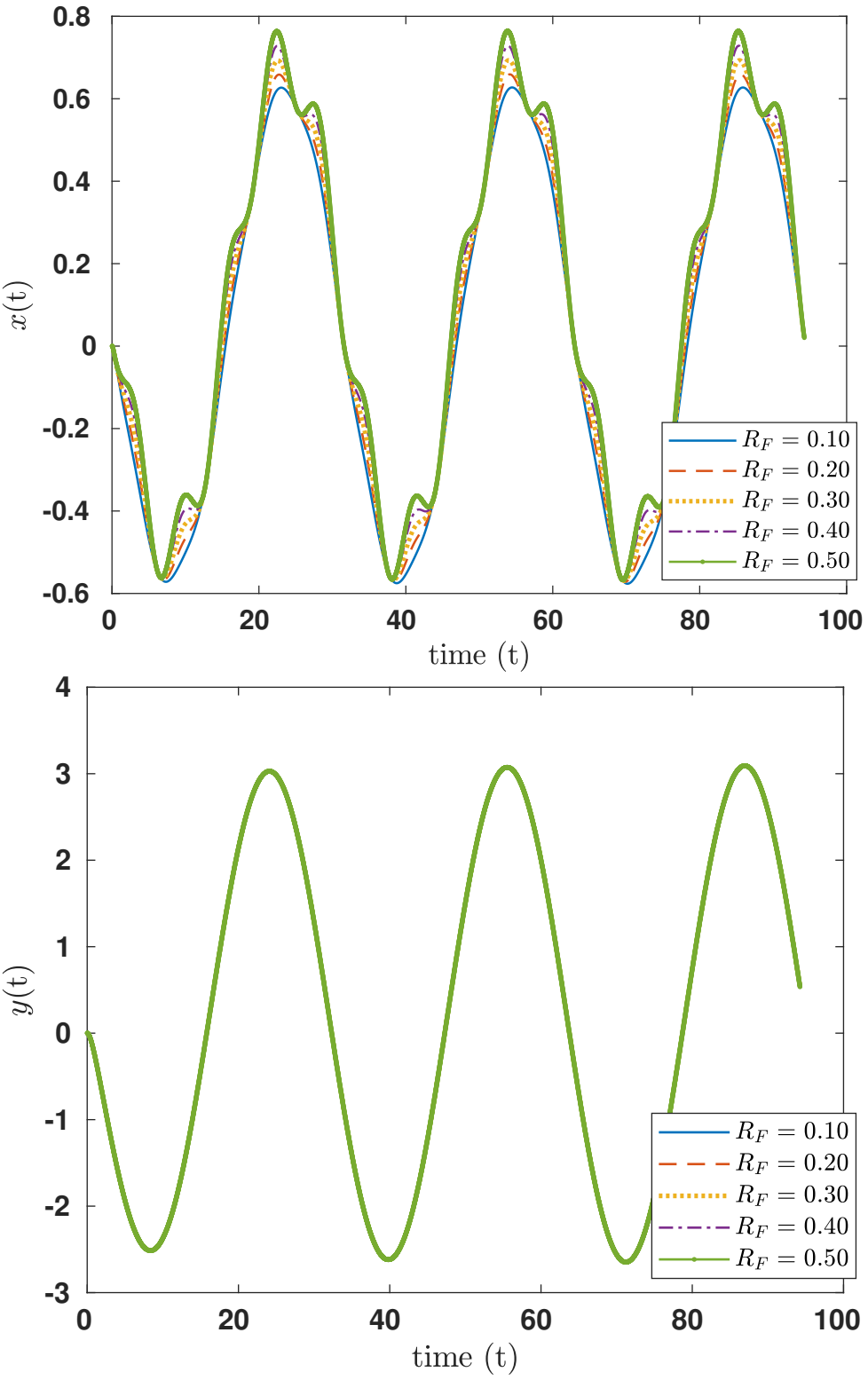

Figure 5.5: The plots showing the variation of x- and y-components of position time series for different amplitude of external force R_F, where $Re = 0.1$, $k_a = 6$ and $\omega = 0.2$.

different Reynolds numbers ranging from 0.01 to 0.1. The phase changes and amplitude of positions for different Reynolds number ($Re = 0.02, 0.04, 0.06, 0.08, 0.10$) for a given aspect ratio of (k_a) 6, external force's amplitude (R_F) of 0.50 and frequency of fluid oscillations (ω) of 0.2 are shown in figures 5.3b and 5.4, respectively. The results show that the increments in amplitudes of position for prolate spheroid considered in the analysis are very small as the Reynolds number increases. The influence in the phase of the particle is negligible as the Reynolds number increases and attain regular orbits as depicted in figure 5.3b.

The influence of amplitude of the external force on the amplitude of position is demonstrated in the time series given in the figure 5.5 for the aspect ratio of $k_a = 6$, fluid oscillation's frequency of $\omega = 0.2$ and Reynolds number of $Re = 0.1$ for different values of the amplitude of external force. It is substantiated from the analysis that the eternal force has a significant effect on the dynamics of the spheroid.

5.5 Conclusions

In this chapter, equations governing the dynamics and analysis of numerical solutions are carried out to determine the dynamical characteristic of a suspended prolate spheroid in an oscillating fluid at a low Reynolds number. The influence of Reynolds number, aspect ratio, the amplitude of external force on the motion of the particles is investigated and analyzed in detail. The dynamics of rigid spheroid suspensions in an oscillating Newtonian fluid at low Reynolds numbers is numerically studied and has been explained in this chapter. We have observed that the dynamics of the spheroid varied significantly as the parameters such as aspect ratio, external force amplitude, Reynolds number, and frequency of the oscillating fluid, changes. In the next chapter, we shall extend this work to an time-dependent uniform flow field.

Chapter 6

Transport of a driven spheroid in a uniform flow at low Reynolds numbers

6.1 Introduction

Micro-particle dynamics in slurry, composite materials, ceramics, colloids, polymers, proteins, and other natural and man-made settings is scientifically and technologically important. The transport properties of the particles occurring in these fields are significant in understanding the macroscopic features of the system, such as sedimentation, aggregation rate, self-diffusion coefficient, thermal conductivity, certain rheological parameters, and so on. These macroscopic properties can be investigated by averaging the solution of dynamics of micro body suspensions over a large volume (Stokes 1851; Pozrikidis 1992; Happel and Brenner 2012). The findings in their work are substantiated (Ramamohan et al. 1994; Kumar et al. 1996) by demonstrating chaotic dynamics of a periodically forced spheroid in a shear flow in certain parametric regions and investigating its strong dependence on rheological parameters. They proposed a method for par-

ticle separation using the dependence of dynamics on shape. It promises a better characterization of fluid suspensions employed in industries. Asokan et al. (2005) have reviewed the investigations done by the group over a decade on the dynamics of driven particles and change of rheological parameters observed due to the forced suspensions in a simple shear flow. Ramamohan et al. (2009) have analyzed the results of dynamics of a dilute suspension of periodically forced and neutrally buoyant spherical particles in a quiescent Newtonian fluid at low Reynolds numbers based on a numerical simulation. They have included the effects of convective and unsteady inertia in their analysis. Effects of inertia on the dynamics and rheology of suspensions have been investigated by Ramamohan et al. (2011). The addition of inertia has resulted in additional terms representing a fading memory of the particle's entire history of motion in the governing equations. The memory term becomes nonlinear due to the presence of convective inertia in the low Reynolds number limit. However, governing equations of suspensions of a particle of arbitrary shape can be easily derived, once the forces induced on the suspended body are identified using the particle geometry.

Lovalenti and Brady (1993b) have derived an approximate expression for the hydrodynamic force exerted on a particle of micro-size translating with the time-dependent fluid motion including both unsteady and convective inertia at low Reynolds numbers. Lawrence and Weinbaum (1986) have also proposed an expression for the hydrodynamic force induced on a suspended particle, including forces due to Stokes drag, added mass, Basset memory, and the secondary memory term generated as a result of the non-spherical geometry of the particle. Madhukar et al. (2010) have used Lovalenti and Brady's formulation for deriving the governing equations of a periodically forced rigid spherical particle in a quiescent flow field at low Reynolds numbers.

Recently, Singh and Kumar (2019) have derived equations describing the transport of harmonically forced spheroid in a quiescent flow in the limit of low Reynolds number, following Lovalenti and Brady (1993b). They have modeled

the problem as a set of ordinary differential equations. The numerical investigation of the problem by varying Reynolds numbers, particle aspect ratios, and external forces revealed that the size of the attractor is increased as the aspect ratio or/and force is increased, whereas it is decreased as the Reynolds number is increased. They have observed sinusoidal variation of position with no phase shift, sinusoidal variation of velocity with a phase shift of nearly $\frac{\pi}{2}$, a delay with the velocity at maximum position, and a strong dependence of the position and velocity on the control variables. These results may have practical importance as given in Singh and Kumar (2019). More details of the applications can be seen from the references therein. Their novel results are presented when fluid at rest, and this motivates us to study the orientation properties of the particle in a disturbed flow.

In this article, we analyse the particle dynamics in a time-dependent uniform flow at low Reynolds numbers. Accordingly, we model the orientation of a periodically forced prolate spheroid suspended in a three-dimensional time-dependent uniform flow in the limit of small Reynolds numbers, and derive the respective equations following the methodology and formulation of an earlier work (Singh and Kumar 2019) of us. This modeling also considers the influence of both fluid and particle inertia on the transport of solid particles, where the flow field far from the spheroid is assumed to be unsteady with a uniform velocity field. First, we derive the governing equations of the typical case and then do the numerical solutions for further analysis. We provide rough phase diagrams of the properties of the solutions as a function of the control variables such as aspect ratio, amplitude, phase of periodic force, Reynolds number, etc. It is found that the acceleration reaction term increases with the increase in aspect ratio, whereas the lift force remains near zero. The dependence of trajectory attractors of position and velocity of orientations on aspect ratio, Reynolds number, and the amplitude of the external field is substantiated. The change of average position, attractor size of position and velocity are the novel properties of this problem. A phase

shift in position, velocity, and drift of trajectories is also observed on varying the parameters. The results may open up new challenges in characterising particle suspension and technologies.

6.2 Governing Equations

We use Newton's second law of motion to derive the governing equations after formulating the expressions for the fluid-induced hydrodynamics force, $\mathbf{F}^{\mathrm{H}}(t)$ and the external force, $\boldsymbol{F}^{ext}(t)$. A general expression of the flow-induced hydrodynamic force on an arbitrary shaped rigid particle undergoing a time-dependent motion in an unsteady Newtonian Fluid at low Reynolds numbers is given in Eq. 8.24 of the work by Lovalenti and Brady (1993b) in the long time limit. Taking a coordinate system with the origin at the instantaneous center of mass of the spheroid and assuming the frame of reference translates with the suspended particle, a simplified form of the hydrodynamic force, $\boldsymbol{F}^{H}(t)$ induced on a particle by the flow at rest is given in Singh and Kumar (2019) as a modification of Lovalenti and Brady (1993b). The simplified expression is given in Eq. (6.1) of their article. In this work, we discuss the dynamics of an externally driven spheroid of arbitrary shape in a time-dependent uniform flow field considering the impact of both particle and fluid inertia, where the flow field far from the spheroid is assumed to be unsteady. Fig. 6.1 presents a schematic representation of the spheroid suspension. Following the formulation of Singh and Kumar (2019), the hydrodynamic force expression Eq. 8.24 of Lovalenti and Brady (1993b) deduces to Eq. (6.1) for a spheroid suspended in a time-dependent uniform flow.

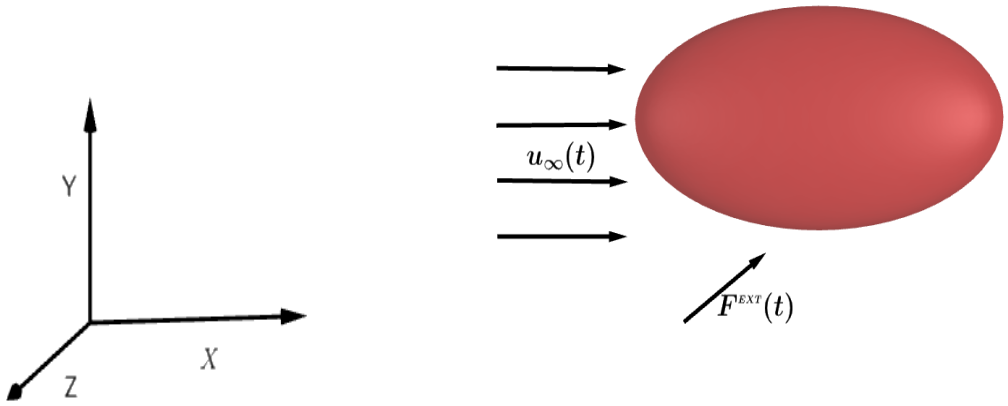

Figure 6.1: Schematic representation of the problem

$$
\begin{aligned}
\boldsymbol{F}^H(t) =& ReSl\mathrm{V}_p\dot{\boldsymbol{u}}_\infty(t) - 16\pi e\left(e_1u_s(t), e_2v_s(t), e_2w_s(t)\right) \\
&- ReSl\left(I_{xx}\dot{u}_s(t), I_{yy}\dot{v}_s(t), I_{zz}\dot{w}_s(t)\right) + \frac{3}{8}\left(\frac{ReSl}{\pi}\right)^{\frac{1}{2}} \\
&\left\{\frac{1024}{9}\pi e^2\left(e_1^2u_s(t), e_2^2v_s(t), e_2^2w_s(t)\right)\left(t^{-\frac{1}{2}} - \epsilon^{-\frac{1}{2}}\right)\right. \\
&\left.+\frac{256}{3}\pi e^2\int_0^{t-\epsilon} B\left(e_1^2u_s(s), e_2^2v_s(s), e_2^2w_s(s)\right)\frac{2ds}{(t-s)^{\frac{3}{2}}}\right\} \\
&- Re\left(L_1(t), L_2(t), L_3(t)\right)
\end{aligned}
\tag{6.1}
$$

Where,

- $\boldsymbol{u}_\infty(t)$ is the velocity of the undisturbed uniform flow field at time $'t'$,
- Sl is the Strouhal number,
- $V_p = \frac{4}{3}\pi ab^2$ is the volume of the spheroid,
- a and b are half of the lengths of the major and minor axes of the spheroid, respectively,
- Re is the Reynolds number,

- e is eccentricity of the particle,
- $e_1 = \frac{e^2}{-2e+(1+e^2)log(\frac{1+e}{1-e})}$,
- $e_2 = \frac{e^2}{-2e+(1-3e^2)log(\frac{1+e}{1-e})}$,
- $u_s(t), v_s(t)$, and $w_s(t)$ are the x,y,z components of the slip velocity of the suspended particle, which is given by $\boldsymbol{u}_p(t) - \boldsymbol{u}_\infty(t)$,
- $\boldsymbol{u}_p(t)$ is the velocity of the translating spheroid.
- B= $\frac{1}{|\mathbf{A}|^2}\left(\frac{\pi^{\frac{1}{2}}}{2|\mathbf{A}|}erf(|\mathbf{A}|) - \exp(-|\mathbf{A}|^2)\right)$,
- A=$\frac{Re}{2}\left(\frac{t-s}{ReSl}\right)^{\frac{1}{2}}\left(\frac{\boldsymbol{Y}_s(t)-\boldsymbol{Y}_s(s)}{t-s}\right)$,
- $\boldsymbol{Y}_s(t) - \boldsymbol{Y}_s(s)$ is the integrated displacement of the particle relative to fluid from the past time s to the current time t,
- $\boldsymbol{Y}_s(t) = \boldsymbol{Y}_p(t) - \boldsymbol{Y}_\infty(t)$,
- $\boldsymbol{Y}_p(t)$ and $\boldsymbol{Y}_\infty(t)$ represent the position vectors of the centre of mass of the particle and fluid respectively at time $'t'$,
- I_{xx}, I_{yy}, and I_{zz} are the principal diagonal elements of the diagonal matrix of order 3, raises from the acceleration reaction term of the problem considered.
- the limit of integration for the problem is from $-\infty$ to the current time, t. Hence there is a singularity at $s = t$ while integrating w.r.t s to obtain the new history integral term at finite Re. The term is thus split into two integrals over $[-\infty, t-\epsilon]$ and $(t-\epsilon, t]$, where $\epsilon > 0$ is an arbitrarily small number. Numerical computations show that the integral over the interval $(t-\epsilon, t]$ tends to zero as ϵ tends to 0 whereas the integral over the interval $[-\infty, t-\epsilon]$ converges. In short, the singularity doesn't create any issue, at least for the present problem. This is computationally proved in our analysis.

- $\boldsymbol{L}(t) = (L_1(t), L_2(t), L_3(t))$ is the lift force calculated for the uniform flow field at time t, using the method explained in Singh and Kumar (2019).

The term, $ReSl\mathrm{V}_p\dot{\boldsymbol{u}}_\infty(t)$ in Eq. 6.1 is the only added term to Eq. 12 of Singh and Kumar (2019) and Eq. 6.1 reduces to Eq. 12 of Singh and Kumar (2019) on taking $\boldsymbol{u}_\infty(t) = 0$ (fluid velocity field is zero). We begin the numerical computation by taking $\boldsymbol{F}^{ext}(t) = (F_1(t), F_2(t), F_3(t))\sin(\omega t)$ as the dimensionless sinusoidal(external) force having frequency ω, $\boldsymbol{Y}_p(t) = (x(t), y(t), z(t))$ as the displacement vector of the particle, $\boldsymbol{u}_p(t) = (u_p(t), v_p(t), w_p(t))$ as the velocity of the particle exerted by the fluid at time t and, the fluid velocity field as $\boldsymbol{u}_\infty(t) = f(t)(1,1,1)$, where $f(t)$ is a real-valued continuous function defined on $(-\infty, \infty)$. We also non-dimensionalize the velocity term by U_c, acceleration by U_c/τ_c, time by ω and length by a, where U_c, τ_c, and a represent the characteristic velocity of the particle, characteristic timescale (defined as $\tau_c = aU_c$) and characteristic length respectively. We obtain the following equations by plugging all these expressions into the Newtonian's second law of motion. For the details of the scheme used in this derivation, the readers are referred to Singh and Kumar (2019), and Lovalenti and Brady (1993b).

$$\begin{aligned}
\dot{u}_p(t) =& \frac{1}{C_1 Re}\left[F_1(t)\sin(\omega t) + ReSl\left(\frac{4}{3}\pi k_a^2 + 1\right) f(t) - 16\pi e e_1 \left(u_p(t) - f(t)\right)\right. \\
&\left. -\frac{3}{8}(P_1 + Q_1)(t) - ReL_1(t)\right] \qquad (6.2)\\
\dot{v}_p(t) =& \frac{1}{C_2 Re}\left[F_2(t)\sin(\omega t) + ReSl\left(\frac{4}{3}\pi k_a^2 + 1\right) f(t) - 16\pi e e_2 \left(v_p(t) - f(t)\right)\right. \\
&\left. -\frac{3}{8}(P_2 + Q_2)(t) - ReL_2(t)\right] \qquad (6.3)\\
\dot{w}_p(t) =& \frac{1}{C_3 Re}\left[F_3(t)\sin(\omega t) + ReSl\left(\frac{4}{3}\pi k_a^2 + 1\right) f(t) - 16\pi e e_3 \left(w_p(t) - f(t)\right)\right. \\
&\left. -\frac{3}{8}(P_3 + Q_3)(t) - ReL_3(t)\right] \qquad (6.4)
\end{aligned}$$

where,

$$\frac{dx(t)}{dt} = u_p(t), \qquad \frac{dy(t)}{dt} = v_p(t), \qquad \frac{dz(t)}{dt} = w_p(t)$$

and

$$\frac{du_p(t)}{dt} = \dot{u}_p(t), \qquad \frac{dv_p(t)}{dt} = \dot{v}_p(t), \qquad \frac{dw_p(t)}{dt} = \dot{w}_p(t),$$

$$\begin{aligned}
k_a =& \frac{a}{b}, \qquad C_1 = \frac{4\pi}{3}\left(\frac{b}{a}\right)^2 + SlI_{xx}, \\
C_2 =& \frac{4\pi}{3}\left(\frac{b}{a}\right)^2 + SlI_{yy}, \qquad C_3 = \frac{4\pi}{3}\left(\frac{b}{a}\right)^2 + SlI_{zz} \\
P_1 =& \frac{256\pi e^2}{3} B \int_0^{t-\epsilon} e_1^2 \frac{\left(u_p(s) - e^{-s}\right)}{(t-s)^{\frac{3}{2}}} ds, \quad P_2 = \frac{256\pi e^2}{3} B \int_0^{t-\epsilon} e_2^2 \frac{\left(v_p(s) - e^{-s}\right)}{(t-s)^{\frac{3}{2}}} ds \\
P_3 =& \frac{256\pi e^2}{3} B \int_0^{t-\epsilon} e_3^2 \frac{\left(w_p(s) - e^{-s}\right)}{(t-s)^{\frac{3}{2}}} ds \quad Q_1 = \frac{1024}{9}\pi e^2 e_1^2 u_s(t)\left(t^{-1/2} - \epsilon^{-1/2}\right) \\
Q_2 =& \frac{1024}{9}\pi e^2 e_2^2 v_s y(t)\left(t^{-1/2} - \epsilon^{-1/2}\right), \; Q_3 = \frac{1024}{9}\pi e^2 e_2^2 w_s(t)\left(t^{-1/2} - \epsilon^{-1/2}\right).
\end{aligned}$$

The above set of decoupled nonlinear equations is numerically solved. The computational results in case of $\omega = 1$ and $f(t) = e^{-t}$ are summarised in the following section. We study the long-term behavior of the particle's orientation directions; hence, more than half of the iterations are removed to ignore the transient dynamics of the body. This means that all graphs generated in this study represent the long-term orientation dynamics of the particle. We observe that the steady-state solution is an orbit for a given set of parameters. In what follows, we characterize the dynamics by analysing the graphs of the orbits for different sets of parameters.

6.3 Results and Discussion

We calculate all necessary expressions and values for different choices of the parameters, and then the above system of integro-differential equations is solved.

The diagonal elements I_{xx}, I_{yy}, and I_{zz} representing the acceleration reaction term, and the components, $L_i(t)$, $i = 1, 2, 3$ representing the lift force exerted on the particle due to the uniform flow are calculated as per the scheme explained in Singh and Kumar (2019) for different values of the aspect ratios(k_a) ranging from 1 to 10 in steps of 1. Note that the diagonal elements representing the acceleration reaction term is constant for the flow at rest and it increases for the uniform flow. The Table. 6.1 shows that all the three diagonal elements of the tensor corresponding to the acceleration reaction term increase with the aspect ratio and hence are significant, where the second and third components are similar for a given choice of the parameter k_a. This similarity may be due to the symmetry in the direction of motion of the spheroid in the current framework. Certainly, these values affect the dynamics of spheroid motion as the aspect ratio increases. Whereas, as can be seen from Table 6.2, the lift force exerted by the uniform fluid flow on the spheroid particle is negligibly small and hence has no influence on the orientation transport of spheroid for $1 < k_a < 10$. For further confirmation, we ran the code for the orientation dynamics for a few sets of parameters and found that the lift force doesn't make any difference in the particle orientation. Accordingly, the respective term is ignored from the numerical solution of motion.

k_a	I_{xx}	I_{yy}	I_{zz}
1			
2	6.01	8.01	9.2
3	6.45	17.03	17.2
4	8.05	25.07	25.25
5	10.34	33.05	33.06
6	11.73	37.05	38.0
7	12.30	40.50	40.50
8	14.85	47.0	47.0
9	19.25	59.0	59.8
10	19.30	60.5	61.50

Table 6.1: The calculated values of the diagonal matrix representing the acceleration reaction term for different values of k_a.

k_a	L_1	L_2	L_3
1			
2	2.96e-09	-1.50e-09	-2.32e-10
3	4.25e-09	-2.30e-09	-3.46e-10
4	5.67e-09	-3.18e-09	-4.74e-10
5	7.22e-09	-4.16e-09	-6.16e-10
6	8.88e-09	-5.22e-09	-7.70e-10
7	1.06e-08	-6.36e-09	-9.35e-10
8	1.25e-08	-7.58e-09	-1.11e-09
9	1.45e-08	-8.88e-09	-1.30e-09
10	1.66e-08	-1.02e-08	-1.50e-09

Table 6.2: The calculated values of components of the lift force as a function of the size of the spheroid.

We solve the system of differential equations, Eqs. 6.2-6.4 numerically using the built-in RK-4 solver of MATLAB for the position and velocity at time t, after incorporating the tabled values corresponding to the acceleration reaction term. The final simplified system of equations contains a set of five parameters, namely, the aspect ratio (k_a), the Reynolds number (Re), the amplitude (F_i), and the phase value (ω) of the external periodic force and the Strouhal number (Sl). Since Sl, always occurs in combination with Re as the present model is restricted for $ReSl << 1$, we can choose the Strouhal number equal to unity without loss of generality, where the limit $Sl << 1$ is automatically attained, once we select the values of Re in the range $0 < Re << 1$. Essentially, we vary the parameters, k_a and F_i appeared in the governing equation for different values of Re within its limit, keeping $\omega = 1$. The effect of parameters on the particle dynamics is summarised in the following sections by analysing the graphs in detail.

6.3.1 The Aspect ratio

The x, y, and z components of position and velocity over time are plotted in Figs. 6.2 and 6.3 respectively. It can be noticed from Fig. 6.2 that the average displacement of the spheroid along the x, y, and z axes is increasing as the aspect

ratio increases, where the increase along x component is dominant than the other two. Further, we observe from Fig. 6.3 that there are no significant changes in the maximum amplitude of velocity-time plots as the aspect increases. A phase shift in position and velocity is also observed with the change in aspect ratios, as can be observed from Fig. 6.2 and 6.3. Fig. 6.2a also reveals that the amplitude of the x-component of the position increases as the aspect ratio increases. At the same time, the maximum amplitudes of y and z components of position are initially increasing up to $k_a = 6$ and then decreasing on varying k_a from the lower value to higher, as can be noticed from Figs. 6.2b and 6.2c. Similar behavior is observed in the case of velocity, where the maximum amplitude increases and later decreases as the aspect ratio increases, as can be seen from Fig. 6.3. This dependence on the size of the attractor as a function of aspect ratio is again substantiated by the enhancement of the area bounded by the attractors as evident from the typical graphs shown in Fig. 6.4, where the Fig. 6.4 represents the component-wise phase space plot of position and velocity as a function of the size of the particle. It is clear that the position-velocity variation along the x axis and y-axis are periodic, as evident from Figs. 6.4a and 6.4b, whereas the variation along the z-axis is quasi-periodic as can be seen from the Fig. 6.4c. Interestingly a forward drift phenomenon of trajectory along the x-axis is observed as evident from Fig. 6.2 and 6.3 as the aspect ratio increases. This forward drift of attractors along the x-axis is further confirmed by Fig. 6.4. The respective 3-dimensional trajectories of position and velocity are shown in Figs. 6.5(a-f). Notably, the orientation of attractors depends on the aspect ratio, as shown in Fig. 6.5. This graphical analysis confirms that the aspect ratio of rigid suspension significantly affects the orientation dynamics of the particle due to its change in inertial effects.

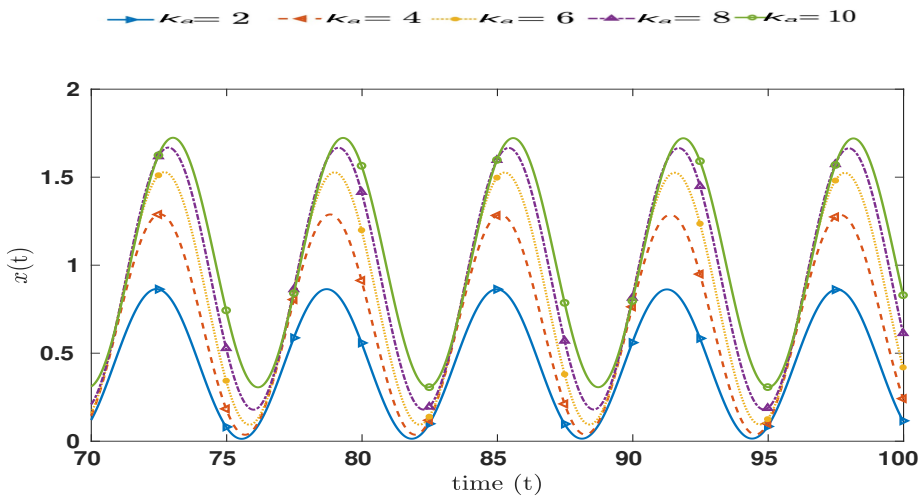

(a)

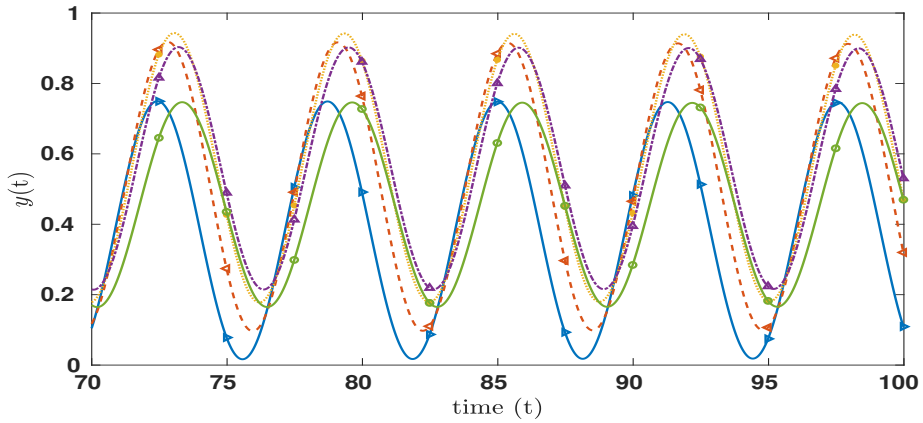

(b)

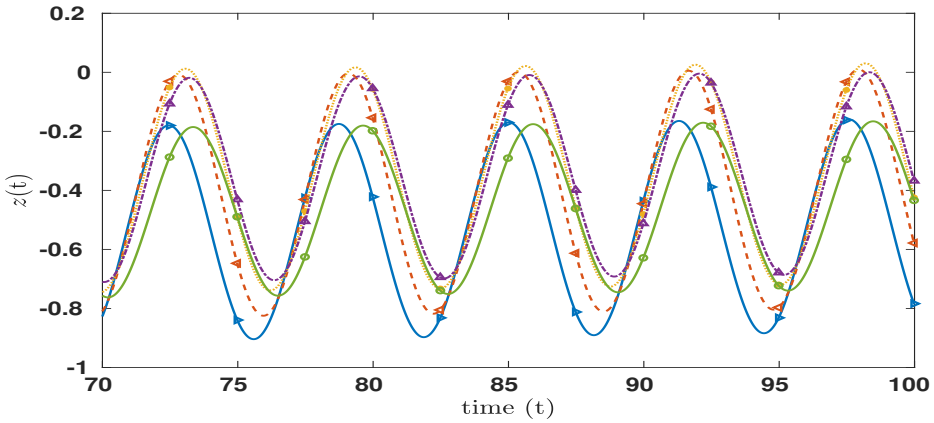

(c)

Figure 6.2: The x, y and z components of position of orientation for $Re = 0.05,$, $F_1 = 1.5$, and different values of $k_a = 2, 4, 6, 8, 10$ are shown respectively in a, b, and c.

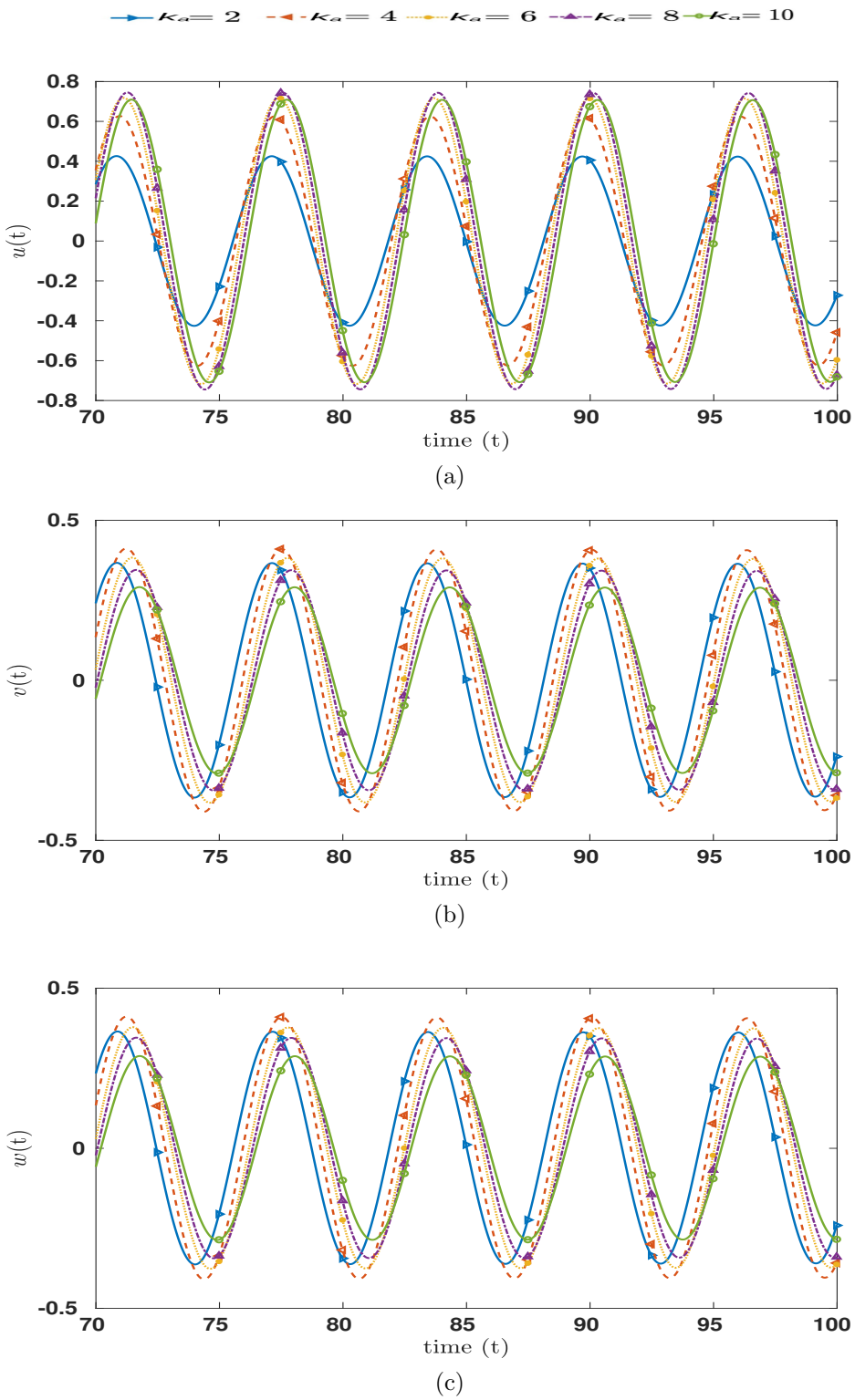

Figure 6.3: The x,y,z-components of velocity of motion for $Re = 0.05, F_1 = 1.5$, and different values of $k_a = 2, 4, 6, 8, 10$.

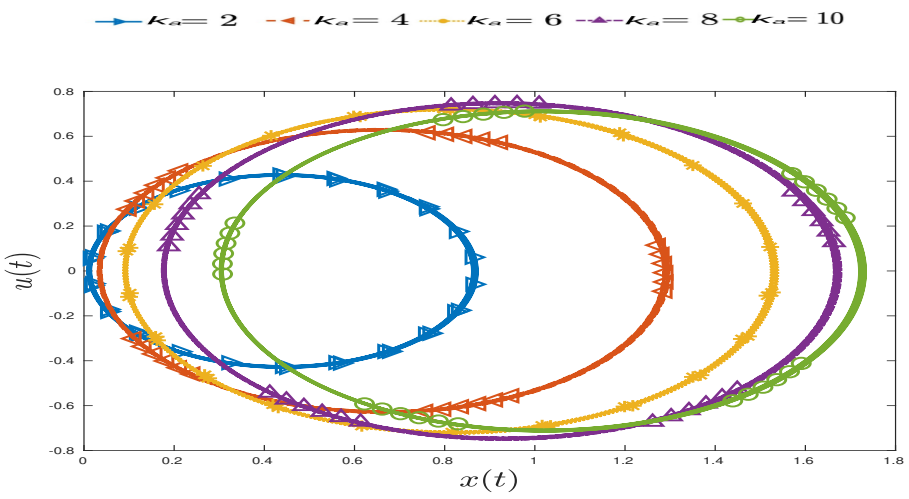

(a)

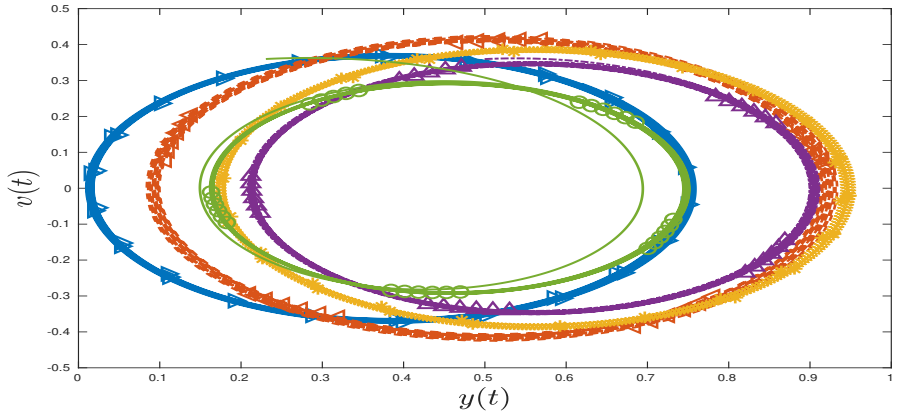

(b)

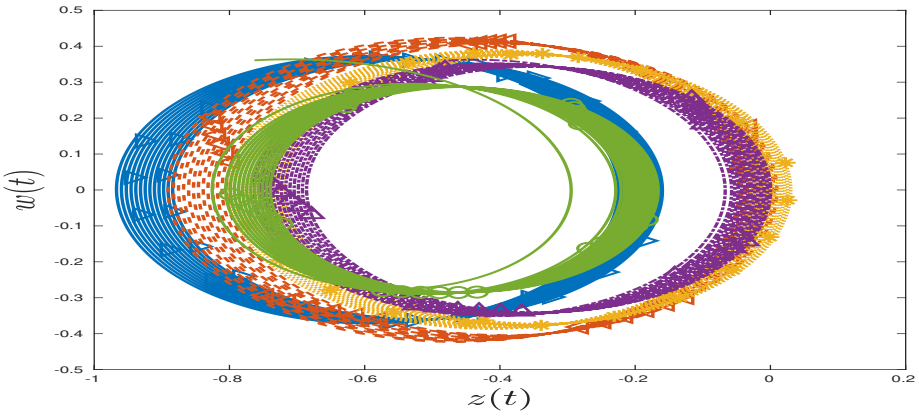

(c)

Figure 6.4: The projections of the phase-space motion of the spheroid in the planes of (a) xy, (b) yz, (c) zx planes, for $Re = 0.05, F_1 = 1.5$, and different values of $k_a = 2, 4, 6, 8, 10$.

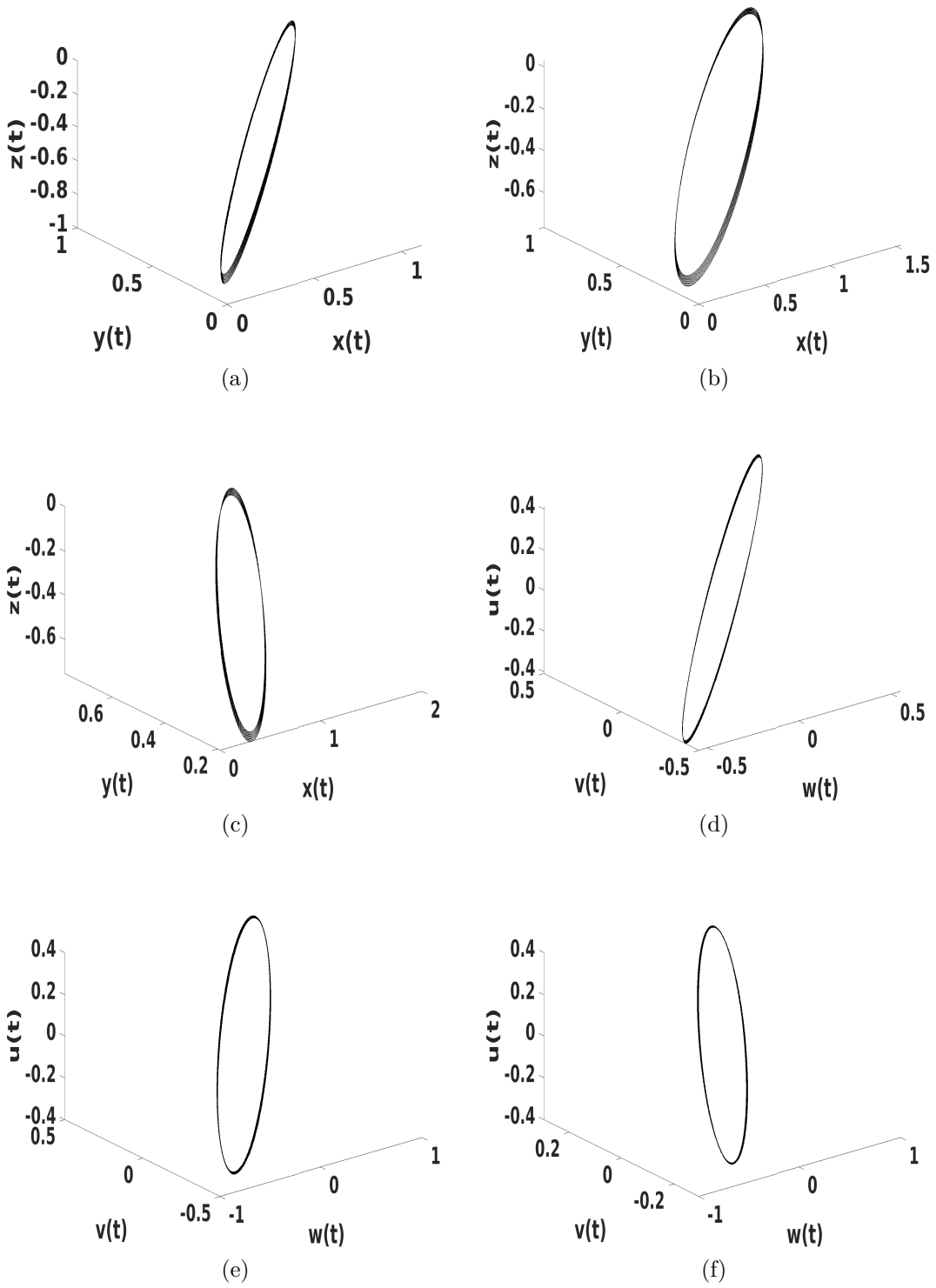

Figure 6.5: The trajectories of positions (a-c) and velocities (d-f) corresponding to the positions for $k_a = 3, 6, 9$, $Re = 0.05$ and $F_1 = 5$.

6.3.2 The Reynolds number

Fig. 6.5 shows that the particle motion aligns along the z-axis as the aspect ratio increases in the limit of low Re, as we have discussed in the previous session. To understanding the stroboscopic effect of Re on the orientation dynamics of suspensions, we plot the time series components of position and velocity by varying Re from 0.05 to 0.45. The plots are presented in Fig. 6.6 and Fig. 6.7, for values of the other parameters. As can be seen from the figures, the orientation resistance increases as Re increases. Moreover, the inertia effects position and velocity at higher Reynolds numbers (in the limit of $0 < Re < 1$), as seen from Figs. 6.7-6.9. The phase space area bounded by x-components of position and velocity of the spheroid decreases as Re increases as depicted in Fig. 6.8a. From Fig. 6.8b, it is evident that the size of the phase plot area of y-component representation tends to zero. In Fig. 6.8c, it can be observed that the phase space area of z-components of the particle drifted away from the zero displacement along axis of position in the negative direction. Fig. 6.9 shows the trajectory of positions in the infinite time limit for different values of Re. The spheroid attains its orbit in equilibrium, and its bounded area decreases as the Reynolds number increases. In addition, the orbit of the spheroid is shifted down along the z-axis as the Reynolds number increases; hence, the dynamics depends significantly on Re within its limit.

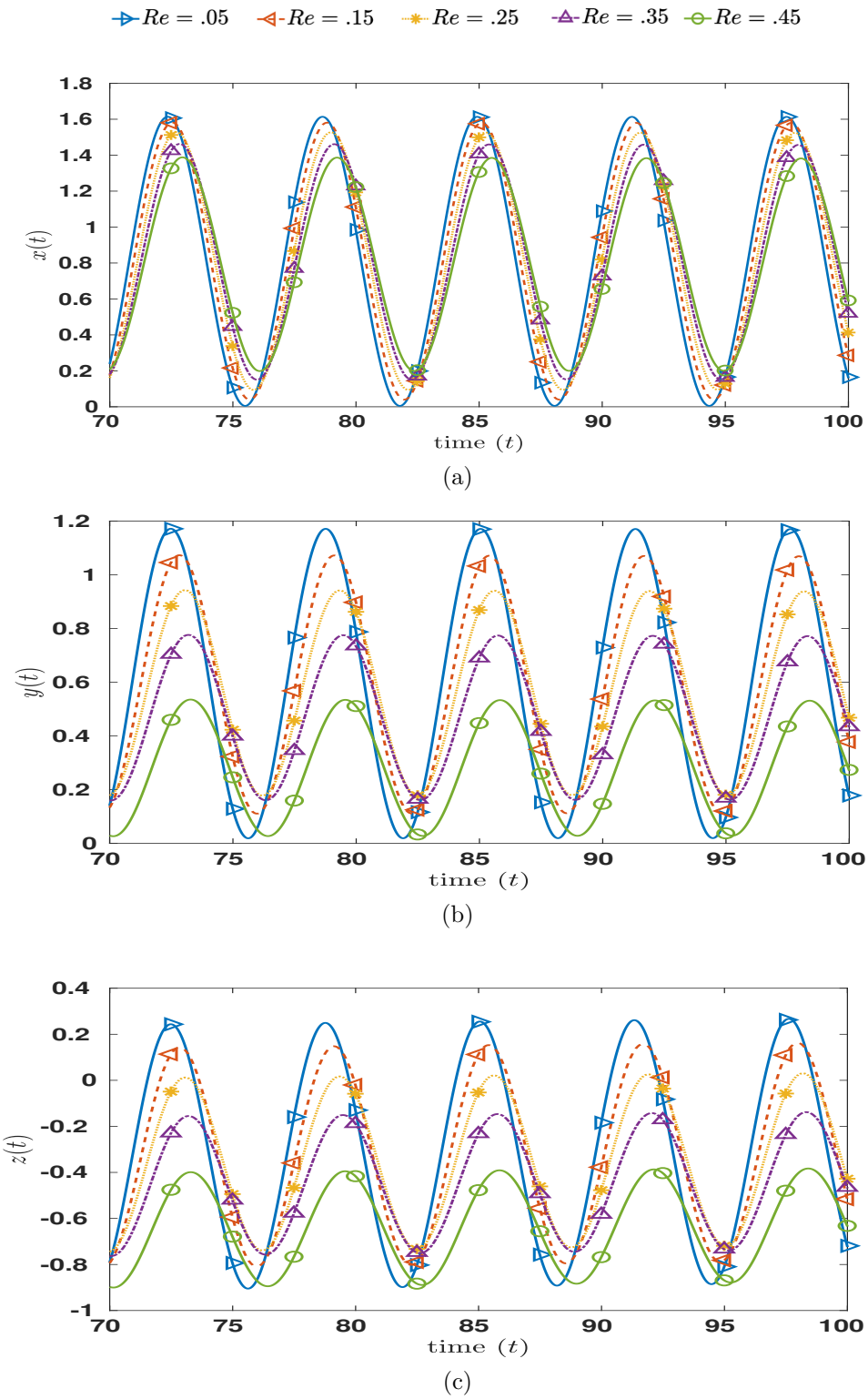

Figure 6.6: The components of position of motion for $F_1 = 1.5$, $\omega = 1$, $k_a = 6$ and $Re = 0.05, 0.15, 0.25, 0.35, 0.45$ (a) x-axis, (b) y-axis, (c) z-axis

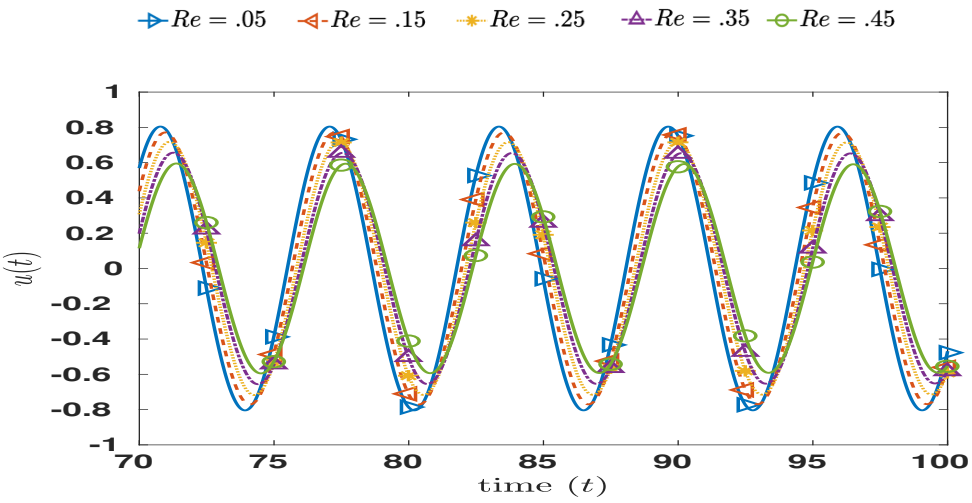

(a)

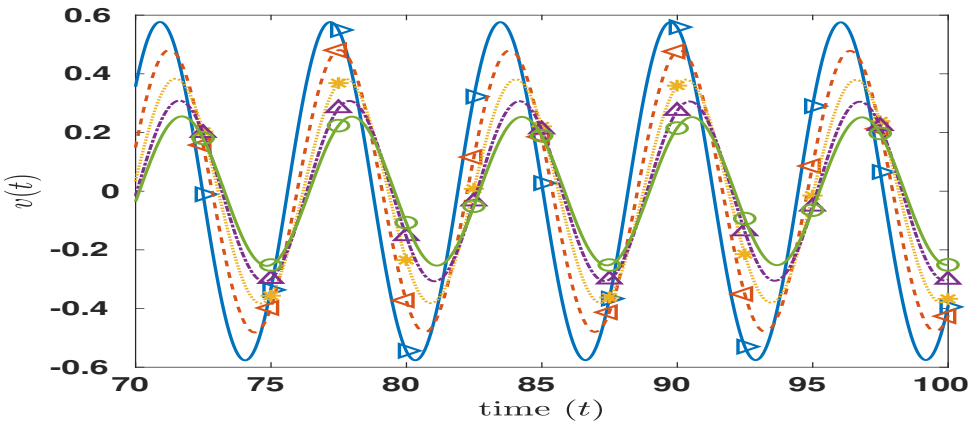

(b)

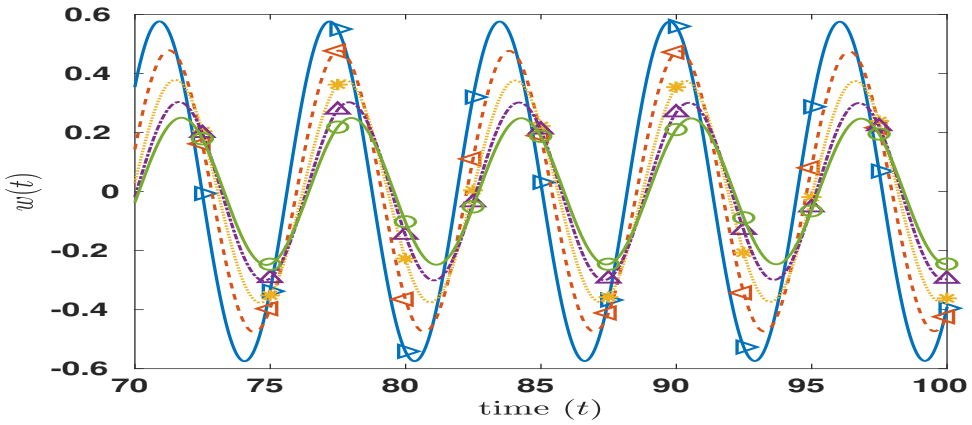

(c)

Figure 6.7: The velocity's components of motion shown in Fig. 6.6 for $F_1 = 1.5$, $\omega = 1$, aspect ratio $k_a = 6$, and $Re = 0.05, 0.15, 0.25, 0.35, 0.45$ are shown above.

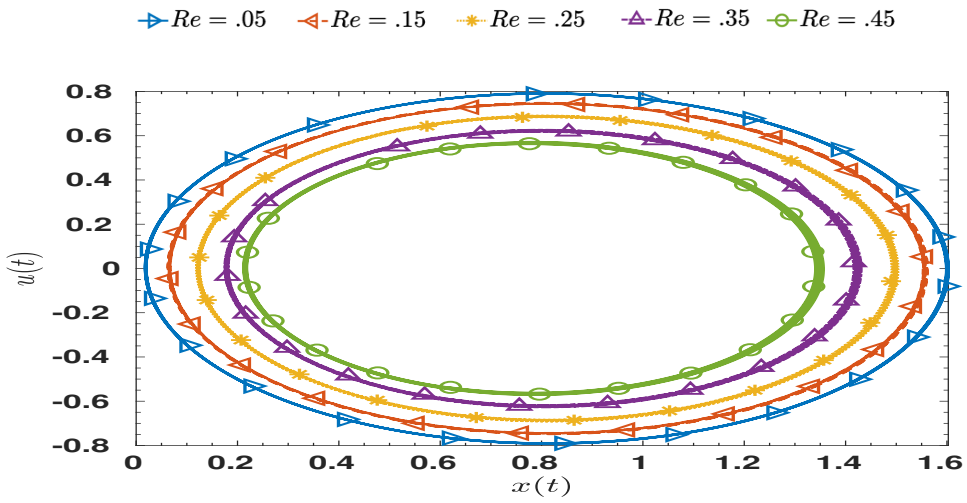

(a)

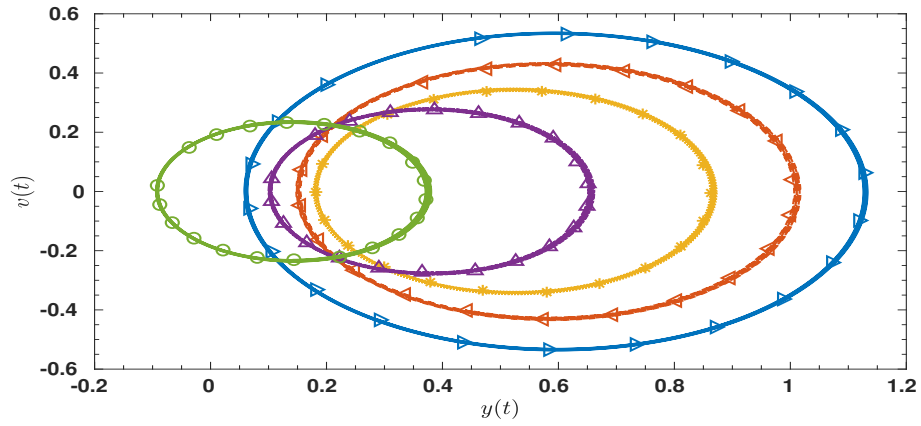

(b)

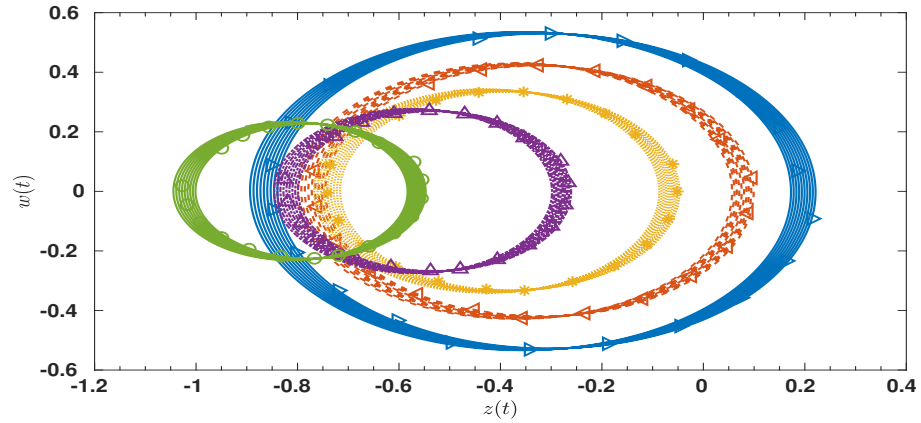

(c)

Figure 6.8: Phase plots of position and velocity for $F_1 = 1.5$, $\omega = 1$ $k_a = 6$, and $Re = 0.05, 0.15, 0.25, 0.35, 0.45$ are plotted. (a) x-components, (b) y-components and (c) z-components.

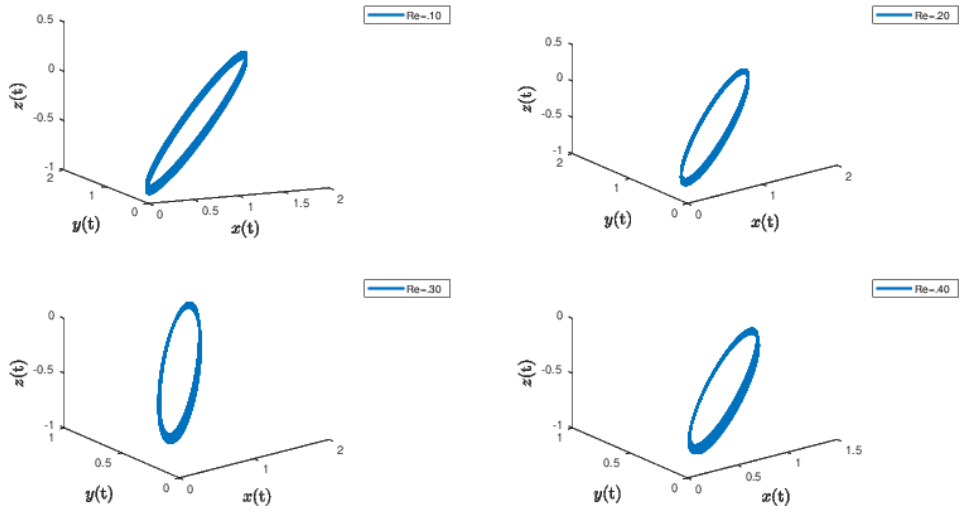

Figure 6.9: The trajectory of position of spheroid for $k_a = 6$, $\omega = 1$, $F_1 = 1.5$, and Reynolds number $Re = .1, 0.2, 0.3, \&0.4$.

6.3.3 The External Periodic Field

The next important parameter in this problem is the amplitude of the external periodic force field. We observe that the steady-state solution is a fixed orbit for a given set of parameters, and the interior area bounded by the orbit reduces with the increase in the amplitude of external force. Figs. 6.10 and 6.11 show the time series of the position and velocity of spheroid motion for different values of F_1, respectively. The amplitude of position and velocity oscillations increases significantly on varying amplitude of the force, as seen from the figures. Interestingly, the average position of particles moves up, whereas average velocity is constant for a given set of parameters, as evident from the graph of position and velocity given in Figs. 6.10 and 6.11. Fig. 6.12 shows the phase space plot of x, y, and z components of position and velocity. The phase space plot enlarges in a particular pattern as the parameter varies, and the area surrounded by the closed trajectory increases as F_1 increases due to the enlargement. The trajectory attractors of position for different values of amplitudes are given in Fig. 6.13, showing the dependence of the dynamics of the particle on external force. From the analysis,

it is confirmed that orientation dynamics rapidly changes as the parameter varies.

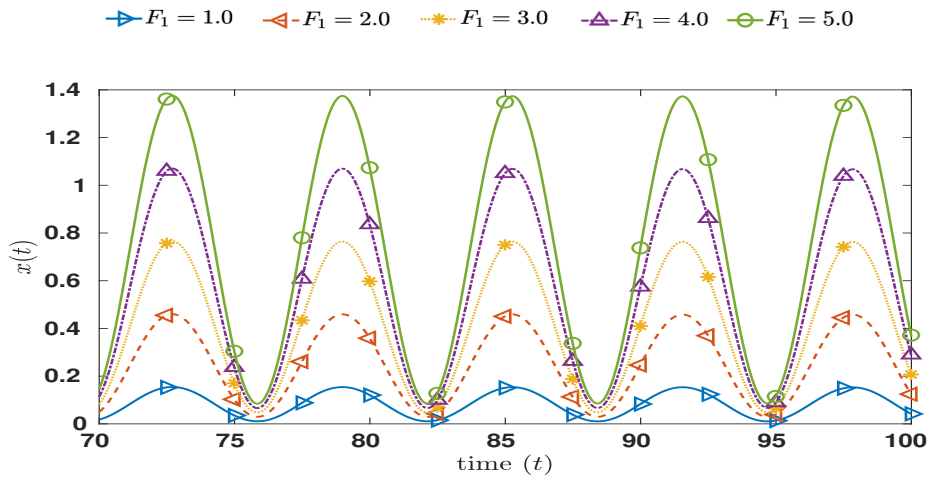

(a)

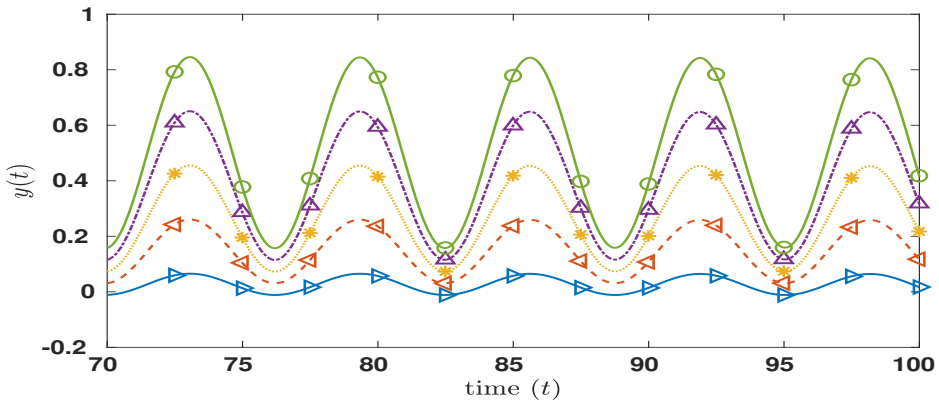

(b)

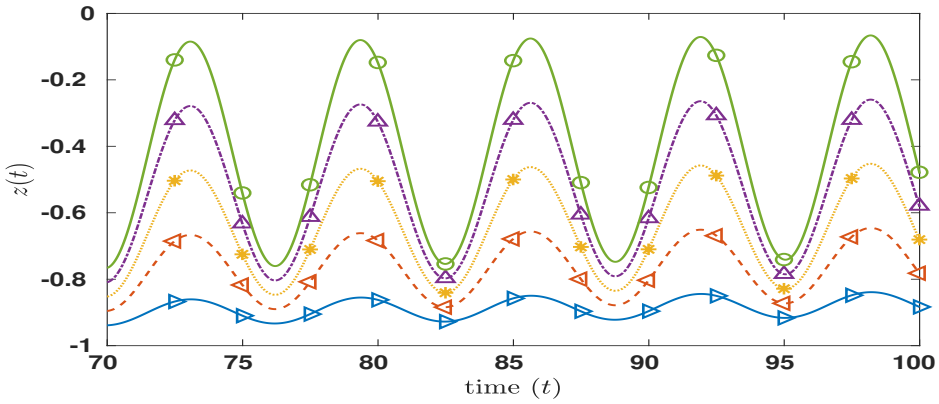

(c)

Figure 6.10: The time series of components of position of motion for $Re = 0.15$,, aspect ratio $k_a = 6$ and F_1 varying from 0.5 to 4.5.

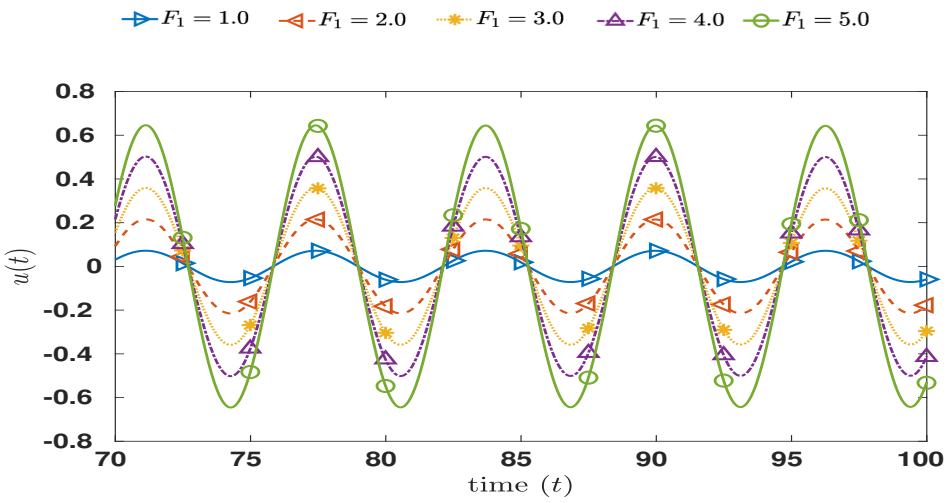

(a)

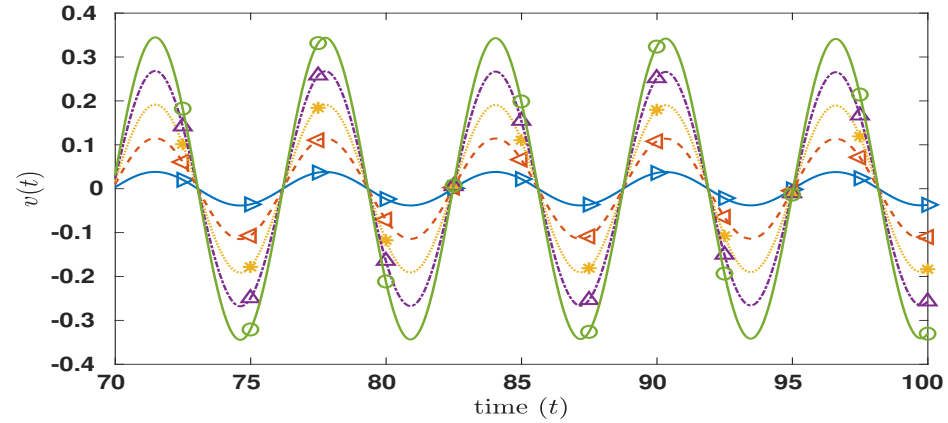

(b)

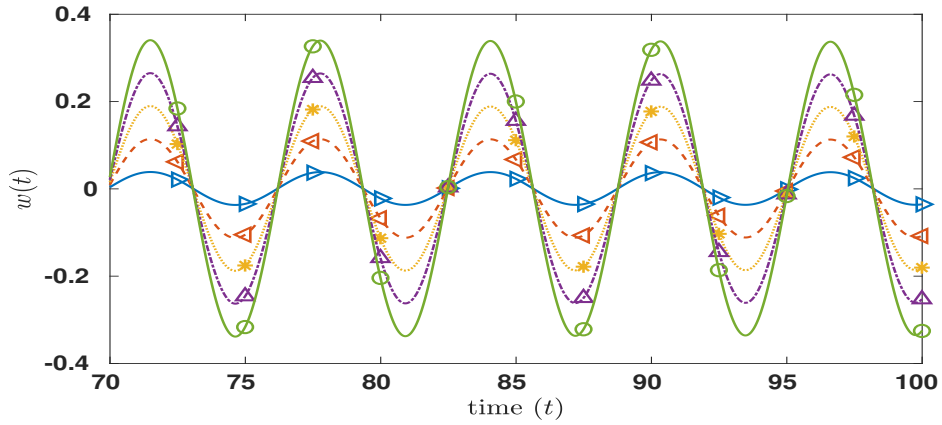

(c)

Figure 6.11: The time series of the velocity of the spheroid for the cases shown in Fig. 6.10.

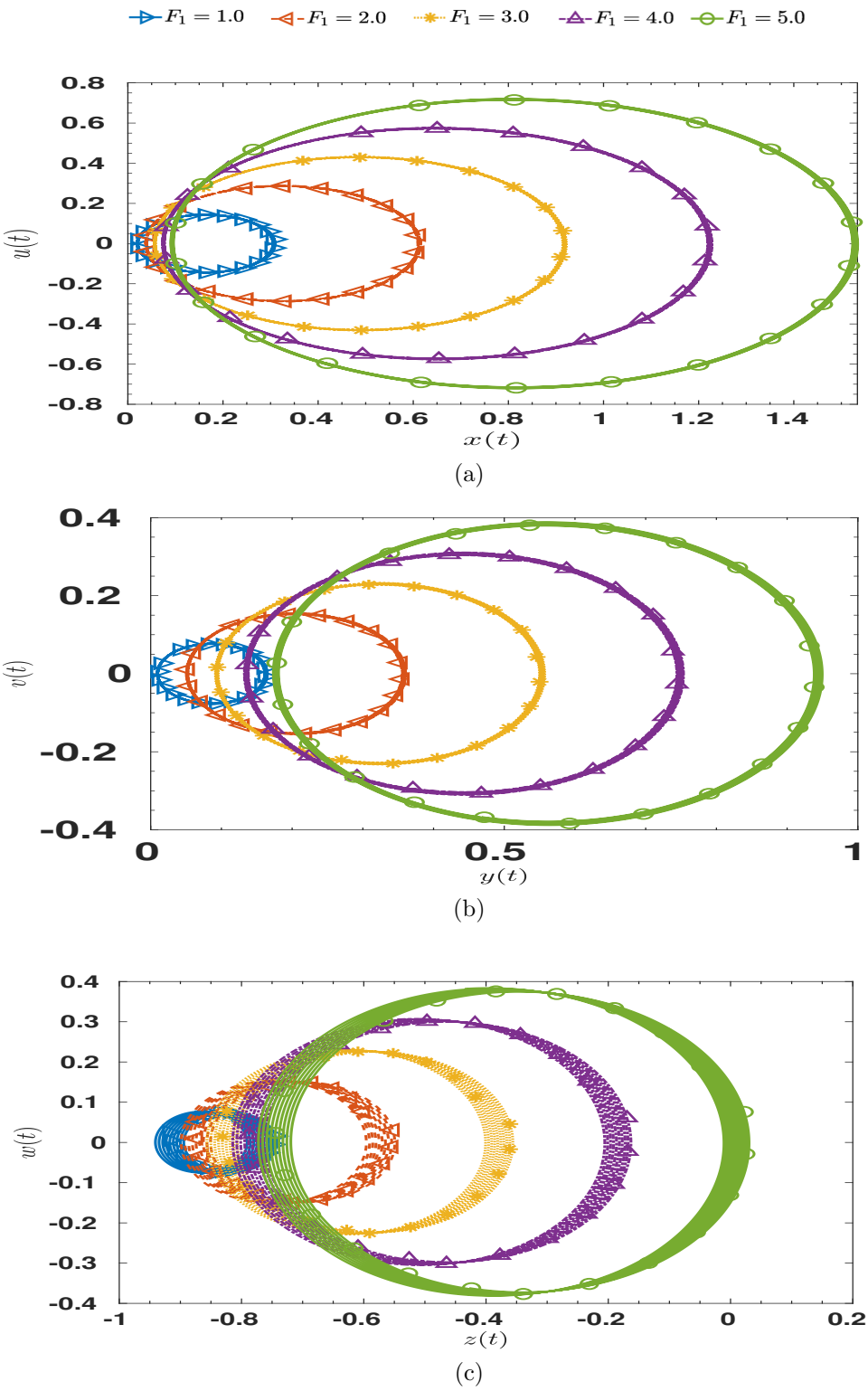

Figure 6.12: Component-wise phase plots of the spheroid for $Re = 0.05$, $k_a = 6$, and for different values of F_1.

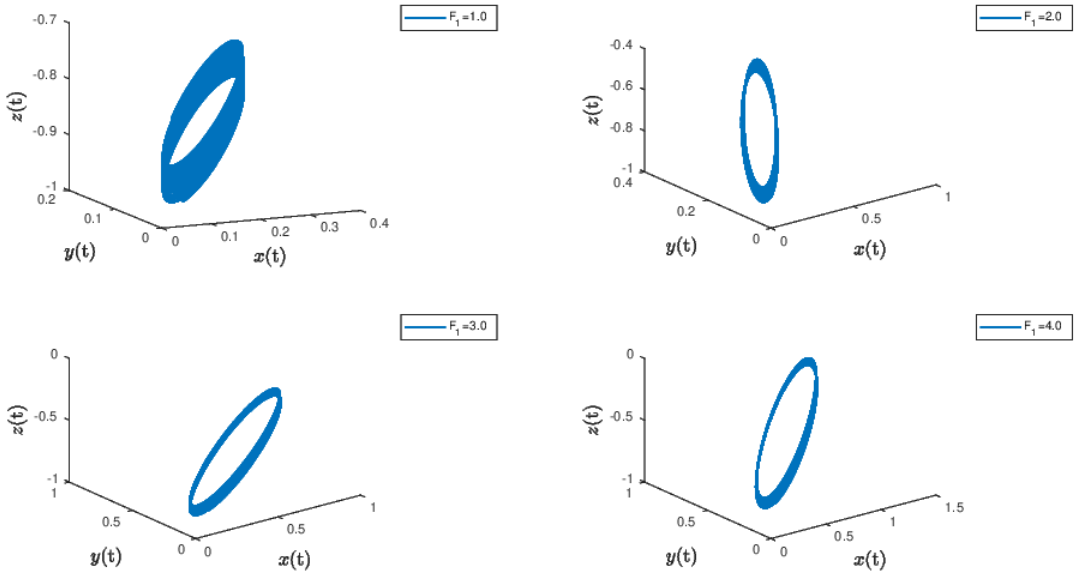

Figure 6.13: Trajectory of position of the spheroid for k_a=2, Re = 0.15, and F_1 = 1.0, 2.0, 3.0&4.0.

6.4 Conclusion

We attempt to examine the dynamics of a prolate spheroid subject to a periodic forcing in a Newtonian fluid flow with a uniform time-dependent velocity at low Reynolds numbers. Fluid and particle inertia terms have been included to study their effect on the orientation dynamics more realistically. The numerical values for the acceleration reaction term and the lift force for different aspect ratios are presented. It is observed that the values corresponding to the acceleration reaction term increase with the increase in aspect ratio and hence contribute to the orientation dynamics of the particle, whereas the values representing the term due to the lift force amount to near zeros and hence contribute no effect to the particle motion. Using this observation and the other essential calculations, a set of integro-differential equations governing the position and velocity of orientations in the limit of low Reynolds number is derived. Then the equations are numerically solved using some standard techniques. The results thus obtained are analysed

carefully by varying the parameters for characterising the changes in the motion behavior. The trajectory attractors of position and velocity of orientations depend on the parameters, aspect ratio, Reynolds number (within the limit), and the amplitude of the external field. It is confirmed that particle dynamics rapidly change as the parameter varies. The average position, the size of the attractors of position, and the respective velocity change as the parameter value changes, whereas the average velocity is zero for any of the parameter values. A phase shift in position, velocity, and drift of trajectories is also observed on varying parameters. These changes in the dynamics of suspension may affect the rheology of the suspension, like stress deformation; hence, the analysis is scientifically and technologically important.

Chapter 7

Summary of the thesis

In this dissertation, We have investigated the fundamental properties of a fluid suspension of a periodically forced spheroid in a Newtonian fluid at low Reynolds numbers. We have analyzed two classes of problems: the translational motion of a spheroid in one dimension and the rotational dynamics of a spheroid in three dimensions in a variety of flows that includes Quiescent fluid fields, Uniform time-dependent fluid fields, and Oscillating fluid fields. The equations governing the dynamics of a periodically driven micro-spheroid in an unsteady viscous fluid at low Reynolds numbers have been derived, and its oscillation properties are studied in the presence/absence of memory forces. These equations have been derived with the help of perturbation analysis of the motion of a sphere. The computed solution depends on the shape, free oscillation frequency, and ratio of particle density to fluid density and it is in agreement with the solutions which are available in the literature for the limiting case of a sphere. The maximum amplitude of the oscillations of an oblate spheroid has been greater than that of a prolate spheroid, showing that the velocity disturbance for an oblate spheroid was higher. The increase in aspect ratio has to lead to the enhancement (reduction) of amplitude peaks in the case of the oblate (prolate) spheroid in the presence and more dominantly in the absence of the force. A reduction in the amplitude

of spheroid oscillations of many multiples due to the memory force has been seen. More vital oscillation variations have been observed on changing natural frequency or particle-fluid density compared to aspect ratio. The variations of the phase value have been similar for both the spheroids on varying the frequency and density ratio, whereas they have reversed on changing the aspect ratio. The linear scaling of amplitude on aspect ratio observed for the spheroids might have given insight into the physics, especially regarding the quantum of velocity disturbances due to particle size. The slopes have been high in the absence of the force, confirming that the presence of the force essentially increases the resistance of spheroid motion.

In addition, we have studied the motion of a spheroid of an average aspect ratio in a viscous fluid under the action of an external harmonic force. Here, first, we have derived the dynamics equation of the particle oscillating along with one of its axes and subject to damping, Basset memory, and second history integral forces at small Reynolds numbers, and then, we have proceeded to obtain an analytical solution of this equation at resonance. With graphical representation, we have observed that for a prolate spheroid, the conventional Q-curves have shown a more significant variation concerning the particle aspect ratio, particle–fluid density ratio, and natural frequency; the variation has been significantly more for the curve corresponding to the second history force. Furthermore, we have found that all three forces affect the amplitude of motion: the amplitude has increased with the strength of damping and the second history integral forces, whereas the presence of Basset memory has decreased it. Remarkably, Basset memory has caused a phase-shift in the oscillations, while the other two forces do not affect the phase. Since our solutions have been analytical, they might have practical application in experiments involving more complex systems, mainly to understand the effect of external force on the transport of micro-particles.

Subsequently, we have discussed a solution for the orientation transport of a periodically driven prolate spheroid suspended in Newtonian fluid oscillating

in the range of low Reynolds number. A set of ordinary differential equations governing the migration of an arbitrarily forced spheroid in a quiescent flow at low Reynolds numbers have been formulated and discussed, assuming a sufficiently dilute suspension to neglect the particle-particle interactions. These governing equations are nonlinear and contain a history term of all the past positions and velocities; hence, obtaining an analytical solution would be difficult. Therefore, we have performed numerical simulations for the numerical approximation of these equations. Since the prolate spheroid has been suspended in a quiescent fluid, the motion of the prolate spheroid has been solely due to the external periodic force acting on the particle. The phase of motion has been helical, and the size of orbits of the helix has decreased as the Reynolds number increases. The spheroid transport has been investigated by varying Reynolds numbers, particle aspect ratios, and external forces. Interestingly, the size of the attractor has increased as the aspect ratio or/and force has increased, whereas it has decreased as the Reynolds number has increased. This decrease has been due to the increase in particle inertia. A delay with the velocity at the maximum position has been observed, as evident from the respective time series. The delay could be that in the absence of inertia, the time at which the velocity reaches its maximum, the position was at its minimum, and when the particle experienced its maximum deviation, the velocity was at its minimum. Since position variation has been almost sinusoidal, the velocity would also be sinusoidal with a phase shift of nearly $\pi/2$. The net migration at zero Reynolds number would be negligible and should have increased with the number increased. Inertia should have changed this to a more considerable extent at higher values of Reynolds number. We have observed that the velocity and displacement increased as the system parameters, such as natural frequency, the aspect ratio of the spheroid, and the magnitude of the externally driving periodic force, increased.

The investigation done in the case of quiescent flow has been repeated with the uniform flow and oscillating flow. The numerical values for the acceleration

reaction term for different aspect ratios have been presented for both cases. We have observed that the amplitude of velocity and displacement increases as frequency, and the aspect ratio of the spheroid or/and force increases in the case of oscillating fluid. Moreover, the amplitude of velocity and displacement decreases as frequency, aspect ratio, or/and force increases. However, the phase plot is reversed when the force is changed in the opposite direction. In the case of time-dependent uniform flow, we stress that the values corresponding to the acceleration reaction term increase as the aspect ratio increases, and hence it is a significant study. On the other hand, the lift force exerted by the uniform fluid flow on the spheroid particle is negligibly small and hence it is insignificant. To illustrate the dynamics, we have provided phase diagrams of the properties of the solutions having functional relations with the particle's geometry, amplitude and phase of an external field, and Reynolds numbers. We have observed a phase shift in position and velocity, a drift in solution trajectories, and orientation properties as a function of aspect ratio, the amplitude of the external field, and the Reynolds number in the low $\Re$ limit. In each chapter, the results have been supplemented with detailed physical arguments, and wherever possible, various tests have been conducted to justify the results. Based on this study, we believe that the dependencies of oscillations on the parameters could be utilized for better separation of particles or characterizing the suspension. The obtained analytical solutions would help in testing software for more complicated and realistic systems and strike a good balance between complication and tractability. The dependence of the position and velocity on the parameters could be characterized by using it as a potential application to particle separation.

Appendix A

Some useful mathematical expressions and tools

A.1 The co-ordinate system

We will denote by $\{r, \theta, \phi\}$ the prolate spheroidal coordinates which have the following domain of definition:

$$r \to [0, \infty), \tag{A.1a}$$

$$\theta \to [0, \pi], \tag{A.1b}$$

$$\phi \to [0, 2\pi]; \tag{A.1c}$$

and are related to the usual Cartesian coordinates (x, y, z) by:

$$x = r \sin(\theta) \cos(\phi), \tag{A.2a}$$

$$y = r \sin(\theta) \sin(\phi), \tag{A.2b}$$

$$z = \sqrt{r^2 + r_\mu^2}\cos(\theta); \tag{A.2c}$$

where the constant parameter r_μ has the meaning of the distance of the foci from the origin of the Cartesian coordinate system. One can see also that surfaces $r = constant$ are prolate spheroids with their foci along the z-axis, and therefore satisfy:

$$\frac{z^2}{r^2 + r_\mu^2} + \frac{x^2 + y^2}{r^2} = 1 \tag{A.3}$$

where the value $r = constant$ correspond to the length of its minor radius and the size of its major radius is equal to $\sqrt{r^2 + r_\mu^2}$. In this coordinates system the line element of the flat Euclidean metric in R^3 acquires the following expression:

$$ds^2 = \left(r^2 + r_\mu^2 \sin(\theta)^2\right)\left(\frac{dr^2}{r^2 + r_\mu^2} + d\theta^2\right) + r^2 \sin(\theta)^2 d\phi^2$$

A.2 Illustration of $I_1(t) = \int_0^\infty \frac{d^2y}{d\tau^2}\frac{d\tau}{\sqrt{t-\tau}}$ and $\int_0^t \frac{d^2y}{d\tau^2}\,\mathrm{erfc}\left[(t-\tau)^{\frac{1}{2}}\right]d\tau$

Let

$$G(\alpha) = \int_{-\infty}^{\infty} \exp(-\alpha x^2)dx \tag{A.4}$$

Since $\exp(-\alpha x^2)$ is even function in domain $(-\infty, \infty)$, therefore by using integral property, we can write it as

$$G(\alpha) = 2\int_0^{\infty} \exp(-\alpha x^2)dx. \tag{A.5}$$

The integral (A.4) and (A.5) is Gaussian integral and its deduced integral over right half domain, respectively. These lead to the value of following integral:

$$\int_{-\infty}^{\infty} e^{-\alpha x^2}dx = \sqrt{\frac{\pi}{\alpha}}\ , \qquad \int_0^{\infty} e^{-\alpha x^2}dx = \frac{1}{2}\sqrt{\frac{\pi}{\alpha}}\ . \tag{A.6}$$

Now if the integrand is complex function, by assuming $\alpha = i$, we have obtained

$$\int_{-\infty}^{\infty} e^{-ix^2} dx = \sqrt{\frac{\pi}{i}} \ , \qquad\qquad \int_{0}^{\infty} e^{-ix^2} dx = \frac{1}{2}\sqrt{\frac{\pi}{i}} \, . \tag{A.7}$$

We know that the square root of i is $\frac{1+i}{\sqrt{2}}$, of course it is principal value (in general $\pm\frac{1+i}{\sqrt{2}}$ or $e^{k\pi i + \frac{\pi i}{4}}$, $k = 0, 1$). Whence we have obtained

$$\int_{-\infty}^{\infty} e^{-ix^2} dx = \frac{(1-i)\sqrt{\pi}}{\sqrt{2}} \, . \tag{A.8}$$

The equation (A.8) may be written as

$$\int_{-\infty}^{\infty} \Big(\cos(x^2) - i\sin(x^2)\Big) \, dx = \sqrt{\frac{\pi}{2}} - i\sqrt{\frac{\pi}{2}} \, . \tag{A.9}$$

Hence we have found

$$\int_{-\infty}^{\infty} \cos(x^2) dx = \int_{-\infty}^{\infty} \cos(x^2) dx = \sqrt{\frac{\pi}{2}} \, . \tag{A.10}$$

$$\begin{aligned} I_1(t) &= \int_0^{\infty} \frac{d^2y}{d\tau^2} \frac{d\tau}{\sqrt{t-\tau}} \\ &= -\frac{\omega^{3/2}\sqrt{\pi}}{2\sqrt{2}} \left[R_1 \left\{\sin(\omega t) + \cos(\omega t)\right\} + R_2 \left\{\sin(\omega t) - \cos(\omega t)\right\}\right] \end{aligned} \tag{A.11}$$

To evaluate it, consider its Laplace transformation

$$\begin{aligned} \hat{I}_1(s) = \ & \mathscr{L}\{\frac{d^2y}{dt^2}\} \, \mathscr{L}\{\frac{1}{\sqrt{t}}\} = \ \mathscr{L}\{-\omega^2 \left(R_1 \cos\omega t + R_2 \sin\omega t\right)\} \, \mathscr{L}\{\frac{1}{\sqrt{t}}\} \\ &= -\omega^2 \frac{R_1 s + R_2 \omega}{s^2 + \omega^2} \sqrt{\frac{\pi}{s}} \\ &= -\omega^2 \sqrt{\pi} \frac{R_1 s + R_2 \omega}{s^2 + \omega^2} \frac{1}{\sqrt{s}} \end{aligned} \tag{A.12}$$

This expression can be further written in terms of a sum of simple fractions,

$$\begin{aligned}\hat{I}_1(s) &= -\omega^2\sqrt{\pi}\left\{\frac{R_1 s}{s^2+\omega^2}\frac{1}{\sqrt{s}} + \frac{R_2\omega}{s^2+\omega^2}\frac{1}{\sqrt{s}}\right\} \\ &= -\omega^2\sqrt{\pi}\left\{\frac{R_1}{2}\left(\frac{1}{\sqrt{s}(s+i\omega)} + \frac{1}{\sqrt{s}(s-i\omega)}\right) - \frac{R_2}{2i}\left(\frac{1}{\sqrt{s}(s+i\omega)} - \frac{1}{\sqrt{s}(s-i\omega)}\right)\right\}\end{aligned} \tag{A.13}$$

The inverse Laplace transformation then leads to

$$\begin{aligned}I_1(t) =& -\omega^2\sqrt{\pi}\left\{\frac{R_1}{2}\left(\frac{e^{-i\omega t}\,\mathrm{erf}(\sqrt{-i\omega t})}{\sqrt{-i\omega}} + \frac{e^{i\omega t}\,\mathrm{erf}(\sqrt{i\omega t})}{\sqrt{i\omega}}\right)\right. \qquad \text{(A.14)} \\ &\left. -\frac{R_2}{2i}\left(\frac{e^{-i\omega t}\,\mathrm{erf}(\sqrt{-i\omega t})}{\sqrt{-i\omega}} - \frac{e^{i\omega t}\,\mathrm{erf}(\sqrt{i\omega t})}{\sqrt{i\omega}}\right)\right\} \\ =& -\frac{\omega^{3/2}\sqrt{\pi}}{2\sqrt{2}}\left[R_1\left\{\sin(\omega t)+\cos(\omega t)\right\} + R_2\left\{\sin(\omega t)-\cos(\omega t)\right\}\right] \qquad \text{(A.15)}\end{aligned}$$

Since, by the obvious, $\mathrm{erf}(\pm\infty) = \pm 1$, or one can find it by using definition of error function along with equations (A.5)-(A.10). On simplifications of all terms reduce to

$$I_1(t) = -\frac{\omega^{3/2}\sqrt{\pi}}{2\sqrt{2}}\left[R_1\left\{\sin(\omega t)+\cos(\omega t)\right\} + R_2\left\{\sin(\omega t)-\cos(\omega t)\right\}\right] \tag{A.16}$$

and also we deduced

$$\begin{aligned}\frac{dI_1(t)}{dt} &= \int_0^\infty \frac{d^2y}{d\tau^2}\left(-\frac{1}{2}\right)\frac{1}{(t-\tau)^{3/2}}d\tau \\ &= \left(-\frac{1}{2}\right)\int_0^\infty \frac{d^2y}{d\tau^2}\frac{1}{(t-\tau)^{3/2}}d\tau\end{aligned} \tag{A.17}$$

Let

$$I_2(t) = \int_0^t \frac{d^2y}{d\tau^2}\,\mathrm{erfc}\left[(t-\tau)^{\frac{1}{2}}\right]d\tau \tag{A.18}$$

here, we have $y(t) = R_1\cos(\omega t) + R_2\sin(\omega t)$ and $\ddot{y}(t) = -\omega^2\left(R_1\cos(\omega t) + R_2\sin(\omega t)\right)$.

Therefore the (A.18) can be written as

$$\begin{aligned} I_2(t) &= \int_0^t -\omega^2 \left(R_1 \cos(\omega t) + R_2 \sin(\omega t)\right) \operatorname{erfc}\left[(t-\tau)^{\frac{1}{2}}\right] d\tau \\ &= -\omega^2 \int_0^t \left(R_1 \cos(\omega t) + R_2 \sin(\omega t)\right) \operatorname{erfc}\left[(t-\tau)^{\frac{1}{2}}\right] d\tau. \end{aligned} \tag{A.19}$$

Letting $f(t) = \operatorname{erfc}(t)$, then the above integration written as convolution of $y(t)$ and $f(t)$,

$$I_2(t) = -\omega^2 \int_0^t y(\tau) f(t-\tau) d\tau. \tag{A.20}$$

Now by considering Laplace transformation of $I_2(t)$ is $\hat{I}(s)$, we have

$$\begin{aligned} \hat{I}_2(s) &= \mathscr{L}(\{I_2(t)\}) \\ &= -\omega^2 \, \mathscr{L}(\{y(t)\}) \, \mathscr{L}(\{f(t)\}) \\ &= -\omega^2 \frac{R_1 s + R_2 \omega}{s^2 + \omega^2} \frac{\sqrt{s+1} - 1}{s\sqrt{s+1}} \\ &= -\omega^2 \frac{R_1 s + R_2 \omega}{s^2 + \omega^2} \left(\frac{1}{s} - \frac{1}{s\sqrt{s+1}}\right) \\ &= -\omega^2 \left[\frac{R_1 \omega - R_2 s}{\omega\left(s^2 + \omega^2\right)} + \frac{R_2}{\omega s} - \frac{1}{1+\omega^2} \left\{ \left(R_1 - R_2 \omega\right) \frac{\sqrt{s+1}}{s^2 + \omega^2} - \left(R_2 + R_1 \omega\right) \frac{s\sqrt{s+1}}{s^2 + \omega^2} \right.\right. \\ &\quad \left.\left. + \frac{R_2}{\omega} \frac{(1+\omega^2)\sqrt{s+1}}{s} + \left(R_1 - R_2 \omega\right) \frac{\sqrt{s+1}}{s+1} \right\}\right] \end{aligned} \tag{A.21}$$

The inverse Laplace transform gives

$$\begin{aligned} I_2(t) = &-\omega^2 \left[\frac{R_1}{\omega} \sin(\omega t) - \frac{R_2}{\omega} \cos(\omega t) + \frac{R_2}{\omega} \left(1 - (\pi t)^{-\frac{1}{2}} e^{-t} - \operatorname{erf}(\sqrt{t})\right) \right. \\ &- \frac{1}{1+\omega^2} \left\{ \frac{\left(R_1 - R_2 \omega\right)}{2} \left(\frac{e^{(-i\omega+1)t} \operatorname{erf}(\sqrt{(-i\omega+1)t})}{\sqrt{(-i\omega+1)}} + \frac{e^{(i\omega+1)t} \operatorname{erf}(\sqrt{(i\omega+1)t})}{\sqrt{(i\omega+1)}} \right) \right. \\ &+ \frac{\left(R_2 + R_1 \omega\right)}{2i} \left(\frac{e^{(-i\omega+1)t} \operatorname{erf}(\sqrt{(-i\omega+1)t})}{\sqrt{(-i\omega+1)}} - \frac{e^{(i\omega+1)t} \operatorname{erf}(\sqrt{(i\omega+1)t})}{\sqrt{(i\omega+1)}} \right) \\ &\left.\left. + \left(R_1 - R_2 \omega\right) (\pi t)^{-\frac{1}{2}} e^{-t} \right\}\right] \end{aligned} \tag{A.22}$$

We obtain after some simplifications

$$I_2(t) = -\,\omega\,(R_1\sin(\omega t) - R_2\cos(\omega t)) \tag{A.23}$$

Bibliography

Abbad M, Souhar M (2004) Effects of the history force on an oscillating rigid sphere at low Reynolds number. Experiments in fluids 36(5):775–782

Abbad M, Souhar M, Caballina O (2006) Note on the memory force on a slightly eccentric fluid spheroid in unsteady creeping flows. Physics of Fluids 18(1):013301

Acrivos A, Lo T (1978) Deformation and breakup of a single slender drop in an extensional flow. Journal of Fluid Mechanics 86(4):641–672

Asokan K, Kumar CVA, Dasan J, Radhakrishnan K, Kumar KS, Ramamohan TR (2005) Review of chaos in the dynamics and rheology of suspensions of orientable particles in simple shear flow subject to an external periodic force. Journal of non-Newtonian fluid mechanics 129(3):128–142

Basset AB (1888a) On the motion of a sphere in a viscous liquid. Philosophical Transactions of the Royal Society of London(A) 179:43–63, DOI 10.1098/rsta.1888.0003

Basset AB (1888b) A treatise on hydrodynamics: with numerous examples, vol 2. Deighton, Bell and Company

Batchelor G (1970) The stress system in a suspension of force-free particles. Journal of fluid mechanics 41(3):545–570

Brenner H (1966) Hydrodynamic resistance of particles at small reynolds numbers. In: Advances in Chemical Engineering, vol 6, Elsevier, pp 287–438

Brenner H (1972) Dynamics of neutrally buoyant particles in low reynolds number flows. In: Proceedings of the International Symposium on Two-Phase Systems, Elsevier, pp 509–574

Brenner H (1974) Rheology of a dilute suspension of axisymmetric Brownian particles. International Journal of Multiphase Flow 1(2):195–341

Bretherton F (1962a) Slow viscous motion round a cylinder in a simple shear. Journal of Fluid Mechanics 12(4):591–613

Bretherton FP (1962b) The motion of rigid particles in a shear flow at low Reynolds number. Journal of Fluid Mechanics 14(2):284–304, DOI 10.1017/S002211206200124X

Buchanan J (1890) The oscillations of a spheroid in a viscous liquid. Proceedings of the London Mathematical Society 1(1):181–215

Buevich YA, Syutkin SV, Tetyukhin VV (1985) Theory of a developed magnetofluidized bed. Magnetohydrodynamics 20(4):333–338

Burgers JM (1995) On the motion of small particles of elongated form. suspended in a viscous liquid. In: Selected Papers of JM Burgers, Springer, pp 209–280

Candelier F, Angilella JR, Souhar M (2005) On the effect of inertia and history forces on the slow motion of a spherical solid or gaseous inclusion in a solid-body rotation flow. Journal of Fluid Mechanics 545:113–139, DOI 10.1017/S0022112005006877

Cebers A (1993a) Chaos in polarization relaxation of a low-conducting suspension of anisotropic particles. Journal of Magnetism and Magnetic Materials 122(1-3):277–280

Cebers A (1993b) Chaos: new trend of magnetic fluid research. Journal of Magnetism and Magnetic Materials 122(1-3):281–285

Chwang AT (1975) Hydromechanics of low-reynolds-number flow. part 3. motion of a spheroidal particle in quadratic flows. Journal of Fluid Mechanics 72(1):17–34

Chwang AT, Wu TY (1976) Hydromechanics of low-reynolds-number flow. part 4. translation of spheroids. Journal of Fluid Mechanics 75(4):677–689

Chwang AT, Wu TYT (1974) Hydromechanics of low-Reynolds-number flow. part 1. rotation of axisymmetric prolate bodies. Journal of Fluid Mechanics 63(3):607–622

Chwang AT, Wu TYT (1975) Hydromechanics of low-Reynolds-number flow. part 2. singularity method for Stokes flows. Journal of Fluid Mechanics 67(4):787–815

Cox R (1970) The motion of long slender bodies in a viscous fluid part 1. general theory. Journal of Fluid mechanics 44(4):791–810

Dabade V, Marath NK, Subramanian G (2016) The effect of inertia on the orientation dynamics of anisotropic particles in simple shear flow. Journal of Fluid Mechanics 791:631–703, DOI 10.1017/jfm.2016.14

Goldsmith H, Mason S (1967) Chapter 2 - the microrheology of dispersions. In: Eirich FR (ed) Rheology, Academic Press, pp 85–250, DOI https://doi.org/10.1016/B978-1-4832-2941-6.50008-8

Goldstein S (1929) The steady flow of viscous fluid past a fixed spherical obstacle at small reynolds numbers. Proceedings of the Royal Society of London Series A, Containing Papers of a Mathematical and Physical Character 123(791):225–235

Guazzelli E, Morris JF (2012) A Physical Introduction to Suspension Dynamics. Cambridge University Press

Happel J, Brenner H (2012) Low Reynolds number hydrodynamics: with special applications to particulate media, vol 1. Springer Science & Business Media

Hassan HK, Stepanyants YA (2017) Resonance properties of forced oscillations of particles and gaseous bubble in a viscous fluid at small Reynolds numbers. Physics of Fluids 29(1):101703, DOI 10.1063/1.5002152

Hassan HK, Ostrovsky LA, Stepanyants YA (2017) Particle dynamics in a viscous fluid under the action of acoustic radiation force. Interdisciplinary Journal of Discontinuity, Nonlinearity, and Complexity 6(3):317–327, DOI 10.5890/DNC.2017.09.006

Hill R, Power G (1956) Extremum principles for slow viscous flow and the approximate calculation of drag. The Quarterly Journal of Mechanics and Applied Mathematics 9(3):313–319, DOI 10.1093/qjmam/9.3.313

Ignatenko NM (1984) Excitation of ultrasonic vibrations in a suspension of uniaxial ferromagnetic particles by volume magnetostriciton. Magnetohydrodynamics 20:237–240

Jeffrey GB (1922) The motion of ellipsoidal particles immersed in a viscous fluid. Proc R Soc London, Ser A 102(715):161–179

Kashevskii BE (1986) Torque and rotational hysteresis in a suspension of single-domain ferromagnetic particles. Magnetohydrodynamics 22:161–168

Keller JB, Rubenfeld LA, Molyneux JE (1967) Extremum principles for slow viscous flows with applications to suspensions. Journal of Fluid Mechanics 30(1):97–125

Klepper D, Kolenkow R (2014) An Introduction to Mechanics. Cambridge University Press

Kulkarni PM, Morris JF (2008) Suspension properties at finite Reynolds number from simulated shear flow. Physics of Fluids 20(4):040602

Kumar CVA, Ramamohan TR (1997) New class I intermittency in the dynamics of periodically forced spheroids in simple shear flow. Physics Letters A 227(1-2):72–78, DOI 10.1016/S0375-9601(97)00030-3

Kumar CVA, Ramamohan TR (1998) Controlling chaotic dynamics of periodically forced spheroids in simple shear flow: Results for an example of a potential application. Sadhana 23(2):131–149, DOI 10.1007/BF02745678

Kumar CVA, Kumar KS, Ramamohan TR (1995) Chaotic dynamics of periodically forced spheroids in simple shear flow with potential application to particle separation. Rheologica Acta 34(5):504–511, DOI 10.1007/BF00396563

Kumar KS, Ramamohan TR (1995) Chaotic rheological parameters of periodically forced suspensions of slender rods in simple shear flow. Journal of Rheology 39:1229–1241

Kumar KS, Savithri S, Ramamohan TR (1996) Chaotic dynamics and rheology of suspensions of periodically forced slender rods in simple shear flow. Japanese Journal of Applied Physics 35(11R):5901

Lagerstrom P, Cole J (1955) Examples illustrating expansion procedures for the navier-stokes equations. Journal of Rational Mechanics and Analysis 4:817–882

Lawrence CJ, Weinbaum S (1986) The force on an axisymmetric body in linearized, time dependent motion: a new memory term. Journal of Fluid Mechanics 171:209–218, DOI 10.1017/S0022112086001428

Lawrence Ct, Weinbaum S (1988) The unsteady force on a body at low Reynolds number; the axisymmetric motion of a spheroid. Journal of Fluid Mechanics 189:463–489, DOI 10.1017/S0022112088001107

Leal L (1971) On the effect of particle couples on the motion of a dilute suspension of spheroids. Journal of Fluid Mechanics 46(2):395–416

Leal LG (1979) The motion of small particles in non-newtonian fluids. Journal of Non-Newtonian Fluid Mechanics 5:33–78

Leal LG, Hinch EJ (1971) The effect of weak Brownian rotations on particles in shear flow. Journal of Fluid Mechanics 46(4):685–703

Lee S, Leal L (1982) The motion of a sphere in the presence of a deformable interface: Ii. a numerical study of the translation of a sphere normal to an interface. Journal of Colloid and Interface Science 87(1):81–106

Lee S, Chadwick R, Leal LG (1979) Motion of a sphere in the presence of a plane interface. part 1. an approximate solution by generalization of the method of lorentz. Journal of Fluid Mechanics 93(4):705–726

Ley MW, Bruus H (2016) Continuum modeling of hydrodynamic particle–particle interactions in microfluidic high-concentration suspensions. Lab on a Chip 16(7):1178–1188

Li X, Sarkar K (2005) Effects of inertia on the rheology of a dilute emulsion of drops in shear. Journal of Rheology 49(6):1377–1394

Lin CJ, Peery JH, Schowalter WR (1970) Simple shear flow round a rigid sphere: inertial effects and suspension rheology. Journal of Fluid Mechanics 44(1):1–17

Looker JR, Carnie SL (2004) The hydrodynamics of an oscillating porous sphere. Physics of Fluids 16(1):62–72

Lovalenti PM, Brady JF (1993a) The force on a sphere in a uniform flow with small-amplitude oscillations at finite Reynolds number. Journal of Fluid Mechanics 256:607–614, DOI 10.1017/S0022112093002897

Lovalenti PM, Brady JF (1993b) The hydrodynamic force on a rigid particle undergoing arbitrary time-dependent motion at small Reynolds number. Journal of Fluid Mechanics 256:561–605, DOI 10.1017/S0022112093002885

MacMillan EH (1989) Slow flows of anisotropic fluids. Journal of Rheology 33(7):1071–1105

Madhukar K, Kumar PV, Ramamohan TR, Shivakumara IS (2010) Dynamics and 'normal stress' evaluation of dilute suspensions of periodically forced prolate spheroids in a quiescent Newtonian fluid at low Reynolds numbers. Sadhana 35(6):659, DOI 10.1007/s12046-010-0050-9

Magnaudet J (2011) A 'reciprocal'theorem for the prediction of loads on a body moving in an inhomogeneous flow at arbitrary Reynolds number. Journal of Fluid Mechanics 689:564–604

Marath NK, Subramanian G (2018a) The inertial orientation dynamics of anisotropic particles in planar linear flows. Journal of Fluid Mechanics 844:357–402

Marath NK, Subramanian G (2018b) The inertial orientation dynamics of anisotropic particles in planar linear flows. Journal of Fluid Mechanics 844:357–402, DOI 10.1017/jfm.2018.184

Mazur P, Bedeaux D (1974) A generalization of Faxén's theorem to nonsteady motion of a sphere through an incompressible fluid in arbitrary flow. Physica 76(2):235–246

McNown JS, Malaika J (1950) Effects of particle shape on settling velocity at low reynolds numbers. Eos, Transactions American Geophysical Union 31(1):74–82, DOI https://doi.org/10.1029/TR031i001p00074

Mueller S, Llewellin E, Mader H (2010) The rheology of suspensions of solid particles. Proceedings of the Royal Society A: Mathematical, Physical and Engineering Sciences 466(2116):1201–1228

Nayfeh A (1981) Introduction to perturbation techniques, john wiley & sons. New York

Nilsen C, Andersson HI (2013) Chaotic rotation of inertial spheroids in oscillating shear flow. Physics of Fluids 25(1):013303

Oberbeck A (1876) Ueber stationäre flüssigkeitsbewegungen mit berücksichtigung der inneren reibung. Journal für die reine und angewandte Mathematik 81:62–80, DOI doi:10.1515/crll.1876.81.62, URL https://doi.org/10.1515/crll.1876.81.62

Oseen CW (1910) Uber die stokes' sche formel und uber eine verwandte aufgabe in der hydrodynamik. Ark f Mat Astr Och Fys 6:29

Oseen CW (1913) title. Ark f Mat Astr Och Fys 9:16

Ostrovsky LA, Stepanyants YA (2018) Dynamics of particles and bubbles under the action of acoustic radiation force. Chaotic, Fractional, and Complex Dynamics: New Insights and Perspectives

Ouellette J (2004) Smart fluids move into the marketplace: Magneto- and electrorheological fluids find new uses. The Industrial Physicist (American Institute of Physics) 9(6):14–17

Patankar NA, Hu HH (2002) Finite Reynolds number effect on the rheology of a

dilute suspension of neutrally buoyant circular particles in a Newtonian fluid. International journal of multiphase flow 28(3):409–425

Pozrikidis C (1992) Boundary integral and singularity methods for linearized viscous flow. Cambridge University Press

Proudman I, Pearson JRA (1957) Expansions at small Reynolds numbers for the flow past a sphere and a circular cylinder. Journal of Fluid Mechanics 2(3):237–262

Radhakrishnan K (1999) Theory for semi-dilute suspensions of periodically forced slender bodies aligned along finite set of directions. Journal of chemical engineering of Japan 32(5):573–580

Radhakrishnan K, Ramamohan TR (2004) Effect of hydrodynamic interactions on chaos control in semi-dilute suspensions of periodically forced slender rods in simple shear flow. J of Chemical Engineering of Japan 37(11):1408–1414, DOI https://doi.org/10.1252/jcej.37.1408

Rallison J (1978) The effects of brownian rotations in a dilute suspension of rigid particles of arbitrary shape. Journal of Fluid Mechanics 84(2):237–263

Rallison J, Acrivos A (1978) A numerical study of the deformation and burst of a viscous drop in an extensional flow. Journal of Fluid Mechanics 89(1):191–200

Ramamohan TR, Savithri S, Sreenivasan R, Bhat CC (1994) Chaotic dynamics of a periodically forced slender body in a simple shear flow. Physics Letters A 190(3-4):273–278

Ramamohan TR, Shivakumara IS, Madhukar K (2009) Numerical simulation of the dynamics of a periodically forced spherical particle in a quiescent newtonian fluid at low reynolds numbers. In: International Conference on Computational Science, Springer, pp 591–600

Ramamohan TR, Shivakumara IS, Madhukar K (2011) The dynamics and rheology of a dilute suspension of periodically forced neutrally buoyant spherical particles in a quiescent Newtonian fluid at low Reynolds numbers. Fluid Dynamics Research 43(4):045–502

Riley N (1967) Oscillatory viscous flows. review and extension. IMA Journal of Applied Mathematics 3(4):419–434

Singh J, Kumar CVA (2019) Dynamics of a periodically forced spheroid in a quiescent fluid in the limit of low Reynolds numbers. Rheol Acta 58:709–18, DOI 10.1007/s00397-019-01169-5

Singh J, Kumar CVA (2021) Oscillations of a periodically forced slightly eccentric spheroid in an unsteady viscous flow at low Reynolds numbers. Theoretical and Computational Fluid Dynamics 35:1–15, DOI https://doi.org/10.1007/s00162-020-00547-7

Stepanyants YA, Yeoh GH (2009) Particle and bubble dynamics in a creeping flow. European Journal of Mechanics-B/Fluids 28(5):619–629, DOI 10.1016/j.euromechflu.2009.04.004

Stepanyants YA, Yeoh GH (2010) Nanoparticle dynamics in a viscous fluid at small Reynolds numbers. In: Proceedings of the 6th Australasian Congress on Applied Mechanics, Engineers Australia, Perth, Australia, 10, p 868

Stokes GG (1851) On the effect of the internal friction of fluids on the motion of pendulums, vol 9. Pitt Press Cambridge

Strand SR (1989) Dynamic rheological and rheo-optical properties of dilute suspensions of dipolar Brownian particles. PhD thesis, The University of Wisconsin-Madison

Strand SR, Kim S (1992) Dynamics and rheology of a dilute suspension of dipolar nonspherical particles in an external field: Part 1. steady shear flows. Rheologica Acta 31(1):94–117

Szeri AJ, Milliken W, Leal LG (1992) Rigid particles suspended in time-dependent flows: irregular versus regular motion, disorder versus order. Journal of Fluid Mechanics 237:33–56

Taylor GI (1923) The motion of ellipsoidal particles in a viscous fluid. Proceedings of the Royal Society of London Series A, Containing Papers of a Mathematical and Physical Character 103(720):58–61, URL `http://www.jstor.org/stable/94096`

Tsebers AO (1986) Numerical modeling of the dynamics of a drop of magnetizable liquid in constant and rotating magnetic fields. Magnetohydrodynamics 22:345–351

Vasil'ev AY, Chashechkin YD (2009) Damping of the free oscillations of a neutral buoyancy sphere in a viscous stratified fluid. Journal of applied mathematics and mechanics 73(5):558–565

Vodop'yanov I, Petrov A, Shunderyuk M (2010) Unsteady sedimentation of a spherical solid particle in a viscous fluid. Fluid Dynamics 45(2):254–263

Vojir D, Michaelides E (1994) Effect of the history term on the motion of rigid spheres in a viscous fluid. International Journal of Multiphase Flow 20(3):547–556

Weinberger HF (1972) Variational properties of steady fall in stokes flow. Journal of Fluid Mechanics 52(2):321–344

Whitehead AN (1889) On the motion of viscous incompressible fluids. Quart J Math 23:78

Williams W (1966) A note on slow vibrations in a viscous fluid. Journal of Fluid Mechanics 25(3):589–590

Publications based on the Thesis

- **International Journals**

1. Singh, J., Kumar, C.V.A. Dynamics of a periodically forced spheroid in a quiescent fluid in the limit of low Reynolds numbers. **Rheologica Acta** 58, 709–718 (2019) Springer, DOI 10.1007/s00397-019-01169-5.
2. Singh, J., Kumar, C.V.A. Oscillations of a periodically forced slightly eccentric spheroid in an unsteady viscous flow at low Reynolds numbers, **Theoretical and Computational Fluid Dynamics**,1–15(2020), Springer Nature, DOI 10.1007/s00162-020-00547-7.
3. Singh, J., Kumar, C.V.A. Periodically driven spheroid in a viscous fluid at low Reynolds numbers, **AIP Advances**,12, 025312 (2022), AIP Publishing DOI 10.1063/5.0080258

- **Books/ Book Chapters**

4. Jogender Singh and C. V Anil Kumar."Dynamics of suspended spheroid in an oscillating Newtonian fluid under the action of external periodic force at low Reynolds numbers"*Application of Soft Computing Techniques in Mechanical Engineering" (ASCME 2021)*, CRC Press (Taylor & Francis Group) DOI 10.1201/9781003257691-9.

- **Communicated and In-progress Papers**

5. Jogender Singh and C. V Anil Kumar. Transport of a driven spheroid in a uniform flow at low Reynolds numbers (**under revision**).

- ## National/International Conferences

7. "Dynamics of Periodically Forced Spheroids in Quiescent fluid at Low Reynolds Number" **International Workshop and Conference on Topology and Applications (IWTCA-2018)** at Rajagiri Institute of Engineering and Technology, Kochi India, 5th- 11th Dec 2018.
8. "Dynamics of suspended spheroid in an oscillating Newtonian fluid under the action of external periodic force at low Reynolds numbers" **International Conference on Energy Conversion and Thermo-fluid Systems (i-CONECTS-21)**, MNIT Jaipur India
9. “Rheology of periodically forced prolate spheroid suspended in a Newtonian fluid at low Reynolds numbers” at the **International Conference on Mathematical Modeling, Computational Intelligence Techniques and Renewable Energy (MMCITRE-2022)** Organized by University of Technology, Sydney, Australia (oral presentation).

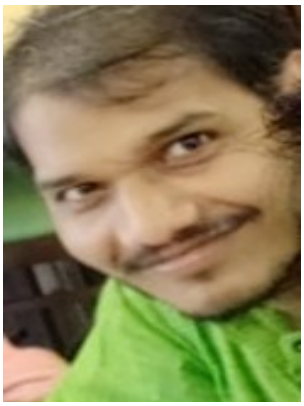

Mr. Jogender Singh is currently employed as Post-Dotoral Fellow at the Indian Institute of Technology Madras (IIT-M) , Chennai, India. He has completed his Doctoral degree (PhD) from Indian Institute of Space Science and Technology, Thiruvananthauram, India. He received a bachelor's degree in Physics and Mathematics as major subjects from CSJM University, Kanpur, Uttar-Pradesh, India, and a master's degree in Mathematics from the Indian Institute of Technology (IIT) Bhubaneswar, India, in 2013 and 2015, respectively. His current research interests include dynamics and rheology of suspended particles in a fluid at low Reynolds numbers and technologies making use of the sensitive dependence on particle shapes. He focuses on locomotion of inertial squirmer, microfluidics, complex fluids, soft matter physics, and non-Newtonian fluids. He has authored three articles and one book chapter and has presented his work at four national and international conferences. Presently, he is a member of International Society for Difference Equations (ISDE). He was a student member of the American Physical Society (APS) from 1st Jan 2020 to 31st Dec 2021.

Jogender Singh

+91-9453982261 / +91-8182354553
js10@iitbbs.ac.in

Research Interests

- Fluid dynamics — micro and macro scale — particulate, complex fluids, two- and multi-phase flow, particle separation
- Soft matter physics — chemistry to mechanics —suspension, rheology.

Academic Qualifications

Doctor of Philosophy (Ph.D.) - Thesis submitted **August 2016 – June 2022**

Department of Mathematics,
Indian Institute of Space Science and Technology (IIST).
Thesis Title: On the dynamics of a periodically driven spheroid in a variety of flows in the limit of low Reynolds numbers
Research Supervisor: Prof. C V Anil Kumar

Master of Science (M. Sc.) **July 2013 – May 2015**

Mathematics
School of Basic Sciences , Indian Institute of Technology Bhubaneswar, India
Specialization: Mathematics
Project Title: The dynamics of wandering domain of entire functions
Project Supervisor: Dr. TaraKanta Nayak
CGPA: 7.78

Bachelor of Science (B. Sc.) **July 2010 – June 2013**

Major: Physics and Mathematics
CSJM University Kanpur, Uttar-Pradesh, India
Percentage: 65.4

Important Course Works Undertaken during Ph.D.

Comutational Fluid Dynamics, Advance Fluid Mechanics, and Nonlinear dynamics, Chaos and Fractals

Research Experience

Indian Institute of Space Science and Technology, Thiruvananthapuram, India
Research Associate (RA) August 2022- Present
Kerala, India
Supervisor : Prof. C. V. Anil Kumar
Thesis title : "The Study of rheology of periodically forced suspended spheroid in Newtonian fluid at low Reynolds number"

Indian Institute of Space Science and Technology, Thiruvananthapuram, India
Research Scholar (PhD) August 2016 – June 2022
Kerala, India
Supervisor : Prof. C. V. Anil Kumar
Thesis title : "On the dynamics of a periodically driven spheroid in a variety of flows in the limit of low Reynolds numbers"

Indian Institute of Technology (IIT) Bhubaneswar, India
Graduate Researcher May 2014 - May 2015
Supervisor : Dr. Tarakanta Nayak, Associate Professor
M.Sc. Project Thesis: "The dynamics of wandering domain of entire functions"

Professional Skills Trainings

1. Advanced Level- *"Diffusion and Sub-Diffusion Problem: Theory, Numeric and Applications"*
   Agency- **National Program on Differential Equation- Theory, Computation and Applications (NPDE-TCA)** Organized by **IIT Bombay & LNM Institute of Information Technology**, Jaipur, India. **Duration- 31st Jan- 5th Feb, 2017**
2. Advanced Level- Training Program on Differential Equations"
   Agency- **National Program on Differential Equation- Theory, Computation and Applications (NPDE-TCA)**
   Organized by **IIT Bombay and IIT Kanpur, India, 25th May- 14th June, 2016.**
3. Postgraduate Level- Training Program on Differential Equations"
   Agency:- **National Program on Differential Equation- Theory, Computation and Applications (NPDE-TCA)**
   Organized by **IIT Bombay & BITS Pilani Hyderabad Campus** , **18th May- 4th June, 2015**.

Publications

Refereed International Journals

1. **Jogender Singh and** C V Anil Kumar**,** "*Dynamics of a periodically forced spheroid in a quiescent fluid in the limit of low Reynolds numbers*" *Rheol. Acta, (Springer)* Vol.- 58(11-12): pages 709–18 (2019) **Springer. DOI:** 10.1007/s00397-019-01169-5
2. **Jogender Singh and** C V Anil Kumar**,** "*Oscillations of a periodically forced slightly eccentric spheroid in an unsteady viscous flow at low Reynolds numbers*", *Theoretical and Computational Fluid Dynamics*, 1–15 (2020), **Springer Nature. DOI:** 10.1007/s00162-020-00547-7
3. **Jogender Singh and** C V Anil Kumar**,** "*Periodically driven spheroid in a viscous fluid at low Reynolds numbers*", *AIP Advances*, 12, 025312 (2022), **AIP Publishing. DOI:** 10.1007/s00162-020-00547-7

Peer-reviewed Reputed International Conferences

1. **Jogender Singh and** C V Anil Kumar**,** "*Dynamics of Periodically Forced Spheroids in Quiescent fluid at Low Reynolds Number*" International Workshop and Conference on Topology and Applications (IWTCA-2018) at Rajagiri Institute of Engineering and Technology, Kochi India, 5th- 11th Dec 2018.
2. **Jogender Singh and** C V Anil Kumar**,** "*Dynamics of suspended spheroid in an oscillating Newtonian fluid under the action of external periodic force at low Reynolds numbers*", International Conference on Energy Conversion and Thermo-fluid Systems (i-CONECTS-21), MNIT Jaipur India.
3. **Jogender Singh and** C V Anil Kumar**,** "*Rheology of periodically forced prolate spheroid suspended in a Newtonian fluid at low Reynolds numbers*" at the International Conference on Mathematical Modeling, Computational Intelligence Techniques and Renewable Energy (MMCITRE-2022) Organized by University of Technology, Sydney, Australia (oral presentation).

Book Chapters

1. *Jogender Singh and C. V Anil Kumar Dynamics of suspended spheroid in an oscillating Newtonian fluid under the action of external periodic force at low Reynolds numbers,* **Application of Soft Computing Techniques in Mechanical Engineering *(ASCME 2022)}*, CRC Press (Taylor \& Francis Group) DOI** 10.1201/9781003257691-9

Awards and Achievements

- Qualified **JAM 2013** Joint Admission test for Masters (JAM) in Mathematics
- Qualified **GATE 2016** Graduate Aptitude Test in Engineering (GATE) in Mathematics
- Qualified **NET 2016** (CSIR-UGC) Mathematical Science (Dec. 2016)
- Qualified **NET 2017** (CSIR-UGC) Mathematical Science (Jun. 2017)
-

Other Responsibilities

- Teaching assistant at Indian Institute of Space Science and Technology – Trivandrum for the Dynamics and Chaos Theory (Graduate) and Calculus (Undergraduate).
- Reviewer of Cogent Engineering (Taylor and Francis).

Technical Expertise

- Modeling and computer simulation, using MatLab, Python, C/C++
- Knowledge of using Ubuntu (Linux), Windows; LaTeX; etc.
- Familiar with CFD and FluidDyn (APIs).

Extracurricular Activities

- Play Billiards
- Swimming

References

1. Prof. C V Anil Kumar, Professor & HOD, Dept. of Mathematics, Indian Institute of Space Science and Technology, Thiruvananthapuram-695547, India. Email : anil@iist.ac.in
Tel: +91-471-2568497

2. Dr. Tarakanta Nayak, Associate Professor, School of Basic Sciences, Indian Institute of Technology (IIT) Bhubaneswar, India Email: tnayak@iitbbs.ac.in
Tel: (+91) 674-713-5166

3. Dr. Sabyasachi Pani, Associate Professor, School of Basic Sciences, Indian Institute of Technology (IIT) Bhubaneswar, India. Email: spani@iitbbs.ac.in
Tel:(+91) 674-713-5138

4. Dr. T.R.Ramamohan, Professor Emeritus, Chemical Engineering Department, M S Ramaiah Institute of Technology, M S R Nagar, Bengaluru - 560 054 India. Email: trr@msrit.edu
Mob: +91-9986469983

5. Prof. K. Satheesh Kumar, Professor and HOD, Department of Future Studies, University of Kerala, Thiruvananthpuram, Kerala, India. Email: kskumar@keralauniversity.ac.in
Mob.: +91-9249438722